Dissertation
Submitted to the
Combined Faculties for the Natural Sciences and for Mathematics
of the Ruperto-Carola University of Heidelberg, Germany
for the degree of
Doctor of Natural Sciences

Identification of $CD4^+$ T cell epitopes specific for the breast cancer associated tumor antigen NY-BR-1 using HLA-transgenic mice

Presented by

Adriane Gardyan

Dissertation

Submitted to the

Combined Faculties for the Natural Sciences and for Mathematics

of the Ruperto-Carola University of Heidelberg, Germany

for the degree of

Doctor of Natural Sciences

Presented by

Diplom-Biologin:	Adriane Gardyan
Born in:	Bottrop, Germany
Oral-examination:	18.02.2014

Identification of $CD4^+$ T cell epitopes specific for the breast cancer associated tumor antigen NY-BR-1 using HLA-transgenic mice

Referees: Prof. Dr. Philipp Beckhove

Prof. Dr. Stefan Eichmüller

Books must follow sciences, and not sciences books.

(Sir Francis Bacon)

Declarations according to § 8 (3) b) and c) oft he doctoral degree regulations:

a) I hereby declare that I have written the submitted dissertation myself and in this process have used no other sources or materials than those expressly indicated,

b) I hereby declare that I have not applied to be examined at any other institution, nor have I used the dissertation in this or any other form at any other institution as an examination paper, nor submitted it to any other faculty as a dissertation.

Heidelberg, 10.12.2013 Adriane Gardyan

Contents

1 Zusammenfassung **1**

2 Abstract **3**

3 Introduction **13**

3.1 Cancer . . . 13
3.2 Breast Cancer . . . 14
3.2.1 Incidence and risk factor . . . 14
3.2.2 Development and classification of breast cancer . . . 16
3.3 Standard therapy of breast cancer . . . 18
3.3.1 Surgery and radiation therapy . . . 18
3.3.2 Chemotherapy . . . 19
3.3.3 Anti-hormonal treatment . . . 21
3.3.4 Targeted therapy . . . 22
3.4 Principles of tumor immunology . . . 25
3.4.1 The immune system . . . 25
3.4.2 T cells . . . 26
3.4.3 The major histocompatibility complex (MHC) . . . 30
3.4.4 Antigen-processing and epitope recognition . . . 30
3.4.5 The T cell receptor: Structure and signaling . . . 31
3.4.6 Tumor antigens as targets for the adaptive immune system . . . 33
3.5 Immunotherapy approaches against breast cancer . . . 34
3.5.1 Passive vaccination strategies . . . 35
3.5.2 Active vaccination strategies . . . 36
3.5.3 Adoptive cellular therapy with TILs . . . 38
3.5.4 Targeting of immune checkpoints . . . 39
3.6 The breast cancer associated antigen NY-BR-1 . . . 40
3.7 Aim of the study . . . 42

4 Materials and Methods **43**

4.1 Materials . . . 43
4.1.1 General instrumentation . . . 43
4.1.2 General disposables . . . 43
4.1.3 General chemicals and reagents . . . 44
4.1.4 Plasmids . . . 45

4.1.5 Kits . . . 45
4.1.6 Antibodies . . . 46
4.1.7 Cytokines . . . 48
4.1.8 Cell culture . . . 48
4.1.9 Software . . . 50
4.1.10 Database . . . 51
4.2 Methods . . . 51
4.2.1 Preparation of buffers and medium . . . 51
4.2.2 Cell culture . . . 54
4.2.3 Protein detection by Western blot analysis . . . 54
4.2.4 Flow cytometry . . . 54
4.2.5 Molecular cloning . . . 55
4.2.6 Transformation and amplification of cloned plasmid . . . 55
4.2.7 NY-BR-1 specific peptide library and synthetic candidate peptides . . . 55
4.2.8 HLA-transgenic mice . . . 56
4.2.9 Isolation of murine PBMCs . . . 57
4.2.10 Analysis of a NY-BR-1-specific T cell response for HLA-DRB1*0301-/*0401-transgenic mice . . . 57
4.2.11 IFN-γ Secretion Assay with murine spleen cells . . . 58
4.2.12 Generation of murine HLA-DRB1*0301- and HLA-DRB1*0401- restricted $CD4^+$ T cell lines . . . 58
4.2.13 Determination of HLA-restriction of established murine T cell lines . . . 59
4.2.14 Generation of human dendritic cells . . . 59
4.2.15 Recombinant adenovirus (Ad5-NY-BR-1) used for infection of human target cells . . . 59
4.2.16 Generation of human dendritic cells (DCs) as antigen presenting cells for murine NY-BR-1-specific HLA-DR restricted T cell lines . . . 60
4.2.17 Histological staining of breast cancer biopsies . . . 60
4.2.18 HLA-typing of patients and healthy donors . . . 60
4.2.19 Detection of NY-BR-1 specific T cells among PBMCs of breast cancer patients and healthy donors . . . 61
4.2.20 Immunofluorescent staining of PBMCs of breast cancer patients and healthy donors . . . 61
4.2.21 Transfection of breast cancer cell lines SK-BR-2, HBL-100 with NY-BR-1-GFP using the X-treame Gene HP DNA Transfection Reagent . . . 62
4.2.22 Transient transfection of human and murine cells with NY-BR-1 . . . 62

4.2.23 Generation of stable NY-BR-1 expressing transfectants 62
4.2.24 Isolation of human PBMCs 63
4.2.25 IFN-γ -treatment of human cell lines 63
4.2.26 MHC surface expression of EL4-NY-BR-1 clones 63

5 Results **64**

5.1 Generation of a NY-BR-1 encoding expression vector suitable for the generation of NY-BR-1 expressing target cells 64
5.2 Generation of stable EL4-Rob/HHD-NY-BR-1 double transfectants 65
5.3 Generation of stable EL4-NY-BR-1 single transfectants 66
5.3.1 Expression of MHC molecules on stable EL4-NY-BR-1 transfectant clones 67
5.4 Identification of NY-BR-1-specific T cell candidate epitopes by using various HLA-transgenic mouse strains 69
5.4.1 Identification of positive NY-BR-1-specific library peptides in HHDtg mice 70
5.4.2 Identification of positive NY-BR-1-specific library peptides in DR3tg mice 74
5.4.3 Identification of positive NY-BR-1-specific library peptides in DR4tg mice 77
5.4.4 *In silico* prediction of HLA-DRB1*0301 and HLA-DRB1*0401-restricted NY-BR-1-specific $CD4^+$ T cell candidate epitopes 84
5.4.5 Detection of $CD4^+$ T cells specific for the NY-BR-1-specific candidate epitopes in HLA-DRB1*0301- and HLA-DRB1*0401-transgenic mice . . 86
5.4.6 Detection of $CD8^+$ T cells specific for NY-BR-1 in DR3tg mice and DR4tg mice 89
5.5 Verification of HLA-DRB1*0301-restriction / HLA-DRB1*0401-restriction of identified NY-BR-1-specific candidate epitopes 91
5.5.1 Establishment of NY-BR-1-specific, HLA-DRB1*0301- and HLA-DRB1*-0401-restricted murine $CD4^+$ T cell lines 91
5.5.2 Verification of HLA-DRB1*0301-/*0401-restriction of NY-BR-1-specific candidate epitopes 92
5.5.3 Peptide affinity differs among established NY-BR-1-specific, murine HLA-DRB1*0301-/*0401-restricted T cell lines 95
5.6 NY-BR-1-derived, HLA-DRB1*0301-/*0401-restricted $CD4^+$ T cell epitopes are endogenously processed in human cells 98
5.6.1 Generation of NY-BR-1 expressing target cells 98
5.6.2 Experiments using Ad5-NY-BR-1 infected melanoma and breast cancer cells as target cells 106

5.6.3 Confirmation of endogenous processing of NY-BR-1-specific candidate epitopes in human cells using HLA-matched, human DCs loaded with lysate generated from Ad5-NY-BR-1 infected tumor cells 110
5.7 Detection of NY-BR-1-specific $CD4^+$ T cells in breast cancer patients and healthy donors 113
5.7.1 Selection of NY-BR-1^+ HLA-matched breast cancer patients 113
5.7.2 NY-BR-1-specific $CD4^+$ T cells were detected among PBMCs of breast cancer patients and healthy donors after peptide stimulation *in vitro* . . . 113
5.7.3 NY-BR-1-specific $CD25^+FoxP3^+CD127^-$ T cells and $CD25^+FoxP3^+CD4^+$ T cells secreting IFN-γ could be detected among PBMCs of breast cancer patients and healthy donors. 118

6 Discussion **122**
6.1 Comparison of a global vaccination approach versus *in silico* epitope-prediction used for the identification of antigen-specific T cell epitopes 122
6.2 Potential limitations and advantages of HLA-tg mouse models for the identification of human tumor antigen-specific T cell epitopes 124
6.3 Chimeric screening for human T cell epitopes using murine $CD4^+$ T cells 126
6.4 Multiple approaches applied to confirm endogenous processing of the newly identified HLA-DRB1*0301- and HLA-DRB1*0401-restricted NY-BR-1-specific epitopes in human cells 128
6.5 Differences in frequencies of NY-BR-1-specific $CD4^+IFN\text{-}\gamma^+$ T cells in the peripheral blood of breast cancer patients and healthy donors 130
6.6 Breast cancer cells as direct targets for NY-BR-1-specific $CD4^+$ T cells 132
6.7 Potential targets of NY-BR-1-specific $CD4^+$ T cells within the tumor stroma . . 132
6.8 Role of Tregs in breast cancer 134
6.9 NY-BR-1 as a target for immunotherapy approaches against breast cancer 136
6.10 Conclusion and outlook 137

7 Supplement material **139**
7.1 Arrangement of the NY-BR-1 peptide library in the first matrix 139
7.2 Screening of a second NY-BR-1-specific library in DR4tg mice 139
7.3 HLA-phenotype of enrolled breast cancer patients and healthy donors 140
7.4 Detection of activated NY-BR-1-specific $CD4^+$ T cells among PBMCs of breast cancer patients and healthy donors by IFN-γ EliSpot assay 140

References **144**

8 Publications and Presentations **175**

8.1 Publications 175

8.2 Presentations 175

9 Acknowledgments **177**

1 Zusammenfassung

Laut der aktuellen weltweiten Statistik über Krebserkrankungen (GLOBOCAN 2008), ist Brustkrebs nicht nur der am häufigsten diagnostizierte Krebs, sondern zudem die Krebsart mit der höchsten Mortalitätsrate bei Frauen.
In den letzten Jahren hat sich die Anwendung einer tumorspezifischen Vakzinierung als eine mögliche Behandlungsoption für bestimmte Krebsarten, unter anderem auch Brustkrebs, etablieren können. Von besonderem Interesse ist es hierbei Vakzinierungen zu entwickeln, die nicht nur eine fortschreitende Metastasierung von Tumorzellen verhindern, sondern im idealen Fall bestehendes Tumorgewebe eliminieren. Klassische Immunzellen, welche eine tumorspezifische und zytotoxische Immunantwort vermitteln sind natürliche Killerzellen (NK Zellen) und zytotoxische $CD8^+$ T Zellen (CTLs). Neben CTLs zeigen auch aktivierte $CD4^+$ T Zellen tumorspezifische Aktivität. Zahlreiche wissenschaftliche Abhandlung beschreiben die Notwendigkeit einer Aktivierung von tumorspezifischen $CD4^+$ Effektorzellen zur Induktion einer effizienten gegen den Tumor gerichteten Immunantwort. Das Brustkrebs assoziierte Antigen NY-BR-1 ist in 60% aller invasiven Brusttumoren exprimiert, zudem liegt eine deutlich erhöhte Expression des NY-BR-1 Proteins in malignem Brustgewebe, im Vergleich zu normalem Brustgewebe vor. Schlussfolgernd stellt das NY-BR-1 Antigen somit möglicherweise ein optimales Zielantigen für eine T Zell basierte, tumorspezifische Immuntherapie dar.
Zielsetzung dieser Arbeit war die Identifizierung neuer *"Major Histocompatibility Complex"* MHC-I- und MHC-II- restringierter, NY-BR-1-spezifischer T Zell Epitope in HLA-transgenen Mäusen. HLA-DRB1*0301-transgenen Mäusen (DR3tg Mäuse) und HLA-DRB1*0401-transgener Mäuse (DR4tg Mäuse) wurden mit einem NY-BR-1-kodierender Experssionsvektor immunisiert um eine NY-BR-1-spezifische T Zell Antwort in den Mäusen zu induzieren. Mittels IFN-γ EliSpot Tests und einer NY-BR-1-spezifischen synthetischen Peptidbibliothek, konnten insgesamt drei neue NY-BR-1-spezifische, HLA-DRB1*0301-restringierte Peptide (BR1-1347, BR1-88, BR1-1238) und drei neue NY-BR-1-spezifische, HLA-DRB1*0401-restringierte Peptide (BR1-537, BR1-1242, BR1-656/-775) in DR3tg Mäusen bzw. in DR4tg Mäusen, identifiziert werden. Daraufhin wurden stabile murine $CD4^+$ T Zell Linien, spezifisch für die neu identifizierten NY-BR-1-spezifische Epitope aus DR3tg und DR4tg Mäusen generiert. Die HLA-Restriktion der murinen $CD4^+$ T Zell Linien wurde auf Grund der spezifischen Erkennung von peptidbeladenden T2/DR3 und T2/DR4 Zielzellen bestätigt. Die endogene Prozessierung der NY-BR-1-spezifischen Epitope BR1-1347, BR1-88, BR1-537 und BR1-1242, konnte anhand der spezifischen Erkennung von humanen Dendritischen Zellen, welche mit Zelllysaten von Ad5-NY-BR-1 infizierten Tumorzellen beladen worden waren, gezeigt werden.
Um eine mögliche klinische Relevanz der neu identifizierten, NY-BR-1-spezifischen Epitope zu

zeigen, wurden periphere mononukleare Zellen (PBMCs) von Brustkrebspatienten, mit passendem HLA-Genotyp, auf das Vorhandensein von NY-BR-1-spezifischen $CD4^+$ T Zellen untersucht. $CD4^+$ T Zellen, spezifisch für die neu identifizierten Epitope BR1-88, BR1-1347, BR1-1238, BR1-537, BR1-1242 und BR1-656/-775, konnten in PBMCs von Brustkrebspatienten detektiert werden.

Die in dieser Arbeit neu identifizierten NY-BR-1-spezifischen $CD4^+$ T Zellepitope könnten zum Beispiel für die Generierung von Tetrameren zum Nachweis NY-BR-1-spezifischer $CD4^+$ T Zellen in Brustkrebspatientinnen, oder zur Überwachung einer NY-BR-1-spezifischen Immunantwort in Brustkrebspatientinnen genutzt werden. Des Weiteren eignen sich NY-BR-1-spezifische Tetramere gegebenenfalls auch zur selektiven Gewinnung NY-BR-1-spezifischer $CD4^+$ T Zellen, welche nach *in vitro* Expansion für einen adoptiven T Zell Transfer verwendet werden könnten. Eine weitere Möglichkeit wäre die Generierung autologer T Zellen, welche einen NY-BR-1-spezifischen T Zell Rezeptor exprimieren und somit für einen adoptiven T Zell Transfer geeignet wären.

NY-BR-1-spezifischen Vakzinierung sollten im idealen Fall sowohl MHC-I als auch MHC-II-restringierte T Zell Epitope beinhalten, so dass zusätzlich zu der Induktion von NY-BR-1-spezifischen $CD8^+$ T Zellen auch NY-BR-1-spezifische $CD4^+$ T Zellen stimuliert werden. Neben der Aufrechterhaltung einer spezifischen, von $CD8^+$ T Zellen vermittelte Immunantwort, können antigen-spezifische $CD4^+$ T Zellen durch Interaktion mit antigenpräsentierenden Tumor assoziierten Makrophagen (TAMs) im Tumorstroma, möglicherweise maßgeblich zu einer gegen den Tumor gerichtete Immunantwort beitragen.

2 Abstract

Out of all malignancies, breast cancer is the second most common cancer worldwide and the leading cause of cancer related death in females. In recent years it has been shown that the anti-tumor vaccination might be a feasible approach for the treatment of certain cancer types, including breast cancer. It is of great interest to develop immunotherapies which not only prevent further dissemination by the tumor cells, but also eliminate tumor tissue and impair the function of immune-suppressive cells, such as regulatory T cells (Tregs), in the tumor microenvironment. Not only antigen-specific cytotoxic $CD8^+$ T cells (CTLs) but also $CD4^+$ T cells show a great capacity to facilitate a specific anti-tumor immune response. Furthermore, successful immunological eradication of tumors depends on the presence of activated tumor antigen-specific $CD4^+$ effector T cells as documented by numerous reports. The differentiation antigen NY-BR-1 has been described to be expressed in 60% of all invasive mammary carcinomas. Since NY-BR-1 protein levels are highly elevated in malignant breast tissues compared to healthy breast tissues, NY-BR-1 might represent a suitable target antigen for T cell based immunotherapy approaches against breast cancer.

The aim of this project was to identify novel MHC-I- and MHC-II-restricted T cell epitopes derived from the breast cancer associated antigen NY-BR-1. A NY-BR-1-specific peptide library was utilized to screen for the presence of MHC-I and MHC-II- restricted T cells in HLA-DRB1*0301-transgenic mice (DR3tg mice) and HLA-DRB1*0401-transgenic mice (DR4tg mice), after global NY-BR-1-DNA vaccination. Splenocytes of immunized mice were screened *ex vivo* for a NY-BR-1-specific T cell response against a synthetic peptide library covering the entire NY-BR-1 protein. So far, novel NY-BR-1-specific, HLA-A2-restricted $CD8^+$ T cell epitopes could not be identified. However, the first NY-BR-1-derived, HLA-DRB1*0301-restricted peptides (BR1-1347, BR1-88, BR1-1238) and the first NY-BR-1 derived, HLA-DRB1*0401-restricted peptides (BR1-537, BR1-1242, BR1-656/-775) were identified in DR3tg mice and DR4tg mice, respectively.

Stable murine $CD4^+$ T cell lines specific for five new epitopes could be established from peptide-immunized DR3tg mice / DR4tg mice, and HLA-DR-restriction of the cell lines was confirmed on peptide loaded T2/DR3 and T2/DR4 target cells *in vitro*. Furhtermore, endogenous processing of HLA-DRB1*0301-restricted NY-BR-1-derived epitopes BR1-88, BR1-1347 and of the HLA-DRB1*0401-restricted NY-BR-1-derived epitopes BR1-537, BR1-1242 could be confirmed by specific recognition of human dendritic cells loaded with cell lysates of melanoma cell line Ma-Mel73a infected with Ad5-NY-BR-1. $CD4^+$ T cells specific for the NY-BR-1 derived, HLA-DRB1*0301-restricted peptides BR1-88, BR1-1347, BR1-1238 and for the HLA-DRB1*0401-restricted peptides BR1-537, BR1-1242, BR1-656/-775 were detected among PBMCs of breast cancer patients stimulated with the respective peptide in vitro for 24 days. Furthermore, $CD4^+$

T cells with the same specificities were also detected among PBMCs of HLA-matched healthy donors, however, frequencies of antigen-specific $CD4^+$ T cells were higher in the peripheral blood of breast cancer patients compared to healthy donors.

The findings of this thesis, such as the identified NY-BR-1-specific, HLA-DRB1*0301-/*0401-restricted $CD4^+$ T cell epitopes, might be used to generate NY-BR-1-specific tetramers which could be applied to monitor immune-responses in breast cancer patients with a tumor expressing the NY-BR-1 antigen. Moreover, the new NY-BR-1-specific, $CD4^+$ T cell epitopes could be applied to expand NY-BR-1-specific autologous $CD4^+$ T cells for an adoptive T cell transfer. Cloning of high affinity TCRs, specific for the newly identified epitopes, to generate TCR-transduced $CD4^+$ T cells for adoptive T cell transfer might be another application for the findings obtained in this work. NY-BR-1-specific therapeutic vaccines could be designed by combination of CTL and $CD4^+$ T cell epitopes to induce NY-BR-1-specific $CD8^+$ T cells as well as NY-BR-1-specific $CD4^+$ T cells. Infect, $CD4^+$ T cells are not only important to sustain a functional $CD8^+$ T cell response, but might also target MHC-II expressing tumor associated macrophages (TAMs) presenting NY-BR-1-specific epitopes on MHC-II, thereby contributing to anti-tumor immunity.

Table of figures

Figure no.	Title	page
Figure 1:	Hallmarks of cancer	14
Figure 2:	Hypothetical models explaining breast tumor subtypes	17
Figure 3:	Structure of the MHC-I and MHC-II molecule	30
Figure 4:	Structure of the T cell receptor	32
Figure 5:	Verification of NY-BR-1 protein expression in transiently transfected human HEK293T cells and MCF-7 cells	65
Figure 6:	NY-BR-1 protein expression in stable EL4-Rob/HHD transfectants	66
Figure 7:	NY-BR-1 protein expression in EL4-NY-BR-1 stable transfectants	67
Figure 8:	Expression of MHC molecules on stable EL4-NY-BR-1 transfectant clones	68
Figure 9:	Workflow, identification of NY-BR-1-specific, HLA-restricted T cell epitopes in HLA-transgenic mice	70
Figure 10:	NY-BR-1 peptide library screening with splenocytes of HHDtg mice	71
Figure 11:	Combinatorial analysis of NY-BR-1 peptide library screening (first matrix) with splenocytes of HHDtg mice	72
Figure 12:	IFN-γ EliSpot results with splenocytes of HHDtg mice employing single NY-BR-1 library peptides	73
Figure 13:	NY-BR-1 peptide library screening with splenocytes of DR3tg mice	75
Figure 14:	Combinatorial analysis of NY-BR-1 peptide library screening (first matrix) performed with splenocytes of DR3tg mice	76
Figure 15:	IFN-γ EliSpot results with splenocytes of DR3tg mice employing single NY-BR1 library peptides	77
Figure 16:	NY-BR-1 peptide library screening with splenocytes of DR4tg mice	78
Figure 17:	Combinatorial analysis of NY-BR-1 peptide library screening (first matrix) performed with splenocytes of DR4tg mice	79
Figure 18:	Arrangement of the NY-BR-1-specific second matrix	79
Figure 19:	Screening of a second level NY-BR-1-specific library in DR4tg mice	80
Figure 20:	Combinatorial analysis of NY-BR-1 peptide library screening (second matrix) performed with splenocytes of DR4tg mice	81
Figure 21:	Screening of pools C1-C19 in DR4tg mice	82
Figure 22:	IFN-γ EliSpot results with splenocytes of DR4tg mice employing single NY-BR1 library peptides	83

Figure 23:	Recognition of NY-BR-1-specific candidate epitopes by splenocytes originating from DR3tg and DR4tg mice	87
Figure 24:	Detection of NY-BR-1-specific $CD4^+IFN\text{-}\gamma^+$ T cells in splenocytes of HLA-DRtg mice	88
Figure 25:	Detection of NY-BR-1-specific, $CD8^+IFN\text{-}\gamma^+$ T cells in splenocytes of HLA-DRB1*0301-/DRB1*0401-transgenic mice	90
Figure 26:	Phenotypic characterization NY-BR-1-specific T cell lines	92
Figure 27:	Recognition of peptide loaded T2, T2/DR3, T2/DR4 cells by HLA-DRB1*0301 and HLA-DRB1*0401restricted T cell lines	94
Figure 28:	Peptide affinity of different NY-BR-1-specific $CD4^+$ murine T cell lines	96
Figure 29:	Identification of NY-BR-1-specific, HLA-restricted T cell epitopes in HLA-transgenic mice	97
Figure 30:	Transfection of breast cancer cell line HBL-100 and SK-BR-2 with pcDNA3.1(-)-NY-BR-1-GFP	99
Figure 31:	Surface expression of HLA-DR-molecules and CAR-receptor in tested breast cancer and melanoma cell lines	101
Figure 32:	NY-BR-1 protein expression in human cell lines after Ad5-NY-BR-1 infection	102
Figure 33:	Identification of optimal infection dose (=MOI) of Ad5-NY-BR-1 on various human melanoma cell lines	103
Figure 34:	NY-BR-1 protein expression in PBMCs of healthy donors after infection with Ad5-NY-BR-1	104
Figure 35:	Phenotypic characterization of in vitro generated human dendritic cells	105
Figure 36:	Incubation of human dendritic cells with AdV-NY-BR-1	106
Figure 37:	IFN-γ EliSpot results on recognition of Ad5-NY-BR-1 infected target cells by novel murine HLA-DR-restricted T cell lines	108
Figure 38:	Western blot analysis of NY-BR-1 protein expression in Ad5-NY-BR-1 infected target cell lines Ma-Mel79b, Ma-Mel21 and SK-BR-2	109
Figure 39:	Western blot analysis of NY-BR-1 protein expression in Ad5-NY-BR-1 infected target cell line Ma-Mel73a.	110
Figure 40:	Recognition of human dendritic cells loaded with lysate generated from Ad5-NY-BR-1 infected tumor cells, by murine HLA-DR-restricted T cell lines	112

Figure 41:	Detection of NY-BR-1-specific $CD4^+$ T cells among PBMCs of breast cancer patients	115
Figure 42:	Detection of NY-BR-1-specific $CD4^+$ T cells among PBMCs of healthy donors	117
Figure 43:	Detection of $CD25^+$ $FoxP3^+CD127^-$ and Treg-like cells secreting IFN-γ among $CD4^+$ T cells of breast cancer patients and healthy donors	120
Figure 44:	Arrangement of the NY-BR-1 peptide library in the first matrix	139
Figure 45:	Screening of a second level NY-BR-1-specific library in DR4tg mice	139
Figure 46:	Experiment 1: Detection of NY-BR-1-specific T cells in breast cancer patient samples 24 days after in vitro	141
Figure 47:	Experiment 2: Detection of NY-BR-1-specific T cells in breast cancer patient samples 24 days after *in vitro* stimulation with NY-BR-1-specific peptides	142

List of tables

Table no.	Title	page
Table 1:	List of figures	5
Table 2:	List of tables	8
Table 3:	Abbreviations	10
Table 4:	General instrumentation	43
Table 5:	General disposables	43
Table 6:	General chemicals	44
Table 7:	General reagents	45
Table 8:	Plasmids used for cloning of the NY-BR-1 breast cancer antigen	45
Table 9:	Kits	45
Table 10:	Antibodies used for Western blot analysis	46
Table 11:	Antibodies used for flow cytometry	46
Table 12:	Antibodies used for EliSpot assays	47
Table 13:	Cytokines	48
Table 14:	Cell culture medium and supplements	48
Table 15:	Murine tumor cell lines	49
Table 16:	Human cell lines	49
Table 17:	Other cells	50
Table 18:	Software	50
Table 19:	Database	51
Table 20:	TBS-T	51
Table 21:	50 x Tris-acetate-EDTA (TAE) buffer, pH 8.0, 1L	51
Table 22:	1 x PBS, pH 7.4, 1L	51
Table 23:	10 x SDS-PAGE running buffer, 1L	51
Table 24:	1 x Tris-buffered saline (TBS), pH 7.6, 1L	52
Table 25:	Transfer buffer, pH 8.5, 1L	52
Table 26:	Stripping buffer, pH 6.8, 100 ml	52
Table 27:	Cell freezing medium	52
Table 28:	LB medium, pH 7.5, 1L	52
Table 29:	FACS buffer	53
Table 30:	MACS buffer	53
Table 31:	Cell culture medium	53
Table 32:	Definition of Milestones	69

Table 33:	*In silico* prediction of HLA-A2 candidate epitopes	72
Table 34:	Arrangement of the NY-BR-1-specific third matrix	81
Table 35:	*In silico* prediction of HLA-A2 candidate epitopes	85
Table 36:	HLA-phenotype of enrolled breast cancer patients and healthy donors	140

Abbreviations

ACT	adoptive cell transfer
Ad5	adenovirus type 5
ADCC	antibody-dependent cellular cytotoxicity
ADP	adenosine diphosphate
AMP	adenosine monophosphate
APC (fluorochrome)	allophycocyanin
APC	antigen presenting cell
ATP	adenosine triphosphate
BCIP/NBT	5-bromo-4-chloro-3´-indolyphophate/nitro-blue tetrazolium
BRCA1/BRCA2	breast cancer 1/2
BSA	bovine serum albumin
CAR	coxsackie virus and adenovirus receptor
CAR	chimeric antigen receptor
CFA	complete Freud´s adjuvant
CAF	cancer associated fibroblasts
CLIP	class II-associated Ii peptide
CTL	cytotoxic T lymphocytes
CTLA-4	cytotoxic T lymphocyte-associated antigen 4
DC	dendritic cell
DMSO	dimethyl sulfoxide
DNA	deoxyribonucleic acid
EDTA	ethylenediaminetetraacetic acid
EGF	epidermal growth factor
EGFR	epidermal growth factor receptor
EliSpot	enzyme-linked immunosorbent spot assay
ER	estrogen receptor
ERAAP	ER-associated amino-peptidase 1/2
FACS	fluorescence-activated cell sorting
FCS	fetal calf serum
FDA	Food and drug administration
FITC	fluorescein isothiocyanate

GM-CSF	granulocyted macrophage-colony stimulating factor
HCl	hydrogen chloride
HEK	human embryonic kidney
HER2	human epidermal growth factor receptor 2
HLA	human leukocyte antigens
HRP	horeseradish peroxidase
ICAM	intercellular adhesion molecule
ICOS	inducible costimulator
IFN-γ	interferon-gamma
IgG	immunoglobulin G
Ii	invariant chain
IL	interleukin
i.m.	intramuscular injection
i.p.	inraperitoneal injection
ITAM	immunoreceptor tyrosine-based activation motif
kDa	kilodalton
LFA-1	lymphocyte function-associated antigen 1
LPS	lipopolysaccharide
mAb	monoclonal antibody
MACS	magnetic cell sorting
MHC	major histocompatibility complex
mRNA	messenger RNA
MUC1	mucin 1
NaCl	sodium chloride
PBMC	peripheral blood mononuclear cell
PBS	phosphate buffered saline
PD1	programmed cell death 1
PDL-1	programmed cell death ligand 1
PE-Cy5	phycoerythrin-cyano dye 5
PerCp	peridinin-chlorophyll-protein complex
PI	propidium iodide
PLC	peptide loading complex
PR	progesterone receptor
ROS	reactive oxygen species

SDS	sodium dodecyl sulfate
TAM	tumor associated macrophages
TAP	transporter associated with antigen processing
TCR	T cell receptor
TBS	Tris-buffered saline
TBS-T	TBS with 0.1% Tween 20
TEMED	tetramethylethylenediamine
TGF-β	tumor growth factor β
TIL	tumor infiltrating lymphocytes
TNF-α	tumor necrosis factor-alpha
Tregs	regulatory T cells
TARP	TCR-γ-chain alternate reading-frame proteins
VEGF	vascular endothelial growth factor

3 Introduction

3.1 Cancer

Based on the latest estimate of the worldwide burden of cancer (GLOBOCAN 2008), cancer represents the leading cause of death (7.6 million cancer deaths in 2008) in the world [72]. An estimate of 200 subtypes of malignant tumors are described, the most common ones in Europe being: colorectal cancer (436.000 cases, 13.6% of total), breast cancer (421.000, 13.1% of the total) and lung cancer (391.000, 12.2% of the total) [72].

Cancer is a single cell based disease which can arise in almost every tissue in the body. Due to their origin, malignant tumors can be classified in three major groups; carcinomas, sarcomas and lymphomas. Carcinomas develop from normal epithelial cells e.g in the breast, colon or lung whereas adenocarcinoma originates in glandular epithelial cells. Sarcomas are arising from mesenchymal tissue such as muscles, bones, fat and cartilage. The last major group of malignant tumors is represented by lymphomas defined as cancers of the hematopoietic system, lymph nodes or blood, respectively. Myeloma, originating from plasma B lymphocytes in the bone marrow can also be classified as a cancer of the hematopoetic system.

One of the fundamental features of cancer is the tumor clonality described by the transformation of a normal single cell into a malignant cell which is characterized by abnormal proliferation due to genetic mutations. The multistep process of cancer development can be accounted to the accumulation of genetic mutations, often leading to uncontrolled cell cycle activity, one example being the mutation of tumor suppressor genes such as BRCA1/BRCA2 (breast cancer 1/2) which are fundamentally involved in DNA repair, DNA recombination, cell cycle control and DNA transcription [258]. Furthermore, aberrant epigenetic information is known to trigger carcinogenesis, one example being hypermethylation of the BRCA1 gene promotor region leading to the silencing of the BRCA1 gene [277]. Acquired mutations of pro-oncogenes, such as chromosome rearrangements in the case of the BCR-ABL gene cause constitutive activation to the Bcr-Abl tyrosinkinase, which subsequently leads to the development of chronic myeloid leukemia (CML) [138]. Moreover, gain of function mutations, for example in the receptor tyrosine kinase c-kit, inducing uncontrolled cell proliferation resulting in malignancies such as gastrointestinal stromal tumors (GIST) [51], are commonly found to induce cancer.

Given the fact of genomic instability being an underlying mechanism for the development of cancer, Hanahan and Weinberg defined the hallmarks of cancer [97] . The ten hallmarks of cancer include - genome instability and mutation, sustained proliferative signaling, evading growth suppressors, resisting cell death, induction of angiogenesis, activating invasion and metastasis, enabling replicative immortality, deregulating cellular energetics, tumor promoting inflammation and evasion of immune destruction, all promoting the development of malignant tumors being the

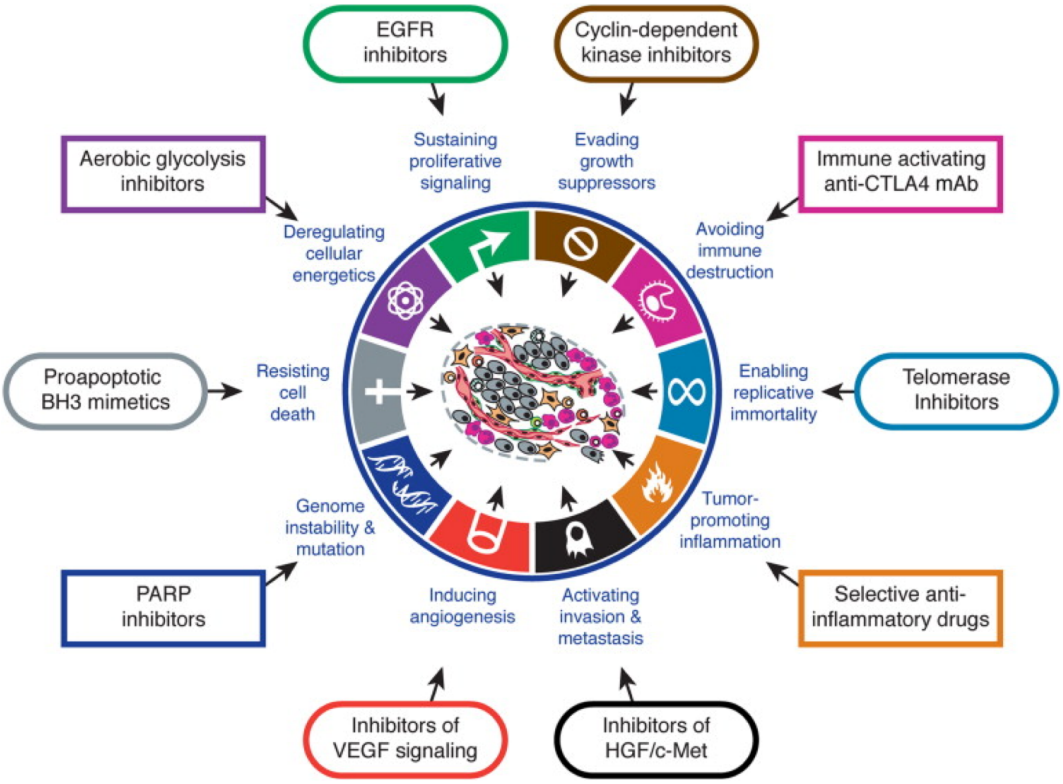

Figure 1: Hallmarks of cancer. This figure illustrates the ten hallmarks of cancer and some of the many approaches employed in developing therapeutics targeted to the known and emerging hallmarks of cancer [97].

attributes of cancer cells [97].

"Evading of immune destruction" being one hallmark of cancer indicates the great importance of the immune system to prevent malignant cell growth in the first place, thus investigation on overcoming the evasion of tumor cells from anti-tumor immunity, as well as promoting a more sustained immune responses, present two attractive strategies in how to interfere with cancer progression and established cancers.

3.2 Breast Cancer

3.2.1 Incidence and risk factor

Based on the latest cancer statistics world wide (GLOBOCAN 2008), breast cancer resembles the most common overall diagnosed cancer in women (1.38 million, 18.2% of total) and the leading cause of cancer related deaths in women (13.7% of total cancer related deaths in women) [72]. In the year 2011, 39.520 breast cancer deaths are expected in women in the United States of America representing the leading cause of death among US women [53]. Important to notice, since 1990 breast cancer related death decreased by 34% among women in the United States [53]. Reduction of breast cancer related death in women is mainly due to mammography screening programs

which invite women at the age of 50-69 to a biannual mammography screening. A comprehensive analysis indicates that the entry age of women included in the screening program is relevant for the overall beneficial effect of mammography screening. Even though the mean reduction of breast cancer related mortality due to mammography screening programs was calculated as 12%, women entering the screening program between the age of 65-70 years statistically reduce their risk of breast cancer related mortality up to 30% [18]. Nevertheless, mammography screening programs have to be evaluated critically since 30% of women enrolled in the breast cancer screening programs are over-diagnosed for breast cancer [90].

The overall likelihood of ones risk for the development of breast cancer can be analyzed due to a number of known personal and familial risk factors. Risks for breast cancer development are elevated if breast cancer cases were diagnosed in close female relatives (mother) before the age of 40 years [42]. Familial risk factors also include inherited breast cancer associated germ line mutations one example being mutations in the BRCA1 tumor-suppressor gene [68]. BRCA1 mutation carriers at the age of 60 were found to have an elevated breast cancer risk of 54% [65]. Furthermore, an increased risk for the development of breast cancer was observed in BRCA1 mutation carriers due to diagnostic radiation exposure thus other imagine techniques e.g. magnetic resonance imaging (MRI), should be considered as an alternative imaging technique in this group of patients [195]. Nulliparity increases the risk of developing breast cancer in women aged 40 years and older whereas on the other hand a full-term pregnancy significantly decreases the occurrence of breast cancer in women, the underlying mechanism still being under investigation [122].

A modifiable risk factor for the disease of breast cancer is obesity in postmenopausal women which is described to correlated with breast cancer incidence [123]. One mechanism underlying elevated risk for the development of breast cancer in obese postmenopausl women might be increased serum levels of secreted insulin and circulating free insulin-like growth factor (IGF-1) often found in obese people [75]. Downstream signaling of the insulin receptor and IGF-1 involves the pro-survival phosphatidylinositol-3 kinase (P13K)/Akt pathway already often unregulated in breast cancers and further stimulated by high levels of insulin and free insulin-like growth factor in obese breast cancer patients [75]. Secondly, in postmenopausal women, estrogen is primarily produced in adipose tissue by aromatization of androgens, hence due to greater availability of adipose tissue, levels of estrogen are highly elevated in obese postmenopausal patients [123]. In consequence, elevated levels of free estrogen in obese breast cancer patients, might induce increased signaling via the estrogen-receptor (ER) in estrogen-receptor positive breast cancers, leading to an enhanced cell proliferation and inhibition of apoptosis in ER- positive breast cancer patients [274][75].

Furthermore, hormone replacement therapy (HRT), substituting the hormone estrogen in post-menopausal women, is associated with a 10% higher breast cancer risk for each five years of

treatment duration [216]. Overall, great mammography density resulting from the proportions of epithelial and stromal tissue composing the breast, which can be identified due to high-density mammography parenchymal patterns, show the greatest impact on the prediction of breast cancer risk of an individual person when compared to known breast cancer risk factors such as family history and age at first birth [28].

3.2.2 Development and classification of breast cancer

Breast cancer is a very common but heterogeneous disease. Many malignancies of the breast are firstly recognized as premalignant lesions. Depending on the cells of origin, premalignant leasions are either termed atypical ductal hyperplasia (ADH) when originating from epithelial cell lining the breast ducts, or atypical lobular hyperplasia (ALH) if epithelial cells of the lobules are the progenitor cells [6]. In many cases premalignant lesions are stable as benign lesions but they are also known to progress into either a ductal carcinoma *in situ* (DCIS) or a lobular carcinoma *in situ* (LCIS). *In situ* carcinomas further on might progress into invasive carcinoma such as invasive ductal carcinoma (IDC) [7] or invasive lobular carcinoma (ILC) which then are prone to form metastasis. Sporadic invasive ductal carcinomas develop from epithelial cells lining the milk ducts. Normal mammary gland breast ducts are composed of two cell layers - luminal epithelial cells surrounding the lumen and myoepithelial cells (also termed basal cells) lining the basement membrane [197]. Basal like breast cancer is characterized by over-expression of genes involved in fatty acid metabolism and steroid hormone-mediated signaling pathways like estrogen receptor (ER) signaling whereas signature genes of the luminal breast cancer phenotypes are genes involved in proliferation and differentiation such as G1-S checkpoint of cell cycle proliferation [239]. Once either myoepithelial cells or luminal epithelial cells experience phenotypically alterations due to the accumulation of pro-oncogenic mutations, one example being mutations in the phsophatidylinsoitol-3-kinase (P13K) involved in the pro-survival Akt signaling pathway [63], a ductal carcinoma *in situ* is established ongoing with a simultaneous loss of myoepithlial cells due to degradation of the basement membrane [197]. Complete loss of the basement membrane and myoepithelial cells indicates an invasive carcinoma, which most likely forms metastasis, commonly spreading to the lung, pleura, liver and bone in breast cancer patients [268].

The three main prognostic determinants for breast cancer patients are lymph node (LN) status, tumor size, and histological grade, also known as the Nottingham Grading System (NGS) which includes the investigation of the percentage of tubule formation, the degree of nuclear pleomorphism and and accurate mitotic count [66]. Patients with four or more involved lymph nodes at initial diagnosis have a high risk of experiencing breast cancer metastasis formation originating from their primary breast tumor [117]. Furthermore, a number of breast cancer metastasis prognostic markers are established in the clinic and will be discussed in the following. The actual

tumor size indicates the risk for metastasis formation, tumors < 2 cm in diameter implicate low risk of metastasis, whereas tumors of 2-5 cm and above hold great potential of metastasis formation. Upon initial diagnosis, axillary lymph nodes are screened for the presence of metastases. Metastasis free axillary lymph node status indicates a low risk of primary tumor metastasis wheres presence of lymph node metastasis relates to a high metastasis risk of the primary tumor [268].

Based on comprehensive gene expression profiling, breast cancer subtypes can be classified due to their hormone receptor status, regarding the expression of hormonal receptors (estrogen receptor (ER), progesterone receptor (PR)) [5], as well as to over-expression of the ERBB2 gene (epidermal growth factor receptor 2), also known as HER2. A HER2 positive breast cancer receptor status is generally associated with a more aggressive cancer phenotype [60] due to HER2 signaling related activation of pro-survival pathways in the cancer cell. The four major breast cancer subtypes classified by receptor status are the luminal A (ER+ and/or PR^+, $HER2^-$, Ki-67<14%), luminal B (ER^+ and/or PR^+, $HER2^-$, Ki-67>14% or ER^+ and/or PR^+, $HER2^+$), HER2-enriched (ER^-, PR^-, $HER2^+$), and triple negative breast cancer (TNBC) (ER^-, PR^-, $HER2^-$) [188].

As shown in figure 2, the "cell of origin model" proposes the initiation of a specific tumor subtype due to its parental cell being either a bipotential stem cell which will give rise to basal-like tumors (ER-, PR-, HER2-), or a luminal progenitor cell which will give rise to either luminal tumors (ER^+, PR^+, $HER2^-$) or $HER2^+$ tumors (PR-, ER-) [197]. A second model of breast tumor subtype-specific transforming events (fig.2) proposes the occurrence of transformations, such as somatic mutations taking place in the bipotential stem cell leading to the development of the major breast tumor subtypes mentioned above [197].

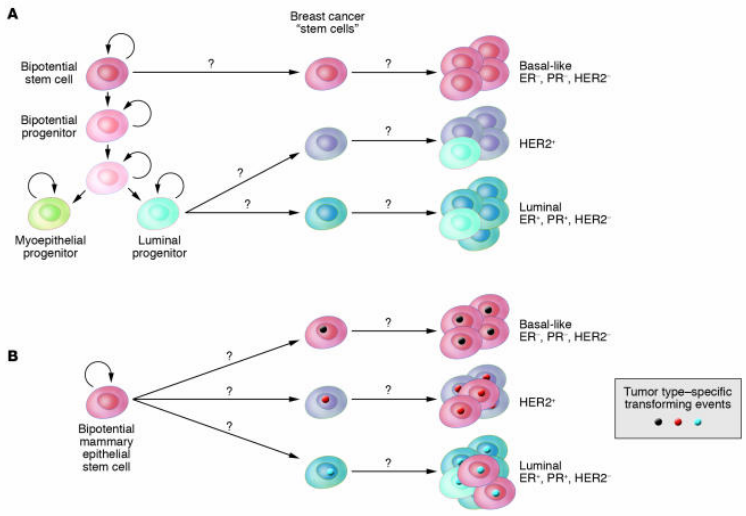

Figure 2: Hypothetical models explaining breast tumor subtypes. Cell of origin **(A)** and tumor subtype-specific transforming event **(B)** models. Based on the cell of origin hypothesis, each tumor subtype is initiated in a different cell type (presumably stem or progenitor cell), whereas according to the model depicted in **B**, the cell of origin can be the same for different tumor subtypes and the tumor phenotype is primarily determined by acquired genetic and epigenetic events [197].

Apart from breast carcinoma cells, genetic profiling has indicated the presence of a variety of different cell types in human breast tumors, such as endothelial cells, stroma cells, B lymphocytes, T lymphocytes and macrophages [193]. Increased lymphocyte infiltration in the tumor and tumor stoma is generally associated with a good prognosis in ER-/HER2-negative breast cancers [148]. Fibroblasts, the predominant cells of the breast stroma are known to possibly convert to cancer associated fibroblasts (CAF) in tumors [232]. Mammary cancer associated fibroblasts are described to influence tumorigenesis by inducing epithelial-to-mesenchymal transition (ETM), whereby expression of the metastatic marker vementin is induced in breast tumor cells by the influence of CAF [238]. Furthermore, breast cancer cells induce CAF to secrete hepatocyte growth factor, this being one example for the crosstalk between malignant cell and CAFs [158]. Hepatocyte growth factor resembles a ligand of the Met receptor tyrosine kinase whereby aberrantly activation of Met is associated with high grade tumor invasiveness[84]. Besides CAF, tumor associated macrophages reside in the breast cancer microenvironment. The majority of macrophages within the tumor site are of a polarized M2 phenotype [154]promoting tumor progression by tissue remodeling, enhanced neo-angiogenesis and suppression of an adaptive immune response due to secretion of interleukin 10 (IL-10) and activation of regulatory T cells (Tregs) [153].

Besides great diversity among individual breast cancer tumor subtypes, a high grade of heterogeneity can also be found within individual mammary tumors. Intratumoral heterogeneity of breast cancer tumors can be accounted to either breast cancer stem cells acquiring mutations in a multistep process with their progeny being of limited proliferation capacity or might follow the competition among different breast cancer tumor cells of distinct phenotypes following the laws of darwinian evolution [174]. Given the facts of intratumoral heterogeneity which might be altered during tumor progression, this most likely explains sudden resistance to breast cancer therapies which will be discussed in the next paragraph.

3.3 Standard therapy of breast cancer

Upon diagnosis of breast cancer, different treatments are available for the patients. Classical breast cancer treatments such as surgery, radiation therapy and chemotherapy, as well as anti-hormonal treatment and targeted therapies of breast cancer. Resectable tumors are often treated with radiation therapy as well as neo-adjuvant chemotherapy to reduce tumor mass prior to surgical removal of the tumor.

3.3.1 Surgery and radiation therapy

Minimal-invasive core needle biopsies as well as fine needle biopsies are widely used to diagnose breast cancer due to histological analysis of the retained tumor sample. Vacuum-assisted core

biopsy instruments remove breast tissue specimens by application of a vacuum at the tumor site, sucking the sample into a small chamber where it is cut by high-speed rotating knives and can be suctioned into a chamber outside of the patients body, available for pathological analysis of the tumor specimens if needed [124].

Due to more advanced diagnostic approaches including diagnostic ultrasound of the breast, magnetic resonance imaging, sentinel lymph node biopsy and mammography screening, most tumors are discovered at early stages, thus breast cancer surgery continues to become more conservative [40]. Breast conserving therapy (BCT) aims on removal of the tumor mass followed by radiation therapy. Certain selection criteria have to be addressed when considering BCT [202], namely the overall tumor size and histology of the tumor. Tumors of a size bigger than 4 cm have to be reduced in size prior to BCT which can be achieved for example by administration of a neo-adjuvant chemotherapy. Furthermore, the breast tumor needs to be non-invasive phenotype to achieve disease-free margins upon breast conserving therapy. Moreover, minimally invasive ablation techniques, such as cryotherapy, radio-frequency ablation or laser interstitial therapy can be applied for the treatment of breast cancer. Cryotherapy aims on disruption of the cellular membrane du to sudden temperature drops in the breast tumor tissue from 37°C to -70°C [241]. In contrast to cryotherapy, radio-frequency ablation (RFA) induced tumor cell death by transmission of frictional heat generated by intracellular irons moving due to an alternating current [235]. Laser interstitial therapy (LITT) causes cell death due to the delivery of thermal laser energy through a fiberoptic probe which is inserted in the breast tumor [59]. Some women might still require palliative radical mastectomy due to chemotherapy-resistant invasive breast tumors as well as prophylactic mastectomy due to a personal or family history of mammary carcinomas. Nevertheless, immediate breast reconstruction, remodeling the shape of the removed breast using the patients own skin, helps to achieve excellent cosmetically results [226]. In addition of primary breast tumor removal, axillary lymph node dissection (ALND) might be performed, especially indicated in patients showing an invasive type of primary breast tumor with axillary lymph nodes already reached by tumor cells originating from the primary breast tumor (node-positive patients) [16].

Radiation therapy of breast cancer often follows surgical treatment, such as breast conservation surgery but is also administered as surgical adjuvant radiotherapy to reduce the tumor size prior to its surgical resection. Surgical adjuvant radiotherapy has been proven to significantly improve the survival of breast cancer patients with operable tumors [255].

3.3.2 Chemotherapy

The use of systemic cytotoxic chemotherapy still remains first choice in both advanced and early stage breast cancer. Chemotherapy can be administered as neo-adjuvant chemotherapy (prior

to any other breast cancer related treatment) or as adjuvant-chemotherapy in combination with other types of breast cancer treatment. A number of cytotoxic agents which can be classified into four major groups are available: Alkylating agents, antimetabolites, anthracyclines and taxane.

Alkylating agents (e.g. cyclophosphamide) induce their cytotoxic effect mainly by DNA damaging due to transfer of an alkyl group (CnH2n+1) to the guanine base of DNA which induces intrastrand and interstrand DNA-crosslinking [184]. Alkylation of nucleotide acid additionally leads to the activation of DNA repair pathways such as base excision repair (BER) and mismatch repair (MMR) [79]thus a combinatorial treatment of alkylating agents based chemotherapy and DNA-repair pathway-blockade should be considered to generate a more effective anti-tumor effect [128].

Platinum based anti-cancer therapy (e.g. cisplatin) target cells‘ DNA by forming DNA adducts via cross-linking of the DNA [265]. Accumulation of DNA-damage leads to the induction of apoptosis in the tumor cell but there is also evidence available that cisplatin induces cellular death due to necrosis [88].

Antimetabolites (e.g. 5-Fluorouracil, gemcitabine) represent chemicals which mimic natural cellular metabolites such as purines and pyrimidines required for DNA-synthesis. By incorporation of the pyrimiden analogue 5-Fluororacil into the DNA during S-phase, cellular replication is inhibited and cellular apoptosis induced, with damaged DNA being the apoptotic signal [150]. Furthermore, 5-fluorouracil inibits the enzyme thymidylated synthase which is important for pyrimidine *de novo* synthesis, resulting in a depletion of dTTP followed by decreased DNA synthesis [177].

Anthracyclines (e.g. doxorubicin and daunorubicin) are cytostatic antibiotics commonly used as adjuvant chemotherapies for the treatment of breast cancer. Activity of anthracyclines is related to the inhibition of topoisomerase II, inducing growth arrest in the G1 and G2 phase of the cell cycle due to anthracycline intercalation in the desoxyribonucleic acid (DNA) [105]. Moreover, Doxorubicin induces cellular apoptosis du to transactivation of the human potent inducer of apoptosis, the CD95 gene (Fas/APO-1 receptor) by binding of activated p53 [217]. Additionally, anthracyclines are capable of reducing oxygen to generating reactive oxygen species (ROS) such as superoxide anion (O_2^-) and hydrogen peroxide (H_2O_2) by adding one electron to their chemical structure, leading to the induction of apoptosis in susceptible tumor cells [162].

The second chemotherapy regimen widely applied is the use of cytostatic active *taxanes* (e.g paclitaxel, docetacel, epirubicin), a class of mitotic inhibitors used in breast cancer systemic chemotherapy. Mitotic cell devision requires the formation of microtubuli structures in the cytoplasm of the cell. Microtubuli are composed of polymerized tubulin which consists of a α-subunit and a β-subunit, assembled into tubulin dimers to form protofilaments lining the microtubuli wall. To fulfill their function of mitosis, maintenance of cell shape and most important by intracellular

trafficking, microtubuli require a high grade of dynamic behavior [228]. Paclitaxel blocks microtubuli by binding to the ß-tubulin subunit in microtubuli. Thereby reducing their dynamics thus impairing cell cycle proliferation by inhibiting the metaphase/anaphase transition of the affected cell [282].

Resistance to individual chemotherapy regimens accounts for failure of tumorregression upon systemic chemotherapy in breast cancer treatment. Multiple factors might contribute to ineffectiveness of cytotoxic agents such as increased drug efflux from the tumor cell, the favoring of pro-survival pathways and down regulation of cell death pathways or drug deactivation [207]. Thus treatment schedules for systemic chemotherapy have to be individualized for every breast cancer patient. Combinatorial treatments approaches composed of different chemo-cytotoxic regimes are especially indicated in the treatment of metastatic breast cancer. Combination of taxan-based chemotherapy regimen paclitaxel and anthracycline cytostatic drug doxorubicin with the addition of a platin regim, generated an objective response rate in stage IV metastatic breast cancer patients [136]. Comprehensive studies have shown a prolonged survival and improved anti-tumor response in patients with metastatic breast cancer receiving a combination chemotherapy [33].

3.3.3 Anti-hormonal treatment

Estrogen (17 β-estradiol) belongs to the group of the steroid hormones which is synthesized in the ovaries in premenopausal women, regulating growth, differentiation and function in many tissues of the body, examples being the regulation of the normal growth and development of the breast and maintenance of the menstrual cycle in women. A number of mammary tumors can be classified as estrogen-positive (ER^+) tumors due to expression of the estrogen-receptor in the tumor cells. Up to now, two isoforms of estrogen receptors are known, ERα and ERβ both members of the nuclear receptor family, with ERα being the predominant regulator of estrogen-induced target gene expression in breast caner patients [185, 175]. Binding of estrogen to its receptor leads to the activation of hormone-responsive genes which promote DNA-synthesis and cell proliferation. Target genes of estrogen in breast cancer cells are the vascular endothelial growth factor (VEGF) [8], c-Myc and cyclin D1 [57].

The first approach of anti-hormonal treatments aims on the inhibition of estrogen receptor signaling by abrogating estrogen binding to its receptor. The anti-estrogen tamoxifen is a selective estrogen modulator which competitively binds to the estrogen receptor, thus inducing growth arrest in the breast cancer cells [81]. Treating early breast cancers with tamoxifen was reported to result in an improvement of 10 year survival rate in women with ER^+ mammary carcinomas [1]. The selective estrogen receptor modulator tamoxifen was approved by the Food and Drug Administration (FDA) for the treatment of postmenopausal women with metastatic breast cancer. Toremifen is structurally similar to tamoxifen, differing in only a single chlorine atom thus having

a similar pharmacological profile. Comparative analysis revealed equal effectiveness of tamoxifen and toremifen in patients with advanced breast cancer [155]. Similar to the effects of tamoxifen and toremifen on estrogen-receptor signaling, a third agent, fulvestrant not only inhibits estrogen induced signaling by blockade of the estrogen-receptor but also accelerates the receptors degradation by the ubiquitin-proteasomal pahtway [149].

Instead of blocking the estrogen receptor, aromatase inhibitors inhibit the enzyme aromatase, a key enzyme in estrogen production. Aromatase is expressed in several tissues such as the subcutaneous fat, liver, muscle, brain and normal breast tissue [172]. In postmenopausal women the predominant source of estrogen is the conversion of androstenedione into physiological active estrogen by the enzyme aromatase [234]. Aromatase inhibitors (e.g. letrozole, anastrozole, exemestane) lack estrogen-agonist activity, therefore not inhibiting estrogen production in the ovaries, but being effective in reducing estrogen serum levels in postmenopausal women by irreversibly binding to the aromatase [83].

3.3.4 Targeted therapy

Targeted therapies specifically inhibit cellular signaling pathways associated with carcinogenesis, such as human epidermal growth factor 2 (HER2), mammalian target of rapamycin (mTor) or vascular endothelial growth factor (VEGF).

The cell surface receptor of human epidermal growth factor number 2 (HER2) is encoded by the ERBB2 tyrosine kinase gene and belongs to the greater family of structurally related receptors: HER1 to HER4 [181]. So far, no HER2 specific ligand has been identified, nevertheless, spontaneous dimerization of the HER2 receptor accelerates the phosphorylation of intrinsic tyrosine kinase domains, finally resulting in the activation of the downstream signaling cascades such as MAPK proliferation pathways or P13K/Akt prosurvival pathways [144]. Activation of MAPK and P13/Akt associated pathways subsequently lead to a cellular growth promoting effect. HER2 functions as the preferred heterodimerization partner for the other ligand-activated human epidermal growth receptors such as EGFR, HER3 and HER4, with the heterodimers being very stable on the cells surface [278] . Hence, by forming heterodimers with associated human epidermal growths factors (e.g. EGFR, HER3, HER4), HER2 contributes to an overall signal amplification of HER-related signaling [126].

The ERBB2 gene is found to be over-expressed in 30% of primary breast tumors in consequence stimulating increased cellular proliferation of these tumor cells [236]. The targeting drug trastuzumab (herceptin), a humanized, recombinant monoclonal antibody binds to the extracellular domain of HER2 thereby inhibiting dimerization of the HER2 receptor leading to down-regulation of HER2 related signaling such as pro-survival PI3K pathway [275]. Binding of the monoclonal antibody trastuzumab to HER2 over-expressing cells additionally engages Fc receptor

mediated immunity, leading to antibody-dependent cellular cytotoxicity (ADCC) in breast cancer cells [9].Moreover, antiangiogenic effects were described for trastuzumab, due to inhibition of the vascular endothelial growth factor pathway [134]. Breast cancer treatment regimens often combine trastuzumab and different chemo-therapeutic approaches, examples being combination of trastuzumab and paclitaxel leading to overall response rates of 62.5% in patients with metastatic breast cancer [45]. Combined therapies might help to overcome trastuzumab resistance such as up regulation of the P13K pathway [17]y or accumulation of p95-HER2, a truncated form of HER2 lacking the trastuzumab binding site [82]. Moreover, trastuzumab-emtansine, a HER2-specific antibody-drug conjugate combines the monoclonal antibody trastuzumab and the cytotoxic agent DM1 (deviate of maytansine) via a stable thioether linker [152]. Efficacy of prolonging progression free survival was proven in HER2 positive advanced breast cancer patients treated with trastuzumab-emtansine [259].

While trastuzumab inhibits ligand-independent dimerization of HER2, the monoclonal antibody pertuzumab binds to HER2 at a distinct epitope of the dimerization domain II from trastuzumab, thereby inhibiting dimerization of HER2-HER3 complexes [13]. In consequence, pertuzumab interferes with ligand dependent HER3-signaling by preventing heterodimers formation of HER2-HER3 [13]. Combined anti-HER2 therapy using both trastuzumab and pertuzumab led to synergistic effects resulting in improved progression free survival of patients with metastatic breast cancer [120].

Secondly, HER2 signaling can be targeted by tyrosine kinase inhibitors (e.g. Lapatinib) disrupting e.g. HER2 downstream signaling due to inhibiting phosphorylation of the protein kinase Akt in the PI3K pathway [262]. Lapatinib, a dual kinase inhibitor of human epidermal growth factor 2-tyrosine kinase and epidermal growth factor (EGFR)-tyrosine kinase [129] proved to be efficient in the treatment of HER2-positive patients with a locally advanced or metastatic breast cancer hence leading to a progression free survival rate of 63% after four months of treatment [87]. Combined therapies of lapatinib and the chemotherapeutic-agent capecitabine was approved by the FDA for the treatment of metastatic breast cancer since the combinatorial therapy was more effective in treating metastatic breast cancer than capecitabine alone [85, 218].

In July 2012, the FDA approved everolimus, a mTor inhibitor for the treatment of advanced hormone receptor-positive, HER2-negative postmenopausal breast cancer patients in combination with the aromatase inhibitor exemestane [176]. mTor is a downstream target of phospathidylinositol-3 kinase (PI3K) signaling initiating cell growth, autophagy and proliferation once activated. The rapamycin analog everolimus, binds to the serine/threonine kinase mTOR (mammalian target of rapamycin), thus inhibiting mTor signaling mediated cell proliferation [221].

Apart from interrupting HER2 mediated signaling, the epidermal growth factor receptor (EGFR), also named human epidermal growth factor 1 (HER1) which is located on the cells´membrane, can

be selectively blocked in breast cancer therapy. Epidermal growth factor (EGF) is a known ligand binding specifically to HER1 [24]. Initiated signaling via EGFR activates the intrinsic tyrosine kinase activity of the EGFR which subsequently results in the activation of pro-proliferative pathways such as the phospathidylinositol-3 kinase (P13K) associated pathway, leading to uncontrolled cell proliferation of EGFR expressing breast cancer cells [147]. Activated EGFR can also be translocated to the nucleus directed by its nuclear localization sequence (NLS) [107]. In the nucleus, EGFR functions as a transcriptional co-activator regulating for example the cyclin D1 gene which is required for highly proliferative activity of the cell [143]. Cetuximab, a chimeric (mouse/human) monoclonal antibody, selectively binds to the EGFR, thus accelerating internalization of the receptor and in consequence decrease of EGFR-surface expression [98]. Furthermore, competitive binding of cetuximab prevents further stimulation of the EGFR by endogenous ligands such as epidermal growth factor (EGF) resulting in the abolishment of pro-proliferation signals in the affected cell [98]. Moreover, binding of cetuximab to EGFR can induce antibody-dependent cellular cytotoxicity in triple negative breast cancer cell lines [210].In combination with the chemotherapeutic drug cisplatin, cetuximab lead to increased progression free survival in patients with metastatic triple-negative breast cancer [12].

Targeting of the tumors´ vascularization represents another group of targeted therapy approaches in breast cancer. The angiogenesis inhibitor bevacizumab (also named Avastin), is a monoclonal antibody targeting the proangiogenic vascular endothelial growth factor (VEGF). Elevated expression of VEGF has been associated with shorter relapse-free survival in primary breast cancer patients [129]. Combinatorial therapy of bevacizumab plus paclitaxel leads to prolongation of progression-free survival in patients with metastatic breast cancer compared to paclitaxel alone [161].

Therapy resistance is one major hurdle of targeted therapies against breast cancer. Loss of sensitivity for example by acquired resistance due to mutations, such as activating mutations in the PI3K gene downstream of HER2, which renders cells to be insensitive for effects of trastuzumab and lapatinib, are just two examples on how cancer cells acquire a therapy resistance [48]. Furthermore, inhibition of signaling pathways such as the Akt-pathway by application of Akt inhibitors, might induce compensatory pathways in the cancer cell, one example being the induced expression and phosphorylation of multiple receptor tyrosine kinases (RTKs) [35].

As discussed above, surgery, chemotherapy, anti-hormonal therapy and targeted therapies are commonly used for the treatment of breast cancer. Nevertheless, tumor-immunotherapy approaches are emerging to become more often the choice of treatment for breast cancer patients. The principles of tumor immunotherapy and current knowledge on immunotherapy in breast cancer patients will be discussed in the following.

3.4 Principles of tumor immunology

3.4.1 The immune system

The immune system is a network of various immune cells, and different lymphoid tissues, orchestrating in protecting the human body against disease. The lymphoid tissues are composed of primary lymphatic tissues (bone marrow, thymus) and secondary lymphatic tissues (lymph node, spleen, mucosa associated lymphatic tissue, skin). Whereas generation of immune cells takes place in the primary lymphatic tissues, mature immune cells migrate to the secondary lymphatic tissues where adaptive immune responses are initiated. Generally, the immune system can be classified into innate immunity and adaptive immunity, both mediated by distinct cell populations. A brief overview on cells of the immune system and their function will be discussed in the following.

Cells of the **innate immunity** develop in the bone marrow before they migrate to the periphery. Monocytes and macrophages, granulocytes, mast cells, dendritic cells and natural killer cells, providing immediate immunity without prior exposure to the antigen. Upon antigen encounter, the innate immunity is the first line response, quickly recognizing antigens in an non-specific way e.g. via pattern recognition receptors. Toll like receptor 4 (TLR4) is a pattern recognition receptor recognizing lipopolysaccharide (LPS) originating from gram-negative bacteria whereas the mannose receptor binds sugar molecules found on the surface of many bacteria and viruses. Antigen capture by cells of the innate immune system triggers for example phagocytosis of pathogen derived antigens by macrophages, cellular cytotoxicity mediated by natural killer cells or the release of toxic granules by granulocytes, overall inducing cellular death. Furthermore, innate immune cells can be activated by binding of antibodies to their Fc receptor, therefore building a bridge between innate immunity and the adaptive humoral immune response. Even though antigenic-response rates are quick, innate immunity fails to establish a long lasting memory response that provides a pre-existing immune response in case of a secondary infection.

The concept of **adaptive immunity** is based on the specific recognition of antigens by antigen-specific receptors present on B lymphocytes and T lymphocytes. In the primary lymphatic organs, such as bone marrow and thymus, lymphocytes are generated from progenitor cells, whereas B lymphocytes are generated in the bone marrow and T lymphocytes are generated in the thymus, respectively. Furthermore, central tolerance of T lymphocytes and B lymphocytes is established in the primary lymphatic organs. In the thymus, one of the main mechanisms of T-cell central tolerance is clonal deletion of self-reacting T cells, whereby immature auto reactive B lymphocytes undergo negative selection and clonal deletion in the bone marrow. Self-reactive B cells might be rescued from clonal deletion by receptor editing which might replace the self-reactive receptor with a non auto-reactive B cell receptor.

Positively selected, mature lymphocytes migrate to the secondary lymphatic organs, such as

the lymph nodes, the spleen and the mucosa-associated lymphoid tissue (MALT). Until encounter of their specific antigen, mature lymphocyte recirculated between the secondary lymphatic organs and the blood. Mature lymphocytes activation by antigen recognition takes place in the secondary lymphatic organs, leading to clonal expansion and maturation of activated lymphocytes. The adaptive immunity is capable of establishing a durable memory response depending on the generation of T lymphocyte memory cells and B lymphocyte memory cells. Lymphoid memory cells are quick in generating an adaptive immune response upon second encounter of an antigen.

B lymphocytes recognize their specific antigen via a B cell receptor (BRC) on the cells surface. Antigen recognition stimulates differentiation of a naive B cell into a plasma cell secreting antibodies with the same specificity as the cells B cell receptor. Different classes of antibodies are described such as IgG, IgM, IgA, IgE and IgD, all belonging to the group of immunoglobulins (Igs) exerting there function via a constant Ig-domain. Pathogens often are opsonized by specific antibodies binding to their surface, accelerating macrophage mediated phagocytosis of the pathogen. A complete antigenic activation of naive B cells require the costimulatory help of antigen-specific T lymphocytes. Since T lymphocytes are the major cell type investigated in this scientific work, they will be analyzed in more detail below.

3.4.2 T cells

T cells develop in the thymus before they migrate into the periphery where they are activated by MHC-restricted antigen recognition. T lymphocytes are characterized by expression of the cluster of differentiation 3 (CD3) and an antigen-specific T cell receptor (TCR). Variety of the T cell receptor repertoire is based on somatic recombination events, the VDJ-recombination. Four different subtypes of T cells are defined: Cytotoxic T cells ($CD8^+$ T cells), $CD4^+$ T cells, NKT cells and $\gamma\delta$-T cells.

$CD8^+$ T cells (Cytotoxic T cells) $CD8^+$ T cells recognize on MHC class I presented epitopes derived from endogenous protein such as virus or antigens derived from malignant cells. Recognition of their specific antigen leads to clonal expansion of activated $CD8^+$ T cells which rapidly clear infected cells by a variety of defense mechanism. Most prominent is the release of granules by cytotoxic T cells in the immunological synapse being in direct proximity to the target cell. The secretory cytotoxic granular contain perforines and and serine proteases such as granzyme A and granzyme B. Upon release, granzymes enter the cytoplasm of the target cell via membrane-pores in the cells plasma membrane formed by perforines [151]. Granzyme A induces single-strand DNA damage by activation of the endonuclease (NM23.H1) and the exonuclease (TREX1) [38]. Moreover, granzyme A disrupts mitochondrial metabolism by cleavage of the NDUFS3 protein in the electron transport complex 1, leading to the release of reactive oxygen

species (ROS) and subsequent cell death in the affected target cell [157]. Granzyme B induced apoptosis of the target cell by activation of pro-caspases e.g. caspase 3, leading to the activation of caspas-induced apoptotic pathways with final DNA-fragmentation [254]. Cytotoxic T cells are also capable of inducing cellular death of a target cell by a Fas mediated apoptosis. Upon activation, $CD8^+$ T cells express the type-II transmembrane protein Fas ligand (FasL, CD95L) on their cells surface which binds Fas receptor expressed on the target cell. Ligation of the FasL and Fas receptor induces Fas dependent apoptosis in the target cell [233].

The main cytokine released by $CD8^+$ T cells is IFN-γ resulting in stimulation of MHC class I antigen presentation pathway by replacement of the constitutive proteasome with the immunoproteasome [92]. In the immunoproteasome the catalytic subunits of the vertebrate 20S proteasome are exchanged for the interferon gamma inducible catalytic subunits LMP2, PMP7 and MECL [92]. Moreover, IFN-γ released by activated $CD8^+$ T cells induces IFN-γ signaling via the Jak-Stat pathway which leads to the phosphorylation of the cytoplasmic transcription factor STAT. Phosphorylated STAT homodimerizes and translocates to the nucleus where it initiates transcription of IFN-γ-inducible genes such as major histo compatibility complex genes (MHC) [285][242].

$CD4^+$ T cells In contrast to $CD8^+$ T cells, $CD4^+$ T cells recognize on MHC class II presented epitopes derived from exogenous protein. MHC-II restricted peptides are recognized by $CD4^+$ T cells by binding of their T cell receptor (TCR) to the peptide-MHC-II complex. TCR-diversity is achieved by somatic recombination of the TCR related genes, name V, D, J genes. In theory, 1 X 10^{15} different TCRs could be composed out of these genes allowing the presence of specific TCRs for every possible antigen presented on MHC molecules [49]. According to their effector function, $CD4^+$ T cells either help to sustain an ongoing immune response by the activation of macrophages and secretion of pro-inflammatory cytokines such as interferon gamma (IFN-γ), or stimulate antigen-specific B cells to mature into antibody-secreting plasma cells by delivery of co-stimulatory signals via CD28. Finally, $CD4^+$ regulatory T cells (Tregs) are necessary to impair an overshooting immune response to maintain homeostasis. Development of the $CD4^+$ T cell linages into T helper cells 1 (Th1), T helper cells 2 (Th2), T helper cells 17 (Th17) and regulatory T cells (Tregs), depends on the cytokine milieu present during $CD4^+$ T cell activation [286] whereas every linage is further on characterized by the specific cytokine profile secreted by these $CD4^+$ T cells.

T helper 1 cells (Th1) cells differentiate from naive $CD4^+$ T cells if the cytokines IFN-γ and interleukin 12 (IL-12) are present in the microenvironment. Once differentiated into Th1 cells, the main cytokines secreted of this $CD4^+$ T cell subpopulation upon antigenic stimulation are IFN-γ, interleukin 2 (IL-2) and tumor necrosis factor β (TNF-β) [215]. Th1 cell can mobilize the cellular arm of the immune system such as cytotoxic T cells, dendritic cells and macrophages,

to combat an infection. Macrophages require two signals for optimal activation: IFN-γ and a sensitizing signal via the CD40 molecule on their cell surface. Th1 cells provide both signals, hence IFN-γ being the cardinal cytokine secreted as well as expression of the CD40 ligand, both leading to microbicidal activity of the macrophages such as production of nitric oxide (NO) [108]. IL-2 secreted by activated Th1 cells stimulates clonal expansion of $CD8^+$ cells during the priming phase and sustains their cytolytic function by upregulated expression of granzyme B [22, 135]. Recruitment of cytotoxic T cells to the site of inflammation is supported $CD4^+$ dependent IFN-γ secretion, one example being the induction of $CD8^+$ T cell chemoattractants such as CXCL10 on the site of inflammation [22]. Furthermore, IFN-γ secreted by activated Th1 cells promotes the expression of MHC class I molecules as well as molecules associated with antigen processing (e.g. TAP) on antigen presenting cells, modulating them indirectly to more effectively prime cytotoxic T cells [78]. Furthermore, Th1 lymphocytes provide help to $CD8^+$ T cells by activating of antigen presenting cells (APC) due to interaction of CD40 ligand and CD40 molecule, in consequence elevating the functional capacity of APCs to confer $CD8^+$ T cell priming. Apart from stimulating $CD8^+$ T cell proliferation and effector function, $CD4^+$ T cells play a pivotal role in generating memory cytotoxic $CD8^+$ T cells. Several lines of evidence suggest that CD27-CD70 receptor/ligand engagement is important in $CD8^+$ T cell memory formation. CD70 is induced on dendritic cells upon CD40-activation and inflammatory stimuli, whereas CD27 is expressed on cytotoxic T cells. CD27 mediated signal on cytotoxic T cells not only engages their expansion in a primary immune response but also allows secondary expansion of CTLs due to avoidance of activation induced cells death by re-encounter with the cognate antigen [71].

T helper 2 cells (Th2), develop in the presence of interleukin 4 (IL-4) and interleukin 2 (IL-2) and later on secrete IL-4 and interleukin 10 (IL-10) as their signature cytokines [215]. Th2 cells are essential for the activation of mature B cells after epitope recognition. Th2 cells mediate host defense against extracellular pathogens, e.g. parasites by induction of antibody secretion of mature B cells. IL-4 secreted by Th2 cells is the major accelerator for a IgE-isotype switch in B cells [227].

Th17 cells expressing a γδ T cell receptor are, contrasting $CD8^+$ T cells and $CD4^+$ T cells expressing an αβ-TCR, are fare less characterized. Tumor growth factor β (TGF-β) as well as inerleukin 6 (IL-6), interleukin 21 (IL-21) in the microenvironment favor the differentiation of Th17 cells, mainly secreting IL-17 upon full maturation [132]. Th17 cells produce pro-inflammatory cytokines such as IL-17, IL-21 and IL-22, their differentiation being initiated by the presence of tumor growth factor β (TGF-β) and IL-6 plus IL-21 [36]. The function of this T cell subtype is not fully elucidated, even though IL-17 receptor signaling is described to be important in the defense of extracellular bacteria and fungi [279]. Increased numbers of γδ T cells in patients´ peripheral blood can be correlated with bacterial and viral infections, the exact function of γδ T

cells in generating an immune response still under investigation [36].

Regulatory T cells (Tregs) are defined as $Foxp3^+$, $CD25^+$ and $CD127^-$ cell population [74]. Tregs can be divided into two subpopulations, natural Tregs and inducible Tregs (iTregs), respectively. Whereas natural Tregs develop in the thymus [266], inducible Tregs differentiate in the periphery upon antigen encounter [139]. Tregs display a great repertoire of immune suppressive effector functions upon antigen recognition via their T cell receptor. Treg effector mechanisms can be suppressive either via direct cell-cell contact, via depleting soluble factors such as IL-2 or via secretion of cytokines associated with suppressive mechanisms, such as IL-10. Regulatory T cells have been shown to express granzyme B and perforin, important for Treg mediated suppression through killing of anti-tumor immune cells present in the tumor microenvironment [31]. Soluble IL-2 is essential for the development and survival of $CD4^+$ T effector cells by binding to the IL-2 receptor. Regulatory T cells over express the α-subunit of the IL-2 receptor (CD25) thereby having an increased affinity for IL-2. In consequence, IL-2 is deprived from binding to T effector cells subsequently leading to cytokine deprivation mediated apoptosis in $CD4^+$ T effector cells [187]. Furthermore, inhibitory cytokines such as tumor growth factor β (TGF-β), interleukin 35 (IL-35) and interleukin 10 (IL-10) suppress T effector cell functions. Soluble IL-10 suppresses T cell proliferation both in Th1 and Th2 cells. TGF-β is suggested to play a role in the generation of Tregs from $CD4^+$ $CD25^-$ precursor T cells by triggering Foxp3 expression in naive $CD4^+$ T cells [80]. Similar to TGF-β, interleukin 35 (IL-35) facilitates the conversion of conventional $CD4^+$ T cells into regulatory T cells (iT(R)35 cells) [43] secreting the IL-35 which exerts a suppressive effect on T cell proliferation [44]. Another important suppressive mechanism of Tregs is the generation of immunosuppressive adenosine [67]. There are several ways of adenosine generation, firstly it can be generated extracellular from ATP and ADP catalyzed by the enzymes CD39 and CD73, secondly adenosine can be generated from intracellular ATP, ADP and AMP via cytoplasmic 5´-nucleotidases. Expression of CD39 and CD73 could be confirmed in human Tregs [3, 4, 246]. Immunosuppressive functions of adenosine are mediated by reduction of pro-inflammatory cytokine secreting (e.g. IFN-γ, IL-12, TNF-α) [99, 137] due to binding of adenosine to the adenosine receptor expressed on antigen presenting cells and Th cell subpopulations. By the constitutive expression of cytotoxic T lymphocyte antigen-4 (CTLA-4), regulatory T cells can bind co-stimulatory molecules such as CD80/86 expressed on antigen-presenting cells, thereby reducing co-stimulatory activity of APCs and subsequently priming of T effector cells, respectively [219].

Activation of T cells requires the binding of their T cell receptor (TCR) and its cognate epitope presented on the respective MHC-restriction element, which will be discussed in more detail in the next paragraph.

3.4.3 The major histocompatibility complex (MHC)

The MHC class I molecule is a heterodimer, expressed by all nucleated cells and is composed out of α-chain with three domains: (α_1 - α_3) and the β_2-micorglobulin non-covalently associated with the α-chains (fig. 3). Up to 800 MHC class I alleles are know in humans [211], encoded by the heavy chain major histocompatibility genes HLA-A, HLA-B, HLA-C, on chromosome 6. The β_2-micorglobulin is encoded in a different locus on chromosome 15. The antigenic binding site of the MHC-I molecule is composed of the α_1- and α_2- domain and preferentially binds peptides with a length of 8-10 amino acids, which are bound in the closed binding cleft of the MHC class I molecule by specific anchor residues such as a Leu at position 2 and Val or Leu at position 9 [52].

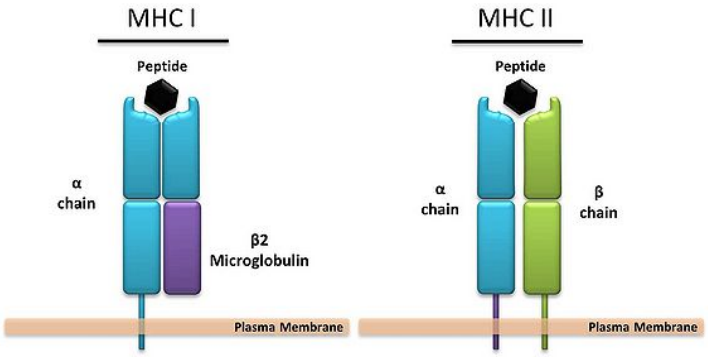

Figure 3: Structure of the MHC-I and MHC-II molecule. The MHC-I molecule is composed of three domains (α_1 - α_3), whereby the α_3-domain anchors the MHC-I molecule to the plasma membrane. Furthermore, the β_2-micorglobulin is non-covalently associated with the α-chains. The MHC-II molecule is composed of one α-chain (subunits α_1 and α_2) one β-chain (subunits β_1 and β_2), both chains anchored to the plasma membrane. (picture taken from: http://www.syncytiabeta.org/~syncyt5/syncytiabeta/index.php?title=Major_Histocompatibility_Complex)

As shown in figure 3, MHC class II molecules are structurally distinct from MHC class I molecules. Three major groups of MHC class II molecules are know in humans, HLA-DR, HLA-DP and HLA-DQ also encoded on chromosome 6. In contrast to MHC class I expression, MHC class II molecules are only expressed on professional antigen presenting cells, such as dendritic cells, macrophages and B lymphocytes. The MHC class II molecule is a heterodimer composed of one α-chain (subunits α_1 and α_2) and one β-chain (subunits β_1 and β_2), while the open peptide binding cleft is composed by the α_1 and β_1 subunits. The morphology of the MHC class II open peptide binding cleft allows binding a peptides with a length of 12-20 amino acids due to the fact that residual parts of the antigen can loosely hang over either side of the peptide binding groove [252].

3.4.4 Antigen-processing and epitope recognition

MHC-class I restricted peptides are derived of endogenous origin and processed via the proteasomal pathway [223]. The 26S proteasome is composed of a 20S subunit harboring the protease activity

and two 19S caps, releasing cleaved precursor peptides proteins into the cytoplasm of the cells [171]. Precursor peptides are transported via the transporter associated with antigen processing (TAP) in the endoplasmatic reticulum [165]. Newly synthesized α_1 domains of the MHC-I molecule are bound to the chaperon calnexin thus hampering MHC-I α_1 domains to leave the endoplasmatic reticulum. Upon binding of β_2-micorglobulin, the MHC-I α_1 domains are released from calnexin building the peptide loading complex including the chaperon calreticulin, tapasin and the ER-associated amino-peptidase 1/2 (ERAAP) . Peptides longer than 10 amino acids are trimmed by the ERAAP before loading on the MHC class I molecule, the process being stabilized by tapasin, calreticulin and ERp57, forming the peptide loading complex (PLC). Upon successful peptide loading, the MHC class I- peptide complex is released from the PLC and transported in vesicles derived from the golgi apparatus to the cell surface where it can be recognized by $CD8^+$ T cells.

Even though peptides presented on MHC class I molecules are generally derive form proteins of endogenous origin, dendritic cells are described to be capable of cross presenting peptides [213]. The process of cross presentation describes the presentation of exogenous peptides on MHC class I molecules. It is believed, that dendritic cells are capable of cross presenting peptides due to an adaption of their endocytic and phagocytic pathways [118].

Peptides presented on MHC class II molecules most commonly are derived from exogenous antigens processed in intracellular vesicles such as lysosomes. MHC class II α- and β-chain assemble in the endoplasmatic reticulum associated with an invariant chain (Ii) to prevent peptide binding. Packed into vesicles, the MHC class II-invariant chain complex is transported in the cytoplasm where it fuses with lysosomes to form the MHC class II-loading compartments (MIICs). In the MIICs, the invariant chain is cleaved into CLIP (class II-associated Ii peptide) due to low pH in the lysosome and eventually being exchanged for an antigenic peptide of exogenous origin, with the help of the dedicated chaperon HLA-DM. Peptide loaded MHC class II molecules are transported in vesicles to the cell membrane where peptides bound to MHC class II are recognized by $CD4^+$ T cells [171].

3.4.5 The T cell receptor: Structure and signaling

$CD8^+$ T cells and $CD4^+$ T cells express a T cell receptor (TCR) on their cells surface. The majority of T cells (95%) express a heterodimic TCR, composed of one α-chain and one β-chain, whereby every chain harbors a variable region and a constant region. As shown in figure 4, the variable region is responsible for epitope recognition thus determining epitope-specificity of the TCR, whereas the constant region anchors the TCR to the cell membrane and is associated with TCR-signaling. A rather small group of T cells express a TCR composed of a γ-chain and a δ-chain instead of the α β-TCR.

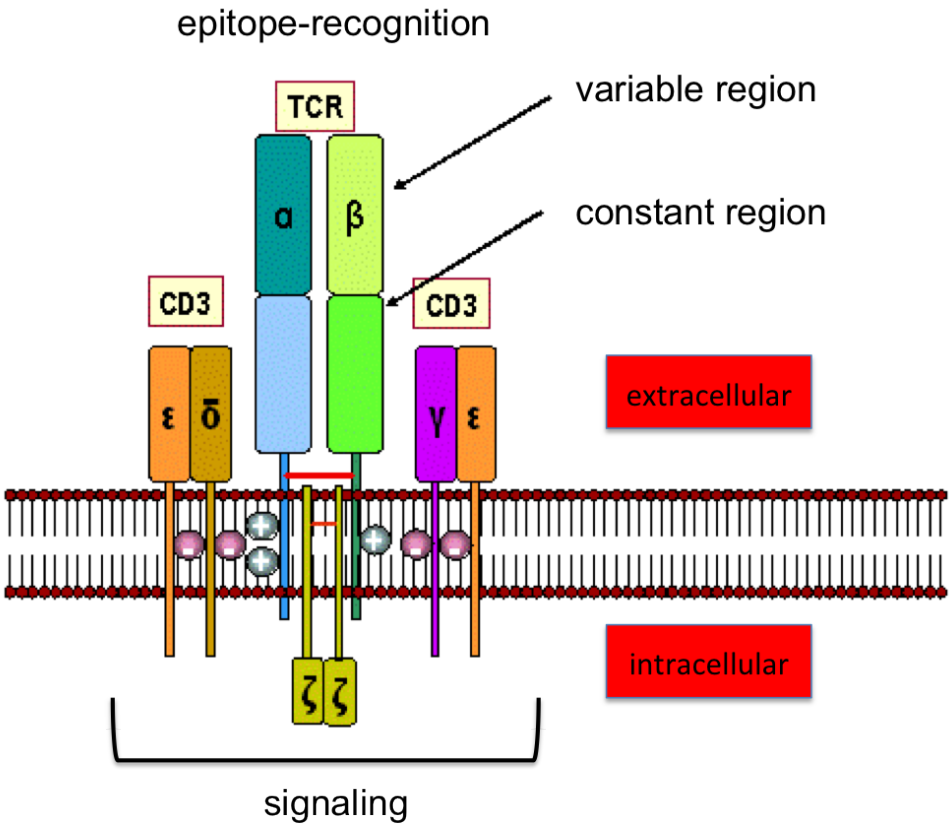

Figure 4: Structure of the T cell receptor. The TCR is composed of one α-chain and one β-chain, whereby the variable domains of the α-chain and β-chain form the TCR-epitope-recognition site. Two CD3 co-receptors are associated with the TCR, harboring ITAM motifs on their intracellular domains, which are phosphorylated during TCR-signaling. Additional ITAM motifs are located within the two intracellular ζ-chains, associated with the TCR, mediating the transition of a TCR-dependent signaling into the cytoplasm of the cell by changing their phosphorylation status. *(modified from epidemiologiamolecular.com)*

Each TCR is associated with two CD3 transmembrane molecule containing immunoreceptor tyrosine-based activation motifs (ITAM) important for TCR-transmitted signaling (fig. 4). Moreover, two ζ-chains are associated with the TCR, harboring six intracellular ITAM motifs, important for TCR-signaling. CD4 and CD8 transmembrane molecules function as co-receptors for the binding of MHC-peptide complexes being the first signal in T cell activation. Only T cells, which also receive a co-stimulatory signal by engagement of their CD28 molecule, pairing with CD80/CD86 on antigen presenting cells, are activated and exhibit TCR-mediated signaling. In the case of absent co-stimulatory signal, the T cell will become anergic and eventually go into apoptosis. A cascade of downstream signaling is activated upon TCR-MHC-peptide complex and CD28-CD80/86 ligation. Antigen recognition initiates receptor clustering and activation of the tyrosine kinase Lak wich is associated with the cytoplasmic domain of the co-receptors CD4/CD8, and the kinase Fyn which is associated with the CD3 molecule. Usually, kinases Lak and Fyn are inhibited in resting cells due to phosphate bound to inhibitory tyrosine residues which are removed by the leukocyte common antigen CD45 upon antigen encounter. Activated Lak and

Fyn kinases phosphorylates the ITAMs in the receptors cytoplasmic tails, thereby recruiting the ζ-chain-associated protein (ZAP-70) which is phosphorylated by Lck. The substrate phosphorylated by activated ZAP-70 is the linker of activation in T cells (LAT) and a second linker protein (SLP-76) in T cells. Transmission of the TCR-mediated signaling from the cell membrane into the cell requires proteins that either bind to phosphotyrosine residues or function as targets for protein tyrosine kinases. The enzyme PLC-γ is phosphorylated at the plasma membrane by Tec kinases which themselves where phosphorylated due to close proximity to the activated TCR upon binding to adaptor proteins such as LAT, SLP-76. PLC-γ initiates two of the major downstream signaling pathways in TCR-signaling by cleavage of phosphatidylinositol bisphosphate (PIP2) into diacylglycerol (DAG) and inositol trisphosphate (IP3). DAG activates the protein kinase C which resulting in activation of the transcription factor NF-$_{\kappa}$B whereas IP3 increases the intracellular $Ca2^{+}$ concentration by stimulation of calcium release in the endoplasmatic reticulum, thus activating the calcium-dependent phosphatase calcineurin which activates nuclear factor of activated T cells (NFAT).

The third major signaling pathway in T cell activation is the MAP kinase pathway, which is activated due to the recruitment and activation of the G-protein RAS by binding to phosphorylated tyrosine residues at the cell membrane. Downstream signaling of MAP kinase pathway leads to the induction of transcription factor AP-1. Genes transcribed by the activated transcription factors NFkB, NFAT and AP-1 are genes associated with T cell proliferation and differentiation e.g IL-2 and IFN-γ [89]. Moreover, TCR engagement increases the expression of co-stimulatory molecules on the T cells surface, one examples being the CD40L [115] leading to enhanced T cell proliferation by interaction the CD40L and the CD40 molecule expressed on dendritic cells [159].

3.4.6 Tumor antigens as targets for the adaptive immune system

One major obstacle in the recognition of cancer cells by the adaptive immune system is self-tolerance due to autologous origin of cancer tissue. Nevertheless, a number of MHC-restricted immunogenic epitopes derived of tumor antigens are presented on MHC molecules on malignant cell, therefore allowing recognition of malignant cells by the adaptive immune system. Tumor antigens can be classified into two major groups: Tumor- associated antigens (TAA) and tumor-specific antigens (TSA).

Tumor specific antigens are solely expressed in malignant cells being completely absent in any healthy tissue, examples being: Mutated antigens, viral antigens and oncofetal antigens.

Mutated tumor antigens are highly immunogenic since they are exclusively expressed in the given tumor entity such as the breast cancer antigen 1/2 (BRCA 1/2) in mammary carcinomas [125]. Moreover, commonly mutated in human cancers are the tumor suppressor gene p53 [103]

and the pro-oncogen Ras [21], thus being possible targets for tumor-immunotherapy approaches. Mutated tumor antigens can arise from germline mutations (e.g. BRCA 1/2) or might be acquired spontaneously during life time (e.g. p53 mutations) resulting in cancer initiation and development.

Oncoviral antigens are encoded by oncogenic viruses examples being the human papilloma virus (HPV) causing cervical carcinoma. The most common HPV-tumor derived antigens are the HPV oncogenes E6 and E7 which are used as targets in tumor immunotherapy approaches [37][198].

Oncofetal antigens are typically expressed in fetal tissue but are not expressed in healthy adult tissue. Nevertheless, expression of oncofetal antigens can be found in malignant adult tissue. An example of oncofetal antigens being the alpha-fetoprotein (afp) receptor (receive) which is usually expressed in undifferentiated cells of either fetal or tumor origin [167]. Expression of the alpha-fetoprotein receptor was found in early stage breast cancer but not in healthy individuals [167] .

Tumor associated antigens are expressed in healthy tissue as well as in malignant tissue, therefore called "shared tumor antigens". Examples being differentiation antigens, overexpressed antigens and cancer-testis antigens.

Differentiation antigens are largely expressed by a single cancer type, examples being gp100 and MART-1 mainly expressed in malignant melanoma [156] and NY-BR-1 being expressed in breast cancer [248]. Nevertheless, differentiation antigens are not only expressed in the given malignancy but also in the healthy tissue the tumor evolved off a fact to keep in mind when design anti-tumor immunotherapies.

Overexpressed antigens are characterized by expression in both normal and malignant tissue whereby levels of expression are highly elevated in the cancerogenic tissue compared to normal tissue. Elevated expression of the human epidermal growth factor 2 (HER2) is found in 30% of all breast cancers [236] being one example for over expressed antigens.

Cancer-Testis antigens are exclusively expressed by cancer cells and adult reproductive tissues, such as testis and placenta. The cancer testis antigen NY-ESO is expressed in malignant melanomas and proven to be immunogenic in clinical trials of autologous $CD4^+$ T cell transfer [108].

3.5 Immunotherapy approaches against breast cancer

Apart from targeted therapies, such as antibody based therapy (refer to part 3.3.4), vaccination strategies are also applied for the treatment of breast cancer. Two principles of anti-cancer vaccines have to be distinguished: Passive vaccination strategies and active vaccination strategies.

3.5.1 Passive vaccination strategies

Passive tumor-immunotherapy relies on the direct anti-tumor effect of the vaccination components. One example for passive immunotherapy approaches in beast cancer are T-cell receptor mimics (TCRm), monoclonal antibodies targeting the the HER2 derived E75 protein [114]. TCRm are monoclonal antibodies with a TCR-like binding domain, recognize HLA-restricted peptides through the TCR engagement leading to antibody dependent cellular cytotoxicity (ADCC) in human cell lines [273].

E75 is a 9mer epitope derived from the extracellular domain of the HER2 protein [163]. TCRm specific for E75, recognize their cognate MHC-I-restricted peptide in all tested HER2$^+$ breast cancer cell lines *in vitro*. Reduction in cell viability was observed possibly due to enhanced apoptosis since a significant increase of caspase 3 activation was found in the cancer cell lines treated with the TCRm [114]. HER2 E75 specific TCRm proved to induce apoptosis in all HER2$^+$ cell lines whereby trastuzumab only lead to increased cell death in HER2$^+$ high expressing cell lines [114], thus TCRm against HER2 seem to be potentially effective in breast tumors with low HER2 surface expression.

Genetically engineered T cells expressing a chimeric antigen receptor (CAR) represent another example of passive immunotherapy approaches. Artificial chimeric T cell receptors (CARs) combine specificity of a monoclonal antibody with T cell signaling properties hence being MHC-independent. Generally, a single chain antibody is coupled to a single lymphocyte activation domain. First generation CARs transmitted T cell activation signals via ITAM-bearing signaling chains like CD3ζ whereas second generation CARs include a CD28 domain to achieve better activation of engrafted T cells. Superior effector functions were observed in third generation CARs which include a second co-stimulatory molecule domain such as CD134 or CD137 [34]. First *in vitro* studies with dual engineered T cell expressing individual chimeric antigen receptors for both ERBB2 and MUC1, whereby ERBB2 is associated with a CD3ζ signaling domain providing cytotoxic functions and IFNγ-production and the antigen MUC1 is associated with a CD28 signaling domain, resulted in increased cell proliferation upon MUC1 antigen engagement. Dual-targeted T cells were found to efficiently kill ERB2$^+$ target cell and to proliferate upon ERBB2 and MUC1 antigen encounter [272]. This study indicates the use of dual-targeted T cells, expressing chimeric antigen receptors as a possible approach to treat ERBB2$^+$, MUC1$^+$ breast cancers *in vivo*.

TCR transduced T cells which express a high affinity T cell receptors, are another approach of passive immunotherapy. The T cell receptor recognizing the HLA-A2-restricted T-cell receptor γ-chain alternate reading-frame protein (TARP)4-13, was cloned into peripheral blood T cells using a lentiviral vector. TARP protein is expressed in normal prostate epithelium but also in adenocarcinomas of the prostate and breast. HLA-A2$^+$ breast cancer cell line MCF-7 which was transduced with a lentiviral vector encoding TARP, were specifically recognized by TARP-specific

TCR transduced T cells *in vitro* [102].

A crucial criterium in therapeutic TCR design is the proper pairing of TCR α-chain and TCR β-chains, to reduce mispairing events, such as dimerization of novel TCR chains with endogenous TCR α-chain and TCR β-chain of the target cell. Addition of exogenous disulfide bonds in the constant domain reduce mispairing events [41].

3.5.2 Active vaccination strategies

Peptide cancer vaccines stimulate the patients own immune response due to the delivery of antigenic peptides of a given tumor entity. One example of a therapeutic peptide cancer vaccine is the HER2-specific peptide vaccine for the treatment of $HER2^+$ breast cancers. Peptides included in this vaccine are 15-18 amino acids long, derived from the extracellular domain (ECD) or intracellular domain (ICD) of the HER2 protein [55]. Patients with stage III or IV breast cancer developed immunity against HER2 derived peptides after receiving the HER2 directed peptide vaccine [56]. One year after receiving the HER2 peptide vaccine, immunity to the HER2 protein was still detectable in 38% of the vaccinated patients [56]. An independent clinical trial investigated the immunogenicity of the HER2 derived peptide E75 in patients with disease-free, node-positive breast cancers. The peptide E75 is a 9 mer HLA-A2-restricted epitope of the extracellular domain of HER2-receptor [164], which is mixed with granulocyte-macrophage colony-stimulating factor prior to vaccination of patients. Overall, the E75 peptide vaccination was reported to elicit a peptide-specific immune response thus reducing the recurrence rate in disease-free patients with $HER2^+$, lymph $node^+$ breast cancer [192]. In a cancer peptide vaccine trial, immunogenicity of the HER2 derived epitopes E75 and GP2 was compared in PBMCs obtained from breast cancer patients. In contrast to E75 being a peptide derived from the extracellular domain of HER2, GP2 is a 9 mer, HLA-A2- restricted epitope derived from the transmembrane domain of HER2 [164]. Immunogenicity of the GP2-peptide/ E75-peptide was evaluated *in vitro*, by stimulation of pre-vaccination, peripheral blood samples (PBMCs) from HLA-$A2^+$ breast cancer patients with autologous GP2-peptide pulsed/E75-peptide pulsed dendritic cells and subsequent analysis of GP2-specific/E75-specific lytic capacity of $CD8^+$ T cells. GP2 stimulated $CD8^+$ T effector cells lysed 44.2 % of $HER2^+$ target cells versus lysis of 43.8% of $HER2^+$ target cells in case of E57 stimulated $CD8^+$ T cells. Overall, immunogenicitiy of the peptide GP2 was proven to be comparable with the immunogenicity of the E57 epitope, thus GP2 vaccine should additionally be considered for the treatment of $HER2^+$ breast cancer patients [163]. A second tumor antigen investigated for potential use in anti-tumor peptide vaccines is the transmembrane glycoprotein MUC1, expressed on glandular epithelium and over-expressed as well as hypo-glycosylated in adenocarcinomas [237]. Vaccination of sixteen metastatic breast cancer patients with a sixteen amino acid long MUC1 peptide conjugated to the carrier protein keyhole limpet hemocyanin (KLA) plus a

DTOX adjuvant lead to induction of detectable amounts of class-I-restricted CTLs against MUC1 in the peripheral blood of these patients. Activity of the MUC1-specific CTLs was confirmed on MHC-I positive adenocarcinoma target cell lines for seven out of eleven vaccinated metastatic breast cancer patients [206].

cDNA based anti-tumor vaccines for example directed against mammaglobin-A (Mam-A), an antigen commonly expressed in human breast cancer [267],were recently investigated in a phase I clinical trial. Breast cancer patients with stage-IV metastatic breast cancer showed an increase of mammaglobin-A specific, $CD4^+$ICOS(hi) activated T cells which efficiently lyse Mam-A^+ target cells *in vitro* concluding that anti-Mam-A cDNA based vaccination induces anti-tumor immunity in breast cancer patients [249]. A pilot clinical trial in patients with metastatic breast cancer, vaccinated with a plasmid DNA encoding HER2 in combination with low dose granulocyte macrophage colony-stimulating factor (GM-CSF) and interleukin 2 (IL-2) induced $CD4^+$ T cell responses agains HER2 and elevated anti-HER2 antibody production in patients receiving the vaccination [178].

Vaccination *viral vectors* is another approach in breast cancer immunotherapy. One breast cancer antigen used in this approach is mucin 1, an oncogene commonly expressed in breast cancers [46]. A new approach of anti-MUC1 immunotherapy currently investigated in a phase I clinical trial is based on a recombinant vaccinia ankara virus based vector encoding MUC1 epitopes and interleukin-2 (IL-2). The vaccinia virus belongs to the group of the poxvirus family, whereby the modified vaccinia virus Ankara shows a deficiency to grow in human cells [244],thus being suitable and safe for tumor immunotherapy approaches. Breast cancer patients with advanced metastatic tumors positive for MUC1, were treated with the viral vector encoding MUC1 epitopes and showed a transient disease stabilization in four out of 13 enrolled patients [212]. Further clinical studies are mandatory to certify anti-tumor efficacy of the vaccinia MUC-1-vaccine.

Dendritic cell based vaccines are successfully used in breast cancer therapy. Autologous dendritic cells are pulsed with HER2-specific, MHC class II restricted epitopes, if the patient is HLA-$A2^+$, dendritic cells were additionally pulsed with two HLA-A2-restricted HER2 epitopes. To induce a pro inflammatory phenotype in HER2-peptide pulsed DCs, the cells were activated *in vitro* with IFN-γ and lipopolysaccharide prior to being re-infused in patients with early $HER2^+$ ductal in situ carcinoma (DCIS) or $HER2^+$ DCIS with microinvasion. The vaccine was reported due induce elevated levels of HER2-specific $CD8^+$ T cells as well as HER2-specific $CD4^+$ T cells in the peripheral blood of vaccinated patients when compared to healthy donors. Furthermore, the HER2-dendritic cell based vaccine led to post vaccination increase in lymphocytic infiltration in the sites of residual DCIS. Most importantly, T cell responses were detectable up to 52 month post-immunization in the peripheral blood of vaccinated breast cancer patients, suggesting clinical value of the DC-based vaccine in the treatment of $HER2^+$ DCIS [133].

The therapeutic effect of a dendritic cell based vaccine specific for the tumor antigen MUC1 was investigated in patients with advanced or metastatic breast cancer. Autologous dendritic cells were loaded with MUC1 antigens or autologous tumor lysate before being re-infused in the patients. Clinical response regarding reduction in tumor size and disappearance of malignant pleural effusion was seen in 7 out of 9 breast cancer patients [131], thus MUC1 derived dendritic cell vaccine can be considered for immunotherapy of breast cancer. Currently investigated in a murine breast cancer tumor mode, efficacy of DC based MUC1-specific tumor vaccines might be increased by fusing recombinant MUC1 protein to a protein transduction domain, e.g. Tat peptide, derived from human immunodeficiency virus (HIV) [26] leading to increased MUC1 antigen uptake by dendritic cells *in vivo*. In a murine MUC1 tumor model, Tat-conjugated MUC1-specific DNA vaccination induced delayed tumor growth more efficiently than unconjugated MUC1 [276].

3.5.3 Adoptive cellular therapy with TILs

The transfer of natural occurring autologous immune cell populations, such as tumor infiltrating lymphocytes, which have been expanded *ex vivo,* is called adoptive cell transfer (ACT). Apart from tumor infiltrating lymphocytes, genetically engineered T cells discussed in part 3.5.1 can also be used for adaptive cellular therapy, whereby the following paragraph will be emphasizing the use of TILs in adoptive cellular therapy.

Many tumors show infiltration of lymphocytes, nevertheless, the tumor persists despite of the presence of anti-tumor targeted lymphocytes. Current opinion is that the tumor infiltrating lymphocytes (TILs) experience immune suppression in the tumor microenvironment due to binding of programmed cell death protein ligand 1 (PDL1) [2] and immunosuppressive cell populations such as myeloid derived suppressor cells, M2 macrophages and Tregs. In preparation for ACT, TILs are recovered from a patients tumor specimen such that they are removed from the immunosuppressive environment and can be expanded *in vitro* in the presence of interleukin 2 (IL-2). Patients usually receive a preparative lymphodepletion using chemotherapy or total-body irradiation before *ex vivo* expanded TILs are re-infused in the patient [208].

In a clinical phase I study, patients with metastatic breast cancer were treated with *ex vivo* expanded tumor-reactive T cells recovered from the bone marrow. Obtained T cells were *in vitro* reactivated with autologous dendritic cells loaded with lysates of MCF-7 breast cancer cells as source of tumor antigen. In seven out of 16 patients (44%), tumor-reactive memory T cells in the peripheral blood were induced after adoptive cell transfer. Patients with an immunological response to the adoptive cell transfer showed in increased median survival of 58.6 month compared to non-responders with a median survival of 13.6 month [58].

On crucial point to consider when applying adaptive cellular therapy is the activation status of transferred autologous cells, such as tumor specific autologous T cells, since the differentiation

state of adoptively transferred T cells is crucial to the success of ACT based treatments. One option might be the use of minimally cultured tumor-infiltrating lymphocytes named "young" TILs [61]. Whereas standard TIL protocols require a complex procedure of many micro-cultures, "young" TILs cultures consist of bulk lymphocytes rather than micro-cultures. "Young" TILs are recovered from the entire resected tumor and minimally expanded *in vitro*, typically about 10-18 days, without any *in vitro* testing for tumor recognition. Compared to standard TILs, "young" TILs have features associated with persistence *in vivo*, such as expression of high levels of co-stimulatory molecules and long telomeres [250]. In patients with metastatic melanoma, $CD8^+$ enriched young TILs mediated an objective tumor regression [61].

3.5.4 Targeting of immune checkpoints

Under physiological conditions, inhibitory pathways (also referred to as "immune checkpoints") such as the CTLA-4 and the PD1 associated pathways, are crucial for the maintenance of self-tolerance. Tumors can disregulate the expression of immune checkpoint proteins by manipulating endogenous anti-tumor immunity.

The cytotoxic T-lymphocyte-associated antigen 4 (CTLA-4) is expressed on activated $CD8^+$ T cells and $CD4^+$ T cells but important to note, also on regulatory T cells (Tregs). CTLA-4 shares identical ligands with the co-stimulatory molecule CD28, the ligands being CD80 and CD86 [76, 256]. Both, CD28 and CTLA-4 are transmembrane protein members of the immunoglobulin gene superfamily whereby CD28 is highly expressed on resting T cells contrasting rather low CTLA-4 surface expression in naive T cells [113]. Low surface expression of the CTLA-4 molecule can be explained by rapid internalization of the CTLA-4 molecule due to interaction of CTLA-4 with the clathrin-associated protein AP50, directing CTLA-4 to clathrin-coated vesicles [39] and allowing endocytosis of the CTLA-4 molecule. CTLA-4 surface expression is upregulated in activated T cells and the CTLA-4 molecule is found to localize in proximity to the TCRs [145]. CTLA-4 engagement dampens the activity of T cells by either competitive binding of the co-stimulatory molecules CD80/86 or by actively delivering inhibitory signals to the T cells such as dephosphorylation of the TCR ζ-chain by a CTLA-4 associated tyrosine phosphatase, therefore abolishing the Lck inducible TCR-signling [140]. Moreover, CTLA-4 is a target gene of the forkhead transcription factor FOXP3 [104, 74] therefore being constitutively expressed in Tregs. The exact mechanism of CTLA-4 mediated enhancement of immunosuppressive functions in Tregs is still unknown. The fully humanized antibodies ipilimumab and tremelimumab are CTLA-4 agonists, their efficacy already being investigated in clinical trials. In a phase 1 clinical study, 26 patients with advanced, hormone-responsive breast cancer were treated with tremelimumab in combination with the aromatase inhibitor exemestane. The treatment was well tolerated and induced increased expression of the inducible costimulator (ICOS) in peripheral $CD4^+$ and $CD8^+$

T cell and an increase in the ratio of ICOS+ T cells to FOXP3+ regulatory T cells [260].

A second immune checkpoint addressed in cancer immunotherapy is the programmed death-1 (PD1) pathway. One function of the PD1 cell surface molecule mediated signaling is to attenuate T cell activation in peripheral tissues by engagement of programmed death-1 ligand (PDL-1) expressed e.g. on tumor cells and PD1 expressed on tumor specific T cells [20]. Engagement of PDL-1 of PD1 results in the inhibition of TCR signaling due to colocalization of PD1 and CD3ζ-chain and subsequent inhibition of TCR-mediated phosphorylation of ZAP70 by the recruitment of SHP-2 (Src homology 2 domain-containing tyrosine phosphatase 2) which induces the dephosphorylation of the proximal TCR signaling molecules [281]. Efficacy of an anti-PDL1 antibody was also investigated in a multicenter phase 1 study. A total of 207 patients with advanced cancer of different entities such as breast cancer (4), non-small-cell lung cancer (75), melanoma (55), colorectal cancer (18), renal-cell cancer (17), ovarian cancer (17), pancreatic cancer (14) and gastric cancer (7). Induced durable tumor regression was observed in 9/25 melanoma patients, 2/17 renal-cell cancer patients, 5/49 non-small-cell lung cancer patients and 1/17 ovarian cancer patients [23].

Currently, at least three active clinical trials are running, evaluating immune checkpoint modulation in breast cancer. Ipilimumab is tested in combination with or without cryoablation in early-stage breast cancer scheduled for mastectomy (clinical trial identification: NCT01502592). Furthermore, anti-PD-L1 monoclonal antibodies are investigated in two clinical trials in a variety of advanced and recurrent solid tumors, including breast cancer (NCT00729664 and NCT01375842).

3.6 The breast cancer associated antigen NY-BR-1

Serological analysis of recombinant tumor cDNA, expression libraries (SEREX), originating from a metastasis of a 60 year old female patient with metastatic ductal carcinoma of the breast, identified the antigen (TAA) NY-BR-1 as a breast cancer-associated tumor antigen [111]. Sequence analysis of NY-BR-1 cDNA, mapped a NY-BR-1 sequence of 4125 base pairs with a continuous open reading frame (ORF) on chromosome 10p11-12 (37 exons).

NY-BR-1 mRNA expression is restricted to the mammary gland (strong expression), testis (strong expression) and placenta (faint expression) [111] but is found to be strongly over expressed in 84% of tested breast tumors. A homologous gene, NY-BR-1.1 was identified on chromosome 9 and is described to display 54% DNA-sequence homology to the NY-BR1 antigen. NY-BR-1.1 mRNA is described to be weakly expressed in breast tissue, testis and brain but so far no expression of the NY-BR-1.1 protein has been described in brain tissue. Analysis of NY-BR-1 and NY-BR-1.1 mRNA expression in breast cancer tumors revealed some tumors to express either antigen exclusively, whereas the majority of tested breast cancer tumors express mRNA for both antigens [111].

The protein sequence for NY-BR-1 (1341aa) includes a predicted DNA-binding site, a bispecific nuclear localization signal, five ankyrin repeats (a unique motif which mediates protein-protein interactions [141]) and a leucin zipper motif. Presence of a nuclear localization signal indicates a preferred nuclear accumulation of the NY-BR-1 protein [111]. In contrast to this finding, NY-BR-1 protein is also described to co-localize with the plasma membrane, implying a possible function as a trans-membrane protein and being attractive for antibody based therapies [225].This finding is supported by the identification of two cis-acting cell membrane targeting domains in the NY-BR-1 amino acid sequence. Ambivalent NY-BR-1 protein localization is confirmed by the findings of *Varga et. al* who describe a nuclear as well as a cytoplasmatic localization of the NY-BR-1 protein [257].

Among normal tissue, NY-BR-1 protein is solely expressed in the ductal epithelium of the breast but strongly over expressed in breast cancer tumors whereas all other normal tissues are found to be negative for NY-B-1 protein expression. Moreover, NY-BR-1 protein expression can not be confirmed in any other carcinomas apart from breast cancer [257]. In fact, 100% of all noninvasive carcinoma lesions, ductal carcinomas *in situ* and lobular neoplasia were described to be NY-BR-1 positive. Moreover, 63.5 % of all invasive breast cancer tumor lesions are NY-BR-1 positive including 80.7 % of combined ductal carcinoma in situ (DCIS) and lobular carcinoma *in situ* (LCIS) [248]. NY-BR-1 protein expression can be found in 77% of grade 1 primary breast carcinomas, in 63% of grade 2 primary breast carcinomas, and in 50% of grade 3 primary breast carcinomas, thus NY-BR-1 protein expression negatively correlates with tumor progression [257]. NY-BR-1 protein expression was found in all samples of ductal carcinoma *in situ* and lobular neoplasia, adjacent to invasive breast carcinoma, immunohistochemically stained for NY-BR-1 protein expression. In invasive carcinoma lesions, NY-BR-1 protein was expressed in 60% of investigated tumors whereby 60% being invasive ductal carcinoma and 59% subtypes of other invasive carcinomas (papillary, tubular, lobular, and mucinous) [257]. Moreover, concordance of NY-BR-1 protein expression in the primary tumor and its metastasis is 88% in grade 2 breast tumors and 91% in grade 3 breast carcinomas [257]. Progression in breast carcinoma grading (grade 1 to grade 3) directly correlates with heterogeneity of NY-BR-1 protein expression[257]. Two splice variants of the NY-BR-1 protein, one shorter variant lacking the 5´-prime sequence compared to the longer splice variant, are described. Equal immunohistochemical staining intensity for both splice variants was observed in primary spermatocytes and in the testis. On the contrary, only weak expression of the shorter splice variant was described in normal breast tissue and invasive breast cancer cells contrasting a very strong expression of the longer splice variant in these tissues [247].

A strong correlation of estrogen receptor (ER) expression and NY-BR-1 expression was described in 66% of tested NY-BR-1 positive tumors [257]. Estrogen-response element (ERE)-like sequences located in proximity to the NY-BR-1 promotor region could be identified, suggesting a

ERα depended regulation of NY-BR-1 protein expression. Studies obtained from patients receiving tamoxifen for treatment of ERα positive breast carcinomas reveal a sustained decrease in NY-BR-1 protein expression under tamoxifen treatment thus suggesting a dose dependent inhibition of NY-BR-1 protein expression by this anti-hormonal therapy [247]. No correlation of NY-BR-1 protein and mRNA expression and menopausal status of women could be detected [247]. Furthermore, an inverse correlation of NY-BR-1 protein expression and both HER2/neu amplification and epidermal growth factor receptor (EGFR) expression was described, thereby identifying NY-BR-1 as a potential therapeutic target for patients with HER2/neu and EGFR negative status [248]. Despite the above described inverse correlation of NY-BR-1 protein expression and HER2/neu amplification, co-expression of these proteins was described in 50% of HER2/neu-amplified and EGFR positive breast cancer tumors [247]. In consequence, combinational therapy options of immunotherapy and HER2-/EGFR-targeted therapies should be considered for future treatment of NY-BR-1$^+$ breast cancers.

Even though the NY-BR-1 protein is found to be expressed in the ductal epithelium of the breast and in metastasis of primary breast cancer tumors as mentioned above, so far no cell line stably expressing NY-BR-1 protein endogenously is available *in vitro,* most likely due to loss of NY-BR-1 protein expression *in vitro,* with the underlying mechanism not yet described.

3.7 Aim of the study

The aim of this project is the identification of novel HLA-restricted NY-BR-1-specific CD4$^+$ and CD8$^+$ T cell epitopes using three different HLA-transgenic mouse strains (HHDtg-, DR3tg- and DR4tg-mice). HLA-restricted NY-BR-1-specific T cell epitopes might be used for: vaccination strategies, immunomonitoring, expansion of T cells for adoptive T cell transfer and the generation of TCR transduced T cells. So far, only a limited number of NY-BR-1 specific epitopes identified by reverse immunology has been described. With the global approach of identifying NY-BR-1 specific epitopes applied in this thesis, further NY-BR-1 specific epitopes, not covered by reverse immunology, were expected to be identified. Furthermore, no CD4$^+$ T cell epitopes had been described so far, thus the aim of this study is to identify novel NY-BR-1 specific T cell epitopes applying the following strategy:

1. Identification of further HLA-A*02 in HHDtg mice
2. Identification of NY-BR-1-specific HLA-DR-restricted candidate epitopes in DR3tg mice and DR4tg mice
3. Verification of natural processing of novel NY-BR-1-specific epitopes in human cells

Finally we would like to investigate the presence of MHC-restricted, NY-BR-1-specific T cells in peripheral blood obtained from breast cancer patients and healthy donors.

4 Materials and Methods

4.1 Materials

4.1.1 General instrumentation

Table 4: General instrumentation

Equipment	Manufacturer
Biofuge Fresco Centrifuge	Heraeus, Hanau, Germany
Biological Safety Cabint	Heraeus, Hanau, Germany
BioPhotometer	Eppendorf, Hamburg, Germany
BioRad Mini-gel apparatus	Bio-Rad, Richmond, CA
CO2 incubator	Binder, Tuttlingen, Germany
Innova 4230 Incubator Shaker	New Brunswick Scientific, Edison, NJ
Leica DM1L Microscope	Leica, Wetzlar, Germany
Microbiological Incubator	Heraeus, Hanau, Germany
MP220 pH Meter	Mettler Toledo, Columbus, OH
Multichannel Pipette	Eppendorf, Hamburg, Germany
Multifuge x3 FR centrifuge	Heraeus, Hanau, Germany
Pipetboy	Brand, Wertheim, Germany
Piepette (P2, P10, P100, P200, P1000)	Gilson, Bad Camberg, Germany
Power PAC 300 power supplier	Bio-Rad, Richmond, Germany
Refrigerator	Liebherr, Ochsenhausen, Germany
Sorvall RT7 Centrifuge	Sorvall, Newton, CT
Thermomixer	Eppendorf, Hamburg, Germany
Verti 96-Well Thermal Cycler	Applied Biosystems, Froster City, CA
AID Elispot plate reader	Autoimmune Diagnostika GmbH, Strassberg, Germany
FACS Calibur Flow Cytometer	Becton Dickinson, Heidelberg, Germany
FACS Canto	Becton Dickinson, Heidelberg, Germany

4.1.2 General disposables

Table 5: General disposables

Material	Manufacturer
Falcon tubes 15ml, 50ml	Greiner, Frickenhausen, Germany
Pipette filter tips (10, 20, 100, 200, 1000µl)	Starlab, Milton Keynes, United Kingdom

Pipette tips (10, 20, 100, 200, 1000µl)	Greiner, Frickenhausen, Germany
Combitips (2.5, 5ml)	Eppendorf, Hamburg, Germany
Sterile serological pipettes (5, 10, 25ml)	Greiner, Frickenhausen, Germany
Safe-Lock tubes (0.5, 1.5, 2ml)	Eppendorf, Hamburg, Germany
Tissue culture flasks (25, 75, 150cm^2)	TPP, Trasadingen, Switzerland
Cell culture test plates, flat bottom (6, 12, 24 wells)	TPP, Trasadingen, Switzerland
Round bottom 96-well plates	TPP, Trasadingen, Switzerland
Petri Dishes	Greiner, Frickenhausen, Germany
Cryotubes	Greiner, Frickenhausen, Germany
Nitrocellulose membrane	Whatmann, Dassel, Germany
Needles (18G, 27G)	Becton Dickinson, Heidelberg, Germany
Inject-F, Syringes	Braun, Melsungen, Germany
EliSpot plates	Merc Miliore, Darmstadt, Germany
Liquid reservoirs	Carl Roth GmbH, Karlsruhe, Germany
FACS tubes	Becton Dickinson, Heidelberg, Germany
Cell strainers	Becton Dickinson, Heidelberg, Germany

4.1.3 General chemicals and reagents

Table 6: General chemicals

Equipment	Manufacturer
Trypsin/EDTA 10x	PAA Laboratories GmbH, Pasching, Austria
Phosphate Buffered Saline (PBS)	Biochrom AG, Berlin, Germany
Dimethyl sulfoxide (DMSO)	Applichem, Darmstadt, Germany
Agarose	Sigma, Saint Louis, MO
Tris Base	Sigma, Saint Louis, MO
Ammonium Persulfate (APS)	Sigma, Saint Louis, MO
Tetramethylethylendiamine (TMED)	Bio-Rad, Saint Louis, MO
Sodium dodecyl sulfate (SDS)	Sigma, Saint Louis, MO
Glycine	GERBU Biotechnik, Gaiberg, Germany
Tween20	GERBU Biotechnik, Gaiberg, Germany
Non-fat milk powder	Carl Roth GmbH, Karlsruhe, Germany
Bovine Serum Albumin (BSA)	Sigma, Saint Louis, MO
Methanol	Sigma, Saint Louis, MO
Ethanol	Sigma, Saint Louis, MO
Ethidium Bromide	Carl Roth GmbH, Karlsruhe, Germany

β-Mercaptoethanol	Sigma, Saint Louis, MO
Paraformaldehyde	Sigma, Saint Louis, MO
Tryptone	Sigma, Saint Louis, MO
Yest extract	GERBU Biotechnik, Gaiberg, Germany
Sodium Chloride (NaCl)	Sigma, Saint Louis, MO
Agar	Sigma, Saint Louis, MO
Leukosept	Greiner, Frickenhausen, Germany

Table 7: General reagents

Material	Manufacturer
Gene Ruler 100bp DNA Ladder	Fermantas, St. Leon-Rot, Germany
O´Gene Ruler 1kb DNA Ladder	Fermantas, St. Leon-Rot, Germany
6x Orange Loading Dye	Fermantas, St. Leon-Rot, Germany
Precision Plus Protein Standard	Bio-Rad, Richmond, CA
Cell Lysis Buffer	Cell Signaling Technology, Beverly, MA
Bio-Rad Protein Assay Reagent	Bio-Rad, Richmond, CA
Restriction enzymes (PvuI, KpnI, NotI, XbaI)	Fermantas, St. Leon-Rot, Germany
FastAP Thermosensitive Alkaline Phosphatase	ThermoFisher Scientific, Schwerte, Germany
BCIP/NBP Liquid Substrate System	Sigma, Saint Louis, MO

4.1.4 Plasmids

Table 8: Plasmids used for cloning of the NY-BR-1 breast cancer antigen

Plasmid	Manufacturer
pcDNA3.1(-)	Invitrogen, Carlsbad, CA
pcDNA3.1(-)zeo	Invitrogen, Carlsbad, CA

4.1.5 Kits

Table 9: Kits

Material	Manufacturer
RNeasy Plus Mini kit	Qiagen, Hilden, Germany
Transcriptor First Strand cDNA Synthesis Kit	Roche, Applied Science, Mannheim, Germany
Rapid DNA ligation	Roche, Applied Science, Mannheim, Germany
QIAquick Gel extraction Kit	Qiagen, Hilden, Germany
QIAGEN Plasmid Maxi Kit	Qiagen, Hilden, Germany

DNA isolation kit	Qiagen, Hilden, Germany
Effectine Transfection Reagent Kit	Qiagen, Hilden, Germany
ECL Plus Western blotting Detection System	GE Healthcare, Buckinghamshire
CD4 (L3T4) MicroBeads mouse	Miltenyi Biotec GmbH, Bergisch Gladbach, Germany
IFN-γ Secretion Assay - Cell Enrichment and Detection kit (PE), mouse	Miltenyi Biotec GmbH, Bergisch Gladbach, Germany
IFN-γ Secretion Assay - Cell Enrichment and Detection kit (PE), human	Miltenyi Biotec GmbH, Bergisch Gladbach, Germany
panT cells MicroBeads human	Miltenyi Biotec GmbH, Bergisch Gladbach, Germany
X-tream Gene HP DNA transfection reagent	Roche, Applied Science, Mannheim, Germany

4.1.6 Antibodies

Table 10: Antibodies used for Western blot analysis

Material	Manufacturer
mouse anti-NY-BR-1 monoclonal antibody clone#2	group of Prof. Jäger, NCT, Heidelberg
mouse anti-β-actin monoclonal (#691001)	MP Biomedicals, Solon, OH
Goat-anti-mouse IgG-HRP (#sc2005)	Santa Cruz Biotechnology, Santa Bruz, CA

Table 11: Antibodies used for flow cytometry

Material	Manufacturer
Mouse anti-human HLA-DR FITC (#347363)	Becton Dickinson, Heidelberg, Germany
Anti-mouse CD4 FITC (#11-0041-81)	eBioscience, San Diego, CA
Anti-human CD4 FITC (#300506)	BioLegend, San Diego, CA
Rat anti-mouse CD8a APC (#553035)	Becton Dickinson, Heidelberg, Germany
Anti-human CD8 APC (#17-0087-42)	eBioscience, San Diego, CA
Mouse anti-human HLA-A2 (hybridoma BB7.2)	Prof. G.J. Hämmerling, DKFZ, Heidelberg, Germany
Goat anti-mouse PE	Dianova, GmbH, Hamburg Germany
Mouse anti-human HLA-A2 PE (#558570)	Becton Dickinson, Heidelberg, Germany
Anti-human CD80 PE (#12-0809-42)	eBioscience, San Diego, CA
Anti-human CD86 PerCp (#46-0869-41)	eBioscience, San Diego, CA
Anti-HLA-DR APC (#559866)	Becton Dickinson, Heidelberg, Germany

Anti-human CD4 PE (BLD-344605)	BioLegend, San Diego, CA
Mouse anti-murine K^b (E3-25)	Prof. G.J. Hämmerling, DKFZ, Heidelberg, Germany
Mouse anti-murine D^b (B22.249)	Prof. G.J. Hämmerling, DKFZ, Heidelberg, Germany
anti-human CD3 PE-Vio770	Miltenyi Biotec GmbH, Bergisch Gladbach, Germany
anti-human CD4 PerCPCy5.5	Becton Dickinson, Heidelberg, Germany
anti-human CD8 APC-H7	Becton Dickinson, Heidelberg, Germany
anti-human CD25 V450	Becton Dickinson, Heidelberg, Germany
anti-human CD127 FITC	Miltenyi Biotec GmbH, Bergisch Gladbach, Germany
anti-human FoxP3 APC	eBioscience, San Diego, CA
anti-human IFN-γ PE	Miltenyi Biotec GmbH, Bergisch Gladbach, Germany
anti-mouse IFN-γ PE	Miltenyi Biotec GmbH, Bergisch Gladbach, Germany
pacific orange	Lifescience, Carlsbad, CA
Milli-Mark™ Anti-CAR-PE, clone RmcB (#FCMAB418PE)	Millipore, Schalbach, Germany
Anti-CAR, clone RmcB (#05-644)	Millipore, Schalbach, Germany

Table 12: Antibodies used for EliSpot assays

Material	Manufacturer
Rat anti-mouse IFN-γ (#551216)	Becton Dickinson, Heidelberg, Germany
Biotinylated rat anti-mouse IFN-γ (#554410)	Becton Dickinson, Heidelberg, Germany
Streptavidin-alkaline phosphatase (#554065)	Becton Dickinson, Heidelberg, Germany
Anti-human IFN-γ mAb (#3420-3-1000)	Mabtech, Nacka Strand, Sweden
Biotinylated anti-human IFN-γ mAb (#3420-6-1000)	Mabtech, Nacka Strand, Sweden

4.1.7 Cytokines

Table 13: Cytokines

Material	Manufacturer
Human IFN-γ recombinant carrier free (#34-8319-82)	eBioscience, San Diego, CA
Recombinant human IL-4 (#204 IL)	R&D Systems, Minneapolis, MN
GM-CSF (Leukine, Sargromastim)	Sanofi, Paris, France
Recombinant TNF-α (#210-TA/CF)	R&D Systems, Minneapolis, MN
Recombinant IL-1β (#210-LB/CF)	R&D Systems, Minneapolis, MN
Prostaglandin E2 (PGE2) (#PG532-1MG)	Sigma, Saint Louis, MO
Recombinant human IL-6 (#206-IL/CF)	R&D Systems, Minneapolis, MN
Recombinant human IL-12 (#219-IL/CF)	R&D Systems, Minneapolis, MN
Recombinant human IL-7 (#C-61712)	Promokine, Heidelberg, Germany
Recombinant human IL-2 (#C61240)	Promokine, Heidelberg, Germany
Recombinant human IL-15 (#247-IL/CF)	R&D Systems, Minneapolis, MN

4.1.8 Cell culture

Table 14: Cell culture medium and supplements

Material	Manufacturer
RPMI 1640	PAA Laboratories, Pasching, Austria
αMinimum Essential Medium Eagle (MEM)	Sigma, Saint Louis, MO
Fetal Calf Serum (FCS)	PAA Laboratories, Pasching, Austria
Penicillin/Streptomycin (Pen/Strep)	PAA Laboratories, Pasching, Austria
Zeocin	Invitrogen, Carlsbad, CA
G418(=Neomycin)	Gibco-Invitrogen, Karlsruhe, Germany
α-methylmannopyranoside	Sigma, Saint Louis, MO
DMEM	PAA Laboratories, Pasching, Austria
Lipopolysacharides (LPS)	Sigma, Saint Louis, MO
Glutamine	Gibco-Invitrogen, Karlsruhe, Germany
McCoy´s 5A	Promocell, Heidelberg, Germany
x-Vivo Medium	Lonza, Basel, Switzerland
Human Serum, type AB, off the clot	Biochrome AG, Berlin, Germany
AIM-V Medium	Invitorgen, Carlsbad, CA

Table 15: Murine tumor cell lines

Cell line	Source	MHC background	Cell line type [Ref]
EL4	German Cancer Research Center, Heidelberg, Germany	H-2^b, C57BL/6 derived	T lymphoma [230]
EL4-Rob/HHD	German Cancer Research Center, Heidelberg, Germany	H-2^b/$\beta_2m^{b-/b-}$, HLA-A*0201	lymphoma [190]
B16	German Cancer Research Center, Heidelberg, Germany	H-2^b, C57BL/6 derived	melanoma [73]
GL261	German Cancer Research Center, Heidelberg, Germany	H-2^b, C57BL/6 derived	glioblastoma [245]

Table 16: Human cell lines

Cell line	Source	MHC background of interest	Cell line type [Ref]
Hek293T	ATCC, Rockville, MD	unknown	human embryonic kidney cells [191][91]
HBL-100	German Cancer Research Center, Heidelberg	HLA-DRB1*301	human breast epithelial cells [32]
Ma-Mel 21	Skin Cancer Unit, DKFZ, Heidelberg, Germany	HLA-DR negative	
Ma-Mel 36	Skin Cancer Unit, DKFZ, Heidelberg, Germany	HLA-DRB1*0301 HLA-DRB1*0401	
Ma-Mel 51	Skin Cancer Unit, DKFZ, Heidelberg, Germany	HLA-DRB1*0301	
Ma-Mel 73a	Skin Cancer Unit, DKFZ, Heidelberg, Germany	HLA-DRB1*0401	
MCF-7	ATCC, Rockville, MD	HLA-DRB1*0301	breast epithelial cell line, derived from metastatic site [240]

SK-BR-3	ATCC, Rockville, MD	HLA-DRB1*	mammary gland/breast, derived from metastatic site [251]
T2	T2 (ATCC®CRL-1992™)	HLA-A*0201	174xCEM.Z2; fusion of B-LCL 721 and T lymphoma [220]
T2/DR3	German Cancer Research Center, Heidelberg	HLA-DRB1*0301, HLA-A*02	transfectant provided by F. Momburg, DkFz
T2/DR4	German Cancer Research Center, Heidelberg	HLA-DRB1*0401, HLA-A*02	transfectant, provided by Harald Kropshofer , Ulm

Table 17: Other cells

Material	Source
TOP10 E.coli competent cells	Invitrogen, Carlsbad, CA

4.1.9 Software

Table 18: Software

Software	Source
Microsoft office 2010	Microsoft, Redmont, USA
GraphPad Prism 5	GraphPad Software, Inc., San Diego, USA
Cell Quest	Becton Dickinson, Heidelberg, Germany
FlowJo	Becton Dickinson, Heidelberg, Germany

4.1.10 Database

Table 19: Database

Database	Source
SYFPEITHI	www.syfpeithi.de

4.2 Methods

4.2.1 Preparation of buffers and medium

Table 20: TBS-T

Component	Amount
1 x TBS, with 0.1% (v/v) Tween 20	

Table 21: 50 x Tris-acetate-EDTA (TAE) buffer, pH 8.0, 1L

Component	Amount
Tris base	242 g
Acetic acid	57.1 ml
500mM EDTA solution	100 ml
H_2O	Adjust final volume to 1L

Table 22: 1 x PBS, pH 7.4, 1L

Component	Amount
PBS Dulbecco w/o CA^{2+}, Mg^{2+}	9.55 g
H_2O	Adjust final volume to 1L

Table 23: 10 x SDS-PAGE running buffer, IL

Component	Amount
Tris base	30 g
10% SDS solution	100 ml
Glycin	144 g
H_2O	Adjust final volume to 1L

Table 24: 1x Tris-buffered saline (TBS), pH 7.6, 1L

Component	Amount
Tris base	2.24 g
Acetic acid	57.1 ml
500mM EDTA solution	100 ml
H_2O	Adjust final volume to 1L

Table 25: Transfer buffer, pH 8.5, 1L

Component	Amount
Tris base	3 g
Glycin	17.5 g
Methanol	200 ml
H_2O	Adjust final volume to 1L

Table 26: Stripping buffer, pH 6.8, 100 ml

Component	Amount
0.5M Tris-HCL (pH 6.8)	6.25 ml
10% (v/v) SDS solution	20 ml
β-Mercaptoethanol	700 µl
H_2O	Adjust final volume to 1L

Table 27: Cell freezing medium

Component	Amount
FCS	90% (v/v)
DMSO	10% (v/v)

Table 28: LB medium, pH 7.5, 1L

Component	Amount
Tryptone	10 g
Yeast extract	5 g
NaCl	10 g
H_2O	Adjust final volume to 1L

Table 29: FACS buffer

Component	Amount
FCS	3% (v/v)
2% NaN_3	5 ml
PBS	Adjust final volume to 500 ml

Table 30: MACS buffer

Component	Amount
0.5M EDTA	4 ml
BSA	5 g
PBS	Adjust final volume to 1L

Table 31: Cell culture medium

Component	supplements
culture medium (RPMI 1640)	10% FCS, 100 U/ml penicillin, 100 µg/ml streptomycin
complete α MEM	10% FCS, 2 mmol/l glutamine , 100 U/ml penicillin, 100 µg/ml streptomycin, 25 ml ConA sup, 25 ml, 50 µmol/l 2-mercaptoethanol
T cell medium (complete α MEM)	5% (v/v) culture supernatant from concavalin A stimulated rat spleen cells, 5% (v/v) Methyl α-D-mannopyranoside (αMM)
Dendritic cell culture medium (RPMI 1640)	200U/ml interleukin (IL)-4, 560 U/ml granulocytes-macrophage growth factor GM-CSF, 10% FCS, 100 U/ml penicillin, 100 µg/ml streptomycin

4.2.2 Cell culture

Melanoma cell lines Ma-Mel21, Ma-Mel36b, Ma-Mel79b, Ma-Mel73a, EL4 cells and T2 cells were cultured in complete RPMI 1640 medium (culture medium). T2/DR3, T2/DR4, EL4-NY-BR-1 transfectants and EL4-Rob/HHD cells were cultured in complete RPMI 1640 medium supplemented with 0.4 mg/ml G418 (Gibco-Invitrogen, Karlsruhe). The breast cancer cell line MCF-7 was cultured in complete DMEM medium. SK-BR-2 and HBL-100 breast cancer cell lines were cultured in McCoys Medium (PAA-Laboratories) supplemented with 10% FCS (PAA Laboratories) and 100 U/ml penicillin, 100 µg/ml streptomycin (PAA Laboratories).

All cell lines were cultured at 37°C in a humidified atmosphere with 5.0 % CO_2.

4.2.3 Protein detection by Western blot analysis

Cell lysates were generated using appropriated amounts of the Cell Lysis Buffer (Cell Signaling) and incubated for 15 min on ice followed by 25 min centrifugation at 13,000 rpm, 4°C. Protein concentration was determined by Bio-Rad Protein Assay reagent on a BioPhotometer. Cell lysates were stored at -20°C.

Heat denatured whole cell protein samples (15 µg- 50 µg) were mixed with 5 x loading dye and separated on a 10% polyacrylamid gel, and electro-transferred onto nitrocellulose membranes. Successful protein transfer was confirmed by Ponceau S staining of the nitrocellulose membrane. Before blocking of the membrane with 5% of non-fat milk in TBS-T, Ponceau S was washed away with TBS-T buffer. After blocking, the membranes were incubated with the respective primary antibody diluted in 0.5% non-fat milk in TBS-T buffer and left rotating at 4°C over night. Next, membranes were washed in intervals of 1 x 10 min and 2 x 5 min with TBS-T before incubated with the respective horseradish peroxidase conjugated secondary antibody diluted in 0.5% non-fat milk in TBST for 1h at RT. Following another interval of washing with TBS-T buffer, protein signals were detected using the enhanced chemiluminescence (ECL) system by exposing blots to an x-ray film.

4.2.4 Flow cytometry

If not otherwise indicated, 1 x 10^6 cells were resuspended in 100 µl FACS buffer and stained in a 1:100 dilution with the respective antibodies for 30 min at 4°C in the dark.

Next, cells were washed two times with FACS buffer and finally resuspended in 200 µl FACS buffer. Data were acquired on a FACS Calibur if not indicated otherwise.

4.2.5 Molecular cloning

NY-BR-1 full length DNA was isolated from pcDNA3.1-NY-BR-1 by Kpn1 and Not1 digestion over night. The resulting interest was separated on a 1% agarose gel by gel-electrophoresis and extracted using the QIAquick Gel Extraction Kit (Qiagen). Prior to ligation into the multiple cloning site, the target vector was dephosphorylated by using FAST alkaline phosphatase (ThermoFisher Scientific), according to the manufacture´s protocol. Successful cloning was verified by digestion of the pcDNA3.1(-)zeo construct with the restriction enzymes Not1 and Kpn1 over night and subsequent gel-electrophoresis.

4.2.6 Transformation and amplification of cloned plasmid

Amplification of the construct was achieve by transformation of Top10 bacteria and subsequent growing of colonies on LB agar with ampicillin. Colonies were picked and used to inoculated 3 ml of LB-medium containing 100 µg/ml ampicillin. Positive clones were further expanded by using the Maxi-Prep Kit (Qiagen) accordingly to the manufacturers instructions. DNA concentration was determined by a BioPhotometer.

4.2.7 NY-BR-1 specific peptide library and synthetic candidate peptides

A NY-BR-1 specific peptide library consisting of 174 peptides (20mers), overlapping by 12 amino acids was purchased. To perform a combinatorial peptide library screening, NY-BR-1 library peptides were organized in 26 pools (K1-K13 and L1-L13), each pool consisting of 13 NY-BR-1 specific library peptides (fig. 44). The final concentration of each library peptide in the respective pool used in IFN-γ Elispot assay was 1.5 µg/ml.

Calculation: Peptide library stock of 200 µg/ml => 13 peptides in each library peptide pool, which leads to a dilution of each single library peptide of 1:13 in the peptide library pool, thus each peptide has a final concentration of 15.4 µg/ml in the peptide pools. Library peptide pools are 1:5 diluted with medium before used in an IFN-γ Elispot assay and further diluted 1:2 on the IFN-γ Elispot assay plate, thus the final concentration of each peptide in the IFN-γ Elispot assay is 1.5 µg/ml.

The second level matrix screened with splenocytes of immunized DR4tg mice was composed of 16 library peptide pools (A1-A8, B1-B8), each one consisting out of eight NY-BR-1-specific library peptides, except for the peptide pools A5, A6, A7, A8 which only harbors seven NY-BR-1-specific library peptides and the peptide pool B8 which only consists out of four NY-BR-1-specific library peptides. The final concentration of each library peptide in the respective pool used in the IFN-γ Elispot assay was 2.1 µg/ml.

Calculation: Peptide library stock of 200 µg/ml => 8 peptides in each library peptide pool,

which leads to a dilution of each single library peptide of 1:8 in the peptide library pool, thus each peptide has a final concentration of 25 µg/ml in the peptide pools. Library peptide pools are 1:6 diluted with medium before used in an IFN-γ Elispot assay and further diluted 1:2 on the IFN-γ Elispot assay plate, thus the final concentration of each peptide in the IFN-γ Elispot assay is 2.1 µg/ml.

Peptide pools C1-C19 were composed out of two individual library peptides and the final concentration of each peptide used in IFN-γ Elispot assay was 2 µg/ml.

Calculation: Library peptide stock of 200 µg/ml => 100 µl of two single library peptides were mixed with 800 µl PBS (1:10 dilution) to generate the peptide pools C1-C19, thus the final concentration of each library peptide in the C pools is 20 µg/ml. Prior to the IFN-γ Elispot assay, peptide pools C1-C19 were diluted 1:5 with medium before used in an IFN-γ Elispot assay and further diluted 1:2 on the IFN-γ Elispot assay plate, thus the final concentration of each peptide in the IFN-γ Elispot assay is 2 µg/ml.

Individual NY-BR-1 specific library peptides were applied as single peptides in the assays at a final concentration of 2 µg/ml in the case of DR3tg mice and DR4tg mice and at a final concentration of 100 ng/ml performing experiments with splenocytes of HHDtg mice. All library peptides were dissolved in DMSO at a concentration of 50 mg/ml and stored at -20°C until use.

Individual candidate peptides selected by the library screen were synthesized and HPLC-purified at the peptide synthesis core facility of the German Cancer Research Center, Heidelberg. All peptides were dissolved in DMSO at a concentration of 50 µg/ml and stored at -20°C until use.

4.2.8 HLA-transgenic mice

Animal experiments were approved by the internal ethics committee of the German Cancer Research center and by the District Government in Karlsruhe. All mice were housed and bred in individual ventilated cages under SFP conditions within the German Cancer Research Center, Heidelberg animal facility.

HLA-DRB1*0301-transgenic mice (HLA-DR3tg) HLA-DRB1*0301-transgenic (HLA-DR3tg) mice express the HLA-DRB1*0301 molecule on a $IA^{0/0}$ H2 background, thus expression of murine MHC-I molecules H2-K^b / H2-D^b is still given [130]. HLA-DRB1*0301 transgene expression was confirmed by analysis of peripheral blood lymphocytes (PBMCs) obtained from the submandibular vein of HLA-DR3tg mice. PBMCs obtained from HLA-DRB1*0301 transgenic mice were stained for 30 min, 4°C with an anti-HLA-DR-FITC antibody (Becton Dickinson, Heidelberg) and analyzed by flow cytometry on a FACS-Calibur.

HLA-DRB1*0401-transgenic mice (HLA-DR4tg) Murine MHC-II deficient, HLA-DRB1*0401-transgenic (HLA-DR4tg) mice express a chimeric version of the HLA-DRB1*0401 molecule (HLA-DRB1*0401:IEd) on a IA0/0 H2 background [110]. More precisely, the HLA-DRB1*0401 chimeric gene contains the human HLA-DRB1*0401 peptide binding α_1 and β_1 domains fused to the murine IEd-α_2 and IEd-β_2 domains. Furthermore, HLA-DR4tg mice also express murine MHC-I, H2-K^b / H2-D^bmolecules.

HLA-A*0201-transgenic mice (HHD-tg) HHDtg mice express the α_1 and α_2 domain of the human HLA-A*0201 molecule and the murine α_3 domain of the murine D^b molecule, linked to the human β_2-microglobulin. In consequence, only HLA-A*0201 restricted $CD8^+$ T cells are generated in HHD-tg mice. In addition, HHDtg mice express IA^b molecules.

4.2.9 Isolation of murine PBMCs

Mouse blood (5-10 drops) drawn from the submandibular veins, were mixed with 100 µl of PBS/Heparin (5U/ml Heparin Natrium 25 000 (Ratiopharm), 2% FCS (PAA Laboratories), 0.1% NaN_3) and incubated on ice. Mouse blood was diluted with 200 µl PBS. Then 200 µl were added on top of 300 µl Bicoll solution (Biochrom, density 1.007mg/ml) without disrupting the Bicoll layer. Samples were centrifuged at 3400 rpm, 15 min. Emerging interphase representing all mononuclear cells was carefully transferred into a fresh eppendorf tube and resuspended in 1 ml PBS. Following another centrifugation step at 2700 rpm, 10 min, cell pellets were resuspended in 200 µl FACS buffer and transferred on a 96 well plate to proceed with anti-HLA-DR staining for 30 min in the dark at 4°C, using the mouse anti-HLA-DR FITC-conjugated antibody 1:100 in FACS buffer. Samples were washed twice with FACS buffer and subsequently analyzed on a FACS Calibur.

4.2.10 Analysis of a NY-BR-1-specific T cell response for HLA-DRB1*0301-/*0401-transgenic mice

DR3tg mice and DR4tg mice were immunized twice (day 0, day 7) by intramuscular (i.m.) injection of 100 µg DNA of the NY-BR-1 encoding expression vector (pcDNA3.1(-)NY-BR-1). To exclude immunogenic effects generated by the expression vector itself, mice immunized with pcDNA3.1(-) served as a control group. On day 14, mice were sacrificed and splenocytes were tested for NY-BR-1 specific T cell responses *in vitro* by recognition of NY-BR-1 specific peptide library pools, individual library peptides (20mers) and candidate epitopes (15mers) in IFN-γ EliSpot assays using the culture medium.

Individual library peptides were tested with a final concentration of 2 µg/ml for DR3tg mice and DR4tg mice and at a final concentration of 100 ng/ml for HHDtg mice. IFN-γ EliSpot assays

were performed using 96 well Multiscreen EliSpot plates (Millipore, Schalbach, Germany) coated with 1 µg/ml rat anti-mouse IFN-γ capture antibody for 1h at 37°C or overnight at 4°C. After blocking the EliSpot plates with culture medium for 1 h, 10^6 – 1.5 x 10^6 splenocytes were co-incubated with the respective library peptide pools or individual library peptides for 18 h in culture medium in a total volume of 200 µl per well. Cells were discarded and plates were washed with PBS Tween20 0.05% twice and PBS three times before adding 1µg/ml biotinylated secondary antibody in 100 µl per well and incubation of plates for 1h at 4°C. Following another washing step with PBS, cells were incubated with streptavidin-conjugated alkaline phosphatase for 30 min and signals were developed by adding 100 µl BCTP/NBT (Sigma, Saint Louis, MO) to the again washed wells. The enzymatic reaction was stopped after 1 min by distilled water to all wells. IFN-γ spots numbers were analyzed on the AID EliSpot Reader classic (Autoimmune Diagnostika GmbH, Strassberg, Germany).

4.2.11 IFN-γ Secretion Assay with murine spleen cells

To analyze $CD4^+$, NY-BR-1 specific T cell responses, splenocytes obtained from immunized mice were stained for $CD4^+$/IFN-γ^+ T cells by mouse IFN-γ Secretion Assay–Cell Enrichment and Detection Kit (PE) (Miltenyi Biotec, Bergisch Gladbach) according to the optimized manufacturer´s protocol in combination with an additional staining for murine $CD8^+$ cells using the CD8-APC antibody (eBioscience, San Diego). Briefly, 2 x 10^7murine spleen cells were seeded in 6 well plates in 2 ml culture medium and over night stimulated with 5 µg/ml of the respective peptide. Cells were transferred to a 96 well plate formate for the IFN-γ-catch period lasting 2 1/2 hours at 37°C, 5% CO_2. Subsequently, cells were additionally stained with mouse-CD4-FITC (eBioscience, San Diego, CA), anti-mouse CD8 APC (eBioscience) and anti-IFN-γ PE (Miltenyi Biotec) were performed. IFN-γ positive cells were enriched according to the manufactures protocol by application of anti-PE microbeads.

All experiments were also performed without the enrichment for IFN-γ positive cells. Data was acquired on a FACS-Calibur and analyzed with FlowJo software.

4.2.12 Generation of murine HLA-DRB1*0301- and HLA-DRB1*0401- restricted $CD4^+$ T cell lines

DR3tg mice were immunized subcutaneously (s.c.) with 100 µg of the 15mer peptides BR1-88, BR1-1238, BR1-1347 and DR4tg mice with the 15 mer peptides BR1-537, BR1-656/-775, BR1-1242. After 13 days, mice were sacrificed and T cell lines were generated from splenocytes upon incubation of 6 x 10^6 splenocytes with 0.2 µg/ml of the respective peptide in 24 well plates in 2 ml complete α-MEM (Sigma-Aldrich, Saint Louis, MO). Every 5 to 7 days, half of the supernatant

was exchanged by the above mentioned medium containing 5% (v/v) of culture supernatant from ConA stimulated rat-spleen cells (= T cell medium), as a source of interleukin (IL)-2. Spleen cell cultures were restimulated every four weeks by addition of 6 X 10^6 irradiated syngeneic feeder cells together with antigenic peptide (0.2 µg/ml).

4.2.13 Determination of HLA-restriction of established murine T cell lines

HLA-DRB1*0301- and HLA-DRB1*0401- restriction of the established murine T cell lines was confirmed in IFN-γ EliSpot assays by co-incubating 10^5 T cells and 5 X 10^4 human T2/DR3 and T2/DR4 cells, respectively in the presence of 1 µg/ml of the cognate peptide. After 18 hrs NY-BR-1 peptide specific signals were detected.

4.2.14 Generation of human dendritic cells

PBMCs were obtained from HLA-DRB1*0301$^+$ and HLA-DRB1*0401$^+$ healthy donors. Adherent PBMCs were cultured in dendritic cell culture medium (RPMI 1640) to induce DC maturation. Five to seven days later, surface expression of DC markers was determined by FACS using anti-CD80-PE(eBioscience, San Diego, CA), anti-CD86-PerCp(eBioscience, San Diego, CA), anti-CD11c-FITC (Becton Dickinson, Heidelberg, Germany), anti-HLA-DR-APC (Becton Dickinson, Heidelberg, Germany) antibodies. Data were acquired on a FACS-Calibur.

4.2.15 Recombinant adenovirus (Ad5-NY-BR-1) used for infection of human target cells

E1-deleted replication deficient recombinant adenoviral vectors, one encoding the NY-BR-1 protein (Ad5-NY-BR-1), the second one being the empty viral vector (Ad5), were purchased at GeneCust (Dudelange, Luxembourg). GenCust provided the recombinant adenoviral vectors at a concentration of 10^{12}pfu/ml which were dissolved in PBS to a final concentration of 5 X 10^8pfu/ml. Optimal multiplicity of infection (MOI) and time point for infection of melanoma cell lines Ma-Mel21, Ma-Mel36b, Ma-Mel79b, MaMel73a and breast cancer cell line SK-BR-2 cell was determined by analysis of NY-BR-1 protein expression, detected by Western blot analysis using the anti-NY-BR-1 antibody (NY-BR-1 monoclonal antibody clone #2). Infections were performed in a final volume of 2 ml of the respective cell culture medium in 6 well plates.

In addition, human PBMCs from healthy donors, depleted of CD3$^+$ cell, and HLA-matched human *in vitro* generated dendritic cells were infected with either Ad5-NY-BR-1 or Ad5 and NY-BR-1 protein expression was analyzed by Western blot 48 hrs after infection. 1 X 10^5 PBMCs depleted of were infected with Ad5-NY-BR-1 at an MOI=100 in a final volume of 2 ml. Infections

of 1 X 10^5 *in vitro* generated dendritic cells were performed with an MOI=1000 in a 96 well formate and in a total volume of 100 µl.

4.2.16 Generation of human dendritic cells (DCs) as antigen presenting cells for murine NY-BR-1-specific HLA-DR restricted T cell lines

Mature HLA-matched dendritic cells were loaded with whole cell lysate obtaind from melanoma cell line (Ma-Mel73a) which was infected with an recombinant adenoviral vector encoding the NY-BR-1 protein (Ad5-NY-BR-1), MOI=100. Infected Ma-Mel73a cells were cultured in six well plates in a volume of 2 ml culture medium and cells were harvested 48hrs after infection and resuspended in PBS. Whole cell protein lysates were generated by repeated thaw-freeze cycles under sterile conditions. Protein concentration was determined by Bradford analysis. Furthermore, NY-BR-1 expression was confirmed by Western blot analysis using the primary NY-BR-1 monoclonal antibody clone #2 (1:1000) and a secondary anti-mouse antibody (SantaCruz Biotechnology, Santa Cruz, CA).

To test for natural processing of the identified epitope, mature DCs (2x10^4) were seeded into each well of an EliSpot plated coated with IFN-γ specific antibody followed by incubation with 20 µg of whole cellular protein derived from Ma-Mel73a cells infected with recombinant Ad5-NY-BR-1 (MOI=100) in 100µl x-Vivo medium (Lonza). Furthermore, mature DCs were pulsed with 1 µg/ml NY-BR-1-specific peptide. After 18 hrs 1 X 10^5 murine T cells were added per well and incubation was continued for another 18 hrs.

4.2.17 Histological staining of breast cancer biopsies

120 tumor biopsies of breast cancer patients were collected by Prof. Schneeweiss at the Heidelberg University Hospital and screened by immunohistology for NY-BR-1 expression (using the NY-BR-1 monoclonal antibody clone #2) at the Pathology Department, University Hospital Heidelberg.

4.2.18 HLA-typing of patients and healthy donors

The HLA genotype of healthy donors and breast cancer patients was determined by high-resolution PCR by an external collaboration partner (Institute for Immunologie and Genetik (Kaiserslautern, Germany). DNA submitted for HLA genotyping was isolated from PBMCs using the DNA-isolation kit (Qiagen) according to the manufactures instructions , kindly done by Elke Dickes, German Cancer Research Center, Heidelberg. Twenty-four patients with positive expression in the tumor specimen were selected due to their HLA genotype (supplement fig. 36).

4.2.19 Detection of NY-BR-1 specific T cells among PBMCs of breast cancer patients and healthy donors

PBMCs of breast cancer patient and healthy donors were thawn and cultured overnight in 50 ml flasks in culture medium. 2 X 10^6 PBMCs/ml were seeded on a 24 well plate in medium supplemented with 20 IU/ml interleukin (IL)-2 (PromoKine, Heidelberg, Germany) and 10 ng/ml interleukin (IL)-7 (PromoKine). Every four days half of the supernatant was exchanged for fresh medium supplemented with (IL)-2 and (IL)-7.

After 17 and 24 days PBMCs were harvested and IFN-γ secretion was analyzed in IFN-γ EliSpot assay. Briefly, IFN- γ EliSpot plates were coated for 2 hrs at 37°C with 10 µg/ml per well with capture IFN-γ mAb. After blocking with culture medium, 10^5 PBMCs/well were incubated with 5 µg/ml of cognate peptide for 16-18 hrs. Plates were washed with PBS and 100 µl/well secondary biotinylated anti-human INF-γ mAb was added at 1 µg/ml per well and incubated for 2 hrs at 37°C. Avidin-conjugated alkaline phosphatase antibody was added after ELISpot plates were washed again with PBS an incubated at room temperature for 30 min. IFN-γ secretion was detected by adding 100 µl BCTP/NBT (Sigma, Saint Louis, MO) to the again washed wells stopping the enzymatic reaction after 1 min by addition of distilled water to the wells. EliSpot results were analyzed using the AID Elispot reader.

4.2.20 Immunofluorescent staining of PBMCs of breast cancer patients and healthy donors

Furthermore, immunofluorescent staining (FACS) was performed on PBMCs obtained from patients and healthy donors after 24 days of *in vitro* stimulation. In more detail, after an *in vitro* stimulation period of 24 days PBMCs were harvested and resuspended at 1 X 10^7 c/ml in x-Vivo medium (Lonza). 1 X 10^6 PBMCs in 200 µl/well x-Vivo medium (Lonza) were plated on a 96 well round bottom plate and incubated over night at 37°C, 5%CO_2 in the presence of 5 µg/ml of antigenic peptide. After 18 hrs, IFN-γ secretion assay was performed according to the manufactures instructions using the IFN-γ secretion Assay - Cell Enrichment and Detection Kit (PE), (Miltenyi). In more detail, after being washed once with MACS-buffer, cells were incubated with the IFN-γ-Catch reagent and incubated for 45 min at 37°C. To distinguish live and dead cells, samples were firstly washed with FACS buffer and then stained with Pac Orange (Lifesciences) in a dilution of 1:1000 in FACS-buffer and incubated on ice for 20 min. Following another washing step with 200 µl FACS-buffer, samples were incubated with IFN-γ-(PE) detection antibody for 10 min on ice in the dark. Next, surface staining for CD3-PE-Vio770 (Miltenyi), CD4-PerCPCy5.5 (Becton Dickinson), CD8-APC-H7 (Becton Dickinson), CD25-V450 (Becton Dickinson), CD127-FITC (Miltenyi) was performed by incubating the samples for 20 min on ice in the dark with the

respective antibodies. Samples were permeabilized by resuspension in 200 µl FIx/PERM Solution (1x) (Becton Dickinson) and incubated for 30 min on ice in the dark. Samples were washed with Perm Buffer (1x) (Becton Dickinson) and incubated for 10 min on ice in the dark. In the last step, intracellular staining for FoxP3 was conducted by incubating the permeabilized samples with FoxP3-APC antibody (eBiosciences) in FACS Perm Buffer (Becton Dickinson) for 30 min on ice in the dark. Finally, samples were washed with FACS-Perm buffer and resuspended in FACS buffer. Cells were measured on a FACS-Canto and date were analyzed with FlowJo software.

4.2.21 Transfection of breast cancer cell lines SK-BR-2, HBL-100 with NY-BR-1-GFP using the X-treame Gene HP DNA Transfection Reagent

Breast cancer cell lines SK-BR-2 (HLA-DRB1*0401) and HBL-100 (HLA-DRB1*0301) were transfected with pcDNA3.1(-)-NY-BR-1-GFP (kindly provided by the group of Prof. Dirk Jäger) using x-treame Gene HP DNA transfection reagent according to the manufactures instructions. Briefly, 3 x 10^5 cells were cultured in 12 well plates in 1ml McCoys medium (PAA laboratories), 100 U/ml penicillin, 100 µg/ml streptomycin (PAA laboratories), until they reached 80% confluence before being transfected with 2 µg NY-BR-1-GFP DNA. Plasmid DNA was set to a concentration of 0.01 µg per 100 µl of diluent (Optimen medium) and mixed with the transfection reagent in a 1:3 ratio. 200 µl of plasmid DNA-diluent mix were added to the cells and cells were harvested 24 hrs and 48 hrs after transfection. In addition, cells were treated with 250 U/ml IFN-γ 24 hrs prior to transfection.

4.2.22 Transient transfection of human and murine cells with NY-BR-1

1 X 10^5 Hek293T cells and MCF-7 cells per well were seeded in a 6 well plated and grown until cells reached 70% confluence. Cells were transfected with the 0.2 µg DNA of the expression vector pcDNA3.1(-)NY-BR-1 whereas EL4 / EL4-Rob/HHD cell lines were transfected with 0.2 µg DNA of the linearized construct pcDNA(3.1)zeo-NY-BR-1 using the Effectine Transfection reagent Kit (Qiagen), according to the manufactures instructions. Linearization of pcDNA3.1(-) was achieved by digesting the plasmid overnight using the restriction enzyme Xba1. Transfections were performed in 6 well plates in a total volume of 2 ml of the respective culture medium.

4.2.23 Generation of stable NY-BR-1 expressing transfectants

1 X 10^5 EL4 or EL4-Rob/HHD cells per well were seeded in a 6 well plate and grown until cells reached 70% confluence. Cells were transfected with 0.2 µg DNA of linearized pcDNA3.1-NY-BR-1(zeo) vector. Limiting dilutions were performed on transfected EL4-NY-BR-1 and EL4-Rob/HHD bulk cultures. To select for stable transfected cell clones, single EL4-NY-BR-1 clones were cultured

in medium containing 0,8 mg/ml G418 (=neomycin) and single EL4-Rob/HHD-NY-BR-1 clones were cultured in medium supplemented with G418 0,4 mg/ml and zeocin 200 µg/ml, respectively.

4.2.24 Isolation of human PBMCs

Human blood samples of NY-BR-1$^+$ breast cancer patients were kindly provided by Prof. Schneeweiss, University Hospital, Heidelberg. EDTA-supplemented patients blood was diluted 1:1 with PBS and and human peripheral mononuclear cells were isolated by using Bicoll solution (Biochrom, density 1.077 g/ml). More precisely, 50 ml falcon tubes were filled with 13 ml of Bicoll solution and diluted EDTA-blood was carefully added on top of the bicoll layer. Samples were centrifuged at 1800 rpm without break and resuspended in 20 ml PBS. After centrifugation, interphase of mononuclear cells collected, transferred to a fresh 50 ml falcon tube and washed 2 times with PBS (1400 rpm, 15 min with brake). Finally, cells were resuspended either in culture medium for *in vitro* culturing or in freezing medium for long term preservation in liquid nitrogen. PBMCs of healthy donors were isolated following the same protocol.

4.2.25 IFN-γ -treatment of human cell lines

HLA-DR expression requires IFN-γ treatment of certain human cell lines. Melanoma cell lines (Ma-Mel79b) and breast cancer cell lines HBL-100, SK-BR-2, were seeded at 5 X 10^5 cells/well on a 6 well plate in a 2 ml RPMI 1640, 10%FCS, 1% PenStrep. The next day, 250 U/ml of human IFN-γ was added to each well. HLA-DR expression was verified 48 hrs later by staining cells with a pan-specific anti-HLA-DR APC antibody (1:100).

4.2.26 MHC surface expression of EL4-NY-BR-1 clones

MHC surface expression of newly generated EL4-NY-BR-1 clones was analyzed by staining of these cell lines with 100 µl of D^b hybridoma (B22.249) supernatant or 100 µl of a K^b hybridoma (E3-25) supernatant, kindly provided by G.J. Hämmerling, Dkfz, for 30 min, 4°C. Cells were washed two times with FACS buffer before staining cells with a secondary goat anti-mouse-IgG FITC antibody (1:100), 30 min, 4°C in the dark. Following another washing step, cells were resuspended in 200 µl FACS buffer and data were acquired on a FACS Calibur. Additionally EL4-NY-BR-1 clonal cell lines were stained for anti-IAb using a directly coupled anti-mouse IA^b- FITC antibody in a 1:100 dilution.

5 Results

The full length NY-BR-1 breast cancer associated antigen was previously cloned into the mammalian expression vector pcDNA3.1(-) and the construct was obtained from Inka Zörnig. Firstly, functionality of the expression vector was tested in mammalian cell lines *in vitro*. Moreover, subcloning of the full length NY-BR-1 DNA into pcDNA3.1-NY-BR-1(-)zeo was required for the establishment of NY-BR-1 expressing target cell lines.

5.1 Generation of a NY-BR-1 encoding expression vector suitable for the generation of NY-BR-1 expressing target cells

In order to test functionality of the expression vector pcDNA3.1(-)NY-BR-1, human embryonic kidney cell line HEK293T and human breast cancer cell lines MCF-7 were transiently transfected with the mammalian expression vector pcDNA3.1(-)NY-BR-1. Untransfected HEK293T cells (fig. 5 A, lanes 1,2) and MCF-7 cells (fig. 5 B, lanes 5,8) cells were used as control groups in this experiment.

NY-BR-1 protein expression was detectable in HEK293T cells 24 hrs after transfection with pcDNA3.1(-)NY-BR-1 (fig. 5 A, lanes 5,6) using 50 µg of cellular protein, in a volume of 20 µl for Western blotting. Signals of the NY-BR-1 protein expression were absent in untransfected HEK293T cells (fig. 5 A, lanes 1,2) as well as in cells transfected with the empty pcDNA3.1(-) vector (fig. 5 A lanes 3,4), indicating that NY-BR-1 protein expression is absent in HEK293T cells and that transfection of the pcDNA3.1(-) vector itself does not lead to any false positive NY-BR-1 expression signals.

In MCF-7 cells, expression of NY-BR-1 protein was analyzed 24 hrs and 48 hrs after transfection of the cells, using 50 µg of cellular protein in a volume of 20 µl for Western blot analysis. NY-BR-1 protein expression was detectable after transfection of MCF-7 cells with pcDNA3.1(-)NY-BR-1(fig. 5 B, lanes 3,6). Intensity of NY-BR-1 protein expression in transfected MCF-7 cells did not differ regarding the investigated time points of 24 hrs and 48 hrs after transfection thus, already 24hrs post transfection was identified as the optimal time point for reaching maximal protein expression in MCF-7 cells transfected with pcDNA3.1(-)NY-BR-1. NY-BR-1 protein expression was neither detectable in untransfected MCF-7 cells (fig. 5 B, lanes 5,8) nor in MCF-7 cells transfected with the empty pcDNA3.1(-) (fig. 5 B, lanes 4,7). Therefore, similar to our findings in HEK293T cells, NY-BR-1 false positive experssion signals of the empty pcDNA3.1(-) expression vector itself, as well a a potential endogenous NY-BR-1 protein expression in MCF-7 cells, could be excluded. HEK293T cells, transfected with pcDNA3.1(-)NY-BR-1 were included as positive control in this experiment (fig. 5 B, lane 1).

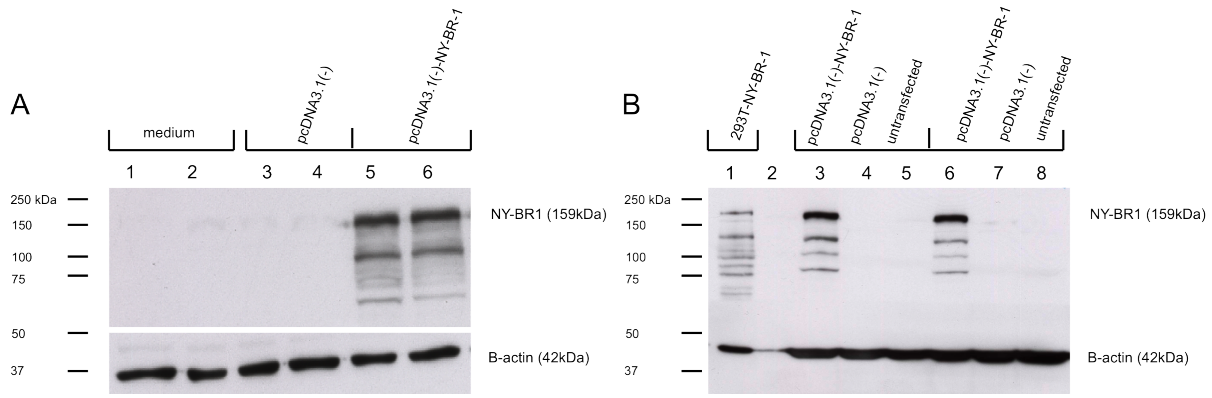

Figure 5: Verification of NY-BR-1 protein expression in transiently transfected human HEK293T cells and MCF-7 cells. A: HEK293T cells, lane 1,2: untransfected cells, **lane 2, 3:** cells transfected with pcDNA3.1(-), **lane 4, 5:** cells transfected with pcDNA3.1(-)NY-BR-1. **B: MCF-7 cells, lane 1:** HEK2937-NY-BR-1 cells, **lane 2, 5:** cells transfected with pcDNA3.1(-), **lane 4, 8:** cells transfected with pcDNA3.1(-)NY-BR-1.

It is important to note that in addition to the NY-BR-1-specific protein band at 160 kDa further protein bands were detected in all NY-BR-1 positive samples.

5.2 Generation of stable EL4-Rob/HHD-NY-BR-1 double transfectants

In order to generate syngeneic cell lines with endogenous NY-BR-1 expression that could be used as stimulator cells for the expansion of HLA-A2-restricted $CD8^+$ T cell lines as well as for investigating HLA-A2-restricted, NY-BR-1-specific CTL responses, we used the murine lymphoma cell line EL4-Rob/HHD which expresses a chimeric HLA-$A2D^b$ molecule as the parental cell lines. However, since EL4-Rob/HHD cells already hold a resistance for neomycin (G418), re-cloning of the NY-BR-1 DNA-sequence from the pcDNA3.1(-)NY-BR-1 constuct, encoding a neomycin resistance, into the pcDNA3.1(-)zeo mammalian expression vector, encoding a zeocin resistance, was performed.

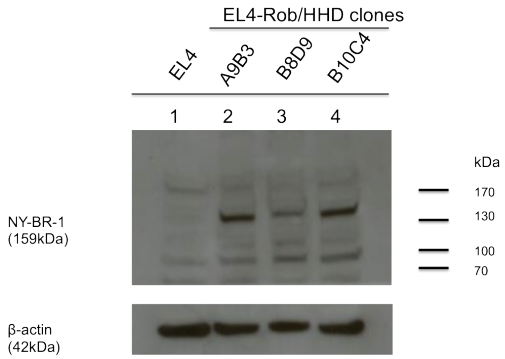

Figure 6: NY-BR-1 protein expression in stable EL4-Rob/HHD transfectants. Stable transfection of EL4-Rob/HHD with pcDNA3.1(-)NY-BR-1zeo, 50 µg of cellular protein in a volume of 20 µl was analyzed for three selected clones. **Lane 1**: EL4 cells, **lane 2**: clone A9B3, **lane 3**: clone B8D9, **lane 4**: clone B10C4

Transfectants with stable NY-BR-1 protein expression were established by limiting dilutions of EL4-Rob/HHD bulk cultures under the selective pressure of 200 µg/ml zeocin. Individual clones obtained by limiting dilutions were screened for NY-BR-1 protein expression. Clones A9B3, B8D9 and clone B10C4 shown as representative results in figure 6. NY-BR-1 protein expression could be detected in clone B10C4 (fig. 6, lane 4) and clone A9B3 (fig. 6, lane 2) whereas it was only to a very low extend detectable in clone B8D9 (fig. 6, lane 3) and not detectable in EL4 cells (fig. 6, lane 1). EL4-Rob/HHD-NY-BR1 clone B10C4 was selected, *in vitro* expanded and cryopreserved for further use, providing a syngeneic murine NY-BR-1-expressing target cell line.

5.3 Generation of stable EL4-NY-BR-1 single transfectants

In vivo tumor models are important to evaluate a translational impact of newly developed T cell lines. The murine lymphoma-blast cell line EL4 was selected as target cell line due to its syngeneic H2 background, thus being suitable for either tumor challenge or tumor protection experiments in C57BL/6 mice. EL4 cells lack murine MHC-II (IA^b) expression on the contrary murine MHC-I molecules ($H2\text{-}D^b$, $H2\text{-}K^b$) are highly expressed on their cell surface. Implantation of EL4-NY-BR-1 transfectants in HLA-tg mice of C57BL/6 background, will allow an evaluation on the contribution of $CD4^+$ HLA-DRB1*0301- /HLA-DRB1*0401-restricted T cells to a $CD8^+$ T cell mediated tumor regression, as well as first insights into the composition of the tumor-miroenvironment regarding a NY-BR-1 positive tumor.

EL4 cells were transfected with a linearized version of the pcDNA3.1(-)zeo to increase transfection efficacy. Next, EL4-NY-BR-1 bulk cultures were further used for the generation of individual El4-NY-BR-1 clones by the process of limiting dilutions. After approximately two weeks, single clones grew out and were expanded *in vitro*. Once enough material was available, NY-BR-1 protein expression was evaluated among the different EL4-NY-BR-1 clones.

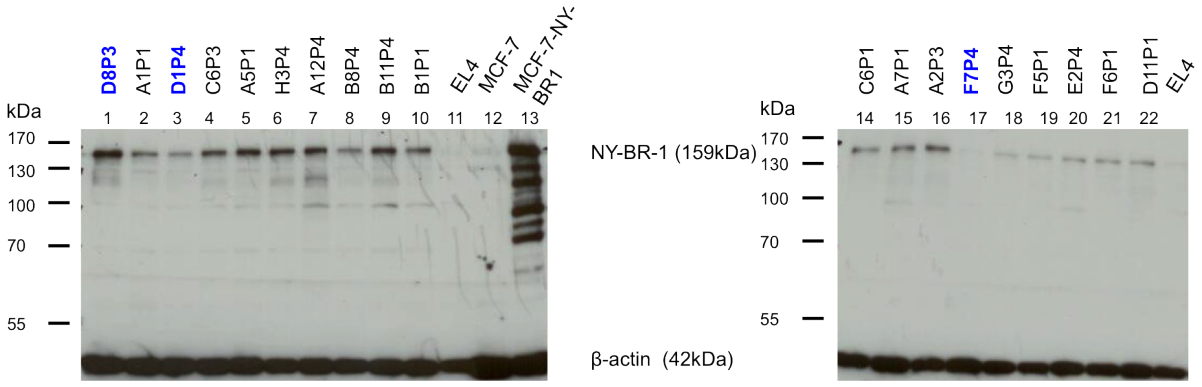

Figure 7: NY-BR-1 protein expression in EL4-NY-BR-1 stable transfectants. NY-BR-1 protein expression was analyzed in indicated individual EL4-NY-BR-1 clones. 15 µg of cellular protein in a volume of 20 µl was analyzed for each sample by Western blot analysis.

Western blot analysis revealed different NY-BR-1 protein expression levels comparing the individual EL4-NY-BR-1 clones (fig. 7). Finally, clone D8P3 was selected as a NY-BR-1^{high}(fig. 7, lane 1) , clone D1P4 was selected as NY-BR-1^{intermediate} (fig.7, lane 3) and clone F7P4 was selected as a NY-BR-1^{low} expressing clone (fig. 7, lane 17) and further expanded i*n vitro*. All remaining clones were cryopreserved and stored in liquid nitrogen. NY-BR-1 protein expression was absent in parental EL4 cells (fig. 7, lane 23). As positive control, NY-BR-1 transfected MCF-7 cells were included in this experiment (fig. 7, lane 13), since NY-BR-1 protein expression was detected previously in MCF-7 cells transfected with pcDNA3.1(-)NY-BR-1 (fig. 5 B).

5.3.1 Expression of MHC molecules on stable EL4-NY-BR-1 transfectant clones

Regarding our attempt to prove the contribution of CD4$^+$ T cells among a CD8$^+$ T cell mediated anti-tumor response, the MHC-phenotype (H2-D^b/K^b IA$^{b-/-}$) of EL4-NY-BR-1 transfectants, was analyzed by immunoflourescent surface molecule staining. Individual EL4-NY-BR-1 clones (D8P3, D1P4, F7P4) were stained with either a murine anti-K^b-specific monoclonal antibody (E3-25), a murine anti-D^b-specific monoclonal antibody (B22.249) or with a IA^b-specific monoclonal antibody. Analysis of acquired flow cytometry data confirmed strong expression of murine H2-K^b, H2-D^b molecules in the tested EL4-NY-BR-1 clones D8P3, D1P4 and F7P4 (fig. 8). However, when comparing the H2-K^b molecule expression levels among the parental EL4 cell line (MFI=786) and the established clones D8P3 (MFI=345), D1P4 (MFI=460) and F7P4 (MFI=399), a reduction of H2-K^b molecule expression levels was observed. Similar tendencies were observed regarding a reduction on expression levels of the H2-D^b molecule, hereby the parental cell line EL4 (MFI=600) and the established clone D8P3 (MFI=533) showed similar expression levels of the H2-D^b molecule. In contrast, H2-Db molecule expression levels were reduced in clones D1P4 (MFI=375) and F7P4 (MFI=305) compared to the parental El4 (MFI=600) cell line (fig. 8).

Reduced expression levels of the surface molecules H2-K^b and H2-D^b among the established EL4-NY-BR-1 transfectants should be considered when using these clones for *in vivo* tumor challenge experiments in mice.

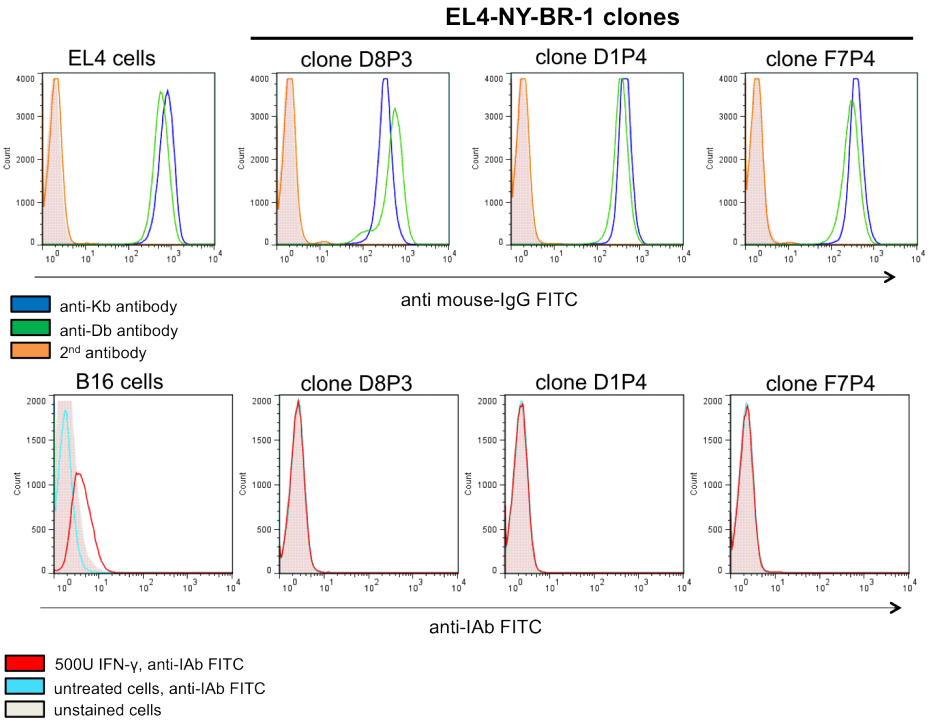

Figure 8: Expression of MHC molecules on stable EL4-NY-BR-1 transfectant clones. EL4-NY-BR-1 transfectants were stained for H2-K^b/D^b expression using the monoclonal antibodies (anti-Kb: E3-25)/(anti-Db: B22.249) detected by an anti-mouse-IgG FITC antibody, and expression of IAb (anti-IA^b-FITC). Cells were treated with 500 U/ml of murine IFN-γ for 48 hrs when indicated.

To test for IA^b molecule expression under the influence of murine IFN-γ, which might be secreted in the tumor microenvironment i*n vivo*, EL4-NY-BR-1 clones were treated with murine IFN-γ prior to flow cytometry staining. Even after IFN-γ treatment, expression of the murine IA^b molecule remained negative for clonal cell line D8P3, D1P4 and F7P4 (fig. 8B) but induced IA^b expression in the murine melanoma cell line B16, which was included as a positive control cell line for IFN-γ induced IA^b expression (fig.8B).

To sum up, selected EL4-NY-BR-1 clonal cell lines D8P3, D1P4 and F7P4 express murine H2-K^b / H2-D^b but no IA^b molecules on the cell surface even upon IFN-γ treatment.

5.4 Identification of NY-BR-1-specific T cell candidate epitopes by using various HLA-transgenic mouse strains

In order to identify novel NY-BR-1-specific HLA-restricted T cell epitopes, three different transgenic mouse strains including HHDtg mice (transgenic for HLA-A*0201), DR3tg mice (transgenic for HLA-DRB1*0301) and DR4tg mice (transgenic for HLA-DRB1*0401) were immunized with global NY-BR-1 antigen, followed by a combinatorial screening of a NY-BR-1-specific peptide library.

The NY-BR-1-specific peptide library was composed of 174 20mers overlapping by 12 aa covering the full length NY-BR-1 protein sequence. Individual library peptides were organized in 26 pools (K1-K13, L1-L13), each pool harboring 13 single library peptides (supplement fig. 44), five library peptides (#24, #146, #166, #171, #173) were not included in the 26 peptide pools (K1-K13, L1-13), but included as single library peptides in the screening process. Upon combinatorial analysis ("matrix screening"), library peptides containing potential NY-BR-1-specific T cell epitopes were determined and further tested as individual library peptides.

Four milestones for the identification of NY-BR-1-specific epitopes in HLAtg mice were defined:

I. Identification of positive NY-BR-1-specific library peptides	**(Milestone I)**
II. Identification of NY-BR-1-specific T cell candidate epitopes in HLA-DR3tg mice and HLA-DR4tg mice	**(Milestone II)**
III. Verification of HLA-restriction of NY-BR-1-specific T cell candidate epitopes	**(Milestone III)**
IV. Verification of processing of NY-BR-1-specific epitopes in human cells	**(Milestone IV)**

Figure 9 shows the workflow on identifying novel NY-BR-1-specific HLA-restricted T cell epitopes using three HLA-tg mouse strains.

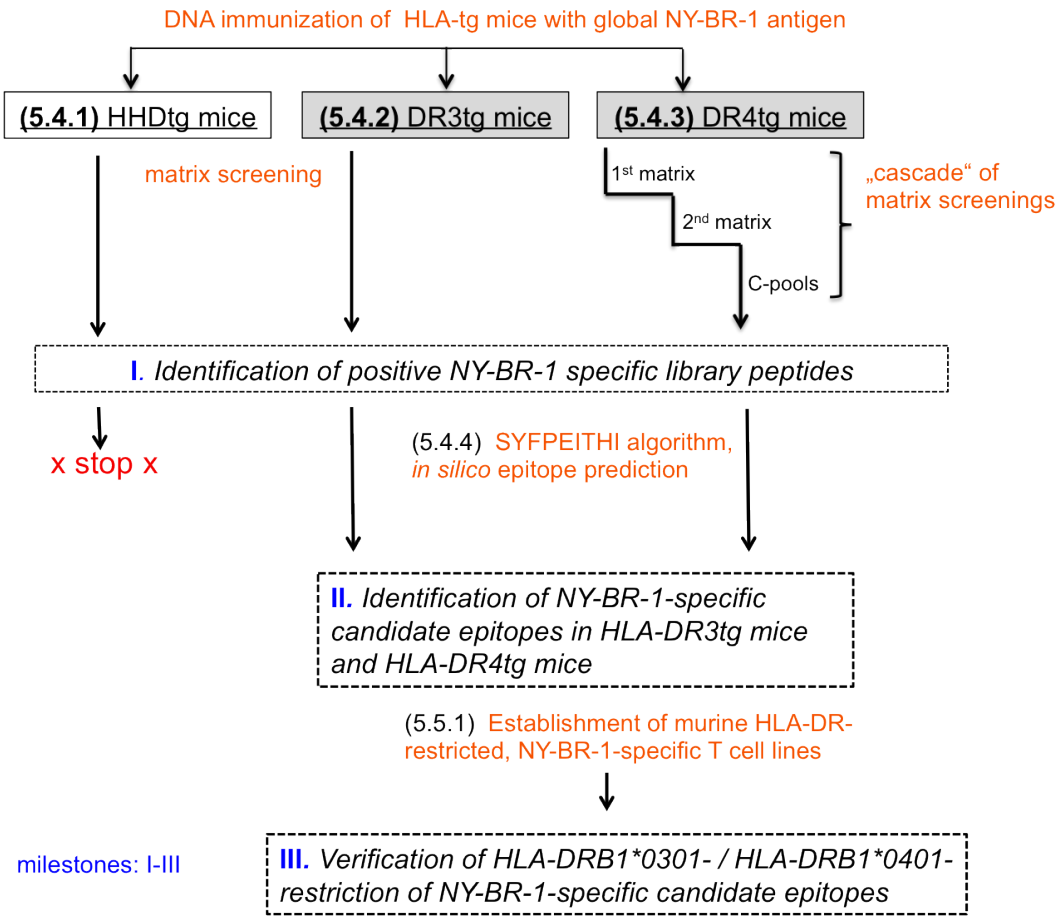

Figure 9: Workflow, identification of NY-BR-1-specific, HLA-restricted T cell epitopes in HLA-transgenic mice. Indicated in blue are the milestones I-III defined for the identification of NY-BR-1-derived $CD4^+$ T cell epitopes in HLA-tg mice.

5.4.1 Identification of positive NY-BR-1-specific library peptides in HHDtg mice

HHDtg mice were immunized either with the pcDNA3.1(-)NY-BR-1 expression vector (recipient mice) or were designated as control group, injected with the empty pcDNA3.1(-) vector. Ten days after immunization, mice were sacrificed and splenocytes, isolated from the immunized mice, could be analyzed for NY-BR-1-specific T cell responses in IFN-γ EliSpot assays. Screening of the NY-BR-1 peptide library resulted in detectable IFN-γ-secretion in 1-2 out of 4 mice, upon stimulation of splenocytes with peptide-pools L1, L3, L5, L7, L10, K2, K6, K10, K11 and K12 (fig.10). Tested peptide library pools showed different immunogenicity when tested with splenocytes obtained from immunized HHDtg mice, since IFN-γ spot numbers varied between 30-40 spots (peptide pools K10, K11, K12 and L7) and were below 30 spots (peptide pools K6, L1, L2 and L10) (fig. 10). Additionally, the already published NY-BR-1-specific, HLA-A*0201 restricted T cell epitopes p158-167 and p960-968 [112] were included in this experiment, however, they did not elicit IFN-γ-secretion among splenocytes obtained from vaccinated HHDtg mice. IFN-γ-secretion was not detectable in any mice of the control group, thus potential immunogenicity of the empty vector

can be considered to be irrelevant in this context (fig. 10).

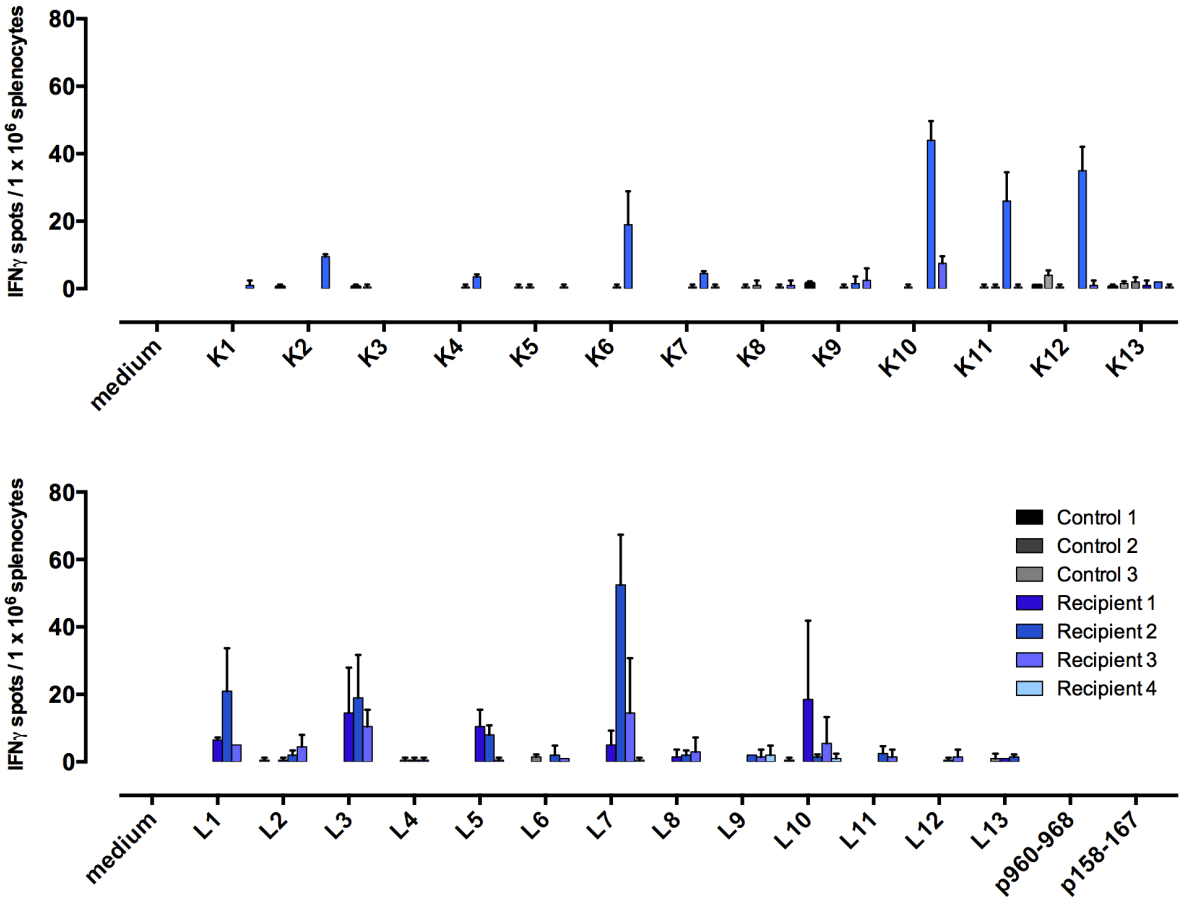

Figure 10: NY-BR-1 peptide library screening with splenocytes of HHDtg mice. IFN-γ EliSpot assay results performed with indicated numbers of splenocytes isolated from DNA vaccinated HHDtg mice. Splenocytes were either incubated for 18 hrs with library peptide pools K1-K13 and L1-L13 or with the known HLA-A*0201, NY-BR-1-specific epitopes #p158-167 and #p160-169. Each column represents one individual mouse; bars, standard error of the mean upon duplicate determination.

As shown in figure 11, following combinatorial analysis, a total of 30 library peptides (25 library peptides identified by combinatorial analysis of the matrix screen and five additional library peptides: #24, #146, #166, #171, #173 which were not included in the first matrix screen) were selected to be tested as individual library peptides in subsequent experiments (fig. 11).

	K1	K2	K3	K4	K5	K6	K7	K8	K9	K10	K11	K12	K13
L1	1	14	27	40	53	66	79	92	105	118	131	144	157
L2	158	2	15	28	41	54	67	80	93	106	119	132	145
L3	174	159	3	16	29	42	55	68	81	94	107	120	133
L4	134	147	160	4	17	30	43	56	69	82	95	108	121
L5	122	135	148	161	5	18	31	44	57	70	83	96	109
L6	110	123	136	149	162	6	19	32	45	58	71	84	97
L7	98	111	124	137	150	163	7	20	33	46	59	72	85
L8	86	99	112	125	138	151	164	8	21	34	47	60	73
L9	74	87	100	113	126	139	152	165	9	22	35	48	61
L10	62	75	88	101	114	127	140	153	170	10	23	36	49
L11	50	63	76	89	102	115	128	141	154	167	11	172	37
L12	38	51	64	77	90	103	116	129	142	155	168	12	25
L13	26	39	52	65	78	91	104	117	130	143	156	169	13

Figure 11: Combinatorial analysis of NY-BR-1 peptide library screening (first matrix) with splenocytes of HHDtg mice. NY-BR-1 library pools which were selected as positive pools due to results obtained in IFN-γ EliSpot assay are depicted in yellow and possible immunogenic NY-BR-1-derived library peptides are depicted in orange.

Due to a limited number of available HHDtg mice for further experiments, no individual tests of active library peptides identified in the first matrix screen (fig. 11), was performed. Instead the potentially activated library peptides determined in the matrix screen were directly submitted to *in silico* analysis, using the SYFPEITHI database (33). According to their SYFPEITHI prediction score, the eighteen first top-scoring predicted HAL-A*0201-restricted, NY-BR-1-specific candidate epitopes were screened as individual library peptides (fig. 12).

aa positiion	predicted epitope (HLA-A201)		library peptide
	sequence	score	
960	SLSKILDTV	28	#120
855	SIPTKALEL	24	#107
1047	KIREELGRI	23	#131
1149	TLKLKEESL	22	#144
1266	NLNYAGDAL	21	#159
593	KINGKLEES	19	#75
74	RTALHWACV	18	#10
286	PLAERTPDT	18	#36
330	SLVEGTSDK	18	#42
525	PAIEMQNSV	18	#66
570	SLCETVSQK	18	#72
179	SITKRSEQI	17	#23
657	LELKNEQTL	16	#83
763	PAIEMQKSV	16	#96
882	PAIEMQKSV	16	#111
1019	KWEQELCSV	16	#127
112	KALQCHQEA	13	#14
139	GNTALHYAV	13	#18
746	DMQTFKAEP	12	#94
943	THQKEMDKI	10	#118
1301	MYQNEQDNV	10	#163
468	FPSESKQEE	5	#59
556	SKQKDYEEN	4	#70

So far screened HLA-A*0201-restricted peptides

Table 33: *In silico* prediction of HLA-A*0201-restricted candidate epitopes. HLA-A*0201-restricted 9mer candidate epitopes were predicted, by using the SYFPEITHI database, for selected NY-BR-1 library peptides as determined by combinatorial matrix screening.

The remaining candidate library peptides #94, #163, #118, #70, #59 as well as the single library peptides not included in the first matrix screening (#24, #146, #166, #171, #173) could not be further investigated due to the limited number of HHDtg mice available.

Nevertheless, first screening of individual library peptides #107, #131, #141 and #120 identified library peptide #107 eliciting a positive IFN-γ response (mean of 25 IFN-γ-spots) (fig.12 A) in one out of three tested mice, NY-BR-1 peptide library pools K10 and L10 were included as technical positive controls in this experiment, since activity of peptide library pools K10 and L10 was observed in the first matrix screening (fig. 10).

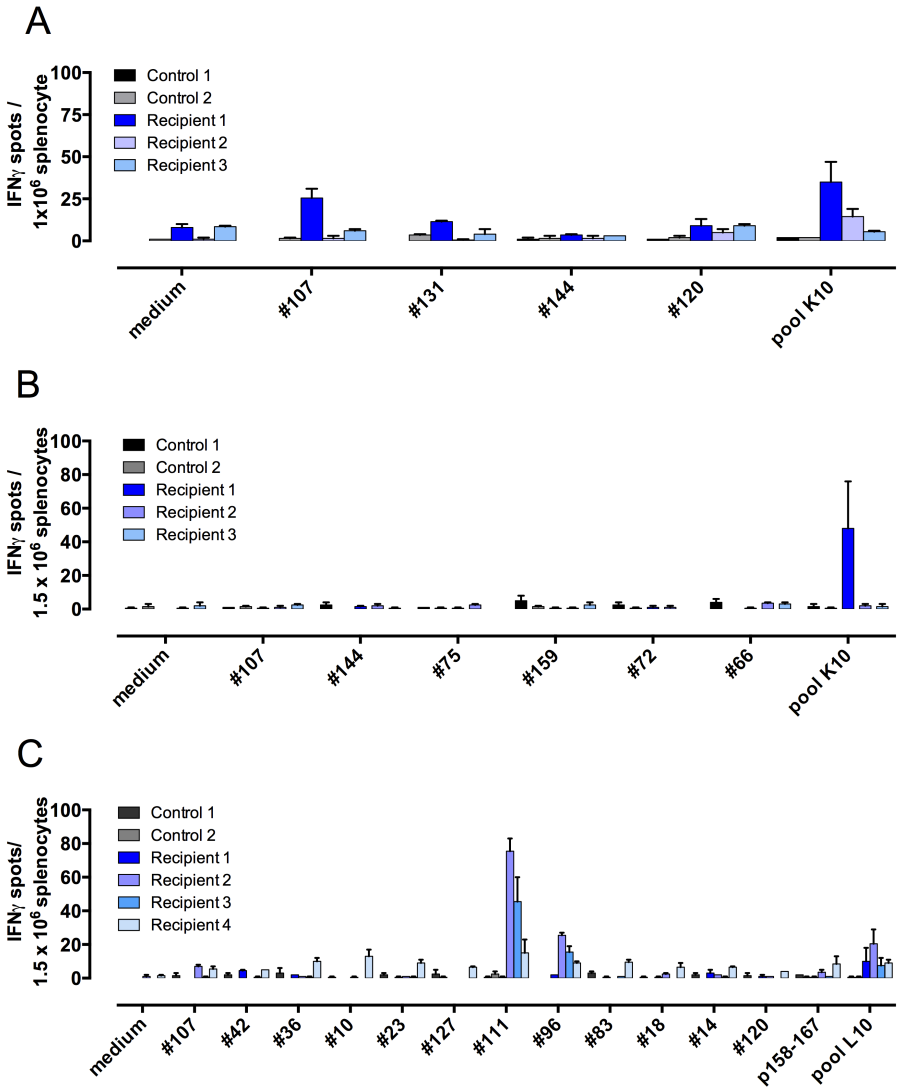

Figure 12: IFN-γ EliSpot results with splenocytes of HHDtg mice employing single NY-BR-1 library peptides. Splenocytes from HHDtg mice immunized with pcDNA3.1(-)NY-BR-1 were isolated and incubated with 2 µg/ml individual library peptides in an IFN-γ EliSpot for 18 hrs. Each column represents one individual mouse; bars, standard error of the mean upon duplicate determination. **Figure 12 A, B, C** represent three individual experiments.

No IFN-γ response could be detected for any of the three mice immunized with the empty

vector pcDNA3.1(-), excluding NY-BR-1-specific immunogenicity of the empty vector itself.

As depicted in figure 12 B, a second screening of individual library peptides with splenocytes obtained from immunized HHDtg mice was conducted, testing individual library peptides #107, #144, #75, #159, #72 and #66. After all, no positive signal could be detected for any of the tested library peptides in this IFN-γ EliSpot assay (fig.12 B). In a third experiment we investigated NY-BR-1 library peptides #107, #42, #36, #10, #23, #127, #111, #96, #83, #18, #14 and #120. IFN-γ secretion was detectable for library peptide #111 and library peptide #96 but not for any other of the remaining NY-BR-1 library peptides (fig.12 C). In conclusion, NY-BR-1 library peptides #111 and #96 should be included in further investigations for the identification of NY-BR-1-specific HLA-A*0201-restricted T cell epitopes. Due to restricted numbers of offsprings resulting in shortage of HHDtg mice, we were not able to carry out further experiments in this mouse strain in the moment, but experiments will continue as soon as suitable numbers of HHDtg mice are available.

Overall, milestone I on identifying probably active NY-BR-1-specific library peptides #96 and #111, was approached by screening a NY-BR-1-specific library in HHDtg mice. However, low response rates in performed IFN-γ EliSpot assays and the lack of reproducibility due to HHDtg mice being not available for further experiments, activity of NY-BR-1-specific library peptides #96 and #111 has to be confirmed in future experiments.

5.4.2 Identification of positive NY-BR-1-specific library peptides in DR3tg mice

In the next step, immunogenicity of the NY-BR-1 antigen was investigated in DR3tg mice. Firstly, DR3tg mice were immunized with the pcDNA3.1(-)NY-BR-1 DNA construct(recipient mice). After 14 days, transgenic mice were sacrificed and IFN-γ EliSpot assay was performed, testing the complete NY-BR-1 peptide library on isolated splenocytes of individual mice. Mice immunized with the empty vector pcDNA3.1(-) served as the control group (control mice). Peptides #24, #146, #166, #171 and #173 were not included in the combinatorial matrix screen but tested as individual peptides later on directly. Out of 26 tested peptide library pools, peptide pools K2, K10, K11, K12, L5, L9, L11, L12 and L13 elicited IFN-γ responses in at least two out of four mice immunized with the pcDNA3.1(-)NY-BR-1 vector but did not induce IFN-γ response in control mice immunized with the pcDNA3.1(-) vector. Remaining peptide library pools K1, K3, K4, K5, K6, K7, K8, K9, L1, L2, L3, L4, L6, L7, L8 and L10 did only induce a marginal IFN-γ response, hence not considered as positive peptide pools (fig.13).

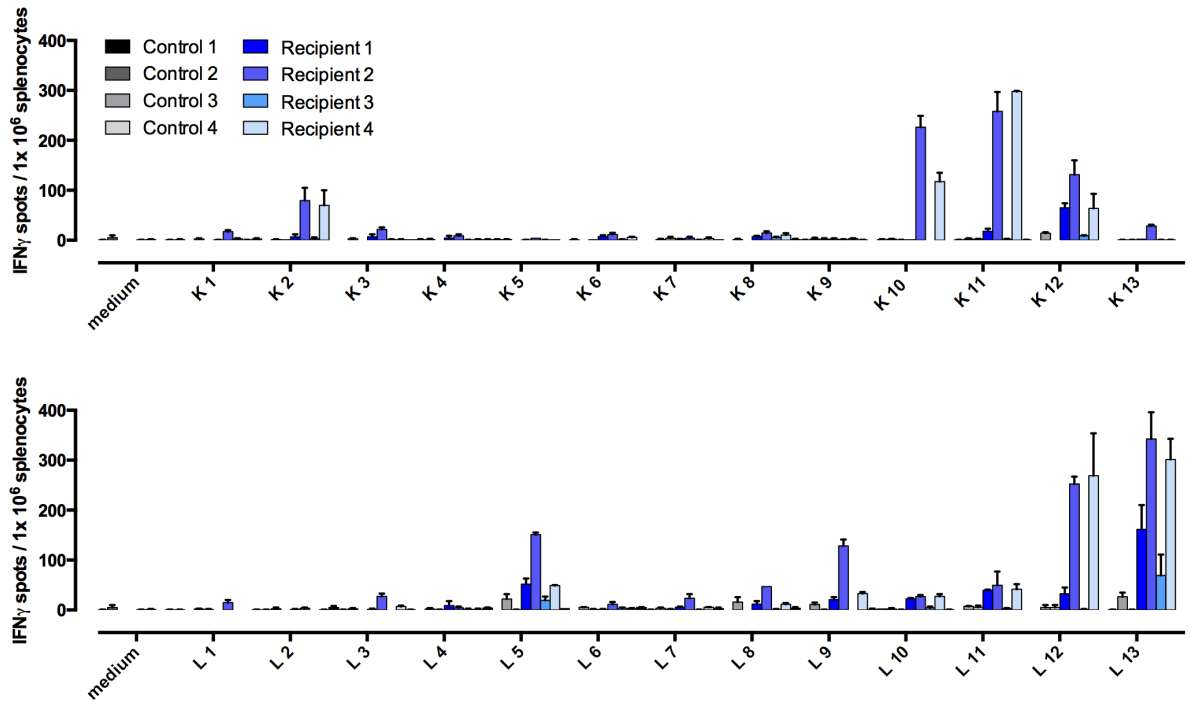

Figure 13: NY-BR-1 peptide library screening with splenocytes of DR3tg mice. IFN-γ EliSpot results on DR3tg splenocytes isolated from DNA vaccinated mice were incubated for 18 hrs with the NY-BR-1 peptide library pools (K1-K13, L1-L13). Each column represents one individual mouse; bars, standard error of the mean upon duplicate determination.

Nine positive pools, namely K2, K10, K11, K12, L5, L9, L11, L12 and L13 were selected and according to the combinatorial peptide matrix system, 20 single potentially immunogenic peptides could be determined (fig. 14)

	K1	K2	K3	K4	K5	K6	K7	K8	K9	K10	K11	K12	K13
L1	1	14	27	40	53	66	79	92	105	118	131	144	157
L2	158	2	15	28	41	54	67	80	93	106	119	132	145
L3	174	159	3	16	29	42	55	68	81	94	107	120	133
L4	134	147	160	4	17	30	43	56	69	82	95	108	121
L5	122	135	148	161	5	18	31	44	57	70	83	96	109
L6	110	123	136	149	162	6	19	32	45	58	71	84	97
L7	98	111	124	137	150	163	7	20	33	46	59	72	85
L8	86	99	112	125	138	151	164	8	21	34	47	60	73
L9	74	87	100	113	126	139	152	165	9	22	35	48	61
L10	62	75	88	101	114	127	140	153	170	10	23	36	49
L11	50	63	76	89	102	115	128	141	154	167	11	172	37
L12	38	51	64	77	90	103	116	129	142	155	168	12	25
L13	26	39	52	65	78	91	104	117	130	143	156	169	13

Figure 14: Combinatorial analysis of NY-BR-1 peptide library screening (first matrix) performed with splenocytes of DR3tg mice. NY-BR-1 peptide library pools which were selected as positive pools due to results obtained in IFN-γ EliSpot assay are depicted in yellow, potential immunogenic individual library peptides are marked in orange.

In the following experiment, 20 library peptides selected upon combinatorial matrix screening in DR3tg mice, namely #11, #12, #22, #35, #39, #48, #51, #63, #70, #83, #87, #96, #135, #143, #155, # 156, #167, #168, #169, #172, and additional five individual library peptides which were not included in the first matrix screened, namely #24, #146, #166, #171 and library peptide #173 were analyzed for recognition by splenocytes of DNA-immunized DR3tg mice. Library peptide #166 was described by others to harbor a published NY-BR-1-specific HLA-DRB1*0301 restricted T cell epitope-sequence [271]. It turned out that peptides #12 and #168 could stimulate an IFN-γ secretion as detected by EliSpot assay in at least 2/4 immunized mice with a range of observed IFN-γ spot numbers between 118 and 161 spots (fig. 15). Mean spot numbers observed were 82-248 IFN-γ-spots upon stimulation of splenocytes originating form DR3tg mice with library peptides #155, #156, #169 and #172 in at least 3/4 immunized DR3tg mice (fig. 15).

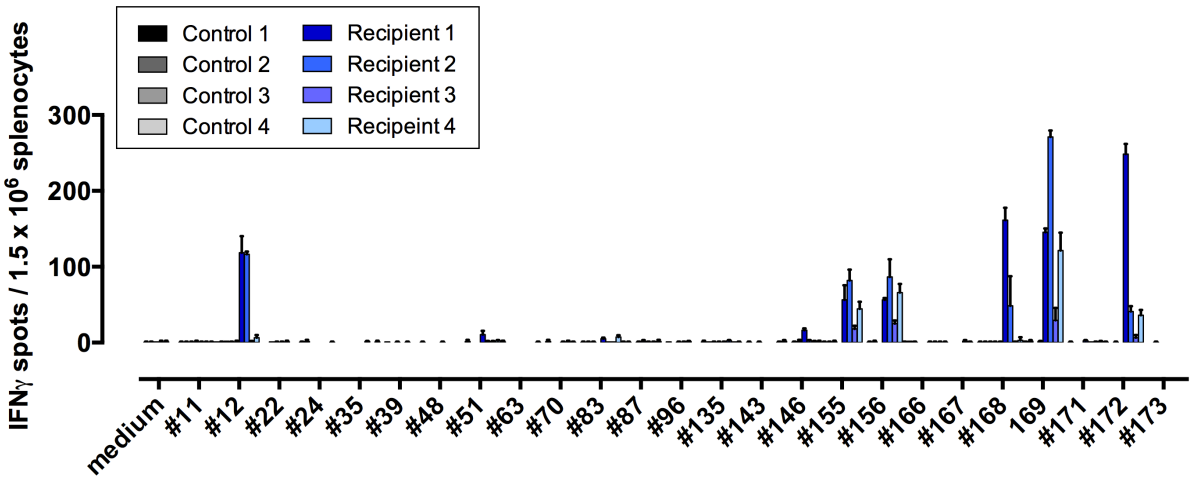

Figure 15: IFN-γ EliSpot results with splenocytes of DR3tg mice employing single NY-BR1 library peptides. 1.5 X 10^6 splenocytes of DNA-vaccinated DR3tg mice were incubated with the respective library peptide for 18 hrs on an IFN-γ EliSpot assay. Each column represents one individual mouse; bars standard error of the mean upon duplicate determination.

In conclusion, library peptides #12, #155, #156, #168, #169 and #172 were considered for further analysis since they represented potential candidates of harboring NY-BR-1-specific, HLA-DRB1*0301-restricted $CD4^+$ T cell epitopes.

Overall, milestone I for DR3tg mice on identifying positive NY-BR-1-specific library peptides was completed by determination of library peptides #12, #155, #156, #168, #169 and #172 as potentially epitope containing NY-BR-1-specific library in DR3tg mice.

5.4.3 Identification of positive NY-BR-1-specific library peptides in DR4tg mice

Similar to the strategy followed for DR3tg mice, DNA-immunized DR4tg mice were divided in two experimental groups: mice immunized with pcDNA3.1(-)NY-BR-1 expression vector (recipient mice) and mice immunized with the empty pcDNA3.1(-) expression vector (control mice). After 14 days, mice were sacrificed and splenocytes of DNA-immunized DR4tg mice were used to screen the NY-BR-1-specific peptide library. As shown in figure 16, peptide pools K3, K4, K8, K10, K11, K13, L2, L3, L4, L5, L6, L7, L8, L9, L10 and L13 were considered positive in stimulating IFN-γ secretion within splenocytes of DNA-immunized DR4tg mice determined by IFN-γ EliSpot assay in at least 1/4 mice. Peptide pools K13 and L3 elicited the greatest IFN-γ response reaching an average of 95-144 IFN-γ-spots in at least 1/4 immunized mice (fig. 16). Overall, splenocytes obtained from recipient mouse two (Recipient 2), elicited greatest IFN-γ-secretion upon incubation with the positive peptide library pools (K3, K4, K8, K10, K11, K13, L2, L3, L4, L5, L6, L7, L8, L9, L10 and L13), when compared to IFN-γ responses obtained with splenocytes originating from the other DR4tg recipient mice. In contrast, IFN-γ secretion was not detected in any member of the control group mice (fig 16).

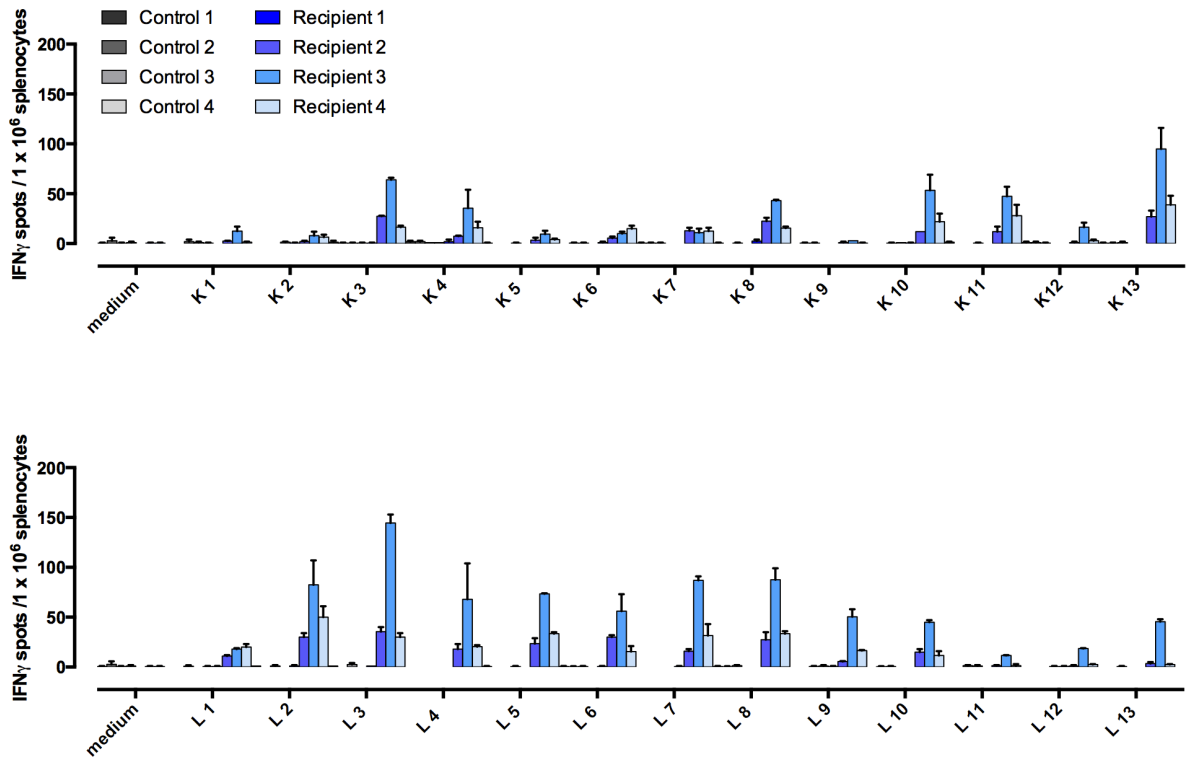

Figure 16: NY-BR-1 peptide library screening with splenocytes of DR4tg mice. IFN-γ EliSpot results on splenocytes isolated from DNA-vaccinated DR4tg mice were incubated for 18 hrs with NY-BR-1 peptide library pools (K1-K13, L1-L13). Each column represents one individual mouse; bars, standard error of the mean upon duplicate determination.

Combinatorial analysis of the results obtained in the first matrix screening with splenocytes of DNA-vaccinated DR4tg mice resulted in a total number of 65 individual library peptides to be screened (60 library peptides resulting from combinatorial analysis of the conducted matrix screen and five additional peptides not included in the initial first matrix screen),(fig. 17).

	K1	K2	K3	K4	K5	K6	K7	K8	K9	K10	K11	K12	K13
L1	1	14	27	40	53	66	79	92	105	118	131	144	157
L2	158	2	15	28	41	54	67	80	93	106	119	132	145
L3	174	159	3	16	29	42	55	68	81	94	107	120	133
L4	134	147	160	4	17	30	43	56	69	82	95	108	121
L5	122	135	148	161	5	18	31	44	57	70	83	96	109
L6	110	123	136	149	162	6	19	32	45	58	71	84	97
L7	98	111	124	137	150	163	7	20	33	46	59	72	85
L8	86	99	112	125	138	151	164	8	21	34	47	60	73
L9	74	87	100	113	126	139	152	165	9	22	35	48	61
L10	62	75	88	101	114	127	140	153	170	10	23	36	49
L11	50	63	76	89	102	115	128	141	154	167	11	172	37
L12	38	51	64	77	90	103	116	129	142	155	168	12	25
L13	26	39	52	65	78	91	104	117	130	143	156	169	13

Figure 17: Combinatorial analysis of NY-BR-1 peptide library screening (first matrix) performed with splenocytes of DR4tg mice. NY-BR-1 library pools which were selected as positive pools due to results obtained in IFN-γ EliSpot assay are depicted in color.

To facilitate screening of the selected 65 candidate library peptides, a second matrix was applied, composed out of 16 pools (A1-A8, B1-B8). Each pool harbored eight individual library peptides, except pools A5-A8 which only contained seven individual library peptides and pool B8 only containing four individual library peptides (fig. 18).

	A 1	A 2	A 3	A 4	A 5	A 6	A 7	A 8
B 1	15	28	80	106	119	145	88	100
B 2	3	16	68	94	107	133	101	113
B 3	160	4	56	82	95	121	153	165
B 4	148	161	44	70	83	109	10	22
B 5	136	149	32	58	71	97	23	35
B 6	124	137	20	46	59	85	49	61
B 7	112	125	8	34	47	73	52	65
B 8	117	143	156	13	PBS	PBS	PBS	PBS

Figure 18: Arrangement of the NY-BR-1-specific second matrix. 65 single NY-BR-1 library peptides were organized in 16 pools (A1-A8, B1-B8). Individual library peptides resulted from the combinatorial analysis of the first matrix screening with splenocytes of DNA-immunized DR4tg mice (fig. 16).

As shown in figure 19, screening of the second matrix by IFN-γ EliSpot assay, identified peptide pools A2, A7, B1 and B6 as truly negative NY-BR-1 peptide pools which were excluded since no IFN-γ-response was observed in any of the recipient mice above an average of 40 IFN-

γ-spots, whereas the remaining peptide pools elicited an average of IFN-γ secretion ranging from 75-316 IFN-γ-spots, in at least 1/4 immunized DR4tg mice (fig. 19). In this particular case, truly negative pools were excluded since data on positive NY-BR-1 peptide pools could only be partially reproduced (supplement figure 45).

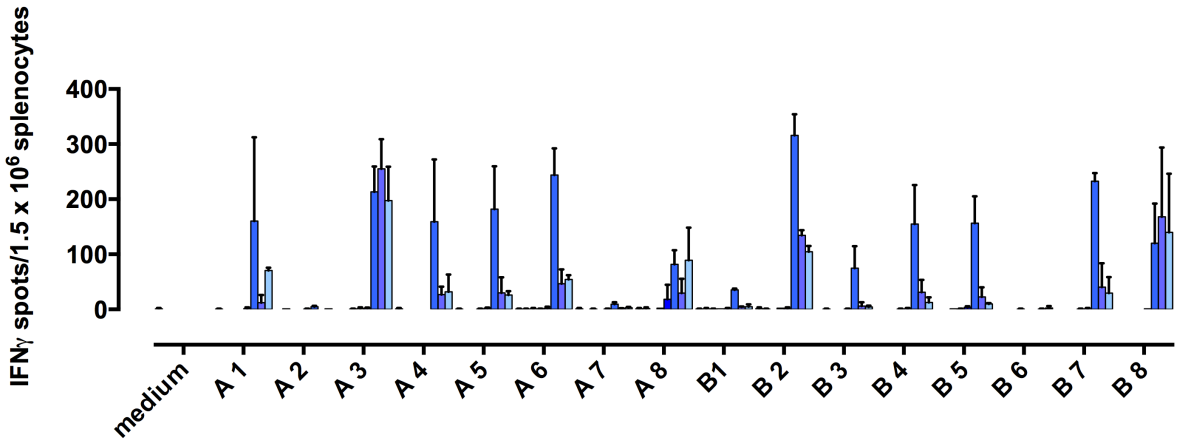

Figure 19: Screening of a second level NY-BR-1-specific library in DR4tg mice. IFN-γ EliSpot assay results on an experiment conducted with splenocytes of DNA vaccinated DR4tg mice. Splenocytes obtained from immunized DR4tg mice were incubated with peptide pools (A1-A7, B1-B8) for 18 hrs. Each column represents one individual mouse; bars, standard error of the mean upon duplicate determination.

As depicted in figure 20, 38 NY-BR-1 library peptides (33 library peptides resulting from combinatorial analysis of the second level matrix screen plus five individual library peptides not included so far in the matrix screen) were selected for further analysis, were identified by combinatorial analysis of the results obtained by screening the second matrix (peptide pools A1-A8, B1-B8) with splenocytes of DNA-immunized DR4tg mice.

	A 1	A 2	A 3	A 4	A 5	A 6	A 7	A 8
B 1	15	28	80	106	119	145	88	100
B 2	3	16	68	94	107	133	101	113
B 3	160	4	56	82	95	121	153	165
B 4	148	161	44	70	83	109	10	22
B 5	136	149	32	58	71	97	23	35
B 6	124	137	20	46	59	85	49	61
B 7	112	125	8	34	47	73	52	65
B 8	117	143	156	13	PBS	PBS	PBS	PBS

Figure 20: Combinatorial analysis of NY-BR-1 peptide library screening (second matrix) performed with splenocytes of DR4tg mice. NY-BR-1 peptide library pools which were selected as positive pools due to results obtained in IFN-γ EliSpot assay (fig. 19) are depicted in yellow, potential immunogenic library peptides are marked in orange.

Given the fact, that the high number of 38 individual library peptides was selected for further screening, these individual NY-BR-1-specific library peptides were organized in a third matrix.

More precisely, the remaining 38 library peptides were organized in pairs of two, composing peptide pools C1-C19 (fig. 34) and subjected to subsequent analysis by IFN-γ EliSpot assay.

peptide pool	library peptides	
C 1	3	68
C 2	94	107
C 3	133	113
C 4	160	56
C 5	82	95
C 6	121	165
C 7	148	44
C 8	70	83
C 9	109	22
C10	136	32

peptide pool	library peptides	
C11	58	71
C 12	97	35
C13	112	8
C14	34	47
C15	73	65
C16	117	156
C17	13	171
C18	173	24
C19	146	166

Table 34: Arrangement of the NY-BR-1-specific third matrix. 38 single NY-BR-1 library peptides were organized in 16 pools (C1-C16). Individual library peptides resulted from screening of the second matrix (fig. 19) with splenocytes of DNA-immunized DR4tg mice.

As depicted in figure 21 A, stimulation of IFN-γ secretion in splenocytes of DR4tg immunized

mice (recipients) was detected for third matrix pools C1, C5, C7, C11, C12 in 4/4 mice with average IFN-γ spot numbers ranging between 40 and 244 spots. Peptide pools C13 and C16 elicited a positive IFN-γ response in at least 1/4 recipient mice, as shown in figure 21 B. However, mean IFN-γ spot numbers determined by EliSpot assay, were low in regard to peptide pool C13 (average 24 IFN-γ-spots). Additionaly, only splenocytes obtained from recipient mouse one (Recipient 1) did elicit a specific IFN-γ response, thus this experiment might not detect all active library peptides containing potential NY-BR-1-specific epitopes due to very low IFN-γ-signals (below an average of 10 IFN-γ-spots) detected among splenocytes obtained from DNA-immunized DR4tg mice.

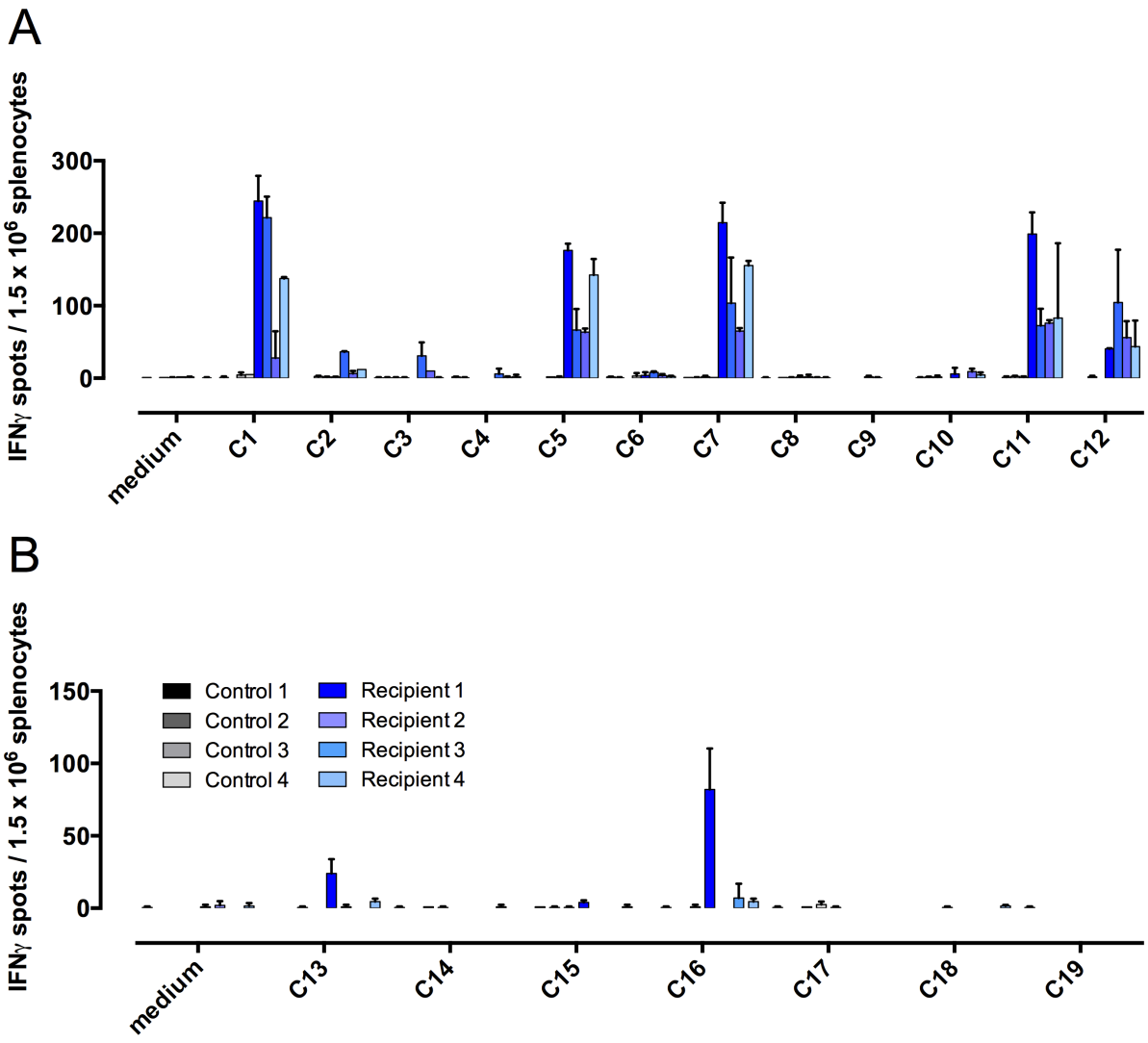

Figure 21: Screening of pools C1-C19 in DR4tg mice. Splenocytes were isolated from DNA vaccinated DR4tg mice and incubated with the respective library pool for 18 hrs on an IFN-γ EliSpot assay. Pools C1-19 were screened in two individual experiments **A:** Screening of pools C1-15, **B:** Screening of pools C16-19. Each column represents one individual mouse; bars, standard error of the mean upon duplicate determination.

Then, we set out to analyze individual library peptides #3, #68, #82, #95, #148, #44, #58, # 71, #97, #35, #112, #8, #117, #156 included in selected positive pools C1, C5, C7, C11, C12, C13 and C16. The results shown in figure 22 indicate immunogenicity of individual library peptides #58, #68, #82 and #97 in 2/4 immunized DR4tg mice with mean IFN-γ spot numbers ranging from 10-57 IFN-γ spots (fig. 22 A, B). Upon stimulation of splenocytes obtained from immunized DR4tg mice, with library peptide #112, a positive IFN-γ response between 172-252 IFN-γ-spots was observed (fig. 22 C). Library peptide #156 elicited a positive IFN-γ response with a mean spot number of 91 IFN-γ-spots in 1/4 immunized DR4tg mice, when incubated with splenocytes obtained from these mice (fig. 22 D). Furthermore, we could detecte a positive IFN-γ-response upon incubation of splenocytes obtained from immunized DR4tg mice, with library peptide #112. Subsequently, the five library peptides #68, #82, #97, #112 and #156 were considered as candidate library peptides potentially containing a NY-BR-1-specific, HLA-DRB1*0401-restricted $CD4^+$ T cell epitopes. Library peptide #58 was so far not further investigated due to technical difficulties but will be included in future experiments.

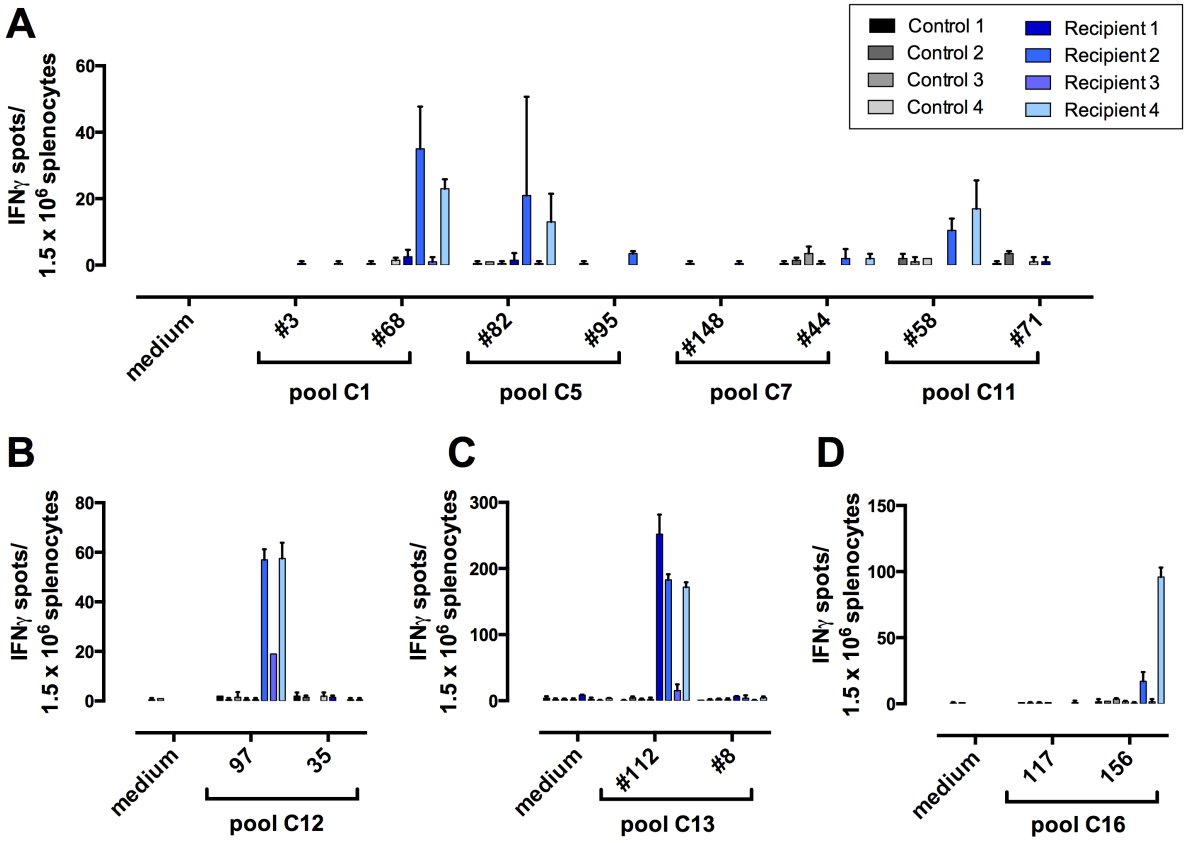

Figure 22: IFN-γ EliSpot results with splenocytes of DR4tg mice employing single NY-BR1 library peptides. IFN-γ EliSpot assay was performed with splenocytes obtained from DNA-immunized DR4tg mice, which were incubated with the indicated library peptides for 18 hrs **(A-D)**. Each column represents one individual mouse; bars, standard error of the mean upon duplicate determination.

We identifying positive NY-BR-1-specific library peptides #58, #68, #82, #97, #112 and #156 which potential harbor NY-BR-1-specific epitopes, by screening a NY-BR-1-specific library in DR4tg mice, thus milestone I was reached.

5.4.4 *In silico* prediction of HLA-DRB1*0301 and HLA-DRB1*0401-restricted NY-BR-1-specific CD4$^+$ T cell candidate epitopes

Potential HLA-DRB1*0301- and HLA-DRB1*0401- restricted CD4$^+$ T cell epitopes contained in NY-BR-1-specific library peptides determined by screening a NY-BR-1-specific peptide library with splenocytes of DNA-immunized DR3tg mice (5.4.2) and DNA-immunized DR4tg mice (5.4.3), were predicted *in silico* by the SYFPEITHI database (fig.35).

The SYFPEITHI algorithm scoring system evaluates the likelihood of binding of a epitope motive to a given anchor position within the MHC-molecule. Among described natural T cell epitopes, the MHC-I-restricted epitope GILGFVFTL, which is derived rom the influenza A matrix protein scores 30 which can be considered as a reference value for "high" SYFPEITHI algorithm scores for HLA-A*02-restricted CTL epitopes. The natural processed MHC-II-restricted epitope $Trp2_{149\text{-}163}$ [183] which is derived from the melanoma differentiation antigen Trp2, scores 21 when submitted to the SYFPEITHI epitope prediction algorithm.

As depicted in table 35 A, analyzing the *in silico* prediction-results of the SYFPEITHI algorithm regarding HLA-DRB1*0301-restricted T cell epitopes contained in the selected NY-BR-1-derived library peptides #12, #169, #155 and #156, poteintial HLA-DRB1*0301-restricted T cell candidate epitopes could be identified. In the case of library peptide #12, prediction of a HLA-DRB1*0301-restricted epitope BR1-88 (prediction score 34) requires an additional vain-residue at aa position 88 to the original library peptide sequence. Library peptide #169 contains the predicted HLA-DRB1*0301-restricted candidate epitope BR1-1347 (prediction score 22). Library peptides #155 and #156 are predicted to contain a H2-D^b restricted CTL epitope, which could be considered as internal control peptide in HLA-transgenic mice with a H2b background. With a SYFPEITHI algorithm score of 15 in case of library peptide #155 and a SYFPEITHI algorithm score of 13 for library peptide #156, both NY-BR-1-derived library peptides are predicted by the SYFPEITHI algorithm with low probability to contain HLA-DRB1*0301-restricted, NY-BR-1 specific T cell epitopes. Even though SYFPEITHI algorithm scores are rather low for NY-BR-1-derived library peptides #155 and #156, the corresponding library peptides were recognized after global NY-BR-1-specific DNA-vaccination in DR3tg mice (fig. 15). Hence, the possible contribution of HLA-DRB1*0301-restricted epitopes BR1-1238 and BR1-1245, contained in library peptides #155 and #156, to positive IFN-γ response determined by EliSpot assay was further investigated. Library peptide #168 was predicted to comprise candidate epitope BR1-1339 (prediction score 18) whereas candidate epitope BR1-1370 (prediction score 17) is located in the aa sequence of

library peptide #172. Both NY-BR-1-derived epitopes were not further investigated in this work due to limited financial resources but will be included into future experiments.

A

library peptide		predicted epitope (HLA-DRB1*0301-restricted)		
no.	sequence[1]	aa position	**score**	designation
#12	**(V)**^{89}**VTFLVDRKCQLDVL**DGEHRT^{108}	88-102	34	BR1-88
#155	^{1233}RKMNV**DVSSTIYNNEVLHQP**^{1252}	1238-1252	15	BR1-1238
#156	^{1241}STIY**NNEVLHQPLSEAQRK**S^{1260}	1245-1259	13	BR1-1245
#168	^{1337}LV**HAHKKADNKSKITID**IHF^{1356}	1339-1353	18	BR1-1339
#169	^{1345}DN**KSKITIDIHFLERKM**QHH^{1364}	1347-1361	22	BR1-1347
#172	^{1369}K**NEEIFNYNNHLKNRI**YQYE^{1388}	1370-1384	17	BR1-1370

B

library peptide		predicted epitope (HLA-DRB1*0401-restricted)		
no.	sequence[1]	aa position	**score**	designation
#68	^{537}**AFELKNEQTLRADPM**FPPES^{556}	537-551	26	BR1-537
#82	^{649}QKSVPNK**ALELKNEQTLRAD**^{668}**(EI)**	656-670	26	BR1-656*
#97	^{769}KSVPNK**ALELKNEQTLRADE**^{788}**(I)**	775-789	26	BR1-775*
#112	^{889}SVPNK**ALELKNEQTLRADQM**^{908}	894-908	26	BR1-894
#156	^{1241}S**TIYNNEVLHQPLSEA**QRKS^{1260}	1242-1256	20	BR1-1242

Table 35: *In silico* **prediction of NY-BR-1-specific T cell epitopes among previously identified NY-BR-1-derived library peptides.** Predicted HLA-DRB1*0301 (A) and HLA-DRB1*0401 (B) restricted, NY-BR-1-specific epitopes are typed in bold; N-terminal and C-terminal amino acid positions are typed in superscript; D^b-restricted $CD8^+$ T cell epitopes are underlined (*Vormehr, unpublished*); *synthetic candidate epitopes with identical aa sequences derived from repetitive stretches within primary sequence of the NY-BR-1 protein; amino acid residues added to the original library peptide sequence are shown in brackets.

As shown in table 35 B, high scoring HLA-DRB1*0401-restricted epitopes were predicted in library peptide #68, #82, #97 and #112. Library peptide #68 harbors the predicted HLA-

DRB1*0401-restricted candidate epitope BR1-537 (prediction score 26). Notably, peptides #82 and #97 are located in a repetitive sequences of the NY-BR-1 protein, thus the predicted candidate epitope BR1-656/-775 (prediction score 26) is identical for these two library peptides. Furthermore, the HLA-DRB1*0401-restricted NY-BR-1-derived epitope BR1-1242 was predicted to be located in the amino acid sequence of library peptide #155 (prediction score 20). NY-BR-1-derived $CD4^+$ T cell epitopes BR1-894, harbored in library peptide #112, so far could not be investigated due to limited financial resources, but will be investigated more thoroughly in future experiments.

To sum up, predicted 15mer NY-BR-1-specific, HLA-DRB1*0301-restricted candidate epitopes BR1-88, BR1-1238, BR1-1347 and HLA-DRB1*0401-restricted candidate epitopes BR1-537, BR1-656/-775, BR1-1242 were synthesized and used for further analysis (fig. 35).

5.4.5 Detection of $CD4^+$ T cells specific for the NY-BR-1-specific candidate epitopes in HLA-DRB1*0301- and HLA-DRB1*0401-transgenic mice

Splenocytes originating from DR3tg mice which were DNA-vaccinated with global NY-BR-1 antigen, elicited a positive IFN-γ response in at least 1/4 mice upon stimulation with 15mer candidate epitopes BR1-88, BR1-1238 and BR1-1347, whereby intensity of induced IFN-γ response, indicated by columns (mean of duplicate determination; bars, standard error of the mean) differed regarding individual mice as well as regarding the three tested candidate epitopes. Mean spot numbers observed were 50-100 spots in 1/3 mice for candidate epitope BR1-88, 180-250 spots in 2/4 mice for candidate epitope BR1-1238 and 100-280 spots in 3/4 mice for candidate epitope BR1-1347. No NY-BR-1-specific IFN-γ response was induced in splenocytes of control mice immunized with the empty pcDNA3.1(-) vector, upon stimulation with candidate epitopes BR1-88, BR1-1238 and BR1-1347 (fig. 23 A).

As shown in figure 23 B, splenocytes originating from DR4tg mice, DNA vaccinated with global NY-BR-1 antigen, were tested for eliciting an IFN-γ response upon stimulation with candidate epitopes BR1-537, BR1-656/-775 and BR1-1242. IFN-γ responses was detectable following stimulation of splenocytes with candidate epitopes BR1-537, BR1-656/-775 and BR1-1242. Candidate epitope BR1-656/-775 elicited an IFN-γ responses ranging from 100-250 spots in 3/4 mice responding, spot numbers observed for candidate epitope BR1-1242 showed a greater diversity regarding immunized mice showing 50-150 spots in 3/4 mice. The range of spot numbers observed for candidate epitope BR1-537 was 100-200 spots with 3/4 mice responding (fig. 23 B).

True for both, experiments performed, as shown in figure 23 A, B, candidate epitopes investigated in this experiment, did not generate a significant NY-BR-1-Specific IFN-γ signal in any of

the control mice immunized with the pcDNA3.1(-) construct (fig. 23 A, B).

Experiments were performed at least three times for each transgenic mouse strain and repeatedly revealed similar results, indicating a NY-BR-1-specific IFN-γ secretion upon stimulation of murine splenocytes with the candidate epitopes BR1-88, BR1-1238 and BR1-1347 in DR3tg mice and candidate epitopes BR1-537, BR1-656/-775 and BR1-1242 in DR4tg mice. Peptides BR1-1245, BR1-1339 and BR1-1370 were not included in IFN-γ EliSpot assays and will be investigated in future experiments.

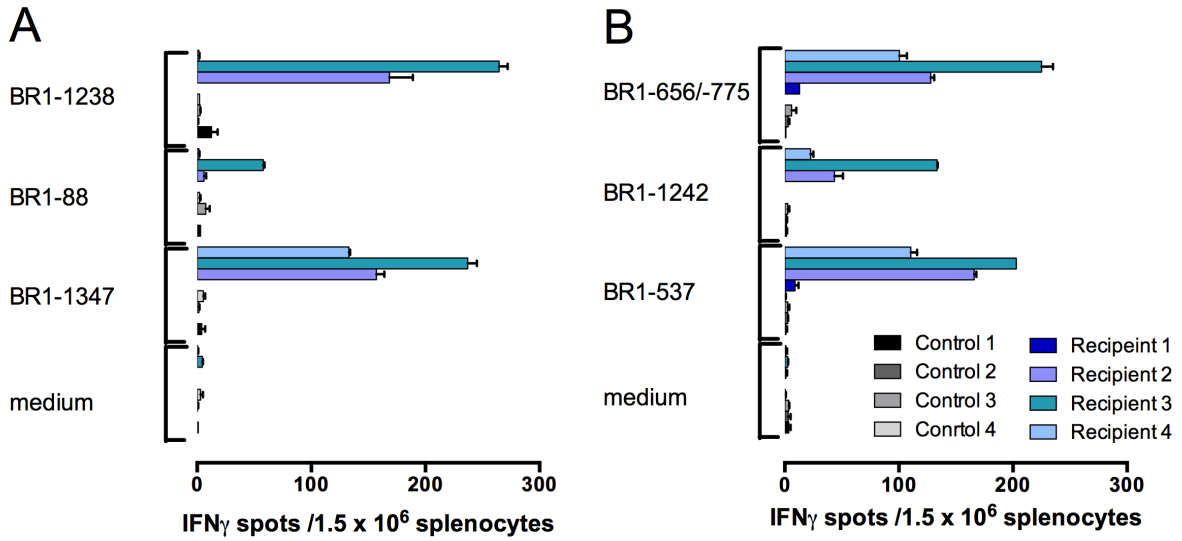

Figure 23: Recognition of NY-BR-1-specific candidate epitopes by splenocytes originating from DR3tg and DR4tg mice. Splenocytes of DR3tg mice **(A)** and DR4tg mice **(B)** DNA-immunized with global NY-BR-1 antigen, were isolated and incubated with the indicated 15mer NY-BR-1-specific candidate epitope for 18 hrs. Each column represents one individual mouse; bars, standard error of the mean upon duplicate determination.

To determine the $CD4^+$ phenotype of the IFN-γ secreting splenocytes upon stimulation with the indicated candidate epitope *in vitro*, IFN-γ secretion assays together with (FACS) immunofluorescence staining of the IFN-γ secreting cells, were performed. $CD4^+$IFN-γ^+ splenocytes were detectable in DNA-immunized DR3tg mice following stimulation of splenocytes with candidate epitopes BR1-1347 and BR1-1238 with frequencies of $CD4^+$IFN-γ^+ cells rangeing from 0.15% to 2.75%. Whereas in control mice immunized with the empty vector, frequencies of $CD4^+$IFN-γ^+ cell were maximum 0.18% (fig. 24 A). Splenocytes of only one immunized DR3tg mouse, which were stimulated with candidate epitope BR1-88, did show a distinct population of $CD4^+$IFN-γ^+ splenocytes with a frequency of 0.17%. However, the epitope BR1-88 was still considered in further experiments, since frequencies of $CD4^+$IFN-γ^+ splenocytes upon stimulation with peptide BR1-88 were higher in recipient mice than among splenocytes isolated from mice immunized with pcDNA3.1(-), (fig. 24 A).

In DR4tg mice, stimulation of HLA-DRB1*0401-transgenic splenocytes with candidate epi-

topes BR1-537 and BR1-656/-775 but not with candidate epitope BR1-1242 resulted in the stimulation of CD4$^+$IFN-γ^+ T cells, detectable by immunoflourescent staining (fig. 24 B). Maximum frequency of CD4$^+$IFN-γ^+ T cells of 0.25% was detected among splenocytes, obtained from an immunized DR4tg mice upont stimulation of the splenocytes with peptide BR1-656/-775. Detected amounts of CD4$^+$IFN-γ^+ T cells were always lower in control mice immunized with pcDNA3.1(-) when compared to amounts of CD4$^+$IFN-γ^+ T cells detected in immunized DR4tg mice (fig. 24 B).

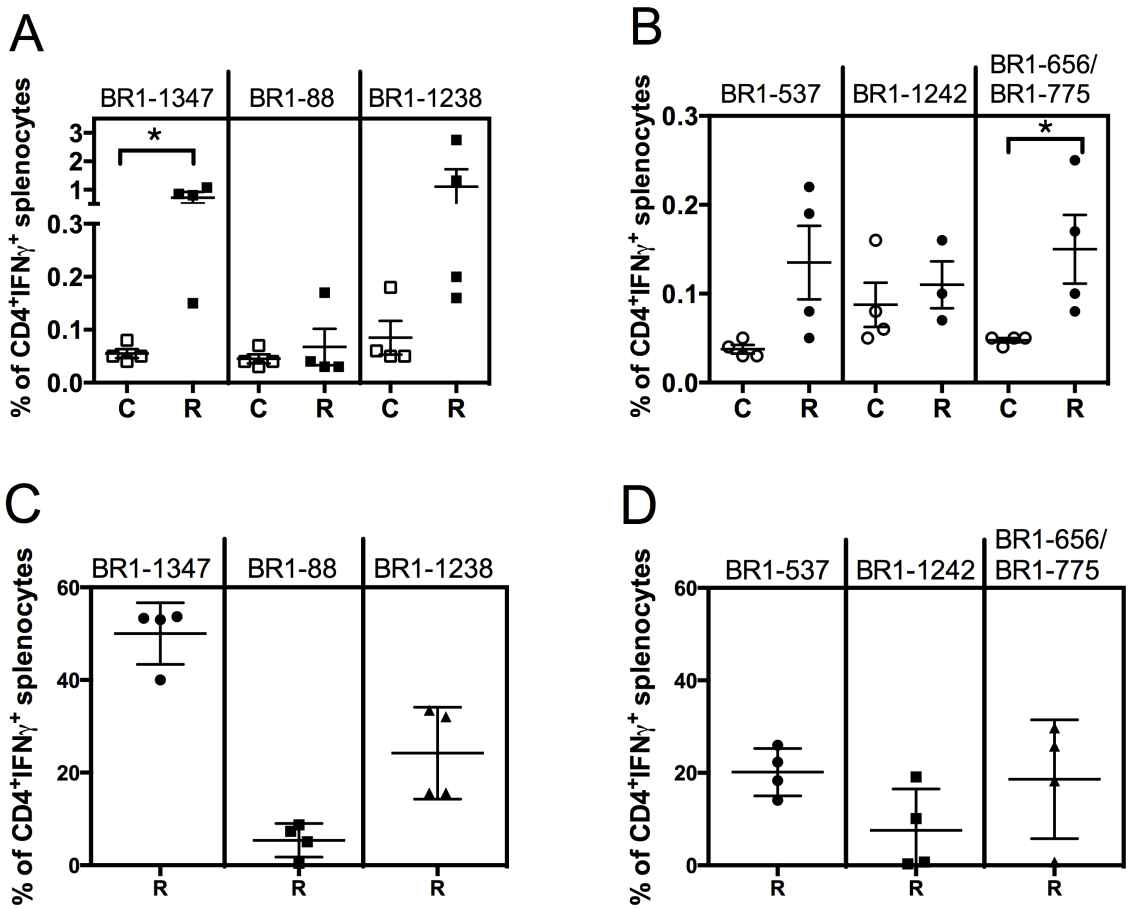

Figure 24: Detection of NY-BR-1-specific CD4$^+$IFN-γ^+ T cells in splenocytes of HLA-DRtg mice. IFN-γ secretion assay results upon stimulation of splenocytes originating from DR3tg mice (**A, C**) and DR4tg mice (**B, D**), immunized with global NY-BR-1 antigen. Splenocytes were stimulated during the assay with the indicated NY-BR-1-specifc candidate epitopes. Samples were enriched for IFN-γ positive cells in DR3tg mice (**C**) and DR4tg mice (**D**) by magnetic sorting. Results are presented as percentag of CD4$^+$IFN-γ^+cell popultions among all viable cells. (Statistic analysis: unpaired t test, significant (*) if $P < 0.05$)

Furthermore, CD4$^+$IFN-γ^+ T cell responses were investigated by a modified IFN-γ secretion assay which includes an enrichment step for IFN-γ-secreting cells. Results obtained from this assay showed that NY-BR-1-specific CD4$^+$IFN-γ^+ T cell among splenocytes of vaccinated DR3tg mice could be enriched up to 53.68% for CD4$^+$ T cells specific for the candidate epitope BR1-1347 and up to 33.48% for CD4$^+$ T cells specific for candidate epitope BR1-1238 (fig. 24 C). In line

with with our findings obtained in the classical IFN-γ secretion assay, amounts of $CD4^+$IFN-γ^+ T cells specific for the promiscuous epitope BR1-88 were very low, thus even after enrichment, the amount of detected $CD4^+$IFN-γ^+ T cells specific for peptide BR1-88 was at maximum 8.74% among total $CD4^+$ T cells (fig. 24 C).

As shown in figure 24 D, NY-BR-1-specific $CD4^+$IFN-γ^+ T cell among splenocytes of vaccinated DR4tg mice, could be enriched for $CD4^+$ T cells specific for candidate epitope BR1-537 up to 25.96% and for candidate epitope BR1-656/-775 up to 29.72% (fig. 24D). Regarding peptide, BR1-1242, peptide-specific $CD4^+$IFN-γ^+ T cells among splenocytes of vaccinated DR4tg mice, could be enriched up to 19.15%.

To sum up, antigen-specific $CD4^+$IFN-γ^+ T cells among splenocytes of vaccinated HLA-DRtg mice could be enriched by the modified IFN-γ secretion assay (fig. 24 C, D), which includes an enrichment step for IFN-γ-secreting cells, thus overall confirming our results obtained with the classical IFN-γ-secretion assay (fig. 24 A, B).

In conclusion, $CD4^+$IFN-γ^+ T cells specific for candidate epitopes BR1-88, BR1-1238 and BR1-1347 could be identified in vaccinated DR3tg mice, whereas $CD4^+$IFN-γ^+ T cells specific for candidate epitopes BR1-537, BR1-656/-775 and BR1-1242 could be identified in vaccinated DR4tg mice. Overall, Milestone II, regarding the identification of NY-BR-1-specific candidate epitopes in DR3tg mice and DR4tg mice was accomplished. Furthermore, we confirmed, that the newly identified NY-BR-1-derived candidate epitopes elicit a $CD4^+$ T cell dependent immune response among splenocytes of DNA-vaccinated, DR3tg mice and DR4tg mice.

5.4.6 Detection of $CD8^+$ T cells specific for NY-BR-1 in DR3tg mice and DR4tg mice

Interestingly, we also observed a NY-BR-1-specific $CD8^+$ T cell response upon stimulation of splenocytes, obtained from DR3tg mice, DNA-vaccinated with global NY-BR-1 antigen, with candidate epitopes BR1-1347 and BR1-1238 (fig. 25A). In splenocytes obtained from DR4tg mice vaccinated with global NY-BR-1 antigen, a NY-BR-1-specific, $CD8^+$ T cell response was observed following stimulation of these splenocytes with candidate epitope BR1-656/-775 in one mouse of four mice (fig. 25B). When stimulating HLA-DRB1*0401-transgenic splenocytes with candidate epitopes BR1-537 and BR1-1242, no NY-BR-1-specific, $CD8^+$ T cell dependent IFN-γ response was observed.

Given the foregoing results on detecting NY-BR-1-specific, $CD8^+$ T cell responses in DR3tg mice, upon stimulation of splenocytes with the 15mer candidate epitope, we investigated the presence of H2-K^b/D^b-restricted NY-BR-1-specific epitopes within the amino acid sequence of

the tested candidate epitopes. In fact, one NY-BR-1 specific, D^b-restricted CTL epitope (amino acid position: NY-BR-$1_{p1242\text{-}1249}$) contained in the amino acid sequence of candidate epitope BR1-1238 (*Vormehr unpublished data*) was described. We postulate, that the newly identified NY-BR-1 specific, D^b-restricted CTL epitope is processed out of the 15mer candidate epitope therefore stimulating a NY-BR-1-specific $CD8^+$ T cell response *in vivo*. Interestingly, we so far could not identify a $H2^b$-restricted CTL epitope harbored in the amino acid sequence of the 15mer library peptide BR1-1347. Even though, as shown in figure 25 A, $CD8^+$ T cells were detected upon stimulation of splenocytes obtained from immunized DR3tg mice with library peptide BR1-1347. Hence, we assume the presence of a $H2^b$-restricted CTL epitope in the amino acid sequence of library peptide BR1-1347 which will have to be further investigated in future experiments. Overall, further experiments, investigating immunogenicity of the newly identified NY-BR-1 specific, $H2^b$-restricted CTL epitope are currently performed in the group of Prof. Eichmueller.

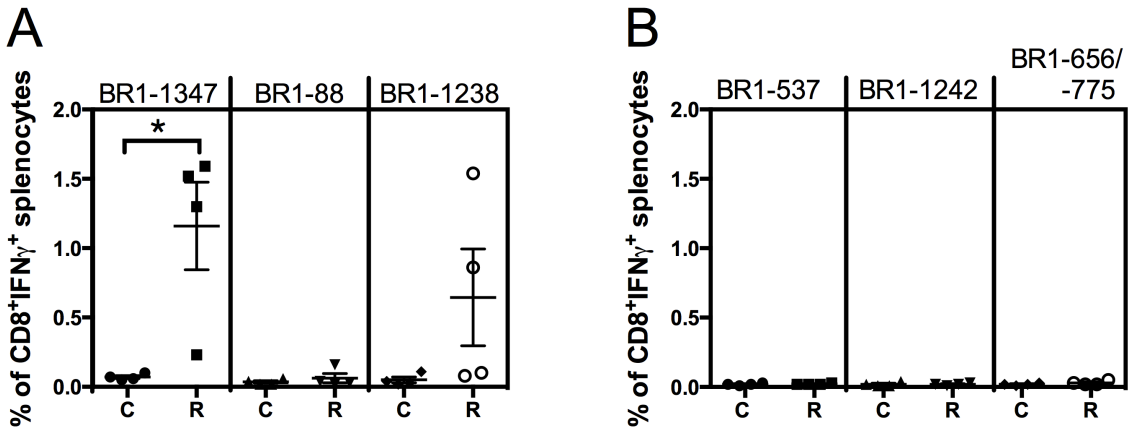

Figure 25: Detection of NY-BR-1-specific, $CD8^+$IFN-γ^+ T cells in splenocytes of HLA-DRB1*0301-/DRB1*0401-transgenic mice. IFN-γ secretion assay results on stimulation of splenocytes originating from DR3tg mice (**A**) and DR4tg mice (**B**), vaccinated with global NY-BR-1 antigen, with the indicated NY-BR-1-derived peptide. Results are presented as percentage of $CD8^+$IFN-γ^+ cell populations. (Statistic analysis: unpaired t test, significant (*) if $P < 0.05$)

5.5 Verification of HLA-DRB1*0301-restriction / HLA-DRB1*0401-restriction of identified NY-BR-1-specific candidate epitopes

5.5.1 Establishment of NY-BR-1-specific, HLA-DRB1*0301- and HLA-DRB1*0401-restricted murine CD4$^+$ T cell lines

In order to establish murine CD4$^+$ T cell lines, DR3tg mice were immunized once with 100 µg peptide of candidate epitopes BR1-88, BR1-1238 or BR1-1347. Individual DR4tg mice were injected with 100 µg peptide of candidate epitopes BR1-537, BR1-656/-775 or BR1-1242. After 13 days splenocytes isolated of immunized DR3tg-/ DR4tg- mice were pooled and cultured in T cell medium supplemented with 0.2 µg/ml of the respective peptide together with irradiated syngeneic feeder cells. After repeatedly restimulation, CD4$^+$ T cell lines specific for candidate epitopes BR1-88, BR1-1347, BR1-537, BR1-656/-775 and BR1-1242 were successfully expanded *in vitro*. Unfortunately, no CD4$^+$ T cell line specific for the candidate epitope BR1-1238 could be established due to poor proliferation capacity of cells and subsequent loss of viable cells in culture.

Flow cytometry analysis was performed to prove a CD4$^+$ phenotype of the newly generated T cell lines BR1-88, BR1-1347, BR1-537, BR1-656/-775 and BR1-1242. Immunoflourescent staining of CD4$^+$ T cell lines was performed by staining the cells using flourochrome-coupled antibodies directed against the surface molecules CD4 and CD8, signals were detected by flow cytometry. T cell lines BR1-88, BR1-1347, BR1-537 and BR1-1242 show a single CD4$^+$ cell population with frequencies of 99%, 98.9%, 96.7%, 97.8 when gated on the lymphocyte population (fig. 26).

As shown in figure 26, T cell line BR1-656/775 not only consists out of a CD4 positive population with a frequency of 64.5%, but also appears to have a CD4$^-$CD8$^-$ cell population within the lymphocyte gate. The specific phenotype of the CD4 negative cell population among the T cell line BR1-656/-775 needs to be further investigated.

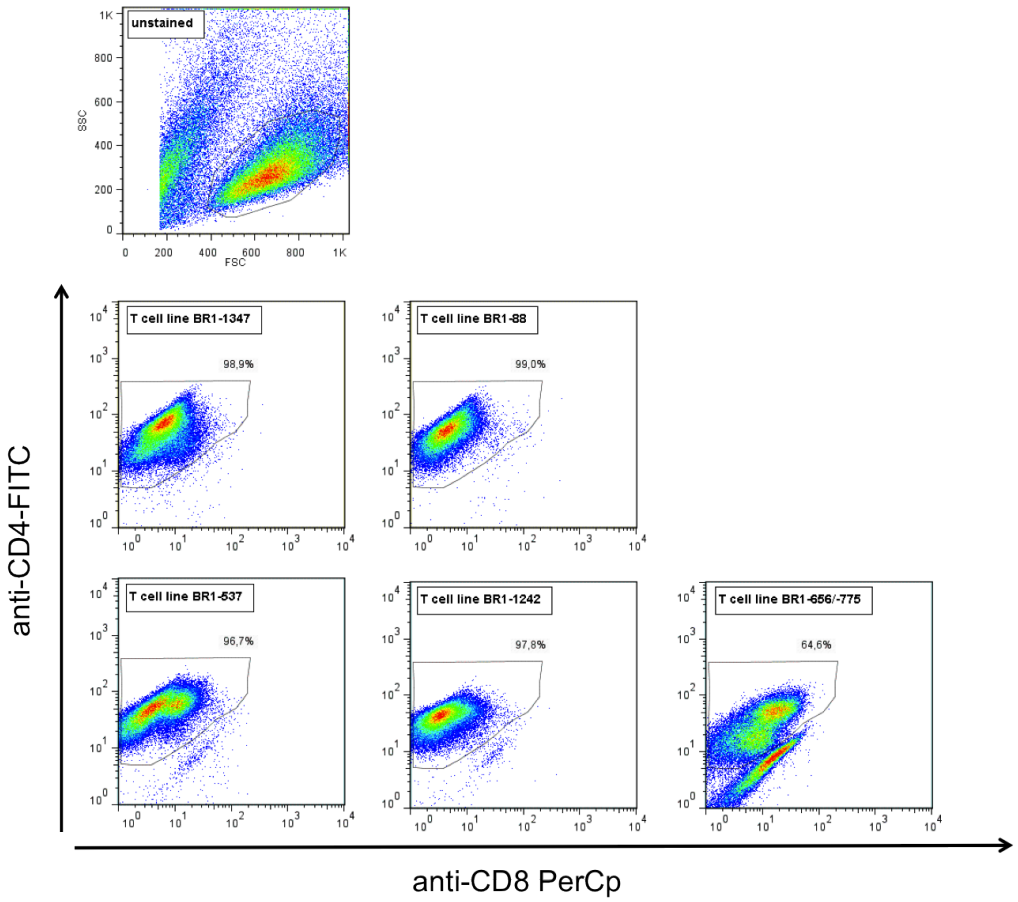

Figure 26: Phenotypic characterization NY-BR-1-specific T cell lines. 1 X 10^6 T cells were stained for anti-CD4-FITC and anti-CD8-FITC. Cells were gated on the lymphocyte population.

Overall, the immunoflourescent staining confirms the established murine T cell lines being dominated by a CD4$^+$ phenotype compared to the amount of cells displaying a CD8$^+$ phenotype, detected by flow cytometry using a FACS-Calibur cytometer. (fig. 26).

5.5.2 Verification of HLA-DRB1*0301-/*0401-restriction of NY-BR-1-specific candidate epitopes

Next, we wanted to prove the HLA-DRB1*0301-/*0401-restriction of the NY-BR-1-specific candidate epitopes BR1-88, BR1-1347, BR1-537, BR1-656/-775 and BR1-1242, by usage of T2/DR3, T2/DR4 transfectants. Those transfectants exclusively express the relevant restriction element on their surface on a MHC-II negative background.

Candidate epitope BR1-88 was clearly recognized by T cell line BR1-88 only if presented on T2/DR3 cells, indicated by detectable IFN-γ-spots in an IFN-γ EliSpot assay (55 IFN-γ-spots) (fig. 27 A). On the contrary, IFN-γ secretion was absent in the case of presenting candidate

epitope BR1-88 on T2/DR4 or T2 cells (IFN-γ-spots < 10), showing that T cell line BR1-88 truly is HLA-DRB1*0301-restricted for recognizing its cognate peptide BR1-88. To prove peptide specificity of the T cell line BR1-88, an irrelevant HLA-DRB1*0301-restricted T cell epitope, derived from the melanoma associated tumor antigen Trp-2, was included in the IFN-γ EliSpot assay. When loaded on T2/DR3 cell, no IFN-γ secretion higher than the negative control was observed, confirming antigen specificity of T cell line BR1-88. T cell line BR1-1347 proved HLA-DRB1*0301 restriction by exclusive recognition of the cognate epitope BR1-1347 loaded on T2/DR3 cells, indicated by 87 IFN-γ-spots in average, but not when loaded onto T2 or T2/DR4 cells indicated by IFN-γ spot numbers below 10 spots. Furthermore, peptide specificity of T cell line BR1-1347 was demonstrated by loading T2/DR3 cells with the irrelevant Trp-2-specific epitope mentioned above which did not result in IFN-γ secretion of T cell line BR1-1347 above the background level of 10 IFN-γ-spots. Unloaded T2, T2/DR3, T2/DR4 cells did not stimulate any IFN-γ secretion in T cell line BR1-1347 (fig. 27 A).

HLA-DRB1*0401-restriction of T cell lines BR1-537, BR1-656/-775 and BR1-1242 was demonstrated by recognition of T2/DR4 target cells loaded with the cognate peptide. True for all three T cell lines, IFN-γ secretion was most prominent when the cognate peptide was loaded on T2/DR4 cells in comparison to T2, T2/DR3 cells loaded with the respective peptide (fig. 27 B).

No IFN-γ secretion was induced in T cell line BR1-537 upon recognition of unloaded T2, T2/DR3, T2/DR4 cells as well upon recognition of T2/DR4 cells loaded with the irrelevant candidate epitope BR1-1242, hereby demonstrating peptide specificity of T cell line BR1-537. But it also has to be taken into consideration, that T cell line BR1-537 apparently also elicits IFN-γ secretion upon encounter of its cognate antigen loaded on T2/DR3 and T2 cells, indicated by 56 IFN-γ-spots and 33 IFN-γ-spots, respectively. This signal has to be considered as being unspecific background activity of T cell line BR1-537.

As shown in figure 27 B, similar results were obtained for T cell line BR1-1242, since the the cognate peptide was only recognized when loaded on T2/DR4 cells, indicated by 67 IFN-γ-spots detected in IFN-γ EliSpot assay, whereby no IFN-γ-spots greater than 10 spots were reached by co-incubation of T cell line BR1-1242 with peptide loaded T2/DR3 and T2 cells or by co-incubation with unloaded T2, T2/DR3 or T2/DR4 cells. Additionally, peptide specificity of T cell line BR1-1242 was demonstrated by loading T2/DR4 cells with the irrelevant candidate epitope BR1-537 which did not induce any IFN-γ secretion of T cell line BR1-1242 (fig. 27 B).

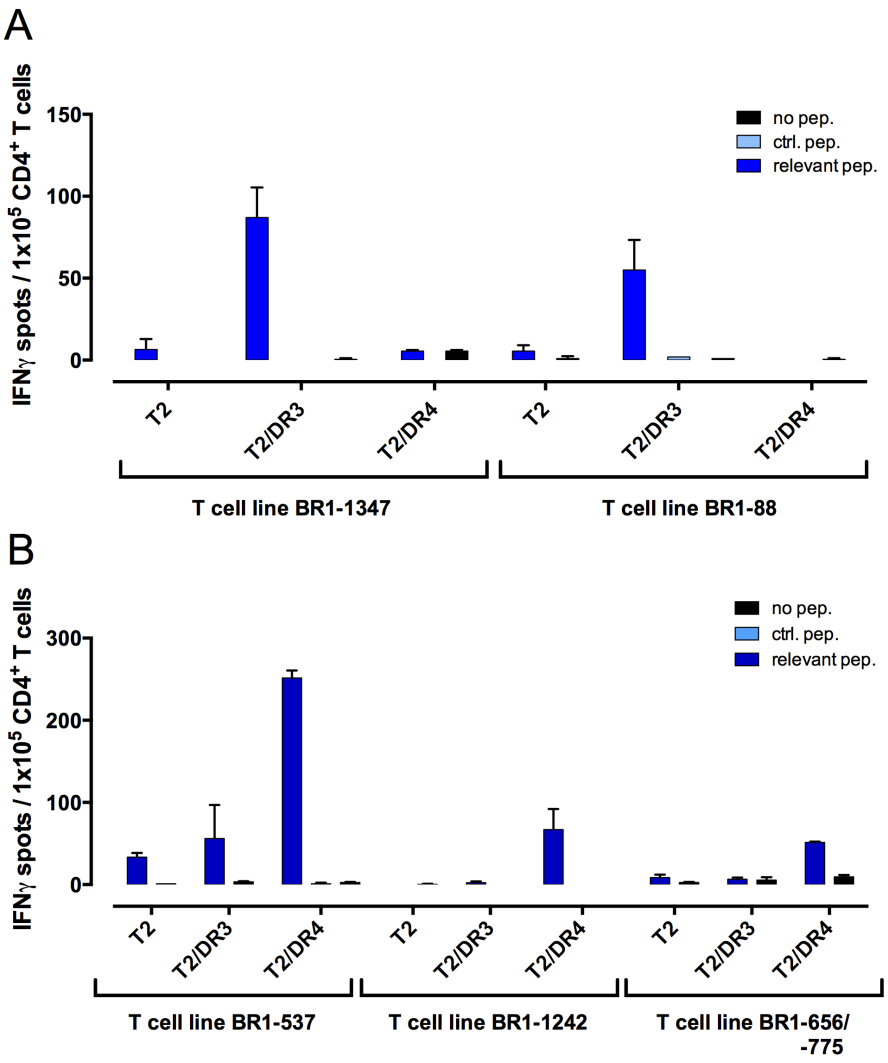

Figure 27: Recognition of peptide loaded T2, T2/DR3, T2/DR4 cells by HLA-DRB1*0301 and HLA-DRB1*0401restricted T cell lines; **A:** HLA-DRB1*0301-restricted T cell lines, **B:** HLA-DRB1*0401-restricted T cell lines. T2, T2/DR3 or T2/DR4 cells were externally loaded with the relevant peptides: BR1-1347, BR1-88 (**A**); BR1-537, BR1-1242, BR1-656/-775 (**B**) or with the control peptide Trp-2 when incubated with T cell line BR1-1347 and T cell line BR1-88. Peptide BR1-1242 was used as a control peptide for T cell line BR1-537 and peptide BR1-537 was used as a control peptide for T cell line BR1-1242 . 1 X 10^5 T cells were co-incubated with peptide loaded T2, T2/DR3 or T2/DR4 cells in an IFN-γ EliSpot assay for 18 hrs. Columns represent reconition of the transfectants by the indicated murine $CD4^+$ T cell line ; bars, standard error of the mean upon duplicate determination; in case of T cell line BR1-1242: bars, standard error of the mean upon triplicate determination.

In the case of T cell line BR1-656/-775, the relevant peptide was recognized when loaded on T2/DR4 cells, indicated by 51 IFN-γ-spots whereby the numbers of IFN-γ-spots detected upon recognition of unloaded T2/DR4, T2/DR3 or T2 cells, were below 10 spots (fig. 27 B). Peptide specificity could so far not be investigated for T cell line BR1-656/-775 due to poor proliferation capacity of this T cell line, but will be analyzed in future experiments.

Importantly, recognition of peptide BR1-537 loaded T2/DR4 cells by T cell line BR1-537 elicited an almost two times higher IFN-γ-response, indicated by 251 IFN-γ-spots in the IFN-γ EliSpot assay, as recognition of peptides BR1-656/-775 and BR1-1242 by their corresponding

T cell lines.

To sum up, NY-BR-1-specific candidate epitopes BR1-88 and BR1-1347 are HLA-DRB1*0301-restricted and NY-BR-1-specific candidate epitopes BR1-537, BR1-656/-775 and BR1-1242 were shown to be HLA-DBRB1*0401-restricted. Overall, reaching milestone III regarding the verification of HLA-DRB1*0301-/*0401-restriction of NY-BR-1-specific candidate epitopes, was accomplished.

5.5.3 Peptide affinity differs among established NY-BR-1-specific, murine HLA-DRB1*0301-/*0401-restricted T cell lines

In the following experiment we aimed to evaluate the peptide affinity of all five generated T cell lines by titration of the cognate peptide starting from 1000 ng/ml followed by 1:2 dilution steps with reaching a final concentration of 62.5 ng/ml. Peptide affinity of HLA-DRB1*0301-restricted T cell lines BR1-88 and BR1-1347 was tested on peptide loaded T2/DR3 cells. As a negative control, unloaded T2/DR3 cells were included in the IFN-γ EliSpot assay. 1000 ng/ml of candidate epitope BR1-1347 loaded on T2/DR3 cells was needed to elicit recognition by T cell line BR1-1347 indicated by IFN-γ secretion, infact none of the lower peptide concentrations resulted in specific recognition of the peptide loaded target cells by this T cell line (fig. 28). T cell line BR1-88 showed a higher affinity for its relevant peptide BR1-88 compared to T cell line BR1-1347 recognizing peptide BR1-1347, since not only at a concentration of 1000 ng/ml but also with 500 ng/ml of cognate peptide loaded on T2/DR3 cells, specific recognition of the cognate peptide BR1-1347 could be detected. It has to be mentioned that in the case of T2/DR3 cells loaded with 500 ng/ml peptide, the average of IFN-γ secretion by T cell line BR1-88 declines to less than 50% of the IFN-γ response observed with a peptide concentration of 1000 ng/ml. Unspecific recognition of T2/DR3 cells was excluded since unloaded T2/DR3 cells did not result in significant IFN-γ secretion in T cell lines BR1-88 and BR1-1347 (fig. 28).

HLA-DRB1*0401-restricted T cell line BR1-656/-775 specifically recognized its cognate peptide BR1-656/-775 at a concentration ranging from 1000 ng/ml to 125 ng/ml, even though it needs to be clarified that overall detected IFN-γ secretion was low for this T cell line compared to the two remaining HLA-DRB1*0401-restricted T cell lines. T cell line BR1-537 elicited a very strong IFN-γ response with any applied concentration of the peptide BR1-537 loaded on T2/DR4 cells which even led to an over saturated signal in case of the two highest peptide concentrations of 1000 ng/ml and 500 ng/ml, applied. Similar findings were obtained with T cell line BR1-1242, here over saturated signals were detected with peptide concentrations ranging from 1000 ng/ml - 250 ng/ml of peptide BR1-1242 loaded on T2/DR4 cells. Strong IFN-γ signals are still detectable for T cell line BR1-1242 recognizing 125 ng/ml and 62.5 ng/ml of peptide BR1-1242 loaded on T2/DR4 cells (fig. 28).

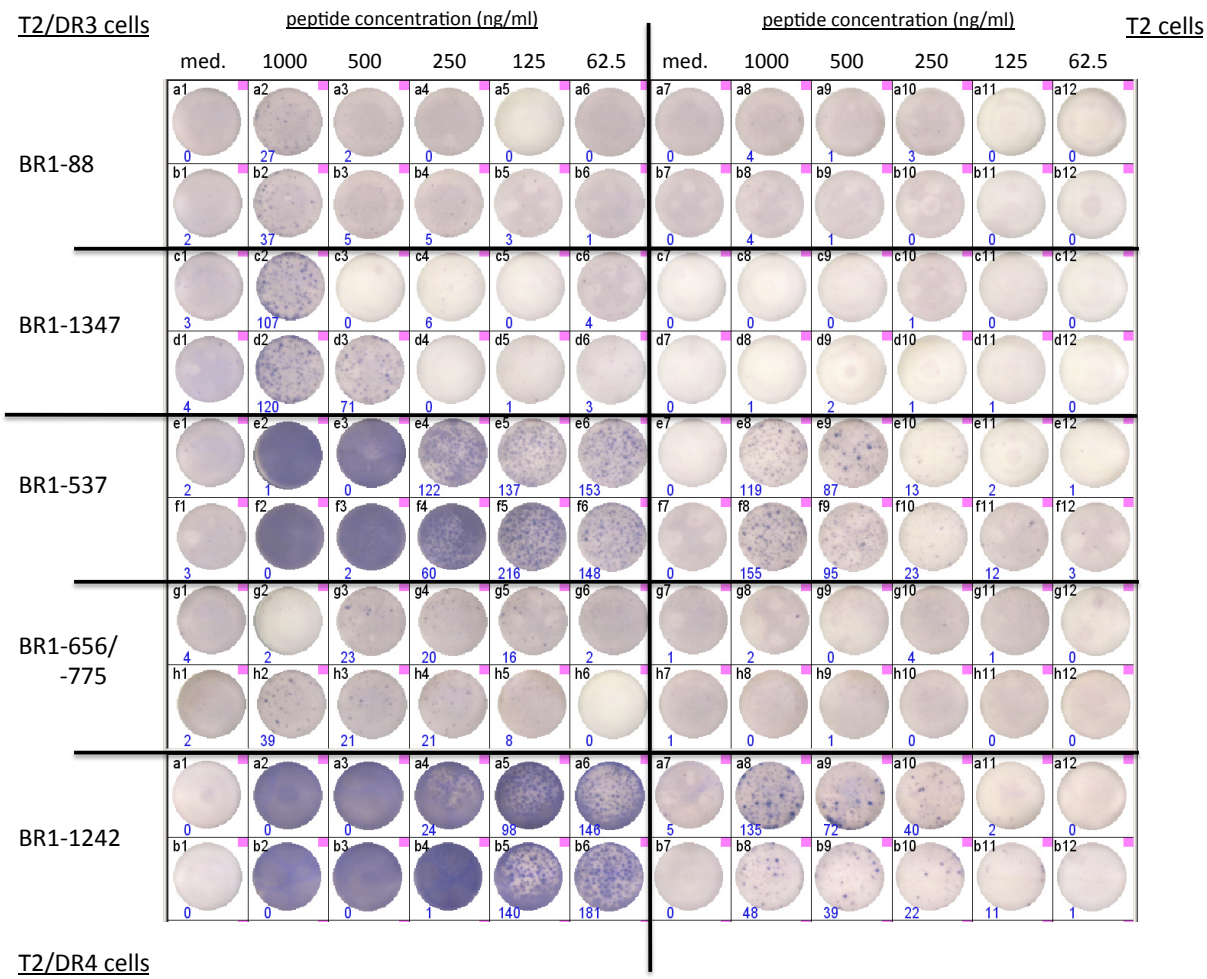

Figure 28: Peptide affinity of different NY-BR-1-specific CD4$^+$ murine T cell lines. 5 X 10^4 T2/DR3, T2/DR4 or T2 target cells/well were externally loaded with 1 µg/ml - 0.0625 µg/ml of indicated candidate epitopes. IFN-γ-secretion was investigated upon recognition of peptide loaded T2/DR3, T2/DR4 cells by indicated peptide-specific T cell lines.

The T cell lines BR1-1242 and BR1-537 represent the highest affinity for their relevant peptide, indicated by specifically recognizing the relevant peptides at a concentration of as little as 62.5 ng/ml. However, the amount of secreted IFN-γ varies between these T cell lines, with the T cell line BR1-1242 eliciting the stronger IFN-γ signal (average of 163 IFN-γ spots) compared to the signal obtained with T cell line BR1-537 (average of 150 IFN-γ spots) . On the other hand, T cell lines BR1-88 and BR1-1347 recognized their peptides BR1-88 and BR1-1347 with a much lower affinity, since the minimum peptide concentrations required to elicit a positive IFN-γ response are 500 ng/ml and 1000 ng/ml, respectively (fig. 28).

In summary, peptide affinity varies among the five newly generated, HLA-DR restricted murine T cell lines as confirmed by specific recognition of peptide loaded T2/DR3, T2/DR4 target cells.

Figure 29 summarizes the NY-BR-1-specific peptide library peptides identified in HHDtg mice, DR3tg mice and DR4tg mice and indicates the potential NY-BR-1-specific candidate 15mer epitopes harbored in identified NY-BR-1-specific library peptides, which were further used to establish murine HLA-DRB1*0301-/ *0401-restricted CD4$^+$ T cell lines.

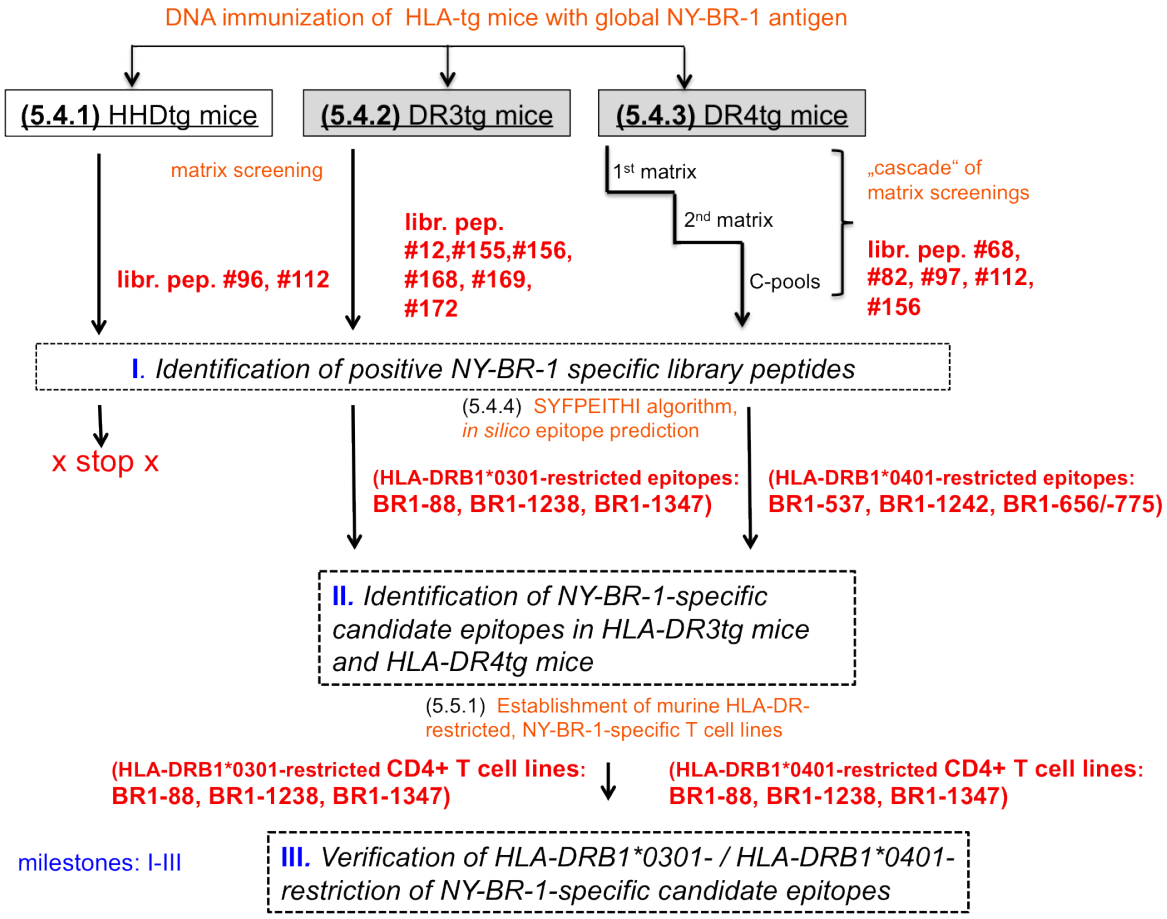

Figure 29: Identification of NY-BR-1-specific, HLA-restricted T cell epitopes in HLA-transgenic mice. Indicated in red are the identified NY-BR-1-specific library peptides and NY-BR-1-specific candidate epitopes as well as the established murine HLA-DR-restricted, NY-BR-1-specific CD4$^+$ T cell lines. Indicated in blue are the milestones I-III reached for the identification of NY-BR-1-derived CD4$^+$ T cell epitopes in HLA-tg mice.

5.6 NY-BR-1-derived, HLA-DRB1*0301-/*0401-restricted CD4$^+$ T cell epitopes are endogenously processed in human cells

Given the fact that only NY-BR-1-specific epitopes naturally processed in human cells are of future clinical relevance, we investigated endogenous processing of the newly identified HLA-restricted, NY-BR-1-specific candidate epitopes in human cells. Various approaches were conducted to confirm natural processing of NY-BR-1-specific, HLA-DR-restricted CD4$^+$ T cell epitopes in human cells.

Finally, NY-BR-1 containing cell lysates were generated from Ad5-NY-BR-1 infected melanoma cell line Ma-Mel73a and used to peptide pulse HLA-matched *in vitro* generated human dendritic cells for recognition by the murine HLA-DR-restricted T cell lines.

5.6.1 Generation of NY-BR-1 expressing target cells

Since no NY-BR-1 expressing human target cell lines were available, we firstly tried to establish a NY-BR-1 expressing target cell by transfection of HLA-matched cell lines with NY-BR-1 encoding expression vector or by using a NY-BR-1 encoding adenoviral construct for the infection of target cells. Apart from HLA-matched human cell lines, HLA-matched CD3-depleted PBMCs and *in vitro* generated HLA-matched dendritic cells were infected with a recombinant adenovirus type 5 (Ad5) to generate NY-BR-1 expressing target cells which could be used to confirm endogenous processing of NY-BR-1-derived candidate epitopes in human cells.

a) Transfection of human breast cancer cell lines SK-BR-2 and HBL-100 with pcDNA3.1(-)NY-BR-1-GFP

To generate HLA-matched, NY-BR-1 expressing breast cancer cell lines, the breast cancer derived cell lines SK-BR-2 (HLA-DRB1*0401 positive) and HBL-100 (HLA-DRB1*0301 positive) were transiently transfected with the pcDNA3.1(-)NY-BR-1-GFP construct. Untransfected cells were included as a control group in this experiment. Expression of the NY-BR-1/-GFP fusion protein in transfected HBL-100 (fig. 30 A) and SK-BR-2 (fig. 30 B) cells was detected by flow cytometry on a FACS-Calibur. GFP-positive cell populations could be detected in both, SK-BR-2 transfected and HBL-100 transfected cell lines, even though percentages of transfected cells were below 10% for both cell lines (3.01% HBL-100-GFP$^+$ cells, 17.18% SK-BR-2-GFP$^+$cells) (fig. 30). Gated on the GFP$^+$ cell population, 37.13% of HLB-100-GFP$^+$ cells also express the surface molecule HLA-DR whereas only 1.73% of all SK-BR-2-GFP$^+$ cells express the HLA-DR surface molecule (fig.30).

Due to the fact, that HLA-DR-expression is naturally low on HBL-100 cells and SK-BR-2 cells, both cell lines were treated with human 500 U/ml of human IFN-γ 24 hrs prior to transfection,

to enhance HLA-DR surface expression.

Given the low frequencies of cells transfected with pcDNA3.1(-)NY-BR-1-GFP, we suggest that the transfection efficacy might be reduced due to the large size of the pcDNA3.1(-)NY-BR-1-GFP vector (10.2 kb) used for transfection leading to a difficulties of the construct entering into the cells´ cytoplasm. Overall, amounts of NY-BR-1/-GFP fusion protein expressing SK-BR-2 and HBl-100 cells generated by this transfection approach were too low for using these cells reliably as NY-BR-1-specific target cell lines.

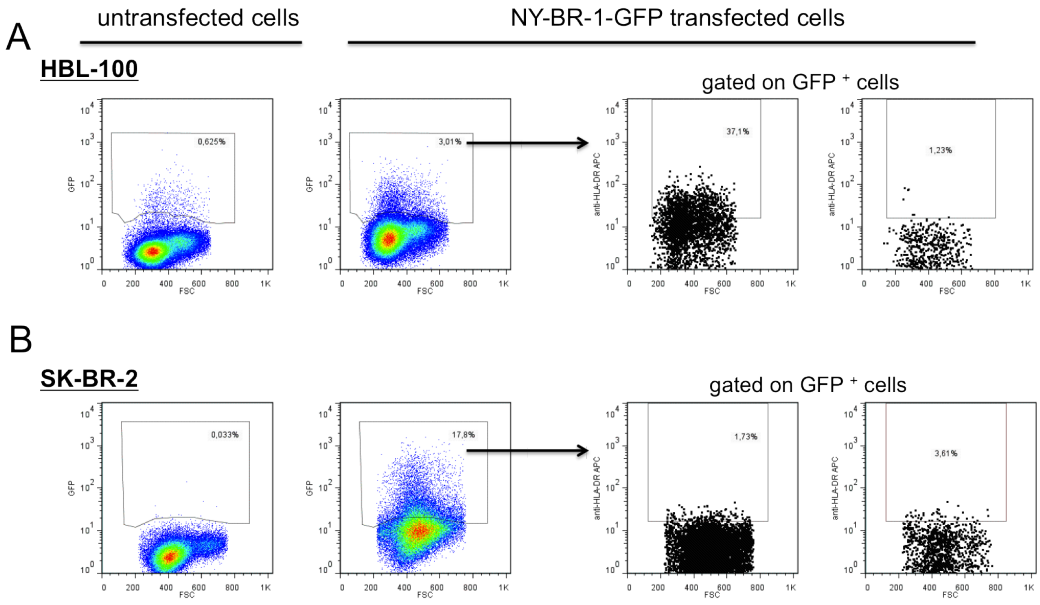

Figure 30: Transfection of breast cancer cell line HBL-100 and SK-BR-2 with pcDNA3.1(-)-NY-BR-1-GFP. Breast cancer cell line HBL-100 (**A**) and SK-BR-2 (**B**) were transfected with a NY-BR-1-GFP DNA construct. NY-BR-1/-GFP fusion protein expression and HLA-DR-expression were analyzed 48 hrs after transfection and IFN-γ treatment (500 U/ml) of cell lines by flow cytometry.

Concluding the results, transient transfection of SK-BR-2 and HBL-100 cell lines with pcDNA3.1(-)NY-BR-1-GFP leads to detectable NY-BR-1/-GFP fusion protein expression in these cell lines. Nevertheless, detection of double positive cells, expressing the NY-BR-1/-GFP fusion protein and the HLA-DR surface molecule was low 37.1% HBL-100 double positive cells and 1.73% double positive SK-BR-2 cells, thus the total amount of double positive cells remains to little to consider this approach as sufficient for the generation of a NY-BR-1-expressing, HLA-matched human target cell line.

b) Infection of a HLA-DR-expressing breast cancer cell lines and a melanoma cell lines with Ad5-NY-BR-1

Infection of target cells by recombinant adenovirus type 5 (Ad5), can be mediated by the coxsackie virus and adenovirus receptor (CAR-receptor), a type 1 transmembrane receptor which has two Ig-like extracellular domains, a transmembrane domain and a cytoplasmic domain [77]. Initially, surface expression of the CAR-receptor was verified on different human breast cancer cell lines and human melanoma cell lines. Furthermore, the surface expression of the HLA-DR molecule was tested on these cell lines, since presentation of relevant epitopes was proven to be restricted to this specific isotype as demonstrated in paragraph 5.5.2.

Breast cancer cell lines HBL-100 ($DR3^+$), SK-BR-2 ($DR4^+$) and melanoma cell lines Ma-Mel21(DR^-) and Ma-Mel79b($DR3^+$) were analyzed for HLA-DR surface expression by staining of the cells with an anti-HLA-DR-FITC antibody.

As shown in figure 31 A, results obtained revealed expression of HLA-DR molecules on the surface of melanoma cell line Ma-Mel79b but only marginal or absent surface expression of HLA-DR molecules in the breast cancer cell lines HBL100 and SK-BR-2. The HLA-DR negative melanoma cell line Ma-Mel21 was included as a negative control in this experiment (fig. 31 A). To induce HLA-DR molecule surface expression, cell lines SK-BR-2, HBL-100 and Ma-Mel79b were treated for 48 hrs with 500 U/ml of human IFN-γ. IFN-γ treatment, induced HLA-DR-surface expression in SK-BR-2 cells and HBL-100 cells (fig. 31 A). Surface expression of the HLA-DR molecule was already present in Ma-Mel79b cells prior to IFN-γ-treatment but could be further increased by treating the cells with human IFN-γ (fig. 31A).

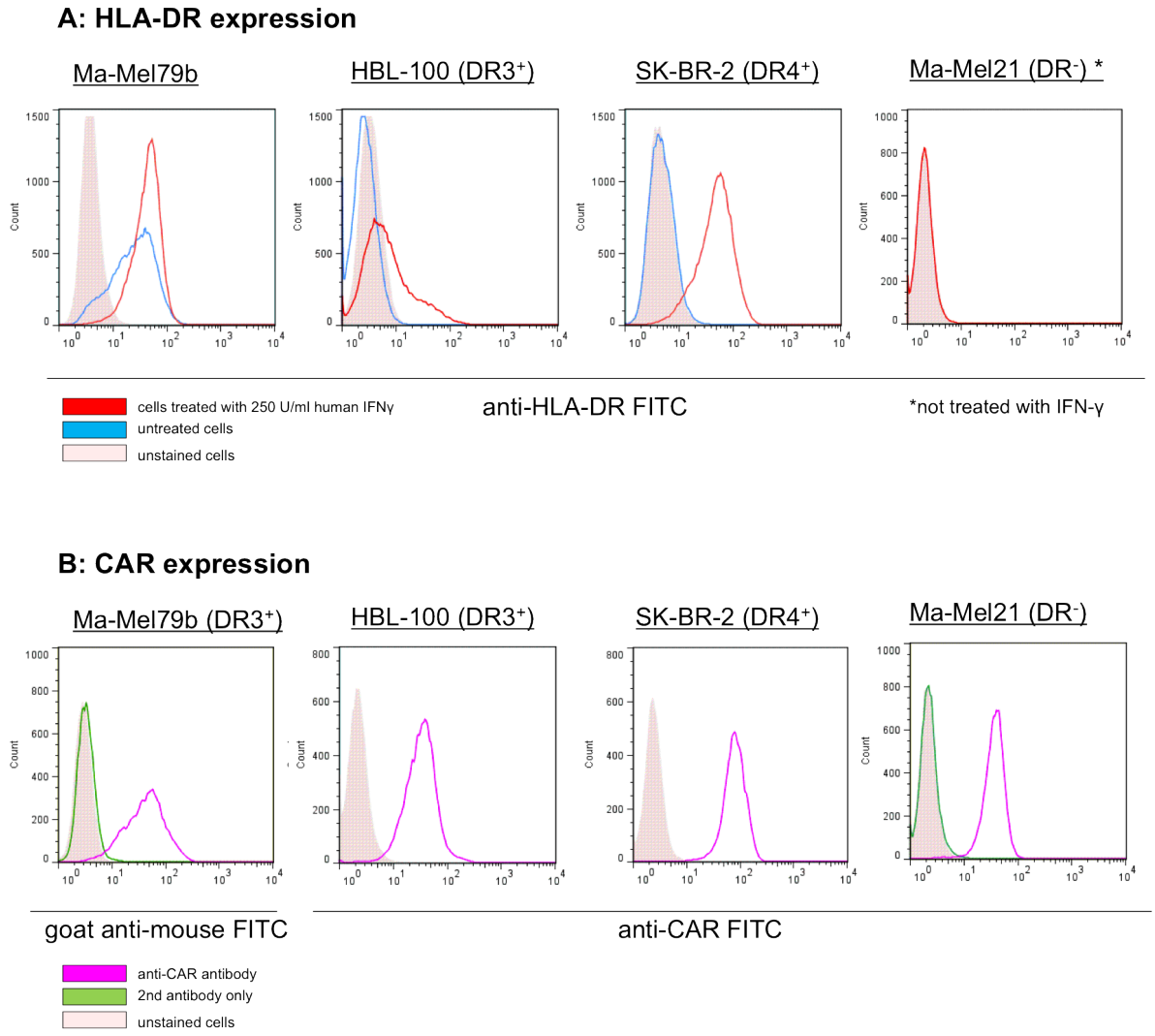

Figure 31: Surface expression of HLA-DR-molecules and CAR-receptor in tested breast cancer and melanoma cell lines. (FACS) immunofluorescence staining including anti-HLA-DR FITC antibody **(A)** and anti-CAR-PE, (in the case of cell line Ma-Mel79b: anti-CAR-IgG antibody detected by a goat-anti-mouse-FITC antibody) **(B)** was performed on breast cancer cell lines HBL-100, SK-BR-2 and melanoma cell lines Ma-Mel21, Ma-Mel79b.

In the next experiment we set out to screen the same panel of melanoma and breast cancer cell lines for surface expression of the CAR-receptor. Data analysis revealed expression of CAR-receptor in cell lines HBL-100, SK-BR-2, Ma-Mel21 and Ma-Mel79b (fig. 31B).

Based on the results obtained by CAR-receptor expression analysis, cell lines SK-BR-2, Ma-Mel21 and Ma-Mel79b were selected to further investigate the optimal time point for maximal NY-BR-1 protein expression after infection of cells with Ad5-NY-BR-1 (fig. 32). In addition, cell lines Ma-Mel21 and Ma-Mel79b were used to determine the optimal viral dose (multiplicity of infection=MOI) needed for successful infection of these cell lines with Ad5-NY-BR-1 (fig. 33).

Firstly, SK-BR-2 cell line was infected with Ad5-NY-BR-1 at an MOI=100. NY-BR-1 protein expression was analyzed at 24 hrs, 48 hrs and 72 hrs after infection of cells. After 24 hrs NY-BR-1

protein expression was detectable (fig. 32 A, lane 1) but signal intensity still increased after 48 hrs (fig. 32 A, lane 3). Interestingly, detectable NY-BR-1 protein expression after 72hrs (fig. 32 A, lane 5) was lower than signals detected after 48 hrs. Uninfected SK-BR-2 cells served as a negative control in this experiment (fig. 32 A, lane 7).

Similar results were obtained for infection of Ma-Mel21 cells and Ma-Mel79b cells with Ad5-NY-BR-1. Detectable NY-BR-1 protein expression was most pronounced 48 hrs after infection of cells with Ad5-NY-BR-1 (fig. 32 B, lane 3, 10) and declined 72 hrs after infection of cells (fig. 32 B, lane 6, 12). Overall, intensity of NY-BR-1 protein expression was higher in Ma-Mel21 cells compared to Ma-Mel79b cells infected with Ad5-NY-BR-1.

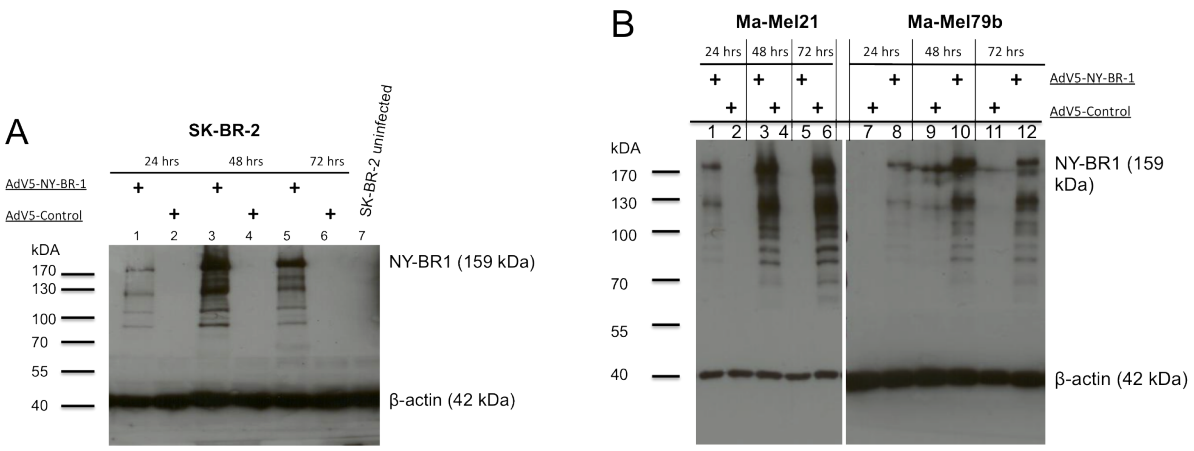

Figure 32: NY-BR-1 protein expression in human cell lines after Ad5-NY-BR-1 infection. SK-BR-1 **(A)**, Ma-Mel21, Ma-Mel79b **(B)** were infected with Ad5-NY-BR-1 (MOI=100) and NY-BR-1 protein expression was investigated in 15 µg of cellular protein, extracted 24 hrs, 48 hrs and 72 hrs after initial infection of cells, by Western blot analysis.

Since we determined 48 hrs after infection of cell lines with Ad5-NY-BR-1 as the time point of optimal NY-BR-1 protein expression, we wanted to investigate in the next set of experiment the optimal virus dose to achieve maximal protein expression in cell lines infected with Ad5-NY-BR-1 at this time point. Selected target cells Ma-Mel21 and Ma-Mel79b were infected with a series of different multiplicities of infection (MOI), MOI=1, MOI=10, MOI=50 and MOI=100, respectively. Western blot analysis revealed highest amounts of NY-BR-1 protein expression 48 hrs after infection of cell lines Ma-Mel79b and Ma-Mel-21 at an MOI=100 (fig.33 A, B: lane 8). NY-BR-1 protein expression was absent after infection of cells with Ad5-NY-BR-1 (MOI=10) but detectable at an MOI=50 (fig.33 A, B: lane 6) and rapidly declined to almost undetectable levels at MOI=10 (fig.33 A, B: lane 4) before being undetectable at an MOI=1 (fig.33 A, B: lane 2). NY-BR-1 protein expression was not detectable in samples of uninfected Ma-Mel21 and Ma-Mel79b cells (fig. 33 A, B: lane 9).

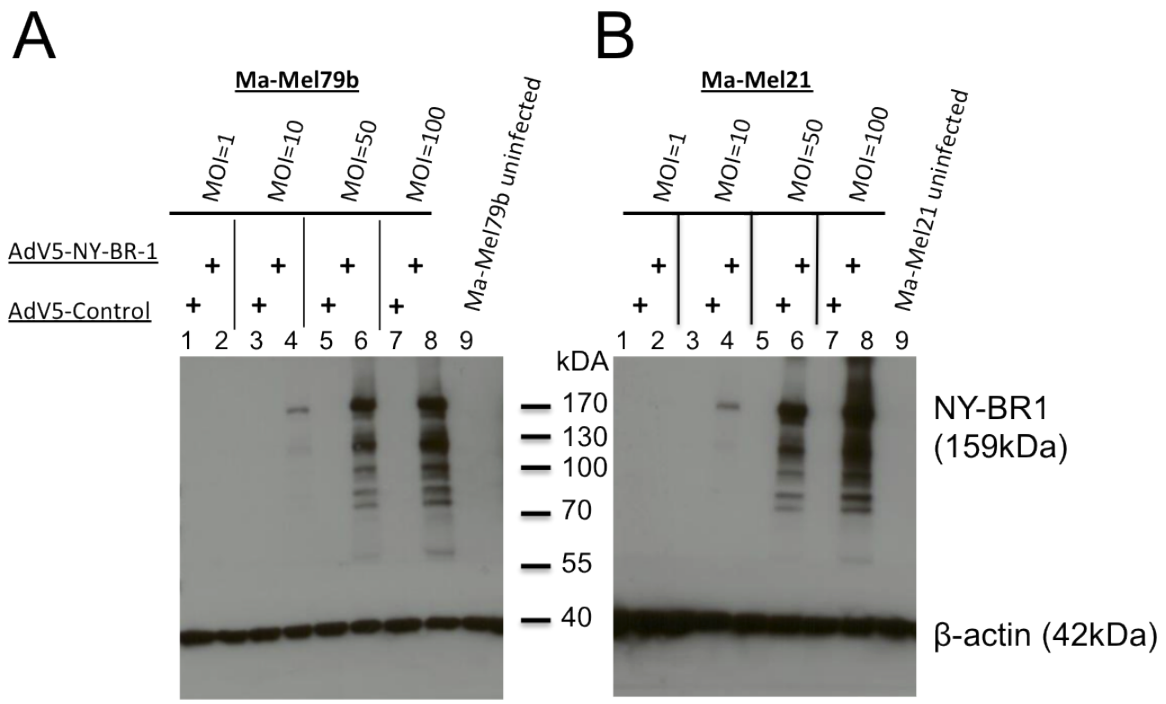

Figure 33: Identification of optimal infection dose (=MOI) of Ad5-NY-BR-1 on various human melanoma cell lines. Melanoma cell lines Ma-Mel21 **(A)**, Ma-Mel79b **(B)** were infected with Ad5 or Ad5-NY-BR-1 at different MOIs; MOI= 1: **lane 1, 2** ; MOI=10: **lane 3, 4**; MOI=50: **lane 5, 6**; MOI=100: l**ane 7, 8**. 15 µg of cellular protein in a volume of 20 µl lysate was analyzed for each sample by Western blotting, 48 hrs post infection.

Infection of cells with Ad5-Control virus did not result in any detectable protein signal at any time point or any of the tested MOIs.

Summing up, we have evidence that 48 hrs after infection of target cells with an MOI=100 is the optimal time point for detection of maximal NY-BR-1 protein expression in the melanoma cell lines tested.

c) Incubation of human PBMCs with Ad5-NY-BR-1

As it was described that human PBMCs depleted of $CD3^+$ cells can be used as target cells after being incubated with an antigen-encoding Ad5 virus [183], we depleted PBMCs obtained from healthy donors of $CD3^+$ T cells, due to the fact that cells of lymphoid origin are considered to be relatively resistant to be infected by adenovirus [199]. The remaining cells, were incubated either with Ad5 or Ad5-NY-BR-1 constructs (MOI=100). Cell lysates obtained from CD3-depleted, PBMCs which were incubated with Ad5-NY-BR-1/Ad5, were tested for NY-BR-1 protein expression by Western blot analysis. As shown in figure 34, NY-BR-1 protein expression was not detectable in CD3-depleted PBMCs incubated with Ad5-NY-BR-1 (lane 3, 6). Cell lysates extracted from Ma-Mel73 cells infected with Ad5-NY-BR-1 were included as a positive control for the detection of NY-BR-1 protein in this experiment (fig 34). Reasons for not detecting NY-BR-1

protein expression after incubation of PBMCs depleted for $CD3^+$ T cells might either be an unsuccessful infection due to the absence of CAR expression, or lack of expression of the Ad5-NY-BR-1 construct in human PBMCs. This question could be answered by investigating surface expression of CAR on PBMCs, and by incubating the western blot membrane with an antibody detecting adenovirus-derived protein. Based on the results obtained, incubatuion of PBMCs depleted for $CD3^+$ T cells with Ad5-NY-BR-1 was not further considered for the verification of endogenous processing of NY-BR-1-specific candidate epitopes in PBMCs of healthy donors.

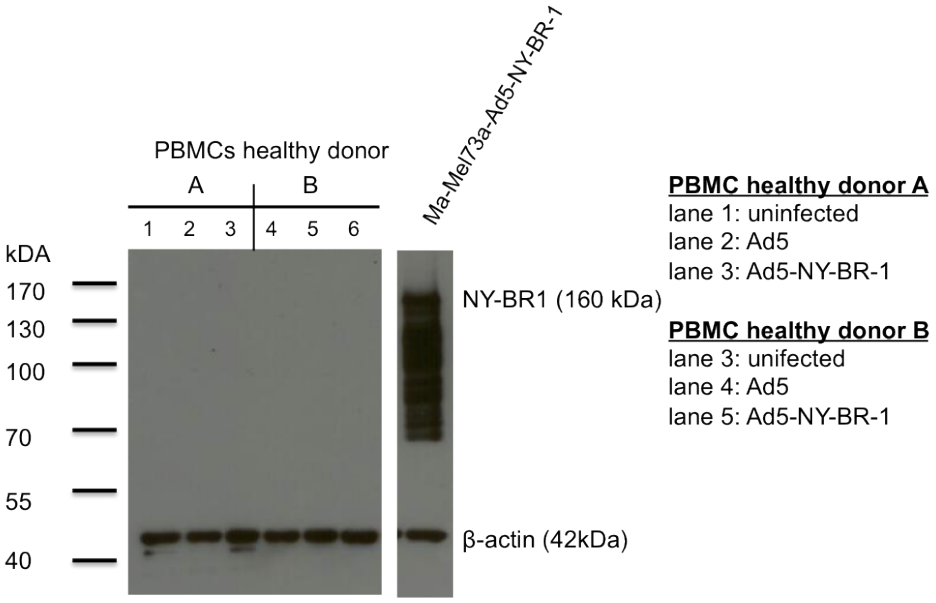

Figure 34: NY-BR-1 protein expression in PBMCs of healthy donors after infection with Ad5-NY-BR-1. NY-BR-1 protein expression in PBMCs depleted for $CD3^+$ T cells, infected at a MOI=100 with Ad5-NY-BR-1, was analyzed by Western blot, 15 µg of cellular protein were analyzed for each sample.

d) Infection of human *in vitro* generate dendritic cells (DCs) with Ad5-NY-BR-1

Since HLA-matched human dendritic cells represent optimal antigen presenting capacity, we wanted to investigate endogenous processing of the NY-BR-1-specific candidate epitopes BR1-88, BR1-1347, BR1-537, and BR1-1242 by recognition of Ad5-NY-BR-1 infected HLA-matched, *in vitro* generated human dendritic cells by established murine HLA-DR-restricted T cell lines.

***In vitro* generation and phenotypic characterization of human dendritic cells (DCs) from HLA-matched healthy donors** Human dendritic cells were generated *in vitro* from PBMCs of HLA-matched healthy donors. *In vitro* generated mature dendritic cells were phenotypically characterized by flow cytometry prior to IFN-γ EliSpot assay experiments. Comprehensive immunoflourescent-staining for the human surface markers CD11c, CD80, CD86 and anti-HLA-DR were performed. Dendritic cells stained for the panel of surface markers, were analyzed by flow

cytometry. As shown in figure 35, 82.53% of *in vitro* generated dendritic cells displayed a double positive phenotype regarding expression of the surface molecules CD11c and HLA-DR. Furthermore, prominent surface expression of the co-stimulatory molecule CD86 was detected among the dendritic cell population expressing both, CD11d and HLA-DR surface molecules (fig.35).

In general it can be testified that these *in vitro* generated dendritic cells show surface molecule expression such as CD11c, HLA-DR and CD86 which are described to be characteristic for mature *in vitro* generated, monocyte derived dendritic cell [194].

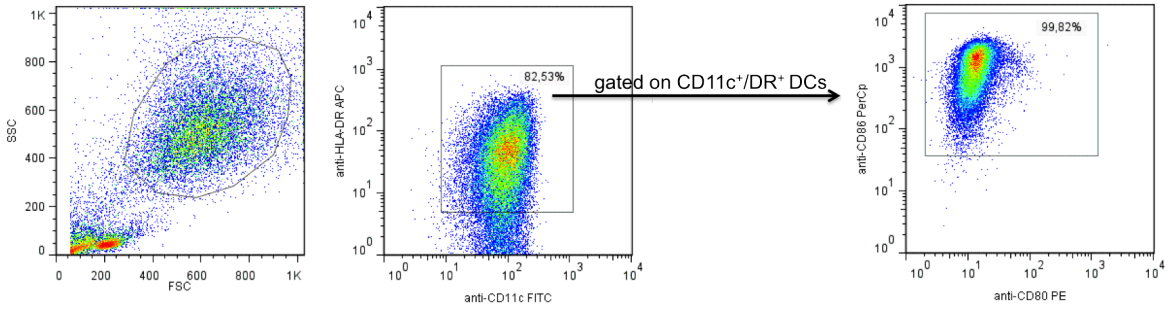

Figure 35: Phenotypic characterization of *in vitro* generated human dendritic cells. Human DCs were generated form PBMCs of healthy donors over a time period of 7 days, receiving IL-4 and GM-CSF every other day. Immunofluorescent staining of differentiated DCs was performed with anti-CD11c FITC, anti-CD80 PE, anti-CD86-PerCp and anti HLA-DR APC antibodies and analyzed by using a FACS-Calibur.

Next, we tried to infected differentiated human DCs with Ad5-NY-BR-1 (MOI=1000) which potentaillly could be recognized by the established murine $CD4^+$ T cell lines BR1-88, BR1-1347, BR1-537 and BR1-1242 in an antigen specific manner. Therefore, we firstly investigated the surface expression of the CAR-molecule on the differentiated dendritic cells (fig. 36 A). Immunoflourescent staining for the adenoviral receptor CAR did reveal absence of receptor surface expression in human dendritic cells (fig. 36 A). However, dendritic cells were incubated with Ad5-NY-BR-1 to possibly generate dendritic cells which express the NY-BR-1 protein after infection with Ad5-NY-BR-1. Incubation of *in vitro* generated dendritic cells with Ad5-NY-BR-1 at a MOI=1000 did not affect viability of the dendritic cells as evaluated by visual inspection of the cells. As shown in figure 36 B, NY-BR-1 protein expression could not be detected in cellular protein samples extracted from DCs which had been incubated with Ad5-NY-BR-1 (lane 1) but was detectable in Ma-Mel73a-Ad5-NY-BR-1 cell lysates included as a positive control in this experiment (lane 4) .

In line with these findings, Ad5-NY-BR-1 infected dendritic cells were not specifically recognized by any of the four tested murine HLA-DR-restricted T cell lines (fig.36 C).

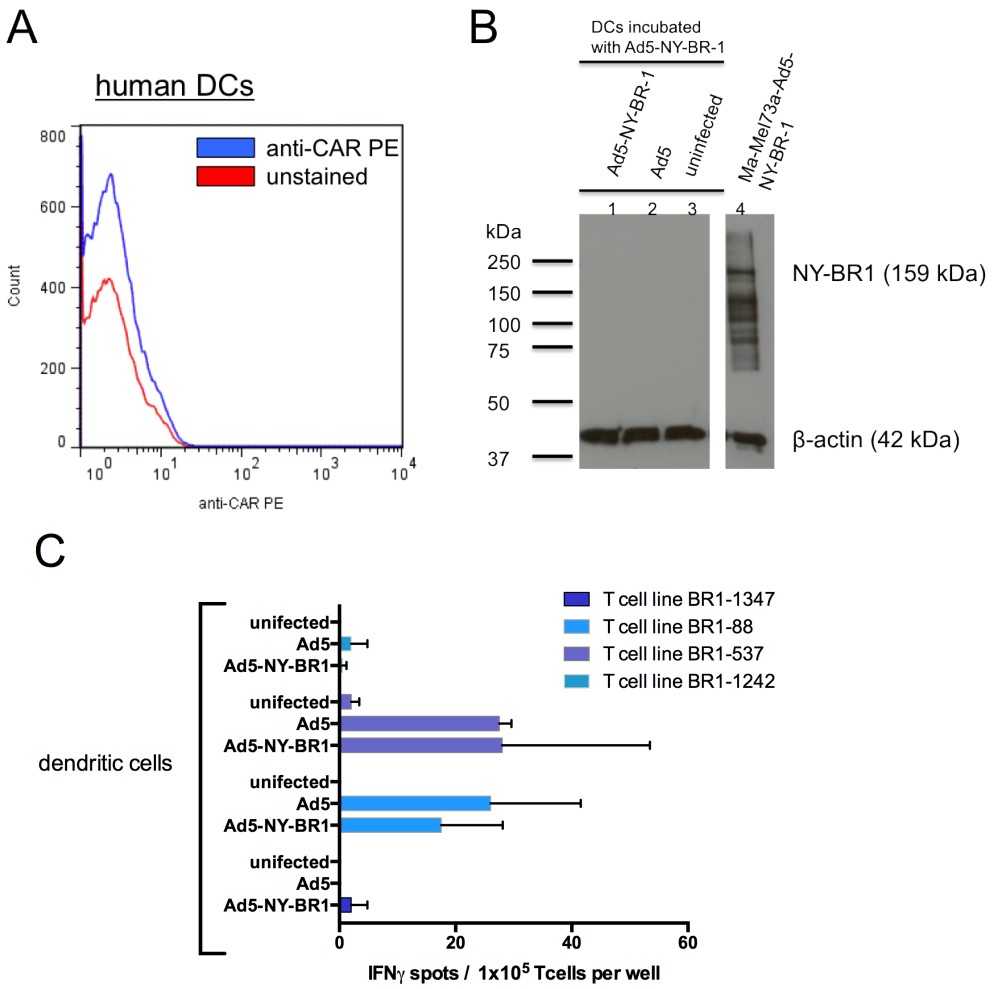

Figure 36: Incubation of human dendritic cells with AdV-NY-BR-1. Surface expression of the CAR-receptor in human dendritic cells, DCs were stained with an anti-CAR PE antibody, data were acquired by flow cytometry (**A**). Western blot analysis of AdV-NY-BR-1 infected dendritic cells, 15 µg of cellular lysate were analyzed per sample (**B**). HLA-matched *in vitro* generated DCs were either incubated with Ad5-NY-BR-1 (MOI=1000) or with Ad5 (MOI=1000). After 24 hrs indicated murine HLA-DR-restricted T cell lines were co-incubated with human DCs in an IFN-γ EliSpot assay for 18 hrs. Columns, mean of duplicate determination; bars standard error of the mean (**C**).

Overall, infection of *in vitro* generated dendritic cells with Ad5-NY-BR-1 was not successful thus these cells were not further considered as target cells for investigation of endogenous processing of NY-BR-1-specific candidate epitopes in human target cells.

5.6.2 Experiments using Ad5-NY-BR-1 infected melanoma and breast cancer cells as target cells

With the following experiment we aimed to investigate endogenous processing of the NY-BR-1-specific candidate epitopes BR1-88, BR1-1347, BR1-537, BR1-656/-775 and BR1-1242 in human cell lines. Therefore, HLA-matched melanoma cell line Ma-Mel79b (DR3$^+$), Ma-Mel21 (DR3$^-$)

and breast cancer cell line SK-BR-2 ($DR4^+$) were infected with Ad5-NY-BR-1 and tested for recognition by NY-BR-1 specific, HLA-DR-restricted murine T cell lines.

HLA-DRB1*0301 positive cell line Ma-Mel79b was infected with Ad5-NY-BR-1 or Ad5 at a MOI=100 and tested for recognition by T cell line BR1-88 and BR1-1347. Ma-Mel21 (DR^-) cells infected with Ad5-NY-BR1 were used as negative control. Additionally, BR1-88/BR1-1347 peptide loaded Ma-Mel79b cells and Ma-Mel21 cells, as well as T2/DR3 cells, loaded with BR1-88/BR1-1347 peptides, were included in the IFN-γ EliSpot assay. HLA-DRB1*0301-restricted T cell lines BR1-88 and BR1-1347 did not recognize Ma-Mel79b and Ma-Mel21 cells infected with Ad5-NY-BR-1, as it was expected for cell line Ma-Mel21(DR^-) but not for cell line Ma-Mel79b ($DR3^+$). However, Ma-Mel79b cells and T2/DR3 cells externally loaded with the cognate peptide were recognized by both T cell lines BR1-88 and BR1-1347. Nevertheless, as shown for T cell line BR1-1347 in figure 37 A, recognition of externally peptide loaded Ma-Mel79b cells (mean of 22 IFN-γ-spots) and peptide loaded T2/DR3 cells (mean of 11 IFN-γ-spots) was low, probably indicating "exhaustion" of the T cell line BR1-1347 on the day of the IFN-γ EliSpot assay. Peptide loaded T2 cells similar to unloaded T2 and T2/DR3 cells, were not recognized by T cell line BR1-1347 (fig.37 A). T cell line BR1-88 recognized peptide loaded Ma-Mel79b cells (71 IFN-γ-spots) to a much greater extent than peptide loaded T2/DR3 cells (mean of 6 IFN-γ-spots). To exclude failure of Ad5-NY-BR-1 infection of the selected target cells, as a potential reason for poor recognition of these target cells by the tested $CD4^+$ T cell lines, NY-BR-1 expression was confirmed for Ad5-NY-BR-1 infected Ma-Mel21 and Ma-Mel79b cells used as target cells in the IFN-γ EliSpot assay by Western blot analysis (fig.38).

HLA-DRB1*0401-restricted T cell lines BR1-537, BR1-565/-775 and BR1-1242 did not specifically recognize Ad5-NY-BR-1 infected SK-BR-2 ($DR4^+$) cells and Ad5-NY-BR-1 infected Ma-Mel21 cells, as expected for HLA-DRB1*0401 negative Ma-Mel-21 cells (fig. 37 C,D,E). Externally loaded target cell lines Ma-Mel-21, SK-BR-1 and T2/DR4 cells with the relevant peptides BR1-537, BR1-565/-775, BR1-1242, were also investigated for recognition by the matching T cell lines. As shown in figure 37 D, only T cell line BR1-1242 induced IFN-γ secretion upon recognition of BR1-1242 peptide loaded target cell line SK-BR-2 (mean of 42 IFN-γ-spots), whereas peptide loaded T2/DR4 cells were specifically recognized by T cell line BR1-537 (mean of 50 IFN-γ-spots) (fig. 37 C) and by T cell line BR1-1242 (IFN-γ-spots not measurable due to signal over-saturation in the well) (fig. 37 D). Important to notice, T cell line BR1-1242 also reacts with IFN-γ secretion upon encounter of peptide loaded T2 cells (mean of 90 IFN-γ spots), this signal has to be considered as background signal of T cell line BR1-1242. Peptide loaded Ma-Mel21 (DR^-) cells were not specifically recognized by any of the HLA-DRB1*0401-restricted murine T cell lines (fig.37 C, D, E).

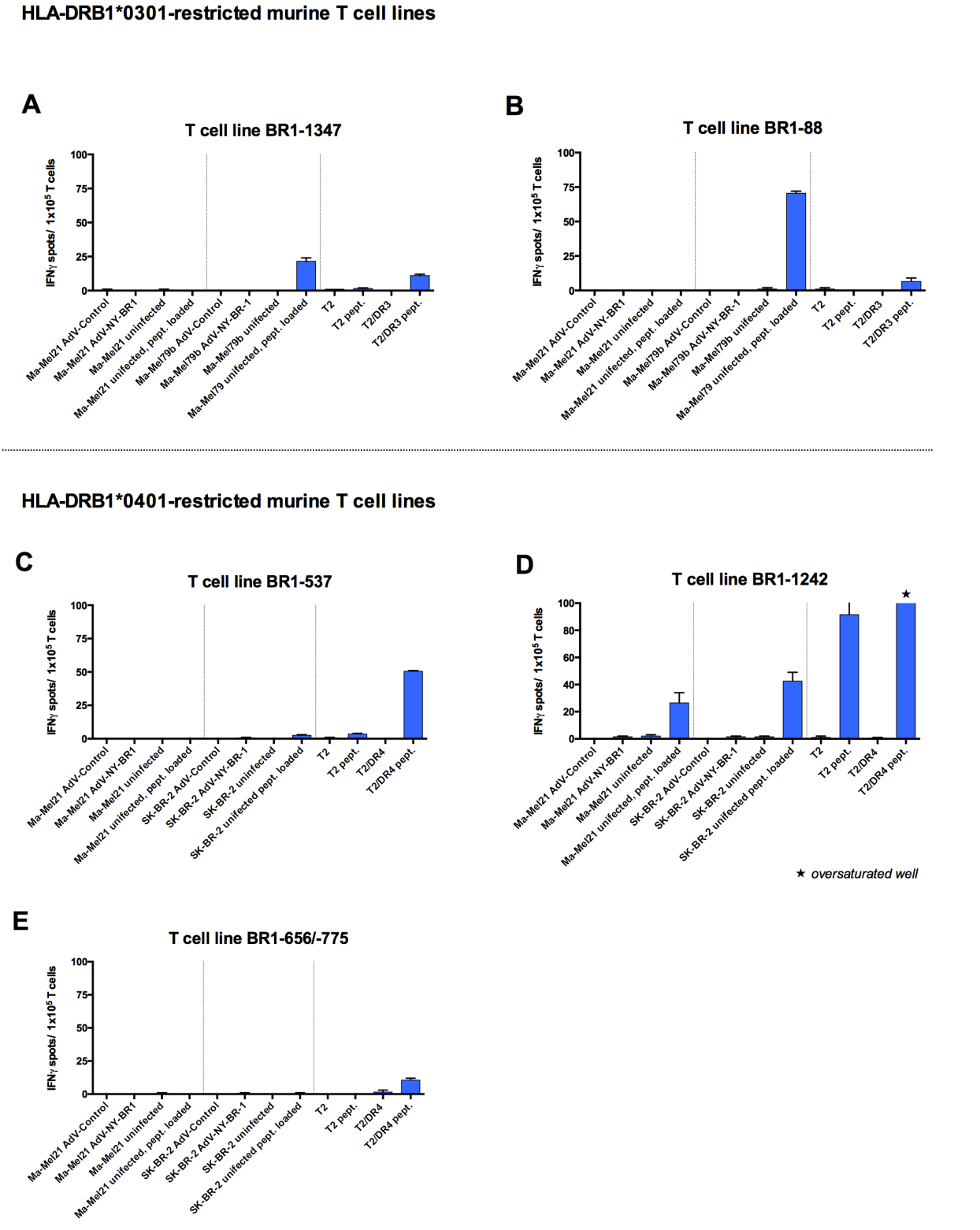

Figure 37: IFN-γ EliSpot results on recognition of Ad5-NY-BR-1 infected target cells by novel murine HLA-DR-restricted T cell lines. Target cell lines SK-BR-2, Ma-Mel79b and Ma-Mel21 were infected with Ad5-NY-BR-1 (MOI=100) and used in IFN-γ EliSpot assay. 5 X 10^4 target cells/ well were incubated with 1 X 10^5 T cells (**A**: T cell line BR1-1347, **B**: T cell line BR1- 88, **C**: T cell line BR1-537, **D**: T cell line BR1-1242, **E**: T cell line BR1-656/775) for 18 hrs. Target cells were peptide loaded with 1 µg of the relevant peptide, when indicated. Columns, mean of duplicate determination; bars standard error of the mean.

However, NY-BR1 protein expression after infection of target cell line SK-BR-2 and Ma-Mel21, with Ad5-NY-BR-1, was confirmed by Western blot analysis (fig. 38). Therefore, lack of specific recognition of HLA-DRB1*0401^{+} target cells by murine HLA-DRB1*0401-restricted CD4^{+} T cell lines, is more likely due to insufficient stimulation of the relevant CD4^{+} T cell line tested, than to a lack of NY-BR-1 antigen expression within the analyzed target cells after infecteion with Ad5-NY-BR-1.

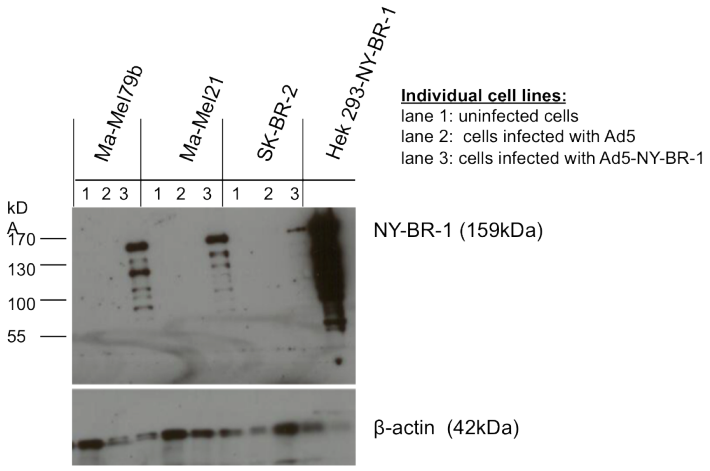

Figure 38: Western blot analysis of NY-BR-1 protein expression in Ad5-NY-BR-1 infected target cell lines Ma-Mel79b, Ma-Mel21 and SK-BR-2. Target cell lines were infected with Ad5-NY-BR-1 (MOI=100). 15 µg of cellular protein was analyzed for each sample by Wester blot analysis.

Collectively, based on the foregoing results, peptide loaded but not Ad5-NY-BR-1 infected target cells are recognized by the newly generated murine HLA-DR-restricted, CD4^{+} T cell lines, thus endogenous processing of the newly identified NY-BR-1-specific T cell epitopes could so far not be confirmed in human cells. This finding is most likely due to an exhausted phenotype of the tested T cell lines as well as a potential lack of affinity of these T cell lines for their cognate peptide at the time point of the performed EliSpot assay. Moreover, it has to be further investigated, if the relevant NY-BR-1-specific epitopes are processing products in the tested target cell lines Ma-Mel79b, Ma-Mel21 and SK-BR-1 upon infection with Ad5-NY-BR-1.

5.6.3 Confirmation of endogenous processing of NY-BR-1-specific candidate epitopes in human cells using HLA-matched, human DCs loaded with lysate generated from Ad5-NY-BR-1 infected tumor cells

Due to the fact that human HLA-matched *in vitro* generated Ad5-NY-BR-1 infected dendritic cells (DCs) failed to be specifically recognized by all murine $CD4^+$ T cell lines (fig. 36, C), we set out and altered the experimental design. *In vitro* generated HLA-matched human DCs loaded with cell lysates containing NY-BR-1 protein might serve as a source to verify endogenous processing of the newly identified NY-BR-1-specific, HLA-DR-restricted epitopes in human cells.

NY-BR-1 containing cell lysates were generated by repeated thaw freeze cycles of Ma-Mel73a cells infected with Ad5-NY-BR-1. The melanoma cell line Ma-Mel73a showed stronger NY-BR-1 protein expression at 48 hrs after infection (MOI=100) of cells with Ad5-NY-BR-1 (fig. 39), when compared to panel of melanoma and breast cancer cell lines tested previously (fig. 33).

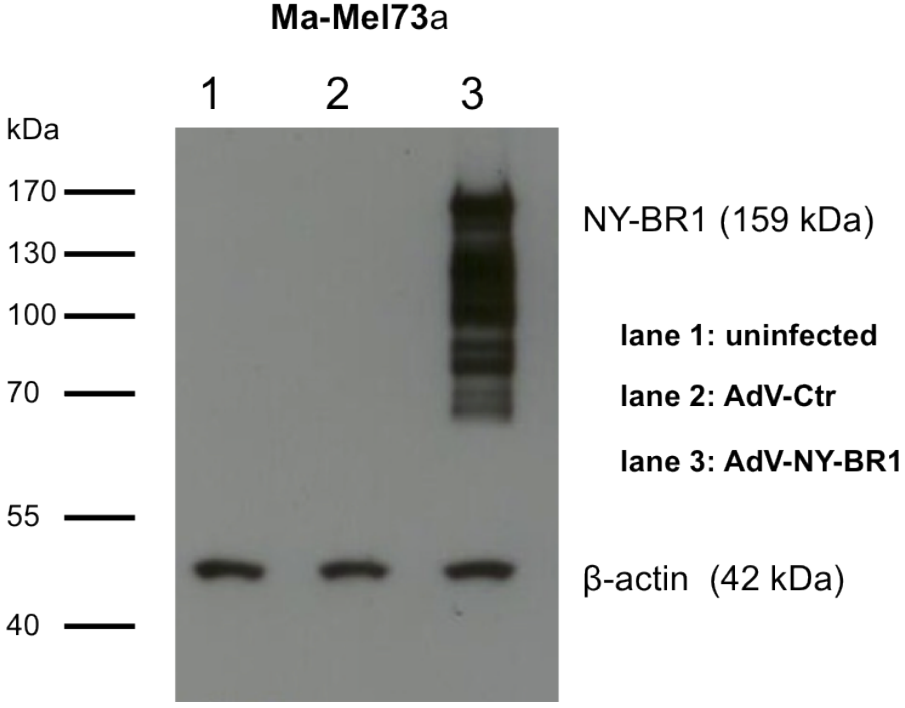

Figure 39: Western blot analysis of NY-BR-1 protein expression in Ad5-NY-BR-1 infected target cell line Ma-Mel73a. Ma-Mel73a were infected with Ad5-NY-BR-1 of Ad5, (MOI=100). 15 µg of cellular protein was analyzed for each sample by Wester blot analysis.

HLA-matched *in vitro* generated dendritic cells were loaded with the NY-BR-1 protein containing cell lysate over night, followed by co-culture with $CD4^+$, HLA-DR-restricted murine T cell lines. Lysates processed from Ma-Mel73a cells infected with Ad5, as well as lysates of uninfected Ma-Mel73a cells were included as control lysates for loading of human dendritic cells.

As shown in figure 40 A, T cell line BR1-1347 specifically recognized dendritic cells loaded

with NY-BR-1-containing cell lysate (mean of 163 IFN-γ-spots), whereas no IFN-γ secretion was detectable for dendritic cells loaded with cell lysate generated from uninfected Ma-Mel73a cells or Ma-Mel73a cells infected with Ad5. Moreover, only dendritic cells pulsed with the cognate epitope (over-saturated IFN-γ signal) but not with the irrelevant Trp-2 epitope were recognized by T cell line BR1-1347 (fig.40 A).

Confirming specificity and HLA-DRB1*0301-restriction, T cell line BR1-88 recognized HLA-matched dendritic cells loaded with lysate of Ma-Mel73a-AdV-NY-BR-1 cells, indicated by IFN-γ secretion detected by IFN-γ EliSpot assay (mean of 153 IFN-γ-spots) (fig. 40 A). Importantly, dendritic cells loaded with cell lysate originating from uninfected Ma-Mel73a cells as well as from Ma-Mel73a cells infected with Ad5, did not promote any IFN-γ secretion of T cell line BR1-88. Exogenous pulsing of dendritic cells with the epitope BR1-88 elicited greatest IFN-γ secretion by T cell line BR1-88 (over-saturated IFN-γ signal), which on the other side was absent in case of dendritic cells pulsed with an irrelevant HLA-DRB1*0301-restricted epitope derived from the melanoma associated antigen Trp2 (fig.40 A).

Similar results could be obtained within the HLA-DRB1*0401-restricted system. Figure 40 B shows the results on specific recognition of *in vitro* generated dendritic cells, obtained from a HLA-DRB1*0401 positive healthy donor, loaded either with cell lysate of Ma-Mel73a cells infected with Ad5-NY-BR-1, or dendritic cells pulsed externally with the epitopes BR1-537 and BR1-1242, by the corresponding T cell lines. T cell line BR1-537 specifically recognized dendritic cells loaded with cell lysate generated from Ad5-NY-BR-1 infected Ma-Mel73A cells (mean of 96 IFN-γ-spots), albeit dendritic cells loaded with cell lysate of cells infected with Ad5 also induced IFN-γ secretion of T cell line BR1-537 upon encounter (mean of 35 IFN-γ-spots), this signal has to be considered background activity for the T cell line BR1-537. Uninfected Ma-Mel73a cells were not recognized by T cell line BR1-537. Besides, T cell line BR1-537 specifically detected BR1-537 peptide pulsed on dendritic cells (mean of 82 IFN-γ-spots) but not the irrelevant HLA-DRB1*0401-restricted epitope BR1-1242 (fig.40 B). Similarly, T cell line BR1-1242 specifically recognized dendritic cells loaded with cell lysate originating from Ma-Mel73a cells infected with Ad5-NY-BR-1 (mean of 163 IFN-γ-spots) and dendritic cells exogenously pulsed with the BR1-1242 epitope (over-saturated IFN-γ signal). Dendritic cells loaded with irrelevant cell lysate originating from uninfected Ma-Mel73a cells or Ma-Mel73a cells infected with Ad5, as well as dendritic cells externally pulsed with the irrelevant HLA-DRB1*0401-restricted epitope BR1-537 did not lead to specific recognition by T cell line BR1-1242 (fig.40 B).

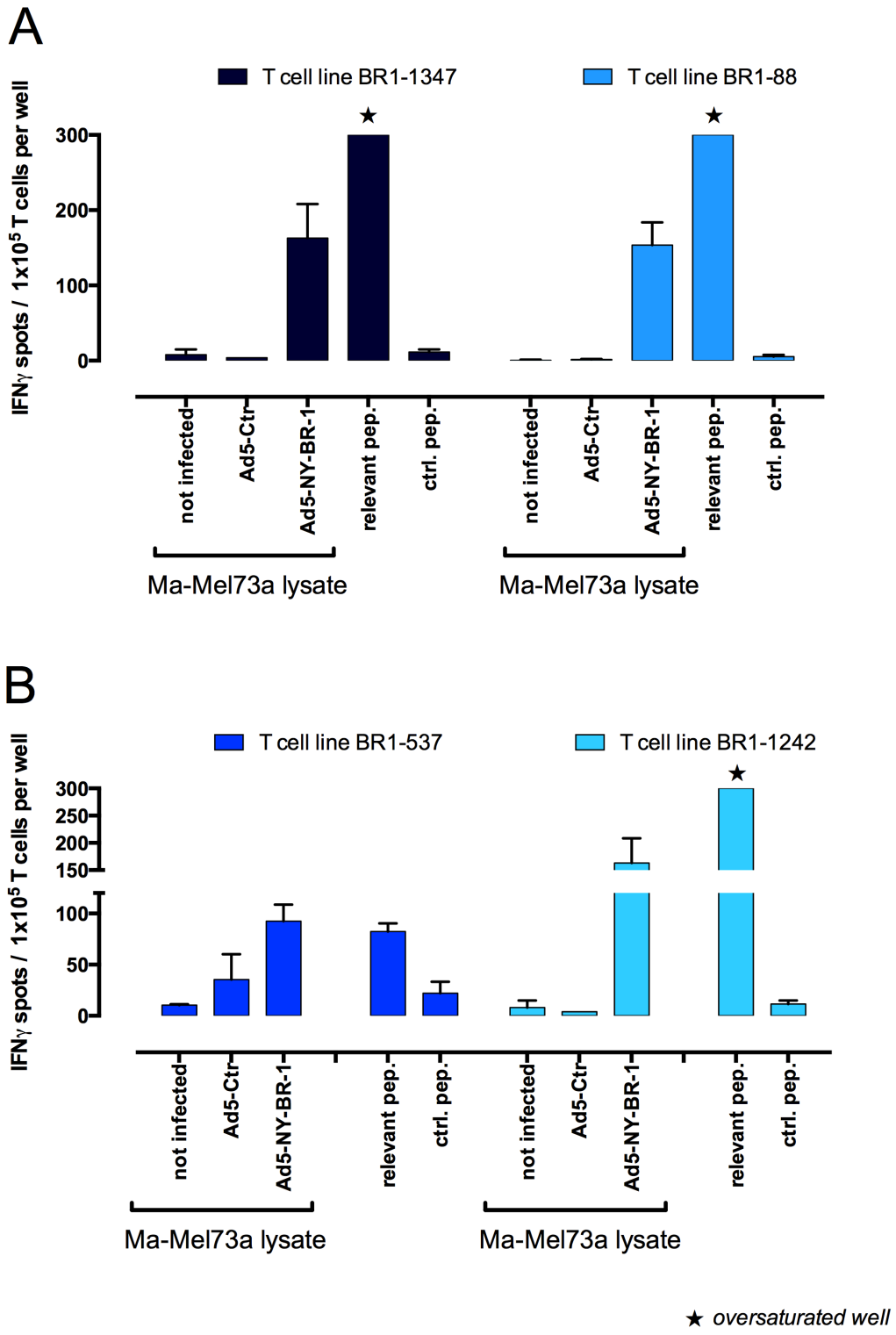

Figure 40: Recognition of human dendritic cells loaded with lysate generated from Ad5-NY-BR-1 infected tumor cells, by murine HLA-DR-restricted T cell lines. *In vitro* generated human dendritic cells were externally loaded with cell lysate originating from Ma-Mel73a cells infected with either Ad5 or Ad5-NY-BR-1 or pulsed with 1 µg of the relevant peptide. 2 X 10^4 *in vitro* generated dendritic cells were incubated with 1 X 10^5 cells of either the HLA-DRB1*0301-restricted T cell line BR1-88 and T cell line BR1-1347 **(A)** or with HLA-DRB1*0401-restricted T cell line BR1-1242 and T cell line BR1-537 **(B)** for 18 hrs on an IFN-γ EliSpot assay. Columns, mean of duplicate determination; bars standard error of the mean.

To sum up, endogenous processing of HLA-DRB1*0301-restricted, NY-BR-1-specific CD4$^+$ T cell epitopes BR1-88 and BR1-1347, as well as endogenous processing of HLA-DRB1*0401-restricted, NY-BR-1-specific CD4$^+$ T cell epitopes BR1-1242 and BR1-537 in human cells was proven by specific recognition of HLA-matched dendritic cells loaded with lysate generated from Ad5-NY-BR-1 infected tumor cells, by murine HLA-DR-restricted T cell lines BR1-88, BR1-1347, BR1-1242 and BR1-537. After all, the milestone IV on verification of processing of NY-BR-1-specific epitopes in human cells was reached.

5.7 Detection of NY-BR-1-specific CD4$^+$ T cells in breast cancer patients and healthy donors

5.7.1 Selection of NY-BR-1$^+$ HLA-matched breast cancer patients

A total of 120 breast tumor biopsy specimens from breast cancer patients were collected at the Heidelberg University Hospital and NY-BR-1 protein expression was confirmed by immunohistochemical stainings, performed at the Pathology department at the Heidelberg University Hospital. 24 Patients with NY-BR-1 positive tumor biopsies were selected, and HLA-genotyping of PBMCs revealed three HLA-DRB1*0301 (BC-1, BC-2, BC-3) and five HLA-DRB1*04 (BC-4, BC-5, BC-6, BC-7, BC-8) positive breast cancer patient samples which were used in the following experiments (Supplement table. 36).

5.7.2 NY-BR-1-specific CD4$^+$ T cells were detected among PBMCs of breast cancer patients and healthy donors after peptide stimulation *in vitro*

Next, we wanted to determine the spontaneous T cell response specific for the NY-BR-1-derived CD4$^+$ T cell epitopes identified in HLA-DRtg mice within the peripheral blood of breast cancer patients and healthy donors.

a) NY-BR-1-specific CD4$^+$ T cells were detected among PBMCs of breast cancer patients

PBMCs obtained from three HLA-DRB1*0301 positive breast cancer patients (samples: BC-1, BC-2, BC-3) and four HLA-DRB1*0401 positive breast cancer patients (samples: BC-4, BC-5, BC-6, BC-7) were *in vitro* stimulated with the relevant HLA-DR-restricted NY-BR-1-specific peptides for 24 days. To detect NY-BR-1-specific CD4$^+$ T cells among the *in vitro* stimulated PBMC cultures, cells were analyzed by immunoflourescent staining. A panel of different markers was investigated, including three cellular surface markers (CD3, CD4, CD8) and one cytokine (IFN-γ).

As shown in figure 41 A, elevated levels of CD4$^+$IFN-γ^+ T cells could be detected among PBMCs of all three HLA-DRB1*0301$^+$ breast cancer patients (BC-1, BC-2, BC-3) upon *in vitro* stimulation with the respective NY-BR-1-derived peptides. Between 0.14% and 2.77% of antigen-specific CD4$^+$IFN-γ^+ T cells were detected among PBMCs of HLA-DRB1*0301$^+$ breast cancer patients (fig. 41 A), when compared to the medium control (m), for all NY-BR-1 derived peptides investigated.

Most elevated levels of antigen-specific CD4$^+$IFN-γ^+ T cells could be detected among PBMCs of three HLA-DRB1*0301$^+$ breast cancer patients, for CD4$^+$IFN-γ^+ T cells specific for the NY-BR-1-derived peptide BR1-1347 (BC-1: 2.77%, BC-2: 0.43%, BC-3: 1.88%), when compared to elevated amounts of activated CD4$^+$IFN-γ^+ T cells specific for peptides BR1-88 (0.24% - 1.24%) and BR1-1238 (0.03 - 0.49%) detected in these patients (fig. 41 A), when compared to the medium control. Collectively, antigen-specific CD4$^+$ T cells for all three NY-BR-1-derived peptides analyzed (fig. 41 A) could be detected among *in vitro* restimulated PBMCs of HLA-DRB1*0301$^+$ breast cancer patients BC-1 and BC-3. However, no elevated levels of CD4$^+$IFN-γ^+ T cells specific for peptides BR1-1238 and BR1-88 could be detected among PBMCs of breast cancer patient BC-2 (fig. 41 A).

As shown in figure 41 C, results obtained in the second experiment (Experiment 2), confirmed the absence of CD4$^+$IFN-γ^+ T cells specific for peptide BR1-1238 and BR1-88 among PBMCs of breast cancer patient BC-2 (fig. 41 C). Moreover, detection of CD4$^+$IFN-γ^+ T cells recognizing their cognate peptides BR1-1347 and BR1-88 was confirmed in the second experiment (fig. 41 C) among PBMCs of BC-2. Albeit, in contrast to the first experiment (Experiment 1), no CD4$^+$IFN-γ^+ T cells specific for peptide BR1-1238 could be detected among PBMCs of breast cancer patient BC-3 (fig. 41 C). As shown in figure 41 B, CD4$^+$ T cells specific for NY-BR-1-derived peptides BR1-537, BR1-1242 and peptide BR1-656/-775 could be detected among PBMCs obtained from HLA-DRB1*0401$^+$ breast cancer patients (BC-4, BC-5, BC-6, BC7). However, differences regarding the frequency of activated, NY-BR-1-specific CD4$^+$ T cells and the immunogenicity of the three NY-BR-1-derived peptides, were observed among individual patients (fig. 41 B). Among PBMCs obtained from HLA-DRB1*0401$^+$ breast cancer patients, highest immunogenicity was observed for peptide BR1-537 with elevated levels of CD4$^+$IFN-γ^+ T cells between 0.97% and 1.42% detected among PBMCs of HLA-DRB1*0401$^+$ breast cancer patient BC-4 and BC-7 (fig. 41 B) compared to the medium control. Albeit, no elevated amounts of activated CD4$^+$IFN-γ^+ T cells specific for peptide BR1-537 could be detected among PBMCs of breast cancer patients BC-5 and BC-6. However, elevated amounts of CD4$^+$IFN-γ^+ T cells specific for the remaining analyzed HLA-DRB1*0401-restricted, NY-BR-1-derived peptides BR1-1242 and BR1-656/-775 up to 0.28% and 0.43% could be detected among PBMCs of patient

BC-5 but did not stimulate CD4$^+$IFN-γ^+ T cells among PBMCs of BC-6 (fig. 41 B), when compard to the medium control.

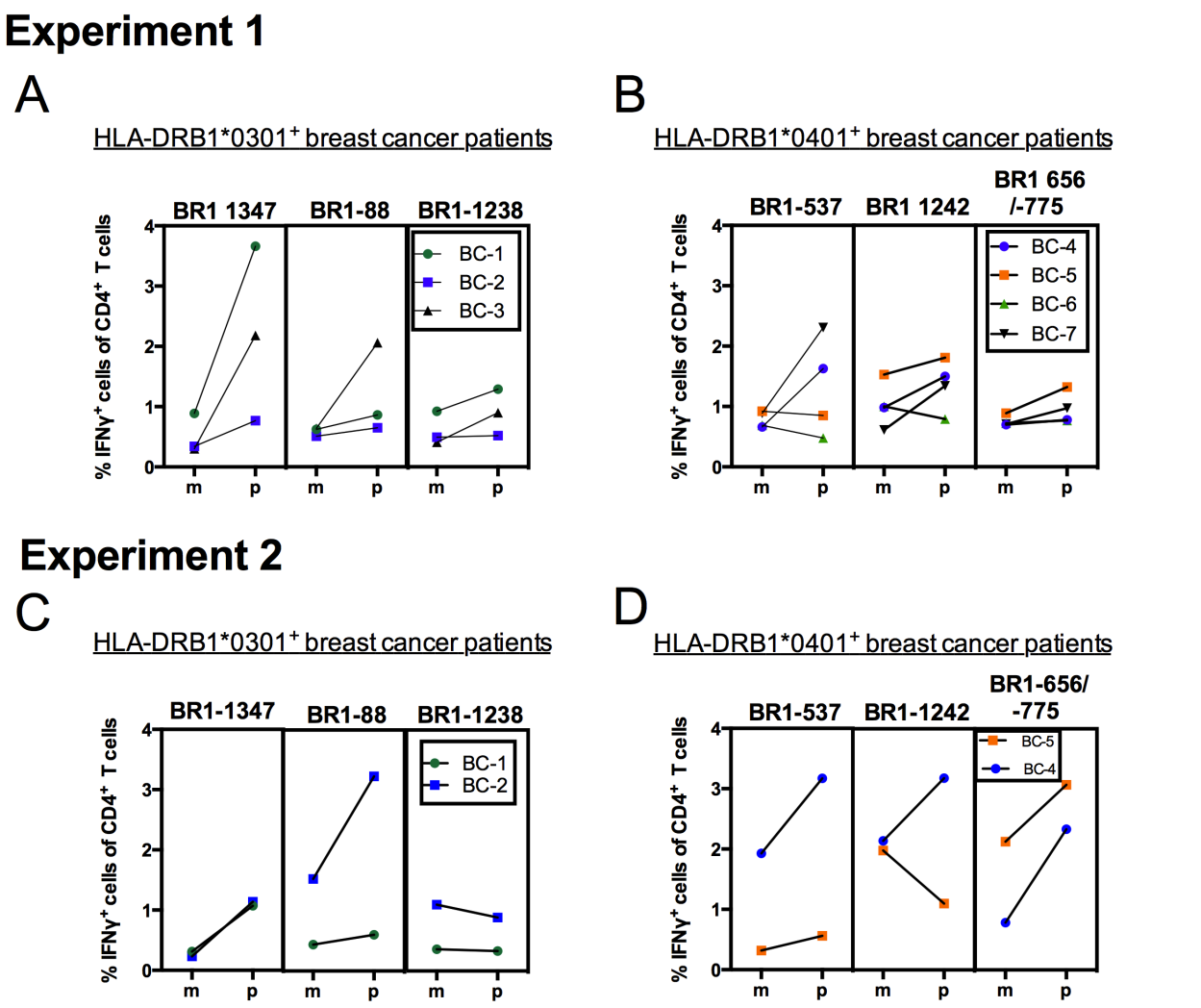

Figure 41: Detection of NY-BR-1-specific CD4$^+$ T cells among PBMCs of breast cancer patients. PBMCs obtained from HLA-DRB1*0301 (**A, C**) and from HLA-DRB1*0401$^+$ breast cancer patients (**B, D**), BC-1 to BC-7 were *in vitro* stimulated for 24 days with the indicated peptides. Antigen-specific CD4$^+$IFN-γ^+ T cells were detected upon stimulation of PBMCs with the relevant peptide for 24 hrs in the assay by immunoflourescent staining of the PBMCs for the surface markers CD3, CD4 and the cytokine IFN-γ. Within the assay, *in vitro* stimulated PBMC cultures were either again stimulated with the **relevant peptide (p)**, or left unstimulated **medium control** (**m**). Data were acquired on a FACS canto and analyzed by using the Flow Jo software. Depicted are percentages of CD4$^+$IFN-γ^+cells among live CD3$^+$ cells.

Upon *in vitro* stimulation of PBMC-samples BC-4 and BC7 with peptide BR1-1242 and BR1-656/-775, CD4$^+$ T cells recognizing their cognate antigen could be detected in both patients for the peptide BR1-1242, with elevated frequencies of CD4$^+$IFN-γ^+ T cells from 1.34% to 1.5% in comparison to the medium control. Among PBMCs obtained from patient BC-7, increased amounts of CD4$^+$IFN-γ^+ T cells specific for peptide BR1-656/-775 (0.26%), but no difference in the frequency of CD4$^+$IFN-γ^+ T cells specific for peptide BR1-1242, were detected when

compared to the medium control (fig. 41 B).

In a second experiment (Experiment 2), as shown in figure 41 D, PBMCs obtained from HLA-DRB1*0401$^+$ breast cancer patients BC-4 and BC-5 were screened for the presence of NY-BR-1-specific CD4$^+$ T cells. Results obtained were in line with the first experiment (fig. 41 B), except for the detection of CD4$^+$ T cells specific for the peptide BR1-656/-775 (elevated fequencie of CD4$^+$IFN-γ^+ T of 0.97%) in BC-4 (fig. 41 D) and the absence of CD4$^+$IFN-γ^+ T cells specific for peptide BR1-1242 among *in vitro* restimulated PBMCs of patient BC-5 (fig. 41 D), in comparison to the medium control.

Overall, the HLA-DRB1*0301-restricted NY-BR-1-derived peptide BR1-1347 and the HLA-DRB1*0401-restricted NY-BR-1-derived peptide BR1-537, stimulated the highest frequencies of CD4$^+$IFN-γ^+ T cells among tested PBMCs of breast cancer patients after *in vitro* stimulation of PBMCs over a time period of 24 days.

In parallel to the immunoflourescent staining of *in vitro* stimulated PBMCs of breast cancer patients (BC-1 to BC-7), IFN-γ^+ EliSpot assays were performed with the PBMCs used in experiment 1 (supplement fig. 46) and experiment 2 (supplement fig. 47). However, the results did not correlated with the data obtained by immunoflourescen staining (fig. 41), due to high background activity of the analyzed samples in the IFN-γ^+ EliSpot assays.

B) NY-BR-1-specific CD4$^+$ T cells were detected among PBMCs of healthy donors

PBMCs obtained from two HLA-DRB1*0301 positive healthy donors (samples: HD-1, HD-2) and from two HLA-DRB1*0401 positive healthy donors (samples HD-3, HD-4), were stimulated *in vitro* with the relevant MHC-restricted NY-BR-1-derived peptides.

Among PBMCs of HLA-DRB1*0301$^+$ healthy donors (HD-1, HD-2), *in vitro* stimulated with peptide BR1-1347, elevated frequencies of antigen-specific CD4$^+$IFN-γ^+ T cells of 1.5% (HD-1) and 0.43% (HD-2) (fig. 42 A), were detected compared to the medium control. CD4$^+$IFN-γ^+ T cells specific for peptide BR1-88 could be detected among PBMCs of HD-1 (fig. 42 A). The results obtained for the detection of CD4$^+$IFN-γ^+ T cells specific for peptide BR1-88 among PBMCs of healthy donor 2 (HD-2) in the medium control, most likely presents an artifact due to technical problems during data acquiring. Results obtained in the second experiment for PBMC-samples of healthy donors HD-1 and HD-2, are in line with date obtained in the the first experiment (Experiment 1) (fig. 42 A).

As depicted in figure 42 B and figure 42 D, elevated frequencies of activated CD4$^+$IFN-γ^+ T cells specific for the HLA-DRB1*0401-restricted peptide BR1-537 could be detected in both experiments among PBMCs obtained from HLA-DRB1*0401$^+$ healthy donor HD-3, compared to the medium control . However, no increased frequencies of CD4$^+$ T cells specific for the NY-BR-

1-derived peptides BR1-1242 and BR1-656/-775, in comparison to the medium control, could be detected in any of the PBMC-samples obtained from HLA-DRB1*0401$^+$ healthy donors (fig. 42 B, D).

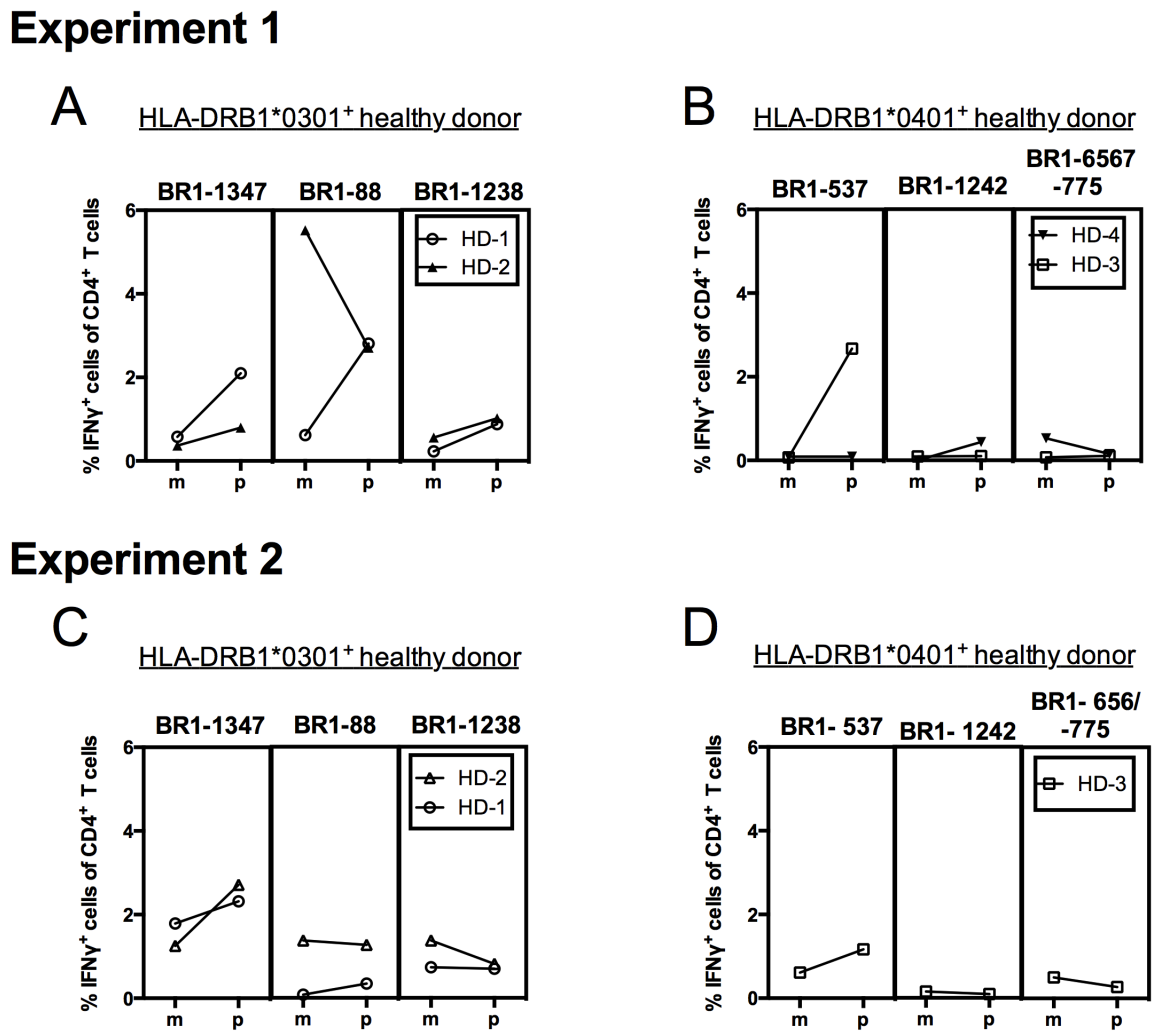

Figure 42: Detection of NY-BR-1-specific CD4$^+$ T cells among PBMCs of healthy donors. PBMCs obtained from HLA-DRB1*0301 (A,C) and from HLA-DRB1*0401$^+$ healthy donors (B,D), were *in vitro* restimulated for 24 days with the relevant peptide. Antigen-specific CD4$^+$IFN-γ^+ T cells were detected upon stimulation of *in vitro* stimulated PBMCs with the relevant peptide for 24 hrs, by immunoflourescent staining of the PBMCs for the surface markers CD3, CD4 and the cytokine IFN-γ. Data were acquired on a FACS Canto and analyzed by using the flow Jo software. Depicted are percentages of CD4$^+$IFN-γ^+cells among live CD3$^+$ cells.

To sum up, CD4$^+$IFN-γ^+ T cells specific for the NY-BR-1-derived HLA-DRB1*0301-restricted peptides BR1-1347, BR1-88, BR1-1238 and HLA-DRB1*0401-restricted peptides BR1-537, BR1-1242 and BR1-656/-775 were detected in the peripheral blood of breast cancer patients upon *in vitro* stimulation for 24 days of PBMCs with the relevant peptide.

Moreover, CD4$^+$ T cells specific for NY-BR-1-derived peptides BR1-1347 and

BR1-537 were also detected among PBMCs of HLA-matched healthy donors upon *in vitro* stimulation for 24 days of PBMCs with the relevant peptide.

5.7.3 NY-BR-1-specific $CD25^+FoxP3^+CD127^-$ T cells and $CD25^+FoxP3^+CD4^+$ T cells secreting IFN-γ could be detected among PBMCs of breast cancer patients and healthy donors.

Among $CD4^+$ T cells of PBMCs obtained from HLA-DRB1*0301$^+$/*0401$^+$ breast cancer patients and healthy donors, we could detect $CD25^+FoxP3^+CD127^-$ T cells (Tregs).

As shown in figure 43 A, frequencies of total Tregs from 9.53% to 13.80% could be detected among PBMCs obtained from breast cancer patient BC-1, whereas the highest frequency of Tregs was observed in PBMC cultures of patient BC-1 which had been stimulated with peptide BR1-88. In contrast to this findings, highest frequencies of Tregs (7.08%), were detected among PBMCs obtained from BC-2 which were *in vitro* stimulated with peptide BR1-1238 (fig. 43 A). Numbers of total Tregs detected among PBMCs obtained from BC-3 with frequencies of 7.08%, 7.20% and 7.09% were similar for all three PBMC cultures analyzed, irrespectively of the NY-BR-1 specific peptide used for *in vitro* stimulation for the PBMC cultures (fig. 43 A). Similar tendencies of total Treg frequencies being independent of the peptide applied for *in vitro* stimulation of PBMC cultures, were observed for the detection of total Tregs among PBMCs obtained from HLA-DRB1*0301$^+$ healthy donors HD-1 and HD-2, hence frequencies of total Tregs varied only from 7.39% to 8.89%, and from 3.37% to 4.00% among PBMCs obtained from HD-1 and HD-2, respectively (fig. 43 A). Collectively, the overall highest frequencies of Tregs among PBMCs obtained from HLA-DRB1*0301$^+$ donors, was detected among PBMCs of breast cancer patient BC-1.

Figure 43 B, shows the frequencies of total Tregs detected among PBMCs of HLA-DRB1*0401$^+$ breast cancer patients and healthy donors. Among PBMCs obtained from breast cancer patient BC-4, 12.% and 11.2% of total Tregs could be detected upon stimulation with peptides BR1-537 and BR1-656/-775, respectively. Whereas, after stimulation of PBMCs obtained from BC-4 with peptide BR1-1242, the lowest frequency (6.31%) of total Tregs among PBMCs of patient BC-4, was detected (fig. 43 B). Interestingly, frequencies of total Tregs among PBMCs obtained from BC-7 were in comparison lower than frequencies of total Tregs detected among PBMCs obtained from BC-4, but showed the same distribution. The lowest frequency of regulatory T cells (2.66%) was detected among PBMCs of breast cancer patient BC-7 which had been stimulated with peptide BR1-1242 (fig. 43 B). In line with this findings, the lowest number of total Tregs of 3.86% among PBMCs of HD-4 was also detected after stimulation of the PBMC sample with peptide BR1-1242. Frequencies of total Tregs detected were similar for all PBMC cultures tested obtained from BC-5, BC-6 and HD-3, irrespectively of the peptide used for *in vitro* stimulation

of the PBMC cultures (fig. 43 B). As depicted in figure 43 B, total numbers of Tregs detected among PBMCs obtained from BC-5, BC-6 and HD-3 varied from 7.66% to 8.13%, from 4.09% to 5.90% and from 10.9% to 12.4%, respectively.

Collectively, frequencies of total $CD25^{+}FoxP3^{+}CD127^{-}$ T cells among $CD4^{+}$ T cells detected ranged from 2.66% (BC-7) to 13.80% (BC1-) independently of the NY-BR-1-derived antigenic stimulus applied during the 24 days of *in vitro* stimulation. Total frequencies of $CD25^{+}FoxP3^{+}CD127^{-}$ T cells among $CD4^{+}$ T cells did not exceed 14% in any of the analyzed samples.

Next, we investigated the presence of $CD25^{+}FoxP3^{+}CD4^{+}$ T cells (Treg-like cells) which secreted IFN-γ, among NY-BR-1-specific $CD4^{+}$IFN-γ^{+} T cells detected in PBMCs of breast cancer patients and healthy donors by immunoflourescent staining of PBMCs. As depicted in figure 43 C, frequencies of $CD25^{+}FoxP3^{+}CD4^{+}$ T cells secreting IFN-γ among total NY-BR-1-specific $CD4^{+}$IFN-γ^{+} T cells, varied between 4.49% and 17.05% in PBMC-samples obtained from HLA-DRB1*0301^{+} breast cancer patients and healthy donors. Even though differences, regarding the total amount of Treg-like cells secreting IFN-γ varied among patient PBMC-samples, total numbers of Treg-like cells were similar among $CD4^{+}$IFN-γ^{+} T cells in all patient PBMC-samples and healthy donor PBMC-samples, irrespectively of the NY-BR-1-derived peptide used for *in vitro* stimulation.

Frequencies of $CD25^{+}FoxP3^{+}CD4^{+}$ T cells secreting IFN-γ detected among $CD4^{+}$IFN-γ^{+} T cells of BC-1 varied from 12.42% to 16.82% and from 11.93% to 14.31% among $CD4^{+}$IFN-γ^{+} T cells in the PBMC-sample of BC-2, upon stimulation of PBMC cultures with NY-BR-1-derived peptides BR1-88, BR1-1347 and BR1-1238 (fig. 43 C). In line with this findings, we detected similar amounts (13.43%, 9.04% and 12.42%) of Treg-like cells secreting IFN-γ among $CD4^{+}$IFN-γ^{+} T cells in the PBMC sample of BC-3 , which had been *in vitro* stimulated with NY-BR-1-specific peptides for 24 days (fig. 43 C).

One exception being, PBMC samples obtained from HLA-DRB1*0301^{+} healthy donors, HD-1 and HD-2, which displayed low levels of $CD25^{+}FoxP3^{+}CD4^{+}$ T cells secreting IFN-γ (from 4.49% to 12.27%) among $CD4^{+}$IFN-γ^{+} T cells, after *in vitro* restimulation of the PBMC sample with the NY-BR-1-derived epitope BR1-1347 and BR1-1238, but displayed higher amounts of Treg-like cells secreting IFN-γ among $CD4^{+}$IFN-γ^{+} T cells upon stimulation of PBMCs with NY-BR-1-derived epitope BR1-88 (from 17.05% to 18.33%), (fig. 43 C). Thereby, indicating a potential peptide specific induction of $CD25^{+}FoxP3^{+}CD4^{+}$ T cells secreting IFN-γ upon stimulation of PBMCs obtained from HD-1 and HD-2 with the NY-BR-1-specific peptide BR1-88.

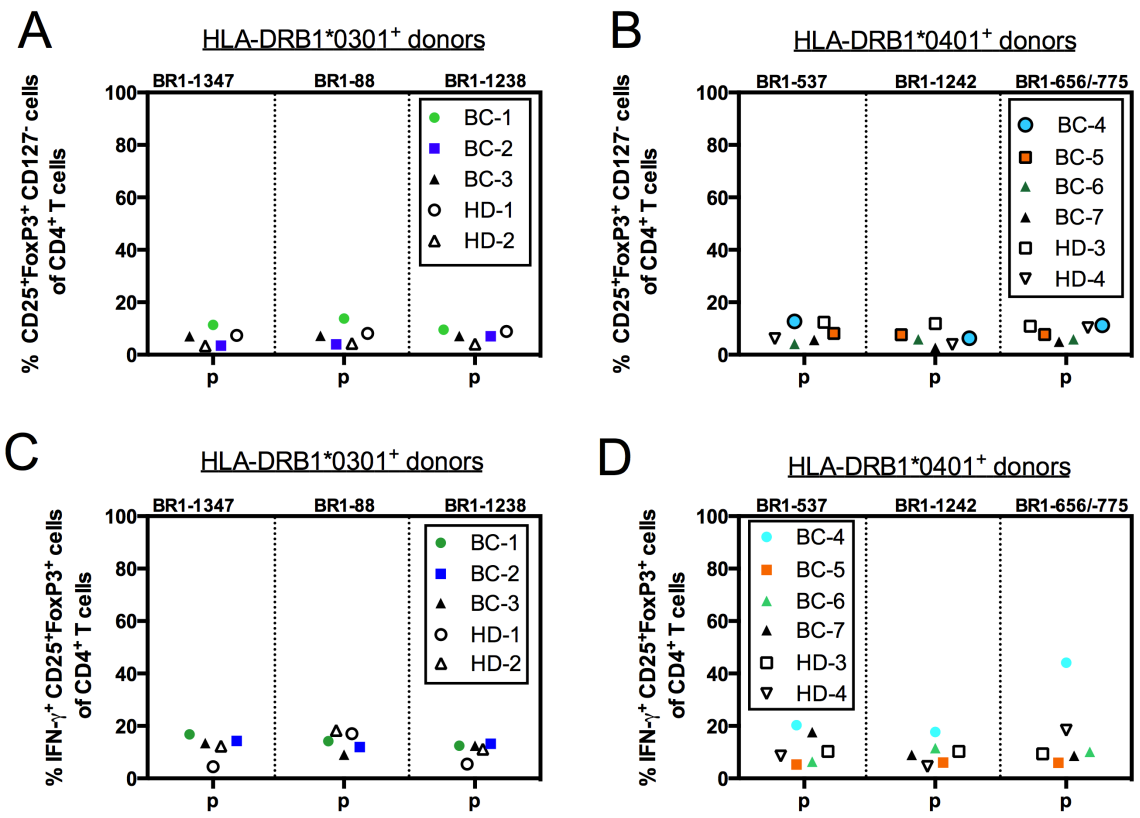

Figure 43: Detection of CD25$^+$ FoxP3$^+$CD127$^-$ and Treg-like cells secreting IFN-γ among CD4$^+$ T cells of breast cancer patients and healthy donors. PBMCs obtained from HLA-DRB1*0301$^+$ breast cancer patients BC-1, BC-2, BC-3 and healthy donors HD-1, HD-2 as well as PBMCs obtained from HLA-DRB1*0401$^+$ breast cancer patients BC-4, BC-5, BC-6, BC-7 and healthy donors HD-3, HD-4, were *in vitro* stimulated for 24 days with the NY-BR-1-derived epitopes BR1-1347, BR1-88, BR1-1238 and BR1-537, BR1-1242, BR1-656/775, respectively. Results depict the frequency of total Tregs (CD25$^+$ FoxP3$^+$CD127$^-$) of CD4$^+$ T cells among PBMCs of HLA-DRB1*0301$^+$ PBMC samples (**A**) and among HLA-DRB1*0401$^+$ PBMC samples (**B**). Frequencies of CD25$^+$FoxP3$^+$CD4$^+$ T cells (Treg-like cells) secreting IFN-γ of CD4$^+$ T cells are depicted for HLA-DRB1*0301$^+$ PBMC samples (**C**) and HLA-DRB1*0401$^+$ PBMC samples (**D**).

As shown in figure 43 B, D, CD25$^+$FoxP3$^+$CD4$^+$ T cells secreting IFN-γ could also be detected among CD4$^+$IFN-γ$^+$ T cells of PBMCs obtained from HLA-DRB1*0401$^+$ breast cancer patients BC-4, BC-5, BC-6, BC-7 and healthy donors HD-3, HD-4.

In PBMC-samples obtained from breast cancer patient BC-4, BC-5, BC-6 and BC-7, total variations in frequencies of Treg-like cells among CD4$^+$IFN-γ$^+$ T cells from 0.7% (BC-%) up to 23.81% (BC-4) were observed.

Similar amounts of Treg-like cells secreting IFN-γ among CD4$^+$IFN-γ$^+$ T cells, varying from 5.3% to 6.04%, irrespectively of the peptide used for *in vitro* stimulation of the PBMC cultures, were detected among PBMCs of breast cancer patient BC-5. CD25$^+$FoxP3$^+$CD4$^+$ T cells secreting IFN-γ detected among CD4$^+$IFN-γ$^+$ T cells in the PBMC-sample of BC-6 varied from 6.37% after stimulation of the PBMCs with peptide BR1-537 to 11.52% and to 10.15%, after stimulation with peptides BR1-1242 or BR1-656/-775. Furthermore, Treg-like cells secreting IFN-γ (17.6%) could be detected among CD4$^+$IFN-γ$^+$ T cells upon stimulation of PBMCs, obtained from BC-7

with peptide BR1-537. In comparison, amounts of Treg-like cells detected upon stimulation of PBMCs obtained from BC-7 with peptide BR1-1242 and BR1-656/-775 were lower with detected freqeuncies of 8.99% and 8.62%, respectively. Important to note, *in vitro* stimulated PBMCs of breast cancer patient BC-4, displayed the overall highest variation in the frequency of Treg-like cells secreting IFN-γ (44.14%), detected among $CD4^+$IFN-γ^+ T cells, after stimulation of PBMCs with the peptide BR1-656/-775, when compared to 20.33% and 17.68% of Treg-like cells secreting IFN-γ after stimulation of PBMCs with peptides BR1-537 or BR1-1242 (fig. 43 D).

Amounts of Treg-like cells secreting IFN-γ detected among $CD4^+$IFN-γ^+ T cells of healthy donor HD-4 varied from 4.57% to 18.36% after stimulation with the peptides BR1-1242 and BR1-656/-775 (fig. 43 D). Whereas, frequencies of Treg-like cells secreting IFN-γ among $CD4^+$IFN-γ^+ T cells were similar (10.27%, 10.30% and 9.38%), after the stimulation of PBMCs with the peptides BR1-537, BR1-1242 and BR1-656/-775, respectively (fig. 43 D).

To sum up, we could detect $CD25^+FoxP3^+CD4^+$ T cells (Treg-like cells) secreting IFN-γ among $CD4^+$IFN-γ^+ T cells of breast cancer patients and healthy donors, whereas frequencies of Treg-like cells secreting IFN-γ were in all stimulated PBMC-samples below 20%. One exception being the detection of 44.14% of $CD25^+FoxP3^+CD4^+$ T cells secreting IFN-γ among $CD4^+$IFN-γ^+ T cells in the PBMC-sample of breast cancer patient BC-4, upon stimulation with the NY-BR-1-derived peptide BR1-656/-775. This finding might indicating an antigen-specific stimulation of Treg-like cells in this particular case.

6 Discussion

6.1 Comparison of a global vaccination approach versus *in silico* epitope-prediction used for the identification of antigen-specific T cell epitopes

To identify NY-BR-1-specific T cell epitopes, a number of different methods are available for the exact mapping of antigen-specific epitopes within the amino acid sequence of the antigen. In this work, a global vaccination approach was applied, followed by *in silico* epitope-prediction, using the SYFPEITHI algorithm. In the following paragraph, advantages and disadvantages of both methods are going to be elucidated.

The global vaccination approach applied in this work was based on immunizing HLA-transgenic mice with a global NY-BR-1 encoding expression vector and followed by the screening of a NY-BR-1-specific peptide library. Hence, the complete NY-BR-1 amino acid sequence was covered by the NY-BR-1-specific peptide library, one advantage of the global approach certainly is the potential of theoretically detecting every possible NY-BR-1-derived T cell epitope. Furthermore, the global vaccination approach allows to investigate candidate epitopes which might be neglected, due to low prediction scores and thresholds of the *in silico* epitope-prediction algorithm. This particular advantage of the global screening approach became especially obvious in the case of identifying NY-BR-1-specific epitopes in DR3tg mice, as candidate epitopes with *in silico* SYFPEITHI algorithm prediction scores < 20 were identified (fig. 35 A). These NY-BR-1-specific, MHC-restricted candidate epitopes would have been neglected relying on reverse immunology.

On the other hand, several limitations of the global vaccination approach used in this project appeared: e.g the antigen-specific candidate epitopes identified in DR3tg mice and DR4tg mice (fig. 35 A,B), could not explain immunogenicity for all peptide pools detected in DR3tg mice (fig. 13) and DR4tg mice (fig. 16).

Moreover, a cascade of matrix screenings had to be applied in DR4tg mice to identify immunogenic NY-BR-1-derived library peptides (fig. 9). Possible reasons for the limitations of the global vaccination approach might be insufficient uptake and expression of intramuscularly injected DNA by muscle cells, since *Dupuis et. al* described that the distribution of DNA vaccines determines their immunogenicity after intramuscular injection in mice [64]. In addition, high numbers of individual library peptides (13 peptides), composing the NY-BR1-library peptide pools K1-13 and L1-13, might cause the observed limitations of the global vaccination approach applied in this work. One explanation being a potential competition of individual library peptides included in one peptide library pool. As crude NY-BR-1 library peptides were used, an accumulation of peptide synthesis byproducts, such as peptide fragments, might lead to poor immunogenicity of the

affected NY-BR-1 synthetic library peptide pool.

Global vaccination strategies using an attenuated adenovirus (Ad5) encoding the NY-BR-1 antigen might be one fruitful alternative to using a global DNA vaccination approach regarding to the immunogenicity of the applied vaccine. *Osen et al.* [183] showed, that antigen-specific T cell epitopes could be identified successfully in HLA-tg mice after immunization with an adenovirus encoding the melanoma tumor associated differentiation antigen Trp-2. Furthermore, reduction in numbers of individual library peptides composing the peptide library pools, as well as the addition of adjuvants, such as additional CpC motives, which enhance immunogenicity of the DNA vaccination by activation of innate immunity [253], might elevate the immunogenic impact of the global vaccination approach.

Overall, application of the global vaccination approach led to the identification of NY-BR-1-derived, immunogenic library peptides in HHDtg mice, DR3tg mice and DR4tg mice (fig. 35), thus this approach might be considered to be suitable for the identification of tumor antigen-derived T cell epitopes in HLA-tg mice.

Even though the global vaccination approach was successfully applied for the identification of immunogenic NY-BR-1-library peptides (20mers), we subsequently relied on *in silico* SYFPEITHI algorithm, to predict candidate epitope sequences within the identified immunogenic NY-BR-1-derived library peptides (fig. 35).

Algorithms available for *in silico* prediction are for example the SYFPEITHI database [204], predicting human and mouse MHC-I and MHC-II human restricted T cell epitopes for a number of MHC-I and MHC-II alleles of several species. The database Rankpep [205] predicts MHC-I and MHC-II epitopes, as well as the proteasomal digestion of given peptides. Epitope-prediction by the SYFPEITHI database is based on the preferential binding of particular amino acids at anchor positions of the MHC-molecules, for example the HLA-A2 molecule most likely binding 9mer amino acid residues with a Leu at position 2 and a Val or Leu at position 9 [189]. *In silico* prediction scores of the SYFPEITHI algorithm are described to be 80% accurate for prediction of MHC-I-restricted epitopes, thus naturally presented epitopes should be among the top-scoring 2% of all predicted epitopes. In case of MHC-II restricted epitope motifs, prediction reliability is estimated to be only 50%, due to the degenerated binding motives and promiscuity of MHC-II ligands [204].

In the present case, limitations of the SYFPEITHI algorithm were especially observed regarding the *in silico* epitope prediction of HLA-DRB1*0301-restricted peptides. HLA-DRB1*0301-restricted NY-BR-1-derived epitope BR1-88 has a very high prediction score by the SYFPEITHI algorithm (SYFPEITHI score: 34) when compared to the HLA-DRB1*0301-restricted epitopes BR1-1238 (SYFPEITHI score: 15) and BR1-1347 (SYFPEITHI score: 22), but did not present

the strongest antigen-specific IFN-γ response among splenocytes obtained from immunized DR3tg mice (fig. 23 A, fig. 24 A). Discrepancies between the *in silico* prediction of antigen-specific HLA-DR-restricted epitopes using the SYFPEITHI algorithm and the observed immunogenicity of the predicted epitopes in HLA-tg mice, might be due to species-specific differences in the MHC-II epitope processing machinery or selection of the T cell repertoire, which will be discussed in the next paragraph.

6.2 Potential limitations and advantages of HLA-tg mouse models for the identification of human tumor antigen-specific T cell epitopes

In this work, we observed differences among the immunogenicity of individual NY-BR-1-derived peptides investigated in mice or humans. The published NY-BR-1-derived, HLA-A*0201-restricted epitopes p158-167, p960-968 [112], did not stimulate splenocytes obtained from HHDtg mice after DNA-vaccination in an antigen-specific manner. In fact, it was expected that HHDtg mice, expressing the HLA-A*0201 molecule, are capable of presenting these epitopes after global DNA-vaccination. Lack of antigen-specific IFN-γ response upon stimulation of murine splenocytes with the epitopes p158-167 and p960-968, can be potentially explained by differences in MHC-I antigen processing machinery among mouse and human species.

It has been described in the literature by *Falk et al.*, that antigen processing for MHC class I restricted presentation is conserved between mouse and humans [70], demonstrated for example by the ovalbumin peptide SIINFEKL being processed in both, human and murine H-2K^b expressing cells [69]. However, interspecies differences among the murine and human MHC-I processing machinery are also described in the literature available. The ATP-dependent transporter associated with antigen processing (TAP) shows differences regarding peptide binding in mouse and humans. Murine TAP are described to preferentially bind peptides with a hydrophobic C-terminus, whereas the human TAP transporter is less selective [224, 165].This difference is also reflected by different peptide anchor residues required by the MHC-I alleles for peptide binding. Murine MHC class I alleles require unvaryingly hydrophobic or aromatic C-terminal residue whereas binding of peptides with either a hydrophobic, aromatic or basic anchor residue is described for human MHC class I alleles [93, 204]. One exception is the HLA-A*0201 motif which also requires, similar to the murine MHC-II molecule, hydrophobic amino acids at the C-terminus of the peptide ligand. Moreover, the length of MHC-peptide ligands, cleaved by the ERAP peptidase which trims precursor peptides to generate peptides with the appropriate length required for binding to the MHC-I molecules, differs among humans and mice, thus generating a different MHC-I-restricted epitope repertoire within these two species [19].Evidence for the differences among human and murine MHC-I ligand

processing has been given by a study conducted in mice transgenic for the human HLA-A*0201 molecule (HHDtg mice), which reported, that certain HLA-A*0201-restricted antigen-specific epitopes found among the peptide repertoire in human cells are not processed in HHDtg mice [243].

Up to now, interspecies differences in the MHC-II antigen-processing pathway among mouse and human are poorly investigated.

Regarding our results obtained in DR3tg mice, even though predicted by the SYFPEITHI database with a high score, HLA-DRB1*0301-restricted NY-BR-1-derived candidate epitope BR1-88 (SYFPEITHI algorithm score 34), did not elicit a strong antigenic response among splenocytes obtained from immunized DR3tg mice, determined by Elispot assay (fig. 23 A) and by IFN-γ-secretion assay. This might be attributed to differences in the presented MHC-II peptide repertoire among mice and humans or differences in T cell selection. The immunogenicity of candidate epitope BR1-88 among PBMCs obtained from breast cancer patients (fig. 41 A), which was detected in the following, supports the assumed inter-species differences in the presented MHC-II peptide repertoire, since the presence of $CD4^+$ T cells specific for the peptide BR1-88 among PBMCs of breast cancer patients clearly indicate that the peptide BR1-88 is presented on MHC-II molecules in humans.

Classical MHC class II molecules do not associate with peptides in the endoplasmic reticulum since the peptide binding groove is shielded by the invariant chain (Ii). The invariant chain Ii is degraded in mice and humans by the protease cathepsin S, generating the CLIP (Class II-associated invariant chain peptide), preventing peptide binding to the MHC-II molecule, before the MHC-II peptide repertoire is fully assembled in the endosomal compartment. Cathepsin S later on further facilitates processing of CLIP and MHC-II restricted epitopes in the endosomal compartment [106]. Apart from Cathepsin S being the major protease in MHC-II antigen processing [15] in humans, several other Cathepsins (Cat) have been described in mice to facilitate cleavage of the invariant chain and peptide loading, such as Cat L, Cat F and Cat K [10]. Subsets of murine antigen presenting cells (APCs) are described to use Cathepsin F to mediate MHC class II invariant chain cleavage and peptide loading [231]. Recruitment of different Cathepsins for peptide cleavage might alter the peptide repertoire presented on murine MHC-II molecules, leading to differences among the NY-BR-1-specific T cell repertoire in mice and humans, which might explain interspecies differences observed regarding the immunogenicity of peptide BR1-88.

However, there are many examples where DR3tg mice have been successfully used to identify human $CD4^+$ T cell epitopes [183, 214, 229]. Since no murine analogue of the human NY-BR-1 protein has been described in mice, it has to be expected that induced NY-BR-1-specific murine T cells are not eliminated due to central tolerance mechanisms. This might enhance NY-BR-1-

specific T cell responses in HLA-tg mice, when applying the global vaccination approach discussed above.

6.3 Chimeric screening for human T cell epitopes using murine CD4$^+$ T cells

A chimeric screening system of using murine CD4$^+$ T cells to verify HLA-DRB1*0301-/*0401-restriction and endogenous processing of the newly identified NY-BR-1-derived peptides was applied in this project. One advantage of this approach is good general feasibility of establishing antigen-specific murine CD4$^+$ T cell cultures, which were used for the generation of murine HLA-DR-restricted, antigen-specific CD4$^+$ T cell lines (fig. 27). Established murine HLA-DR-restricted T cell lines showed high peptide affinity when recognizing their cognate peptide on human MHC-molecules (fig. 28). Nevertheless, peptide affinity differed among the five established, NY-BR-1-specific murine, HLA-DR-restricted CD4$^+$ T cell lines since amounts between 62.5 ng/ml and 1000 ng/ml of peptide (fig. 28), externally loaded on human T2/DR3, T2/DR4 cells, were required to elicit specific recognition of the target cells by murine T cell lines. Cloning of the T cell lines by limiting dilutions would probably help to select for high affinity T cell clones, specific for peptides BR1-88, BR1-1347 and BR1-656/-775. Moreover, the protocol of *in vitro* restimulation of murine CD4$^+$ T cell lines should be optimized to minimize the risk of inducing CD4$^+$ T cell lines to become exhausted T cells, which are characterized by a state of T cell dysfunction, commonly observed after chronic antigen-exposure [270]. In our work we might have detected a stage of an exhausted T cell phenotype when applying the murine CD4$^+$ T cell lines for the specific recognition of Ad5-NY-BR-1 infected melanoma cell lines and breast cancer cell lines (fig. 38). A potential exhausted phenotype of the murine CD4$^+$ T cell lines during the performed IFN-γ-EliSpot assay might be indicated by reduced recognition of the positive controls (peptide loaded T2/DR3, T2/DR4 cells) included in this experiment, compared to specific recognition of peptide loaded T2/DR3, T2/DR4 cells by these T cell lines in earlier experiments (fig. 27).

In addition, insufficient interaction of co-stimulatory molecules during priming and of further accessory molecules, such as lymphocyte function-associated antigen 1 (LFA-1) during restimulation might occur due to interspecies barriers, leading to an impaired T cell activation. It has been described, that murine LFA-1 does not bind to human intercellular adhesion molecule (ICAM), although binding-specificity can be mapped to the human LFA-1 alpha subunit [119].

Moreover, the interaction of the CD8-molecule and the MHC-I complex works in a species dependent manner, thus suboptimal interaction of the CD8-molecule with the alpha 3 domain of xenogenic MHC-I molecules may be an important contribution to poor xenoreactivity [109].

Furthermore, it was described in humans, that interaction of the HLA-DR molecule and the human CD4 molecule requires specific amino acid residues at position 110 and 139 of the β_2-domain of the human class II molecules, for proper binding [186]. Experiments in HLA-DRtg mice, have shown, that amino acid 110 of the second domain of human HLA-DR-molecules contributes also to the interaction between murine $CD4^+$ T cells and human class II [127], thus inter-species binding of human MHC molecules and murine $CD4^+$ T cells can be successful. However, interspecies barriers were reported for the interaction of human $CD4^+$ T cells and murine H2-E β_2-domain [203], thus possible xenogenic barriers might also exist (vice versa) for the interaction of murine $CD4^+$ T cells and HLA-DR-molecules.

The DR4tg mice used in this thesis express a chimeric HLA-DRB1*0401 molecule with a murine α_2- and β_2- domain, in comparison to DR3tg mice which express the complete human HLA-DRB1*0301 molecule. Therefore, potential interspecies differences in binding of murine $CD4^+$ T cells to the relevant transgenic HLA-DR molecule were expected to be more pronounced in DR3tg mice compared to an effect in DR4tg mice. Our results show that IFN-γ responses determined by EliSpot assay, upon screening of the synthetic NY-BR-1-specific peptide library, were suboptimal in DR4tg mice (fig. 16) compared to DR3tg mice (fig. 13). Furthermore, the amounts of antigen-specific $CD4^+$ T cells detected *ex vivo* among splenocytes of immunized HLA-DR transgenic mice, were on average greater in DR3tg mice than in DR4tg mice (fig. 24 A, B). This might indicate a suboptimal activation of murine $CD4^+$ T cells by the chimeric HLA-DRB1*0401 molecule expressed in DR4tg mice. In line with this findings are the results obtained on recognition of lysate loaded human HLA-matched dendritic cells by the relevant HLA-DR-restricted T cell line. We could observe on average a higher IFN-γ secretion in HLA-DRB1*0301-restricted murine $CD4^+$ T cells lines compared to HLA-DRB1*0401-restricted $CD4^+$ T cell lines upon recognition of NY-BR-1 protein containing cell lysate loaded human DCs (fig. 40 A, B).

However, signal intensity might have been additionally reduced for some established NY-BR-1-specific T cell lines due to impaired interaction between accessory molecules such as LFA-1 and ICAM. One example for impaired LFA-1 and ICAM interaction might be the T cell lines BR1-656/-775, which showed low affinity for recognition of the cognate HLA-DR-restricted peptide on peptide loaded T2/DR4 cells (fig. 28). It is conceivable, that optimal interaction of co-stimulatory and accessory molecules probably are required to achieve maximal T cell activation upon antigen-recognition in the case of T cell line BR1-656/-775.

In summary, the conclusion can be drawn that the compatibility of the human HLA-DRB1*0301 and HLA-DRB1*0401 molecules is sufficient for binding and activation of murine HLA-DR-restricted $CD4^+$ T cells.

6.4 Multiple approaches applied to confirm endogenous processing of the newly identified HLA-DRB1*0301- and HLA-DRB1*0401-restricted NY-BR-1-specific epitopes in human cells

Given the fact that endogenous processing of the newly identified NY-BR-1-derived peptides needed to be verified in human cells, this work we took advantage of the already established NY-BR-1-specific murine HLA-DR-restricted $CD4^+$ T cell lines to examine this scientific question. The overall strategy aimed at the chimeric approach of antigen-specific recognition of NY-BR-1 expressing human target cells by murine T cell lines.

Up to now, no human cell line endogenously expressing NY-BR-1 *in vitro* is available, thus we firstly focused on the generation of NY-BR-1 expressing human target cells on the relevant MHC-background. Melanoma cell lines and breast cancer cell lines were infected with an attenuated adenovirus encoding the NY-BR-1-protein (Ad5-NY-BR-1). Surface-expression of the CAR-receptor (fig. 31), one major receptor associated with infection of target cells by adenovirus Type 5 [284], as well as surface-expression of HLA-DR molecules (fig. 31) was confirmed, double positive tumor cells (CAR^+, HLA-DR^+), were considered as promising NY-BR-1-protein expressing target cells upon Ad5-NY-BR-1 infection. However, no antigen-specific recognition of Ad5-NY-BR-1 infected, HLA-matched target cells could be observed (fig. 37) for any of the investigated murine T cell lines, although, NY-BR-1-protein expression in the tumor cell lines was confirmed by Western blot analysis (fig. 38). Possible reasons for the observed results might be insufficient processing of MHC-II-restricted peptides in the tested target cell lines, since the melanoma and breast cancer cell lines tested, do not belong to the group of professional antigen-presenting cells, which might impair processing of the relevant epitopes in these cell lines. Moreover, MHC-II surface expression needed to be induced by IFN-γ treatment, resulting in a maybe only transient effect leading to suboptimal amounts of MHC-II surface molecules and subsequently to insufficient antigen-specific stimulation of the $CD4^+$ T effector cells, in combination with impaired interaction of the MHC-DRB1*0301/*0401 molecule and the murine $CD4^+$ T cell line.

Furthermore, persistent antigenic stimulation of the murine $CD4^+$ T cell lines might have induced an "exhausted" phenotype in these T cell lines [280]. T cell exhaustion is defined by poor effector functions and expression of molecules associated with immune-suppressive pathways, such as the PD1 molecule [270]. In line with this thought, murine HLA-DR-restricted $CD4^+$ T cell lines used in this experiment, only showed poor recognition of the included positive control (peptide loaded T2/DR3, T2/DR4 cells),(fig. 38). However, to confirm induction of T cell exhaustion, an immunofluorescent staining for T cell exhaustion markers such as CD244, CD160 and PD1 [283] of the murine $CD4^+$ T cell lines would have been to be performed additionally.

Failure of recognition of HLA-matched human target cell lines, endogenously expressing the

NY-BR-1 protein upon infection with Ad5-NY-BR-1(fig. 38), might also have been due to the fact that IFN-γ is a suboptimal cytokine used as read out for potential $CD4^+$ T cell stimulation. Taken into consideration that $CD4^+$ T cell responses might potentially be a Th2 associated T cell response, cytokines characteristic for a Th2 $CD4^+$ T cell response, such as IL-4 and IL-13, should also be investigated. Moreover, NY-BR-1 expressing target cells might induce antigen specific Tregs, thus cytokines associated with stimulation of regulatory T cells such as TGF-β or IL-10 might be an important additional cytokine read out for this assay. Taken together, so far we could not demonstrate recognition of NY-BR-1 protein expressing, HLA-matched human tumor cell lines, by the established murine $CD4^+$ T cell lines, probably due to the various reasons discussed above.

The following attempts of infecting human PBMCs and human dendritic cells with Ad5-NY-BR-1 did not reveal NY-BR-1-protein expression in infected cells (fig. 34, 36). We could show, that expression of the CAR-receptor was absent in human dendritic cells, which gives a reason for insufficient infection of human dendritic cells with Ad5-NY-BR-1 (fig. 36).

It has been described previously, that human PBMCs, depleted of $CD3^+$ lymphocytes, are specifically recognized by human $CD4^+$ T cell lines after incubation with antigen-encoding Ad5-constructs [183]. Reasons for inefficient infection of human PBMCs, depleted of $CD3^+$ lymphocytes, with Ad5-NY-BR-1 in this work remain unexplained. Application of an antibody detecting Ad5-derived protein could be included in the Western blot analysis to discriminate between unsuccessful infection of target cells and lack of endogenous epitope processing, thereby elucidating the capacity of Ad5-NY-BR-1 to infect human PBMC fractions.

Finally, endogenous processing of the HLA-DR-restricted, NY-BR-1-derived epitopes BR1-88, BR1-1347, BR1-537 and BR1-1242 was verified by the use of human dendritic cells loaded with NY-BR-1-protein containing whole cell lysate. *In vitro* generated mature human dendritic cells (fig. 35) loaded with cellular lysate containing the NY-BR-1-protein (fig. 39), were specifically recognized by murine HLA-DR-restricted $CD4^+$ T cell lines in an antigen-specific manner (fig. 40). In fact, due to our findings, endogenous processing of the above mentioned epitopes can be postulated in human cells. Nevertheless, it remains questionable if the epitopes are processed in the melanoma cell line Ma-Mel73a or by the human dendritic cell from whole cellular lysate, containing NY-BR-1 protein, used for exogenous loading of the dendritic cell. Blockade of the MHC-II processing machinery within the human dendritic cells, for example by using simvastin which inhibits the MHC class II pathway of antigen presentation by impairing Ras superfamily GTPases [86], could give first insights to resolve this question.

6.5 Differences in frequencies of NY-BR-1-specific CD4$^+$IFN-γ^+ T cells in the peripheral blood of breast cancer patients and healthy donors

A collective of PBMC samples of three HLA-DRB1*0301$^+$ (BC1 to BC-3) and four HLA-DRB1*-0401$^+$ breast cancer patients (BC-4 to BC-7) was analyzed for the presence of NY-BR-1-specific, CD4$^+$IFN-γ^+T cells, after 24 days of *in vitro* stimulation with the relevant NY-BR-1-derived peptides.

Analysis of PBMCs obtained from breast cancer patients indicated the presence of CD4$^+$ T cells specific for the identified NY-BR-1-derived peptides BR1-1347, BR1-88, BR1-537, BR1-1242 and BR1-656/-775 in the peripheral blood of tested breast cancer patients (fig. 41). Peptide specific stimulation of CD4$^+$IFN-γ^+ T cells was detected in at least 1/3 tested PBMC samples obtained from HLA-DRB1*0301$^+$ breast cancer patients upon stimulation with the HLA-DRB1*0301-restricted, NY-BR-1-specific peptides BR1-1347 and BR1-88. Based on these findings, we assume that the NY-BR-1-specific peptides BR1-1347 and BR1-88 identified in HLA-transgenic mice, are among the presented MHC-II peptide repertoire in NY-BR-1$^+$ breast cancer patients, which is indicated by the presence of CD4$^+$IFN-γ^+T cells in the peripheral blood of these patients. Interestingly, the frequencies of CD4$^+$IFN-γ^+ T cells specific for the peptide BR1-88 detected among splenocytes obtained from immunized DR3tg mice were very low compared to the detected frequencies of CD4$^+$IFN-γ^+ T cells specific for peptide BR1-1238 (fig. 24). In contrast, we could detect CD4$^+$IFN-γ^+ T cells specific for the peptide BR1-88 with a higher frequency (2.06% CD4$^+$IFN-γ^+ T cells) than CD4$^+$IFN-γ^+ T cells specific for the peptide BR1-1238 (1.29% CD4$^+$IFN-γ^+ T cells), in the peripheral blood of breast cancer patients (fig. 41). This finding, might demonstrate inter-species related differences in frequencies of NY-BR-1-specific, CD4$^+$IFN-γ^+ T cells due to differences in the peptide repertoire presented on MHC-II molecules in mice and humans, as discussed above. So far, we could not demonstrate the endogenous processing of the NY-BR-1-derived HLA-DRB1*0301-restricted peptide BR1-1238 in human cells, hence this epitope might not be among the peptide repertoire presented on MHC-II in breast cancer patients. Therefore, potentially explaining very low to non-detectable amounts of CD4$^+$ T cells specific for this antigen detected among PBMCs of HLA-DRB1*0301$^+$ breast cancer patients.

Moreover, CD4$^+$IFN-γ^+ T cells specific for the HLA-DRB1*0401-restricted, NY-BR-1-specific peptides BR1-537, BR1-1242 and BR1-656/-775 were also detected among PBMCs in at least 1/4 tested breast cancer patient samples. Frequencies of CD4$^+$IFN-γ^+ T cells specific for peptide BR1-537, were the highest (1.34% CD4$^+$IFN-γ^+ T cells) among all HLA-DRB1*0401-specific CD4$^+$ T cell responses detected, which correlates with our data obtained in DR4tg mice (fig. 24 B).

It was expected to detect NY-BR-1-specific $CD4^+$ T cells in the peripheral blood of breast cancer patients with NY-BR-1^+ tumors, since NY-BR-1-specific immunogenic peptides might be released by dying tumor cells into the tumor stroma, and further on processed and presented on MHC-II molecules for example by dendritic cells or tumor associated macrophages (TAMs). Notably, it should be taken into considereation that frequencies of NY-BR-1-specific $CD4^+$ T cells in the peripheral blood of breast cancer patients might be low, as observed within the PBMC sample of BC-6 (fig. 41 B), since mature $CD4^+$ T cells show enhanced migratory properties toward the bone marrow, thus the bone morrow might function as a secondary lymphoid organ [54]. Thereby, withdrawing NY-BR-1-specific $CD4^+$ T cells from the peripheral blood, leaving no or very low levels of antigen-specific $CD4^+$ T cells behind which could not be detected by the immunofluorescent staining applied in this project (fig. 41).

NY-BR-1-specific $CD4^+$ T cells were not only detected in PBMCs obtained from breast cancer patients, but were also detectable among PBMCs obtained from healthy donors (fig. 42).

In this work, we detected frequencies from 0.77% to 3.66% versus from 0.8% to 2.7% of $CD4^+$IFN-γ^+ T cells specific for the NY-BR-1-derived peptide BR1-1347 in PBMCs obtained from HLA-DRB1*0301 positive breast cancer patients and healthy donors, respectively (fig. 41 A, 42 C). In line with these findings, elevated numbers from 0.6% to 3.23% versus from 0.3% to 2.81% of $CD4^+$ T cells specific for their cognate antigen BR1-88 could be detected among PBMCs of breast cancer patients compared to healthy donors (fig. 41 C, 42 A).

In the case of HLA-DRB1*0401-restricted NY-BR-1-specific epitopes BR1-537, BR1-1242 and BR1-656/-775, frequencies of antigen-specific $CD4^+$IFN-γ^+ T cells were higher in PBMCs obtained from breast cancer patients in comparison to PBMCs obtained from HLA-matched healthy donors (fig. 41 B, D; fig. 42 B, D), except for antigen-specific $CD4^+$ T cells detected in PBMCs obtained from healthy donor HD-3 (fig. 42 C, D). In this case we would postulate high frequencies of $CD4^+$ T cells specific for the NY-BR-1-derived peptide BR1-537 in healthy donor HD-3, due to cross-reactivity of $CD4^+$ T cells with a different antigen-specificity. Overall, it needs to be further investigated if antigen-specific $CD4^+$ T cell responses detected among PBMCs obtained from healthy donors are true NY-BR-1-specific $CD4^+$ T cell responses or are based on cross-reactivity of $CD4^+$ T cells in a NY-BR-1 independent manner.

It has been described in the literature, that frequencies of circulating antigen-specific $CD8^+$ T cells were found to be higher in CML patients compared to healthy donors [209]. Moreover, frequencies of $CD4^+$ T cells specific for the melanoma associated differentiation antigen Trp-2 were described to be elevated among PBMCs of melanoma patients in comparison to healthy donors [183]. The data obtained in this thesis might support the fact, that frequencies of NY-BR-1-specific, $CD4^+$ T cells circulating in the peripheral blood of healthy donors, are reduced in comparison to frequencies of NY-BR-1-specific, $CD4^+$ T cells detected in the peripheral blood of

breast cancer patients.

Overall, conclusions are difficult to be drawn due to very limited numbers of breast cancer patients and healthy donors available for our studies. Further experiments are required to confirm the so far obtained data on the detection of antigen-specific $CD4^+$ T cells in the peripheral blood of NY-BR-1^+ breast cancer patients and healthy donors.

6.6 Breast cancer cells as direct targets for NY-BR-1-specific $CD4^+$ T cells

Breast cancer cells might be a direct target for antigen-specific $CD4^+$ T cells with cytotoxic effector function, such as secretion of perforin and FasL-mediated cytolytic activity [27]. Specific targeting of tumor cells by cytotoxic $CD4^+$ T cells has been described to be efficient in tumor control in melanoma [166]. However, in contrast to melanoma cells, which are described to express MHC-II molecules on there cell surface [25], this might not be the case in breast cancer cells.

In the literature, MHC molecules are described to be down regulated in 20% to 50% of primary breast tumors and cell lines, and MHC-II expression could only be detected in around 30% of breast tumors [29]. Given this fact, also the majority of NY-BR-1 expressing breast tumors are most likely to be MHC-II negative. Reduction of MHC-II expression might be due to unresponsiveness of the tumors to IFN-γ caused by defects in the class II transactivator (CIITA) synthesis at the transcriptional or translational level [170]. Moreover, cell surface exposure of MHC-II can be down regulated by the interaction of ubiquiting ligases of the membrane-associated RING-CH family [180]. Hereby, addition of ubiquitin molecules to the cytoplasmic tail of the MHC-II molecules, enhances intracellular sequestration and degradation of the MHC-II molecules, leading to reduced MHC-II surface expression [263].

Our data obtained on the MHC-II surface expression in breast cancer cell lines has indicated, that most of the tested tumor cell lines were negative for MHC-II expression (fig. 31). *In vitro*, MHC-II surface expression could be induced by IFN-γ-treatment, however, this would not be applicable *in vivo* in breast cancer patients, due to severe side effects, such as cytokine-storms anticipated. In conclusion, tumor cells might not be targeted by NY-BR-1-specific $CD4^+$ T cells directly due to the absence or down regulation of MHC-II surface expression.

6.7 Potential targets of NY-BR-1-specific $CD4^+$ T cells within the tumor stroma

Immune cells of the tumor stroma such as tumor associated macrophages (TAMs), myelo-derived suppressor cells (MDSCs) and regulatory T cells (Tregs) might represent direct interaction partners

for antigen-specific $CD4^+$ T cells.

Tumor associated macrophages (TAMs) reside in the tumor microenvironment and can constitute up to 50% of the tumor-mass of breast cancers [121]. Especially, when considering a NY-BR-1-specific $CD4^+$ T cell based immunotherapy, antigen-presenting cells within the stroma, such as TAMs might be the link for a $CD4^+$ T cell mediated anti-tumor response. However, TAMs display a dual face of firstly classically activated macrophages (M1) and secondly tumor promoting macrophages (M2-like) .

M1 macrophages can be induced by the influence of IFN-γ and bacterial products [154]. Once activated, M1 macrophages function as antigen presenting cells, thus being considered to promote anti-tumor immunity by e.g. activating NY-BR-1-specific $CD4^+$ Th1 cells. Moreover, activated M1 macrophages can directly eliminate tumor cells by activation of the inducible NO synthase (iNOS) gene leading to the production of nitric oxide (NO) [179]. Phenotypically, M1 macrophages can be characterized by the expression-markers iNOS and IL-12p70 [101].

M2-like macrophages, or alternatively activated macrophages, are activated in association with the cytokines IL-4, IL-10, IL-13 and glucocorticoid hormones [154]. Under hypoxic conditions in breast cancer tumors, M2-like macrophages secrete IL-10 which inhibits immune effector T- cells [168][179]. Moreover, IL-10 secretion drives the development of Th2 cells and enhances Treg activity, supported by the expression of chemokine ligand 22 (CCL22) on M2-like macrophages which recruits Tregs into the tumor microenvironment [201, 47]. Furthermore, it has been described, that M2-like macrophages may affect the clinical course of breast cancer patients by non-immune mechanisms, such as induction of angiogenesis via secretion of VEGF[196] and promotion of tumor cell invasion and metastasis [200, 142]. Breast cancer cell invasion and metastasis is potentiated by M2-like macrophages via the production of several enzymes which can degrade the extracellular matrix (ECM), one example being the metalloproteinases MMP-2 and urokinase-type plasminogen activator (uPA) [169]. Breast cancer patients with primary tumors and high levels of uPA were reported to have a significant shorter disease-free interval when compared to patients with normal uPA levels [62].

Recently it has been described that interaction of M2-like macrophages with tumor infiltrating Th1 $CD4^+$ T cells can favor a re-polarization of M2-like macrophages to a M1-like phenotype, thus promoting anti-tumor immunity [100]. Re-polarization of M2-like macrophages is achieved by exposure of the cells to IFN-γ-secreting and CD40-ligand expressing Th1 cells, indicated by elevated expression of co-stimulatory molecules, elevated IL-12 secretion and loss of typical M2-like markers, such as CD206 and CD163, in affected M2-like macrophages [100]. To sum up, cognate interaction of M2-like macrophages and IFN-γ secreting Th1 cells in synergy with CD40 activation, can initiate a switch of tumor-promoting M2-like macrophages to classical M1-like

macrophages with anti-tumor capacities. NY-BR-1-specific $CD4^+$ T cells activated *in vitro* or NY-BR-1-TCR transduced $CD4^+$ T cells, used for an adoptive cell transfer in breast cancer patients, could maybe promote a phenotypic-switch of tumor-promoting M2 macrophages into classical M1-like macrophages, reducing immune-suppressive capacity orchestrated by the breast tumor stroma. However, this implies the uptake and processing of exogeneous NY-BR-1 antigen, for example originating from necrotic tumor cells, by M2 macrophages [11].

Further experiments will have to be performed to gain more profound knowledge on the composition of the tumor-miroenvironment in NY-BR-1^+ breast tumors. Currently an orthotopic NY-BR-1 tumor model is established in DR3tg mice in the group of Prof. Eichmueller, which will be applied to investigate not only a possible $CD4^+$ T cell mediated support for an NY-BR-1-specific $CD8^+$ T cell anti-tumor response, but can also be further used to investigate the composition of the NY-BR-1^+ tumor stroma in mice.

6.8 Role of Tregs in breast cancer

As depicted in figure 43 A, B, we could detect $CD25^+$ $FoxP3^+CD127^-CD4^+$ T cells (Tregs) among $CD4^+$ cells of HLA-DRB1*0301^+/*0401^+ breast cancer patients and healthy donors. Total frequencies of Tregs among $CD4^+$ T cells of breast cancer patients and healthy donors did not exceed 13% and were independent of the NY-BR-1-derived peptide used for *in vitro* stimulation of the PBMC cultures (fig. 43 A, B).

In this work we did not detect overall differences regarding the frequencies of total Tregs among $CD4^+$ T cells among PBMCs of breast cancer patients and healthy donors.

However, it was described in the literature that in patients with breast cancer, regulatory Tregs are increased in both, peripheral blood and malignant effusions [146][50]. Furthermore, Treg numbers are reported to increase in the peripheral blood of breast cancer patients with developing progression of a stage I breast cancer into a stage IV classified breast tumor [264]. In line with this, it has been described that total frequencies of tumor associated Tregs in breast cancer patients can be directly associated with disease progression in invasive and non-invasive breast tumors, whereas invasive tumors display greater numbers of Tregs than non-invasive tumor specimens [14].

We further on investigated the frequency of $CD25^+FoxP3^+CD4^+$ T cells (Treg-like cells) secreting IFN-γ among $CD4^+$ T cells detected among PBMCs of breast cancer patients and healthy donors (fig. 42). This experiment was performed to elucidate the possible induction of antigen-specific Treg-like cells by the NY-BR-1-derived peptides BR1-1347, BR1-88, BR1-1238, BR1-537, BR1-1242 and BR1-656/-775. To confirm a true regulatory T cell phenotype, further

assays addressing the functional activity of Treg-like cells, for example antigen-specific suppression of $CD4^+$ effector cells or the release of Treg associated cytokine such as IL-10 and TGF-β upon antigenic stimulation, should be performed.

Total numbers of $CD25^+FoxP3^+CD4^+$ T cells secreting IFN-γ among $CD4^+$IFN-γ^+ T cells, did generally not exceed numbers higher than 20% in both, breast cancer patients and healthy donors. Furthermore, frequencies of Treg-like cells among $CD4^+$IFN-γ^+ T cells of breast cancer patients and healthy donors were independent of the NY-BR-1-derived peptide used for *in vitro* stimulation of the PBMC cultures (fig. 43 C,D). One exception was, that elevated amounts of Treg-like cells up to 44.14%, specific for the NY-BR-1-derived peptide BR1-656/-775 could be detected among $CD4^+$IFN-γ^+ T cells obtained from breast cancer patient BC-4 versus 9.38%-18.36% of T cells with the same phenotype detected among $CD4^+$IFN-γ^+ T cells of healthy donors (fig. 43 B). In this particular case, amounts of potential antigen-specific Treg-like cells among $CD4^+$ T cells are higher in the peripheral blood of breast cancer patients, compared to healthy donors. Based on this finding, we assume an NY-BR-1-specific induction of Treg-like cells among PBMCs obtained from breast cancer patient BC-4.

Especially when considering for example a NY-BR-1-specific anti-tumor vaccine for the treatment of NY-BR-1^+ tumors in breast cancer patients, it is crucial to consider a potential antigen-specific induction of regulatory T cells. In the literature it has been described, that antigen-specific Tregs develop from $CD4^+CD25^-Foxp3^-$ T cells by activation with an immunogenic antigen and TGFβ, in a non-inflammatory environment [94]. There is evidence that antigen-specific Tregs are superior in their immunosuppressive function when compared to natural Tregs, hence antigen-specific Tregs suppress the immune response at ratios below 1:10 ($CD4^+CD25^+$: $CD4^+CD25^-$) T cells, whereby natural T cells are described to induce tolerance in a 1:1 ratio [95, 96]. Even though, IFN-γ not being the classical cytokine associated with regulatory T cells, it has been described in mice, that antigen-specific Tregs can acquire an effector phenotype of IFN-γ secreting cells upon antigen-encounter [182].

Recently *Schmidt et. al*, reported that mammaglobin-reactive, antigen-specific Tregs can be found in the peripheral blood of breast cancer patients. The authors postulated, that pre-existing antigen-specific regulatory T cells are induced by encounter of their cognate antigen on professional antigen presenting cells, such as dendritic cells [222]. Moreover, regulatory T cells expressing IFN-γ were described to be found selectively expanded in the peripheral blood of patients with metastatic melanoma upon peptide vaccination, impairing an effective Th1 effector response [116].

When considering to apply a NY-BR-1-specific vaccine as a therapy to treat breast cancer, a potential activation of antigen-specific regulator T cells should be very closely monitored, to prevent an overshooting activation of suppressive antigen-specific Tregs, which might even result

in tumor-progression.

6.9 NY-BR-1 as a target for immunotherapy approaches against breast cancer

HLA-DRB1*0301-restricted epitopes BR1-88, BR1-1347 and HLA-DRB1*0401-restricted epitopes BR1-537, BR1-1242 were identified as NY-BR-1-specific epitopes naturally processed in human cells (fig. 40). Promising results in cancer immunotherapy have been reported combining $CD4^+$ T cell epitopes and $CD8^+$ T cell epitopes by generating long synthetic peptides leading to profound immunity against human papilloma virus [269]. So far two HLA-A*0201 restricted NY-BR-1-specific epitopes have been identified by *Jaeger et al.* [112], thus combining these MHC-I restricted epitopes with the newly identified MHC-II epitopes might result in fruitfully anti-cancer treatment. NY-BR-1-specific epitopes could be combined for composition of a synthetic long peptide used for peptide vaccination of NY-BR-1^+ breast cancer patients. Immunotherapy of malignant tumors has been described using synthetic long peptide vaccines, here delivery of peptides to antigen presenting cells (APCs) plays a pivotal role [160]. Hence, a possible NY-BR-1 peptide vaccine should not only include MHC-I and MHC-II restricted NY-BR-1-specific epitopes but also a signal to enhance delivery of the vaccine to dendritic cells as described for DNA-vaccines, one example being the fusion of antigenic DNA to a dendritic cell direct single chain antibody fragment (scFv) specific for a DC-restricted surface molecule (DEC-205) [30].

Moreover, identified HLA-DR-restricted, NY-BR-1-specific epitopes deliver antigenic-sequences for generating NY-BR-1-specific tetramers. Tetramers could be used for monitoring a NY-BR-1 specific immune response in patients *ex vivo* and after NY-BR-1 specific immunotherapy. MHC class II specific tetramers allow detection of very low frequency of antigen specific $CD4^+$ T cells circulating in the peripheral blood. Biophysical studies identified tetramers of pMHC superior to monomeric and dimeric forms of pMHC, since off-rate analysis suggested that multivalent binding of tetrameric pMHC is most effective for reliable T cell imaging and isolation of antigen-specific T cells by fluorescence-activated cell sorting (FACS) [173].

As discussed above in paragraph 6.5, we could detect activated NY-BR-1-specific $CD4^+$ T cells in the peripheral blood obtained from breast cancer patients (fig. 41), thus adoptive cellular transfer presents a possible treatment approach for breast cancer patients with NY-BR-1 expressing tumors. We suggest, that detected $CD4^+$ T cells specific for the newly identified NY-BR-1-derived, HLA-DR-restricted T cell epitopes circumvent mechanism of peripheral tolerance in the breast cancer patient and could therefore possibly be further restimulated and expanded *in vitro*. Successful expansion of NY-BR1- specific $CD4^+$ T cells could be achieved by co-incubation

of purified $CD4^+$ T cells and *in vitro* generated dendritic cells loaded with cognate antigen *in vitro*. Expanded cell-populations could be subsequently used for an adoptive T cell transfer in breast cancer patients. Moreover, genetically engineered T cells could be designed encoding a NY-BR-1 specific T cell receptor (TCR). Currently, RNA isolated from HLA-DR-restricted, NY-BR-1-specific murine T cell lines BR1-88, BR1-1370, BR1-537, BR1-656/-775 and BR1-1242 is sequenced for identification of the TCRs α-chains and β-chains. Once NY-BR-1-specific murine TCR-sequences are available, they could be applied for retroviral insertion of TCR-genes into autologous lymphocytes obtained from HLA-matched breast cancer patients. Similar as described by *Voss et al.* it might be favorable to generate a chimeric antigen-specific TCR, expressing a murine constant α-domain (Cα) and human variable α domain (Vα), variable β domain (Vβ) and human constant β (Cβ). *Voss et al.* report, that the chimeric TCR showed superior functional T-cell avidities compared to a double transgenic TCR. Moreover, human $CD8^+$ T cells transduced with a chimeric T cell receptor, specific for the melanoma antigen gp100, did show superior delay in tumor-growth in a engrafted melanoma model in NOD/SCID mice compared to a double chain transgenic TCR [261].

Collectively, the breast cancer associated antigen NY-BR-1 might therefore present a suitable target for anti-tumor immunotherapy by various approaches discussed above.

6.10 Conclusion and outlook

In this work, we identified two novel NY-BR-1-derived, HLA-DRB1*0301-restricted $CD4^+$ T cell epitopes and two novel NY-BR-1-derived, HLA-DBR1*0401-restricted $CD4^+$ T cell epitopes as natural processing products in human cells, which could be directly implemented in the design of NY-BR-1 targeted anti-tumor immunotherapies. However, immune escape mechanisms, such as reduced MHC-molecule expression on the tumor and establishment of a suppressive tumor microenvironment, hamper a successful anti-tumor response. To overcome these limitations, targeting of the tumor stroma, for example by induction of a more M1 macrophage dominated tumor stroma, would be one possible approach. Moreover, we would like to gain more insight into the cellular composition of the tumor-microenvironment in a NY-BR-1-expressing breast tumor, with special regard on understanding the plasticity of tumor associated macrophages, possibly influenced by NY-BR-1-specific $CD4^+$ T effector cells. Furthermore, NY-BR-1-specific anti-tumor immunotherapy might be most effective when administered as an adjuvant therapy in combination with negative checkpoint blockade, such as blockade of the CTL-A4, PD-1, CD39 and CD73 associated pathways. We would like to further investigate the immunogenicity of adoptively transferred HLA-DR-restricted, NY-BR-1-specific murine $CD4^+$ T cell lines, also in combination with blockade of suppressive pathways as indicated above, in transplantable murine tumor models. We are especially interested in the contribution of NY-BR-1-specific $CD4^+$ T cells

to an effective anti-tumor response. Relevance of the newly identified HLA-DR-restricted $CD4^+$ T cell epitopes should be further confirmed in humans by incorporating larger numbers of breast cancer patients and healthy individuals. Furthermore, we would be interested in investigating the repertoire of pre-existing antigen-specific $CD4^+$ T cells and antigen-specific regulatory T cells among PBMCs obtained from breast cancer patients and healthy donors. Finally, it would be desirable to translate our so far gained immunological knowledge regarding the breast cancer associated antigen NY-BR-1 into the clinics by launching a first clinical study on NY-BR-1-specific, anti-tumor immunotherapies in breast cancer patients.

7 Supplement material

7.1 Arrangement of the NY-BR-1 peptide library in the first matrix

	K1	K2	K3	K4	K5	K6	K7	K8	K9	K10	K11	K12	K13
L1	1	14	27	40	53	66	79	92	105	118	131	144	157
L2	158	2	15	28	41	54	67	80	93	106	119	132	145
L3	174	159	3	16	29	42	55	68	81	94	107	120	133
L4	134	147	160	4	17	30	43	56	69	82	95	108	121
L5	122	135	148	161	5	18	31	44	57	70	83	96	109
L6	110	123	136	149	162	6	19	32	45	58	71	84	97
L7	98	111	124	137	150	163	7	20	33	46	59	72	85
L8	86	99	112	125	138	151	164	8	21	34	47	60	73
L9	74	87	100	113	126	139	152	165	9	22	35	48	61
L10	62	75	88	101	114	127	140	153	170	10	23	36	49
L11	50	63	76	89	102	115	128	141	154	167	11	172	37
L12	38	51	64	77	90	103	116	129	142	155	168	12	25
L13	26	39	52	65	78	91	104	117	130	143	156	169	13

Figure 44: Arrangement of the NY-BR-1 peptide library in the first matrix. 174 single NY-BR-1 library peptides were organized in 26 pools (K1-K13, L1-L13), each pool containing 13 individual peptides. Library peptides #24, #146, #166, #171, #173 were not included in the NY-BR-1 matrix but screened as individual library peptides directly.

7.2 Screening of a second NY-BR-1-specific library in DR4tg mice

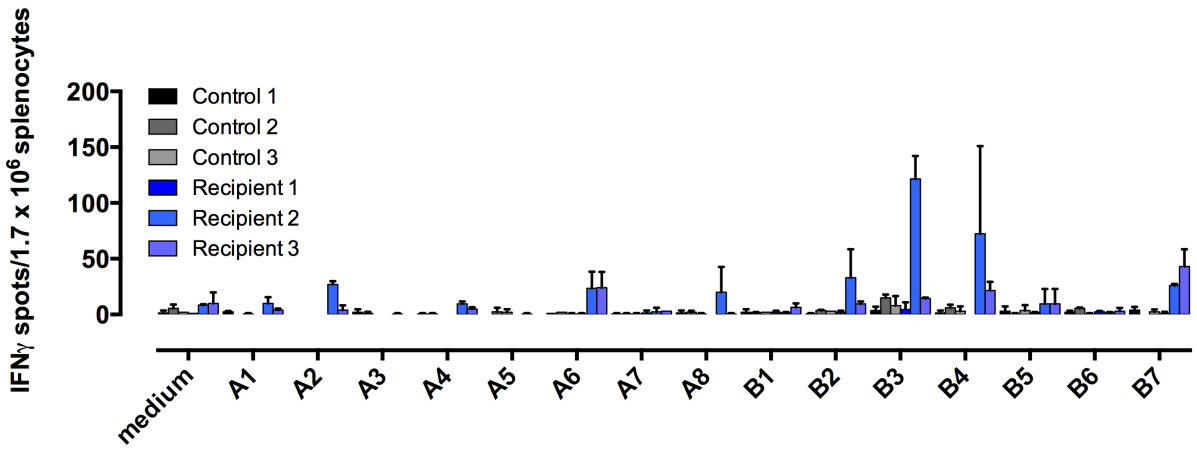

Figure 45: Screening of a second level NY-BR-1-specific library in DR4tg mice. IFN-γ EliSpot assay result on an experiment conducted with splenocytes of DR4tg mice vaccinated with global NY-BR-1 DNA. Splenocytes isolated from DNA-immunized DR4tg mice were incubated with peptide pools (A1-A7, B1-B8) for 18 hrs. Each column represents one individual mouse; bars, standard error of the mean upon duplicate determination.

7.3 HLA-phenotype of enrolled breast cancer patients and healthy donors

PBMC samples	HLA-phenotye	gender
BC -1	HLA-DRB1*0301	female
BC -2	HLA-DRB1*0301	female
BC -3	HLA-DRB1*0301	female
BC -4	HLA-DRB1*0401	female
BC -5	HLA-DRB1*0401	female
BC -6	HLA-DRB1*0401	female
BC -7	HLA-DRB1*0401	female
BC -8	HLA-DRB1*0401	female
HD -1	HLA-DRB1*0301	female
HD -2	HLA-DRB1*0301	male
HD -3	HLA-DRB1*0301/ HLA-DRB1*0401	male
HD -4	HLA-DRB1*0401	male

Table 36: HLA-phenotype of enrolled breast cancer patients and healthy donors. Out of 24 HLA-typed breast cancer patients, eight HLA-matched breast cancer patients (BC 1-8) which were tested for a NY-BR-1 positive tumor lesion and five healthy HLA-matched donors (HD 1- 5) were selected.

7.4 Detection of activated NY-BR-1-specific $CD4^+$ T cells among PBMCs of breast cancer patients and healthy donors by IFN-γ EliSpot assay

In parallel to the immunoflourescent staining of *in vitro* stimulated PBMCs obtained from breast cancer patients and healthy donors (fig. 41), IFN-γ EliSpot assays were performed with the same PBMC-samples. Significant amounts of $CD4^+$IFN-γ^+ T cell specific for the peptide BR1-1242 could be detected among PBMCs obtained from breast cancer patient BC-7. Indicated by elevated IFN-γ spots/well, tendencies for the presence of preexisting NY-BR-1-specific CD4+ T cells could be detected for peptide BR1-1347 among PBMCs obtained from breast cancer patient BC-3 and for peptides BR1-1242 and BR1656/-775 among PBMCs obtained from breast cancer patients BC-6 and BC-8, respectively.

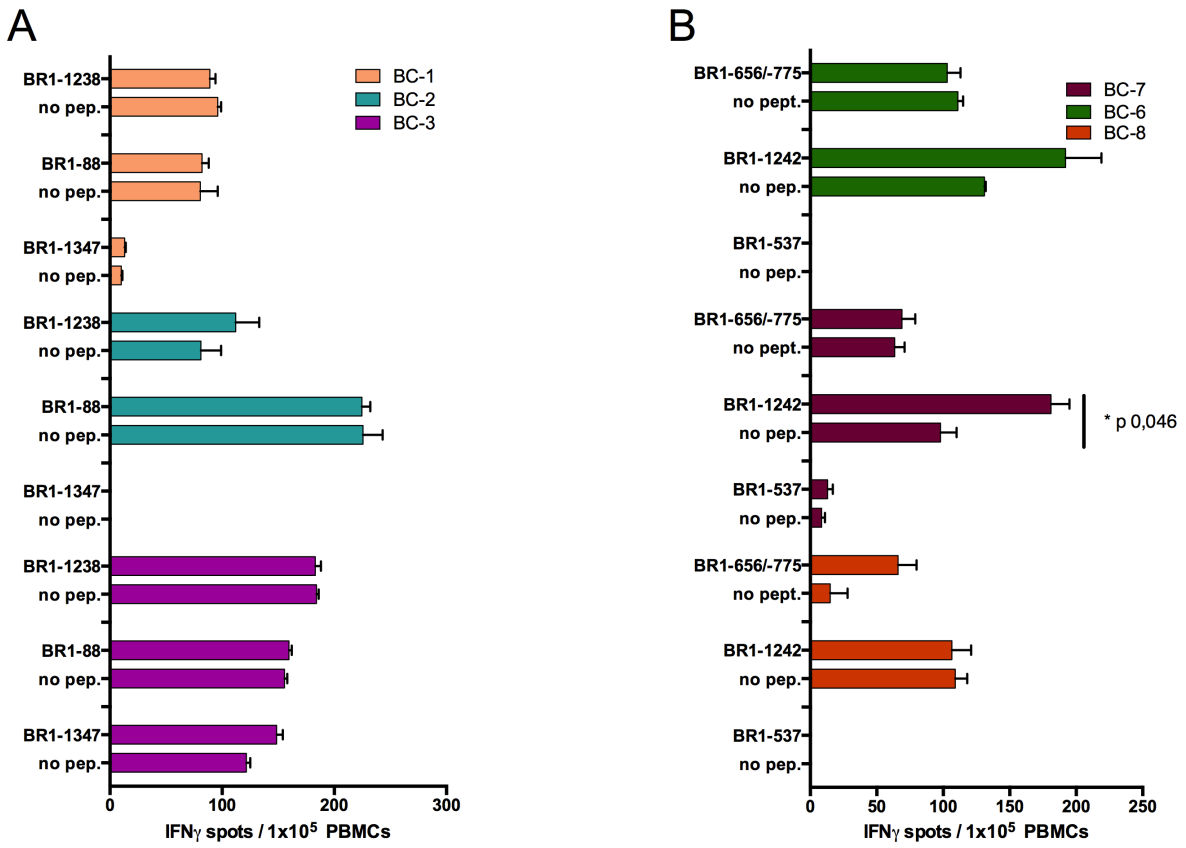

Figure 46: Experiment 1: Detection of NY-BR-1-specific T cells in breast cancer patient samples 24 days after *in vitro* stimulation with NY-BR-1-specific peptides. 1 X 10^5 isolated breast cancer PBMCs were incubated with 5 µg/ml of the indicated peptide for 18hrs in an IFN-γ-EliSpot assay. PBMCs were *in vitro* stimulated for 24 days with the same peptide used in the IFN-γ-EliSpot assay. Colums, mean of duplicate determination; bars standard error of the mean. (Statistic analysis: unpaired t test, significant (*) if $P < 0.05$)

In the IFN-γ EliSpot assay performed in parallel to the second experiment of detecting NY-BR-1-specific $CD4^+$ T cells among PBMCs of breast cancer patients (fig. 41), significant levels of $CD4^+$ T cells specific for their cognate antigen BR1-1347 could be detected among PBMCs obtained from breast cancer patient BC-3 (fig. 47 A), indicated by significantly elevated IFN-γ spot numbers/well compared to the medium control (no. pep.). Moreover, significantly elevated levels of $CD4^+$ T cells specific for the NY-BR1 derived peptide BR1-1242 could be detected among PBMCs of breast cancer patient BC-6 (fig. 47 B).

As depicted in figure 47 D, significant elevated levels of BR1-1242 antigen-specific $CD4^+$ T cells could be detected among PBMCs obtained from healthy donor HD-3, indicated by elevated IFN-γ spot numbers in the IFN-γ EliSpot assay.

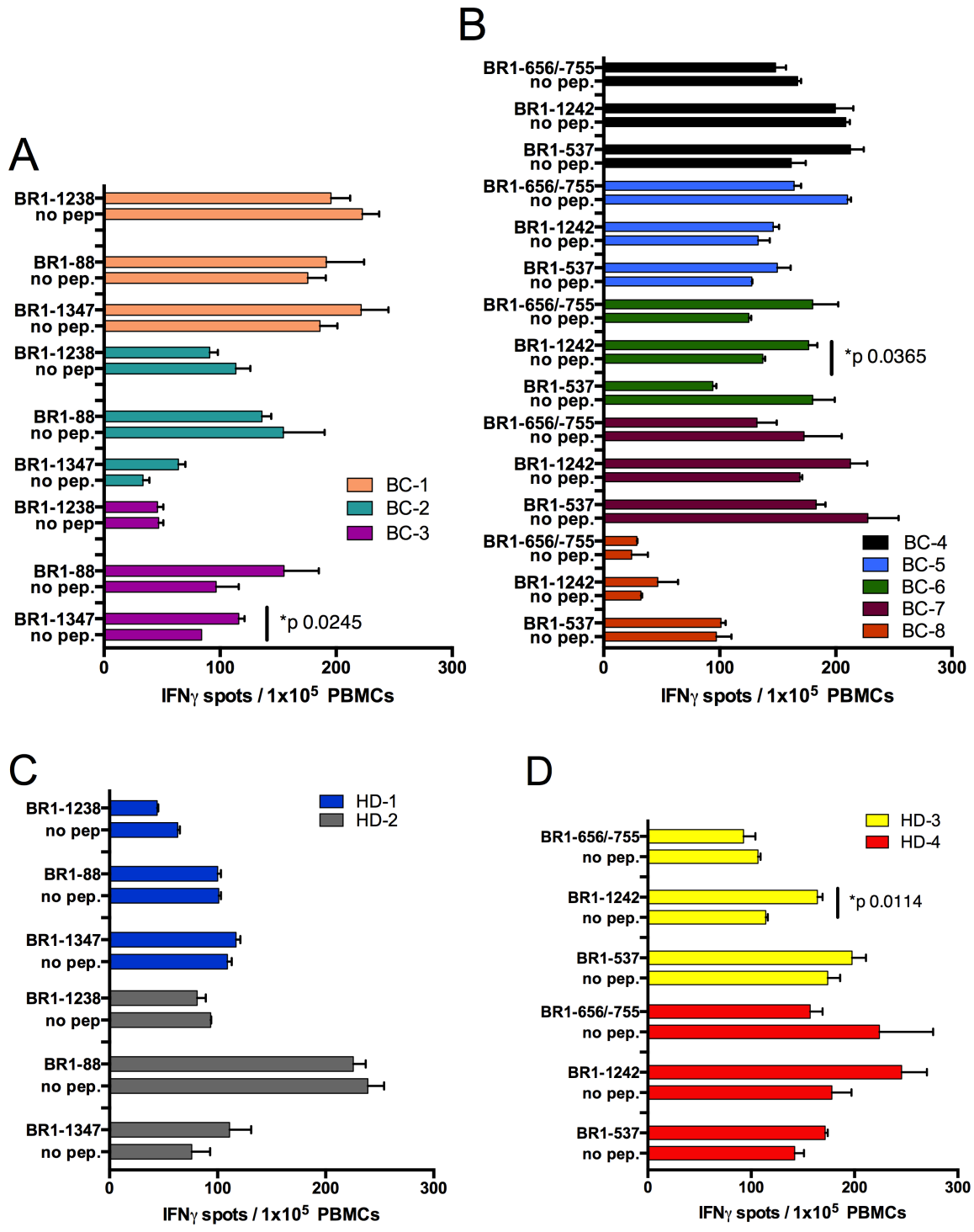

Figure 47: Experiment 2: Detection of NY-BR-1-specific T cells in breast cancer patient samples 24 days after *in vitro* stimulation with NY-BR-1-specific peptides. 1 X 10^5 isolated breast cancer PBMCs were incubated with 5 µg/ml of the indicated peptide for 18hrs in an IFN-γ-EliSpot assay. PBMCs were *in vitro* stimulated for 24 days with the same peptide as used in the IFN-γ-EliSpot assay. Columns, mean of duplicate determination; bars standard error of the mean. (Statistic analysis: unpaired t test, significant (*) if $P < 0.05$)

To sum up, antigen-specific secretion of IFN-γ among PBMCs obtained from breast cancer patients could be obtained, but results are not consistent within two independent IFN-γ Elispot assays performed (fig. 46,47), and do not correlated with the data on antigen-specific $CD4^+$ T cells among PBMCs of breast cancer patients and healthy donors obtained by immunoflourescent staining of the cells (fig. 41, 42). Background IFN-γ signal was very hight in this IFN-γ EliSpot assay, to obtain more reliable data, firstly background IFN-γ signals should be reduced and secondly the assay should be repeated with a greater amount of PBMC-samples obtained from HLA-matched breast cancer patients and healthy donors.

References

[1] Tamoxifen for early breast cancer: an overview of the randomised trials. early breast cancer trialists' collaborative group. *Lancet*, 351(9114):1451–1467, May 1998.

[2] Mojgan Ahmadzadeh, Laura A. Johnson, Bianca Heemskerk, John R. Wunderlich, Mark E. Dudley, Donald E. White, and Steven A. Rosenberg. Tumor antigen-specific CD 8 T cells infiltrating the tumor express high levels of PD -1 and are functionally impaired. *Blood*, 114(8):1537–1544, Aug 2009.

[3] M. S. Alam, C. C. Kurtz, J. M. Wilson, B. R. Burnette, E. B. Wiznerowicz, W. G. Ross, J. M. Rieger, R. A. Figler, J. Linden, S. E. Crowe, and P. B. Ernst. A2a adenosine receptor (ar) activation inhibits pro-inflammatory cytokine production by human CD4+ helper T cells and regulates helicobacter-induced gastritis and bacterial persistence. *Mucosal Immunol*, 2(3):232–242, May 2009.

[4] Mohammad S. Alam, Courtney C. Kurtz, Robert M. Rowlett, Brian K. Reuter, Elizabeth Wiznerowicz, Soumita Das, Joel Linden, Sheila E. Crowe, and Peter B. Ernst. CD73 is expressed by human regulatory T helper cells and suppresses proinflammatory cytokine production and helicobacter felis-induced gastritis in mice. *J Infect Dis*, 199(4):494–504, Feb 2009.

[5] D. C. Allred, J. M. Harvey, M. Berardo, and G. M. Clark. Prognostic and predictive factors in breast cancer by immunohistochemical analysis. *Mod Pathol*, 11(2):155–168, Feb 1998.

[6] D. C. Allred, S. K. Mohsin, and S. A. Fuqua. Histological and biological evolution of human premalignant breast disease. *Endocr Relat Cancer*, 8(1):47–61, Mar 2001.

[7] D Craig Allred. Ductal carcinoma in situ: terminology, classification, and natural history. *J Natl Cancer Inst Monogr*, 2010(41):134–138, 2010.

[8] Martine Perrot Applanat, Helene Buteau-Lozano, Marie Astrid Herve, and Armelle Corpet. Vascular endothelial growth factor is a target gene for estrogen receptor and contributes to breast cancer progression. *Adv Exp Med Biol*, 617:437–444, 2008.

[9] L. Arnould, M. Gelly, F. Penault-Llorca, L. Benoit, F. Bonnetain, C. Migeon, V. Cabaret, V. Fermeaux, P. Bertheau, J. Garnier, J-F. Jeannin, and B. Coudert. Trastuzumab-based treatment of HER2-positive breast cancer: an antibody-dependent cellular cytotoxicity mechanism? *Br J Cancer*, 94(2):259–267, Jan 2006.

[10] Jacek Bania, Evelina Gatti, Hugues Lelouard, Alexandre David, Fanny Cappello, Ekkehard Weber, Voahirana Camosseto, and Philippe Pierre. Human cathepsin S, but not cathepsin L, degrades efficiently MHC class II-associated invariant chain in nonprofessional APCs. *Proc Natl Acad Sci U S A*, 100(11):6664–6669, May 2003.

[11] R. N. Barker, L. Erwig, W. P. Pearce, A. Devine, and A. J. Rees. Differential effects of necrotic or apoptotic cell uptake on antigen presentation by macrophages. *Pathobiology*, 67(5-6):302–305, 1999.

[12] Jose Baselga, Patricia Gomez, Richard Greil, Sofia Braga, Miguel A. Climent, Andrew M. Wardley, Bella Kaufman, Salomon M. Stemmer, Antonio Pego, Arlene Chan, Jean-Charles Goeminne, Marie-Pascale Graas, M John Kennedy, Eva Maria Ciruelos Gil, Andreas Schneeweiss, Angela Zubel, Jutta Groos, Helena Melezinkova, and Ahmad Awada. Randomized phase ii study of the anti-epidermal growth factor receptor monoclonal antibody cetuximab with cisplatin versus cisplatin alone in patients with metastatic triple-negative breast cancer. *J Clin Oncol*, 31(20):2586–2592, Jul 2013.

[13] Jose Baselga and Sandra M. Swain. Novel anticancer targets: revisiting ERBB2 and discovering ERBB3. *Nat Rev Cancer*, 9(7):463–475, Jul 2009.

[14] Gaynor J. Bates, Stephen B. Fox, Cheng Han, Russell D. Leek, Jose F. Garcia, Adrian L. Harris, and Alison H. Banham. Quantification of regulatory T cells enables the identification of high-risk breast cancer patients and those at risk of late relapse. *J Clin Oncol*, 24(34):5373–5380, Dec 2006.

[15] Courtney Beers, Karen Honey, Susan Fink, Katherine Forbush, and Alexander Rudensky. Differential regulation of cathepsin S and cathepsin L in interferon gamma-treated macrophages. *J Exp Med*, 197(2):169–179, Jan 2003.

[16] A. Bembenek and P. M. Schlag. Lymph-node dissection in breast cancer. *Langenbecks Arch Surg*, 385(4):236–245, Jul 2000.

[17] Katrien Berns, Hugo M. Horlings, Bryan T. Hennessy, Mandy Madiredjo, E Marielle Hijmans, Karin Beelen, Sabine C. Linn, Ana Maria Gonzalez-Angulo, Katherine Stemke-Hale, Michael Hauptmann, Roderick L. Beijersbergen, Gordon B. Mills, Marc J. van de Vijver, and Rene Bernards. A functional genetic approach identifies the PI3K pathway as a major determinant of trastuzumab resistance in breast cancer. *Cancer Cell*, 12(4):395–402, Oct 2007.

[18] Donald A. Berry. Breast cancer screening: Controversy of impact. *Breast*, 22 Suppl 2:S73–S76, Aug 2013.

[19] Nicolas Blanchard and Nilabh Shastri. Coping with loss of perfection in the MHC class I peptide repertoire. *Curr Opin Immunol*, 20(1):82–88, Feb 2008.

[20] Christian Blank, Thomas F. Gajewski, and Andreas Mackensen. Interaction of PD-L1 on tumor cells with PD-1 on tumor-specific T cells as a mechanism of immune evasion: implications for tumor immunotherapy. *Cancer Immunol Immunother*, 54(4):307–314, Apr 2005.

[21] J. L. Bos. Ras oncogenes in human cancer: a review. *Cancer Res*, 49(17):4682–4689, Sep 1989.

[22] Rinke Bos and Linda A. Sherman. CD4+ T-cell help in the tumor milieu is required for recruitment and cytolytic function of CD8+ T lymphocytes. *Cancer Res*, 70(21):8368–8377, Nov 2010.

[23] Julie R. Brahmer, Scott S. Tykodi, Laura Q M. Chow, Wen-Jen Hwu, Suzanne L. Topalian, Patrick Hwu, Charles G. Drake, Luis H. Camacho, John Kauh, Kunle Odunsi, Henry C. Pitot, Omid Hamid, Shailender Bhatia, Renato Martins, Keith Eaton, Shuming Chen, Theresa M. Salay, Suresh Alaparthy, Joseph F. Grosso, Alan J. Korman, Susan M. Parker, Shruti Agrawal, Stacie M. Goldberg, Drew M. Pardoll, Ashok Gupta, and Jon M. Wigginton. Safety and activity of anti-PD-L1 antibody in patients with advanced cancer. *N Engl J Med*, 366(26):2455–2465, Jun 2012.

[24] Toni M. Brand, Mari Iida, Chunrong Li, and Deric L. Wheeler. The nuclear epidermal growth factor receptor signaling network and its role in cancer. *Discov Med*, 12(66):419–432, Nov 2011.

[25] E. B. Broecker, L. Suter, and C. Sorg. HLA-DR antigen expression in primary melanomas of the skin. *J Invest Dermatol*, 82(3):244–247, Mar 1984.

[26] Hilary Brooks, Bernard Lebleu, and Eric Vives. Tat peptide-mediated cellular delivery: back to basics. *Adv Drug Deliv Rev*, 57(4):559–577, Feb 2005.

[27] Deborah M. Brown, Cris Kamperschroer, Allison M. Dilzer, Deborah M. Roberts, and Susan L. Swain. IL-2 and antigen dose differentially regulate perforin- and FasL-mediated cytolytic activity in antigen specific CD4+ T cells. *Cell Immunol*, 257(1-2):69–79, 2009.

[28] C. Byrne, C. Schairer, J. Wolfe, N. Parekh, M. Salane, L. A. Brinton, R. Hoover, and R. Haile. Mammographic features and breast cancer risk: effects with time, age, and menopause status. *J Natl Cancer Inst*, 87(21):1622–1629, Nov 1995.

[29] Michael Campoli, Chien-Chung Chang, Sharon A. Oldford, Allison D. Edgecombe, Sheila Drover, and Soldano Ferrone. HLA antigen changes in malignant tumors of mammary epithelial origin: molecular mechanisms and clinical implications. *Breast Dis*, 20:105–125, 2004.

[30] Jun Cao, Yiqi Jin, Wei Li, Bin Zhang, Yang He, Hongqiang Liu, Ning Xia, Huafeng Wei, and Jian Yan. DNA vaccines targeting the encoded antigens to dendritic cells induce potent antitumor immunity in mice. *BMC Immunol*, 14:39, 2013.

[31] Xuefang Cao, Sheng F. Cai, Todd A. Fehniger, Jiling Song, Lynne I. Collins, David R. Piwnica-Worms, and Timothy J. Ley. Granzyme B and perforin are important for regulatory T cell-mediated suppression of tumor clearance. *Immunity*, 27(4):635–646, Oct 2007.

[32] C. Caron de Fromentel, P. C. Nardeux, T. Soussi, C. Lavialle, S. Estrade, G. Carloni, K. Chandrasekaran, and R. Cassingena. Epithelial HBL-100 cell line derived from milk of an apparently healthy woman harbours SV40 genetic information. *Exp Cell Res*, 160(1):83–94, Sep 1985.

[33] Sue Carrick, Sharon Parker, Charlene E. Thornton, Davina Ghersi, John Simes, and Nicholas Wilcken. Single agent versus combination chemotherapy for metastatic breast cancer. *Cochrane Database Syst Rev*, (2):CD003372, 2009.

[34] Marc Cartellieri, Michael Bachmann, Anja Feldmann, Claudia Bippes, Slava Stamova, Rebekka Wehner, Achim Temme, and Marc Schmitz. Chimeric antigen receptor-engineered T cells for immunotherapy of cancer. *J Biomed Biotechnol*, 2010:956304, 2010.

[35] Sarat Chandarlapaty, Ayana Sawai, Maurizio Scaltriti, Vanessa Rodrik-Outmezguine, Olivera Grbovic-Huezo, Violeta Serra, Pradip K. Majumder, Jose Baselga, and Neal Rosen. AKT inhibition relieves feedback suppression of receptor tyrosine kinase expression and activity. *Cancer Cell*, 19(1):58–71, Jan 2011.

[36] Zhi Chen and John J. O'Shea. Th17 cells: a new fate for differentiating helper T cells. *Immunol Res*, 41(2):87–102, 2008.

[37] Wen-Fang Cheng, Ming-Cheng Chang, Wei-Zen Sun, Yu-Wei Jen, Chao-Wei Liao, Yun-Yuan Chen, and Chi-An Chen. Fusion protein vaccines targeting two tumor antigens generate synergistic anti-tumor effects. *PLoS One*, 8(9):e71216, 2013.

[38] Dipanjan Chowdhury, Paul J. Beresford, Pengcheng Zhu, Dong Zhang, Jung-Suk Sung, Bruce Demple, Fred W. Perrino, and Judy Lieberman. The exonuclease TREX1 is in the SET complex and acts in concert with NM23-H1 to degrade DNA during granzyme A-mediated cell death. *Mol Cell*, 23(1):133–142, Jul 2006.

[39] E. Chuang, M. L. Alegre, C. S. Duckett, P. J. Noel, M. G. Vander Heiden, and C. B. Thompson. Interaction of ctla-4 with the clathrin-associated protein ap50 results in ligand-independent endocytosis that limits cell surface expression. *J Immunol*, 159(1):144–151, Jul 1997.

[40] Hiram S Cody, 3rd. Current surgical management of breast cancer. *Curr Opin Obstet Gynecol*, 14(1):45–52, Feb 2002.

[41] Cyrille J. Cohen, Yong F. Li, Mona El-Gamil, Paul F. Robbins, Steven A. Rosenberg, and Richard A. Morgan. Enhanced antitumor activity of T cells engineered to express T-cell receptors with a second disulfide bond. *Cancer Res*, 67(8):3898–3903, Apr 2007.

[42] G. A. Colditz, W. C. Willett, D. J. Hunter, M. J. Stampfer, J. E. Manson, C. H. Hennekens, and B. A. Rosner. Family history, age, and risk of breast cancer. prospective data from the nurses' health study. *JAMA*, 270(3):338–343, Jul 1993.

[43] Lauren W. Collison, Vandana Chaturvedi, Abigail L. Henderson, Paul R. Giacomin, Cliff Guy, Jaishree Bankoti, David Finkelstein, Karen Forbes, Creg J. Workman, Scott A. Brown, Jerold E. Rehg, Michael L. Jones, Hsiao-Tzu Ni, David Artis, Mary Jo Turk, and Dario A A. Vignali. IL-35-mediated induction of a potent regulatory T cell population. *Nat Immunol*, 11(12):1093–1101, Dec 2010.

[44] Lauren W. Collison, Creg J. Workman, Timothy T. Kuo, Kelli Boyd, Yao Wang, Kate M. Vignali, Richard Cross, David Sehy, Richard S. Blumberg, and Dario A A. Vignali. The inhibitory cytokine IL-35 contributes to regulatory T-cell function. *Nature*, 450(7169):566–569, Nov 2007.

[45] Alison K. Conlin, Andrew D. Seidman, Ariadne Bach, Diana Lake, Maura Dickler, Gabriella D'Andrea, Tiffany Traina, Michael Danso, Adam M. Brufsky, Mansoor Saleh, Alicia Clawson, and Clifford A. Hudis. Phase II trial of weekly nanoparticle albumin-bound paclitaxel with carboplatin and trastuzumab as first-line therapy for women with HER2-overexpressing metastatic breast cancer. *Clin Breast Cancer*, 10(4):281–287, Aug 2010.

[46] Maria V. Croce, Marina T. Isla-Larrain, Sandra O. Demichelis, Jorge R. Gori, Mike R. Price, and Amada Segal-Eiras. Tissue and serum MUC1 mucin detection in breast cancer patients. *Breast Cancer Res Treat*, 81(3):195–207, Oct 2003.

[47] Tyler J. Curiel, George Coukos, Linhua Zou, Xavier Alvarez, Pui Cheng, Peter Mottram, Melina Evdemon-Hogan, Jose R. Conejo-Garcia, Lin Zhang, Matthew Burow, Yun Zhu, Shuang Wei, Ilona Kryczek, Ben Daniel, Alan Gordon, Leann Myers, Andrew Lackner, Mary L. Disis, Keith L. Knutson, Lieping Chen, and Weiping Zou. Specific recruitment of regulatory T cells in ovarian carcinoma fosters immune privilege and predicts reduced survival. *Nat Med*, 10(9):942–949, Sep 2004.

[48] Bhuvanesh Dave, Ilenia Migliaccio, M Carolina Gutierrez, Meng-Fen Wu, Gary C. Chamness, Helen Wong, Archana Narasanna, Anindita Chakrabarty, Susan G. Hilsenbeck, Jian Huang, Mothaffar Rimawi, Rachel Schiff, Carlos Arteaga, C Kent Osborne, and Jenny C. Chang. Loss of phosphatase and tensin homolog or phosphoinositol-3 kinase activation and response to trastuzumab or lapatinib in human epidermal growth factor receptor 2-overexpressing locally advanced breast cancers. *J Clin Oncol*, 29(2):166–173, Jan 2011.

[49] M. M. Davis and P. J. Bjorkman. T-cell antigen receptor genes and T-cell recognition. *Nature*, 334(6181):395–402, Aug 1988.

[50] Peter DeLong, Richard G. Carroll, Adam C. Henry, Tomoyuki Tanaka, Sajjad Ahmad, Michael S. Leibowitz, Daniel H. Sterman, Carl H. June, Steven M. Albelda, and Robert H. Vonderheide. Regulatory T cells and cytokines in malignant pleural effusions secondary to mesothelioma and carcinoma. *Cancer Biol Ther*, 4(3):342–346, Mar 2005.

[51] G. D. Demetri. Targeting c-kit mutations in solid tumors: scientific rationale and novel therapeutic options. *Semin Oncol*, 28(5 Suppl 17):19–26, Oct 2001.

[52] K. Deres, W. Beck, S. Faath, G. Jung, and H. G. Rammensee. MHC/peptide binding studies indicate hierarchy of anchor residues. *Cell Immunol*, 151(1):158–167, Oct 1993.

[53] Carol Desantis, Jiemin Ma, Leah Bryan, and Ahmedin Jemal. Breast cancer statistics, 2013. *CA Cancer J Clin*, Oct 2013.

[54] Francesca Di Rosa and Reinhard Pabst. The bone marrow: a nest for migratory memory T cells. *Trends Immunol*, 26(7):360–366, Jul 2005.

[55] M. L. Disis, K. H. Grabstein, P. R. Sleath, and M. A. Cheever. Generation of immunity to the HER-2/neu oncogenic protein in patients with breast and ovarian cancer using a peptide-based vaccine. *Clin Cancer Res*, 5(6):1289–1297, Jun 1999.

[56] Mary L. Disis, Theodore A. Gooley, Kristine Rinn, Donna Davis, Michael Piepkorn, Martin A. Cheever, Keith L. Knutson, and Kathy Schiffman. Generation of T-cell immunity to the

HER-2/neu protein after active immunization with HER-2/neu peptide-based vaccines. *J Clin Oncol*, 20(11):2624–2632, Jun 2002.

[57] S. F. Doisneau-Sixou, C. M. Sergio, J. S. Carroll, R. Hui, E. A. Musgrove, and R. L. Sutherland. Estrogen and antiestrogen regulation of cell cycle progression in breast cancer cells. *Endocr Relat Cancer*, 10(2):179–186, Jun 2003.

[58] Christoph Domschke, Yingzi Ge, Isa Bernhardt, Sarah Schott, Sophia Keim, Simone Juenger, Mariana Bucur, Luisa Mayer, Maria Blumenstein, Joachim Rom, Joerg Heil, Christof Sohn, Andreas Schneeweiss, Philipp Beckhove, and Florian Schuetz. Long-term survival after adoptive bone marrow T cell therapy of advanced metastasized breast cancer: follow-up analysis of a clinical pilot trial. *Cancer Immunol Immunother*, 62(6):1053–1060, Jun 2013.

[59] Dowlatshahi, Kambiz and Francescatti, Darius S. and Bloom, Kenneth J. Laser therapy for small breast cancers. *Am J Surg*, 184(4):359–363, Oct 2002.

[60] Dowsett, M. and Cooke, T. and Ellis, I. and Gullick, W. J. and Gusterson, B. and Mallon, E. and Walker, R. Assessment of her2 status in breast cancer: why, when and how? *Eur J Cancer*, 36(2):170–176, Jan 2000.

[61] Mark E. Dudley, Colin A. Gross, Michelle M. Langhan, Marcos R. Garcia, Richard M. Sherry, James C. Yang, Giao Q. Phan, Udai S. Kammula, Marybeth S. Hughes, Deborah E. Citrin, Nicholas P. Restifo, John R. Wunderlich, Peter A. Prieto, Jenny J. Hong, Russell C. Langan, Daniel A. Zlott, Kathleen E. Morton, Donald E. White, Carolyn M. Laurencot, and Steven A. Rosenberg. CD8+ enriched "young" tumor infiltrating lymphocytes can mediate regression of metastatic melanoma. *Clin Cancer Res*, 16(24):6122–6131, Dec 2010.

[62] M. J. Duffy, P. O'Grady, D. Devaney, L. O'Siorain, J. J. Fennelly, and H. J. Lijnen. Urokinase-plasminogen activator, a marker for aggressive breast carcinomas. Preliminary report. *Cancer*, 62(3):531–533, Aug 1988.

[63] Jennifer Dunlap, Claudia Le, Arielle Shukla, Janice Patterson, Ajia Presnell, Michael C. Heinrich, Christopher L. Corless, and Megan L. Troxell. Phosphatidylinositol-3-kinase and AKT1 mutations occur early in breast carcinoma. *Breast Cancer Res Treat*, 120(2):409–418, Apr 2010.

[64] M. Dupuis, K. Denis-Mize, C. Woo, C. Goldbeck, M. J. Selby, M. Chen, G. R. Otten, J. B. Ulmer, J. J. Donnelly, G. Ott, and D. M. McDonald. Distribution of DNA vaccines determines their immunogenicity after intramuscular injection in mice. *J Immunol*, 165(5):2850–2858, Sep 2000.

[65] D. F. Easton, D. Ford, and D. T. Bishop. Breast and ovarian cancer incidence in BRCA1-mutation carriers. Breast Cancer Linkage Consortium. *Am J Hum Genet*, 56(1):265–271, Jan 1995.

[66] C. W. Elston and I. O. Ellis. Pathological prognostic factors in breast cancer. I. The value of histological grade in breast cancer: experience from a large study with long-term follow-up. *Histopathology*, 19(5):403–410, Nov 1991.

[67] Peter B. Ernst, James C. Garrison, and Linda F. Thompson. Much ado about adenosine: adenosine synthesis and function in regulatory T cell biology. *J Immunol*, 185(4):1993–1998, Aug 2010.

[68] D Gareth Evans, Andrew Shenton, Emma Woodward, Fiona Lalloo, Anthony Howell, and Eamonn R. Maher. Penetrance estimates for BRCA1 and BRCA2 based on genetic testing in a Clinical Cancer Genetics service setting: risks of breast/ovarian cancer quoted should reflect the cancer burden in the family. *BMC Cancer*, 8:155, 2008.

[69] K. Falk, O. Roetzschke, S. Faath, S. Goth, I. Graef, N. Shastri, and H. G. Rammensee. Both human and mouse cells expressing H-2Kb and ovalbumin process the same peptide, SIINFEKL. *Cell Immunol*, 150(2):447–452, Sep 1993.

[70] K. Falk, O. Roetzschke, and H. G. Rammensee. Specificity of antigen processing for MHC class I restricted presentation is conserved between mouse and man. *Eur J Immunol*, 22(5):1323–1326, May 1992.

[71] Sonia Feau, Zacarias Garcia, Ramon Arens, Hideo Yagita, Jannie Borst, and Stephen P. Schoenberger. The CD4+T-cell help signal is transmitted from APC to CD8+T-cells via CD27-CD70 interactions. *Nat Commun*, 3:948, 2012.

[72] Jacques Ferlay, Hai-Rim Shin, Freddie Bray, David Forman, Colin Mathers, and Donald Maxwell Parkin. Estimates of worldwide burden of cancer in 2008: GLOBOCAN 2008. *Int J Cancer*, 127(12):2893–2917, Dec 2010.

[73] I. J. Fidler. Biological behavior of malignant melanoma cells correlated to their survival in vivo. *Cancer Res*, 35(1):218–224, Jan 1975.

[74] Jason D. Fontenot, Marc A. Gavin, and Alexander Y. Rudensky. Foxp3 programs the development and function of CD4+ CD25+regulatory T cells. *Nat Immunol*, 4(4):330–336, Apr 2003.

[75] Nikki A. Ford, Kaylyn L. Devlin, Laura M. Lashinger, and Stephen D. Hursting. Deconvoluting the Obesity and Breast Cancer Link: Secretome, Soil and Seed Interactions. *J Mammary Gland Biol Neoplasia*, Oct 2013.

[76] G. J. Freeman, F. Borriello, R. J. Hodes, H. Reiser, J. G. Gribben, J. W. Ng, J. Kim, J. M. Goldberg, K. Hathcock, and G. Laszlo. Murine B7-2, an alternative CTLA4 counter-receptor that costimulates T cell proliferation and interleukin 2 production. *J Exp Med*, 178(6):2185–2192, Dec 1993.

[77] P. Freimuth, L. Philipson, and S. D. Carson. The coxsackievirus and adenovirus receptor. *Curr Top Microbiol Immunol*, 323:67–87, 2008.

[78] K. Frueh and Y. Yang. Antigen presentation by MHC class I and its regulation by interferon gamma. *Curr Opin Immunol*, 11(1):76–81, Feb 1999.

[79] Dragony Fu, Jennifer A. Calvo, and Leona D. Samson. Balancing repair and tolerance of DNA damage caused by alkylating agents. *Nat Rev Cancer*, 12(2):104–120, Feb 2012.

[80] Shuang Fu, Nan Zhang, Adam C. Yopp, Dongmei Chen, Minwei Mao, Dan Chen, Haojiang Zhang, Yaozhong Ding, and Jonathan S. Bromberg. TGF-beta induces Foxp3 + T-regulatory cells from CD4 + CD25 - precursors. *Am J Transplant*, 4(10):1614–1627, Oct 2004.

[81] B. J. Furr and V. C. Jordan. The pharmacology and clinical uses of tamoxifen. *Pharmacol Ther*, 25(2):127–205, 1984.

[82] Joan T. Garrett and Carlos L. Arteaga. Resistance to HER2-directed antibodies and tyrosine kinase inhibitors: mechanisms and clinical implications. *Cancer Biol Ther*, 11(9):793–800, May 2011.

[83] J. Geisler, N. King, G. Anker, G. Ornati, E. Di Salle, P. E. Lonning, and M. Dowsett. In vivo inhibition of aromatization by exemestane, a novel irreversible aromatase inhibitor, in postmenopausal breast cancer patients. *Clin Cancer Res*, 4(9):2089–2093, Sep 1998.

[84] Alessandra Gentile, Livio Trusolino, and Paolo M. Comoglio. The Met tyrosine kinase receptor in development and cancer. *Cancer Metastasis Rev*, 27(1):85–94, Mar 2008.

[85] Charles E. Geyer, John Forster, Deborah Lindquist, Stephen Chan, C Gilles Romieu, Tadeusz Pienkowski, Agnieszka Jagiello-Gruszfeld, John Crown, Arlene Chan, Bella Kaufman, Dimosthenis Skarlos, Mario Campone, Neville Davidson, Mark Berger, Cristina Oliva,

Stephen D. Rubin, Steven Stein, and David Cameron. Lapatinib plus capecitabine for HER2-positive advanced breast cancer. *N Engl J Med*, 355(26):2733–2743, Dec 2006.

[86] Raffaella Ghittoni, Giorgio Napolitani, Daniela Benati, Cristina Ulivieri, Cristina Uliveri, Laura Patrussi, Franco Laghi Pasini, Antonio Lanzavecchia, and Cosima T. Baldari. Simvastatin inhibits the MHC class II pathway of antigen presentation by impairing Ras superfamily GTPases. *Eur J Immunol*, 36(11):2885–2893, Nov 2006.

[87] Henry L. Gomez, Dinesh C. Doval, Miguel A. Chavez, Peter C-S. Ang, Zeba Aziz, Shona Nag, Christina Ng, Sandra X. Franco, Louis W C. Chow, Michael C. Arbushites, Michelle A. Casey, Mark S. Berger, Steven H. Stein, and George W. Sledge. Efficacy and safety of lapatinib as first-line therapy for ErbB2-amplified locally advanced or metastatic breast cancer. *J Clin Oncol*, 26(18):2999–3005, Jun 2008.

[88] V. M. Gonzalez, M. A. Fuertes, C. Alonso, and J. M. Perez. Is cisplatin-induced cell death always produced by apoptosis? *Mol Pharmacol*, 59(4):657–663, Apr 2001.

[89] Balachandra K. Gorentla and Xiao-Ping Zhong. T cell Receptor Signal Transduction in T lymphocytes. *J Clin Cell Immunol*, 2012(Suppl 12):5, Oct 2012.

[90] Peter C. Gotzsche and Margrethe Nielsen. Screening for breast cancer with mammography. *Cochrane Database Syst Rev*, (4):CD001877, 2009.

[91] F. L. Graham, J. Smiley, W. C. Russell, and R. Nairn. Characteristics of a human cell line transformed by DNA from human adenovirus type 5. *J Gen Virol*, 36(1):59–74, Jul 1977.

[92] T. A. Griffin, D. Nandi, M. Cruz, H. J. Fehling, L. V. Kaer, J. J. Monaco, and R. A. Colbert. Immunoproteasome assembly: cooperative incorporation of interferon gamma (IFN-gamma)-inducible subunits. *J Exp Med*, 187(1):97–104, Jan 1998.

[93] Tom A M. Groothuis, Alexander C. Griekspoor, Joost J. Neijssen, Carla A. Herberts, and Jacques J. Neefjes. MHC class I alleles and their exploration of the antigen-processing machinery. *Immunol Rev*, 207:60–76, Oct 2005.

[94] H. Groux, A. O'Garra, M. Bigler, M. Rouleau, S. Antonenko, J. E. de Vries, and M. G. Roncarolo. A CD4+ T-cell subset inhibits antigen-specific T-cell responses and prevents colitis. *Nature*, 389(6652):737–742, Oct 1997.

[95] Bruce M. Hall, Karren M. Plain, Nirupama D. Verma, Giang T. Tran, Rochelle Boyd, Catherine M. Robinson, Mark R. Nicolls, Manuela E. Berger, Masaru Nomura, and Suzanne J. Hodgkinson. Transfer of allograft specific tolerance requires CD4+CD25+T cells but not

interleukin-4 or transforming growth factor-beta and cannot induce tolerance to linked antigens. *Transplantation*, 83(8):1075–1084, Apr 2007.

[96] Bruce M. Hall, Catherine M. Robinson, Karren M. Plain, Nirupama D. Verma, Nicole Carter, Rochelle A. Boyd, Giang T. Tran, and Suzanne J. Hodgkinson. Studies on naÃ¯ve CD4+CD25+T cells inhibition of naive CD4+CD25- T cells in mixed lymphocyte cultures. *Transpl Immunol*, 18(4):291–301, Feb 2008.

[97] Douglas Hanahan and Robert A. Weinberg. Hallmarks of cancer: the next generation. *Cell*, 144(5):646–674, Mar 2011.

[98] Joanne Harding and Barbara Burtness. Cetuximab: an epidermal growth factor receptor chemeric human-murine monoclonal antibody. *Drugs Today (Barc)*, 41(2):107–127, Feb 2005.

[99] G. Hasko, D. G. Kuhel, J. F. Chen, M. A. Schwarzschild, E. A. Deitch, J. G. Mabley, A. Marton, and C. Szabo. Adenosine inhibits IL-12 and TNF-[alpha] production via adenosine A2a receptor-dependent and independent mechanisms. *FASEB J*, 14(13):2065–2074, Oct 2000.

[100] Moniek Heusinkveld, Peggy J. de Vos van Steenwijk, Renske Goedemans, Tamara H. Ramwadhdoebe, Arko Gorter, Marij J P. Welters, Thorbald van Hall, and Sjoerd H. van der Burg. M2 macrophages induced by prostaglandin E2 and IL-6 from cervical carcinoma are switched to activated M1 macrophages by CD4+ Th1 cells. *J Immunol*, 187(3):1157–1165, Aug 2011.

[101] Moniek Heusinkveld and Sjoerd H. van der Burg. Identification and manipulation of tumor associated macrophages in human cancers. *J Transl Med*, 9:216, 2011.

[102] Victoria Hillerdal, Berith Nilsson, Bjoern Carlsson, Fredrik Eriksson, and Magnus Essand. T cells engineered with a T cell receptor against the prostate antigen TARP specifically kill HLA-A2+ prostate and breast cancer cells. *Proc Natl Acad Sci U S A*, 109(39):15877–15881, Sep 2012.

[103] M. Hollstein, D. Sidransky, B. Vogelstein, and C. C. Harris. p53 mutations in human cancers. *Science*, 253(5015):49–53, Jul 1991.

[104] Shohei Hori, Takashi Nomura, and Shimon Sakaguchi. Control of regulatory T cell development by the transcription factor Foxp3. *Science*, 299(5609):1057–1061, Feb 2003.

[105] G. N. Hortobagyi. Anthracyclines in the treatment of cancer. An overview. *Drugs*, 54 Suppl 4:1–7, 1997.

[106] Lianne C. Hsing and Alexander Y. Rudensky. The lysosomal cysteine proteases in MHC class II antigen presentation. *Immunol Rev*, 207:229–241, Oct 2005.

[107] Sheng-Chieh Hsu and Mien-Chie Hung. Characterization of a novel tripartite nuclear localization sequence in the EGFR family. *J Biol Chem*, 282(14):10432–10440, Apr 2007.

[108] Naomi N. Hunder, Herschel Wallen, Jianhong Cao, Deborah W. Hendricks, John Z. Reilly, Rebecca Rodmyre, Achim Jungbluth, Sacha Gnjatic, John A. Thompson, and Cassian Yee. Treatment of metastatic melanoma with autologous CD4+ T cells against NY-ESO-1. *N Engl J Med*, 358(25):2698–2703, Jun 2008.

[109] M. J. Irwin, W. R. Heath, and L. A. Sherman. Species-restricted interactions between CD8 and the alpha 3 domain of class I influence the magnitude of the xenogeneic response. *J Exp Med*, 170(4):1091–1101, Oct 1989.

[110] K. Ito, H. J. Bian, M. Molina, J. Han, J. Magram, E. Saar, C. Belunis, D. R. Bolin, R. Arceo, R. Campbell, F. Falcioni, D. Vidovi?, J. Hammer, and Z. A. Nagy. HLA-DR4-IE chimeric class II transgenic, murine class II-deficient mice are susceptible to experimental allergic encephalomyelitis. *J Exp Med*, 183(6):2635–2644, Jun 1996.

[111] D. Jaeger, E. Stockert, A. O. Guere, M. J. Scanlan, J. Karbach, E. Jaeger, A. Knuth, L. J. Old, and Y. T. Chen. Identification of a tissue-specific putative transcription factor in breast tissue by serological screening of a breast cancer library. *Cancer Res*, 61(5):2055–2061, Mar 2001.

[112] Dirk Jaeger, Julia Karbach, Claudia Pauligk, Inka Seil, Claudia Frei, Yao-Tseng Chen, Lloyd J. Old, Alexander Knuth, and Elke Jaeger. Humoral and cellular immune responses against the breast cancer antigen NY-BR-1: definition of two HLA-A2 restricted peptide epitopes. *Cancer Immun*, 5:11, 2005.

[113] C. B. Jago, J. Yates, N Olsen Saraiva CÃ¢mara, R. I. Lechler, and G. Lombardi. Differential expression of CTLA-4 among T cell subsets. *Clin Exp Immunol*, 136(3):463–471, Jun 2004.

[114] Rinki Jain, Amit Rawat, Bhavna Verma, Maciej M. Markiewski, and Jon A. Weidanz. Antitumor activity of a monoclonal antibody targeting major histocompatibility complex class I-Her2 peptide complexes. *J Natl Cancer Inst*, 105(3):202–218, Feb 2013.

[115] A. I. Jaiswal, C. Dubey, S. L. Swain, and M. Croft. Regulation of CD40 ligand expression on naive CD4 T cells: a role for TCR but not co-stimulatory signals. *Int Immunol*, 8(2):275–285, Feb 1996.

[116] Camilla Jandus, Gilles Bioley, Danijel Dojcinovic, Laurent Derre, Lukas Baitsch, Sebastien Wieckowski, Nathalie Rufer, William W. Kwok, Jean-Marie Tiercy, Immanuel F. Luescher, Daniel E. Speiser, and Pedro Romero. Tumor antigen-specific FOXP3+ CD4 T cells identified in human metastatic melanoma: peptide vaccination results in selective expansion of Th1-like counterparts. *Cancer Res*, 69(20):8085–8093, Oct 2009.

[117] I. Jatoi, S. G. Hilsenbeck, G. M. Clark, and C. K. Osborne. Significance of axillary lymph node metastasis in primary breast cancer. *J Clin Oncol*, 17(8):2334–2340, Aug 1999.

[118] Olivier P. Joffre, Elodie Segura, Ariel Savina, and Sebastian Amigorena. Cross-presentation by dendritic cells. *Nat Rev Immunol*, 12(8):557–569, Aug 2012.

[119] S. C. Johnston, M. L. Dustin, M. L. Hibbs, and T. A. Springer. On the species specificity of the interaction of LFA-1 with intercellular adhesion molecules. *J Immunol*, 145(4):1181–1187, Aug 1990.

[120] Gillian M. Keating. Pertuzumab: in the first-line treatment of HER2-positive metastatic breast cancer. *Drugs*, 72(3):353–360, Feb 2012.

[121] P. M. Kelly, R. S. Davison, E. Bliss, and J. O. McGee. Macrophages in human breast disease: a quantitative immunohistochemical study. *Br J Cancer*, 57(2):174–177, Feb 1988.

[122] J. L. Kelsey, M. D. Gammon, and E. M. John. Reproductive factors and breast cancer. *Epidemiol Rev*, 15(1):36–47, 1993.

[123] T. J. Key, P. N. Appleby, G. K. Reeves, A. Roddam, J. F. Dorgan, C. Longcope, F. Z. Stanczyk, HE Stephenson, Jr, R. T. Falk, R. Miller, A. Schatzkin, D. S. Allen, I. S. Fentiman, T. J. Key, D. Y. Wang, M. Dowsett, H. V. Thomas, S. E. Hankinson, P. Toniolo, A. Akhmedkhanov, K. Koenig, R. E. Shore, A. Zeleniuch-Jacquotte, F. Berrino, P. Muti, A. Micheli, V. Krogh, S. Sieri, V. Pala, E. Venturelli, G. Secreto, E. Barrett-Connor, G. A. Laughlin, M. Kabuto, S. Akiba, R. G. Stevens, K. Neriishi, C. E. Land, J. A. Cauley, L. H. Kuller, S. R. Cummings, K. J. Helzlsouer, A. J. Alberg, T. L. Bush, G. W. Comstock, G. B. Gordon, S. R. Miller, C. Longcope, and Endogenous Hormones Breast Cancer Collaborative Group . Body mass index, serum sex hormones, and breast cancer risk in postmenopausal women. *J Natl Cancer Inst*, 95(16):1218–1226, Aug 2003.

[124] Wojciech Kibil, Diana Hodorowicz-Zaniewska, Antoni Szczepanik, and Jan Kulig. Ultrasound-guided vacuum-assisted core biopsy in the diagnosis and treatment of focal lesions of the breast - own experience. *Wideochir Inne Tech Malo Inwazyjne*, 8(1):63–68, Mar 2013.

[125] Mary-Claire King, Joan H. Marks, Jessica B. Mandell, and New York Breast Cancer Study Group . Breast and ovarian cancer risks due to inherited mutations in BRCA1 and BRCA2. *Science*, 302(5645):643–646, Oct 2003.

[126] L. N. Klapper, M. H. Kirschbaum, M. Sela, and Y. Yarden. Biochemical and clinical implications of the ErbB/HER signaling network of growth factor receptors. *Adv Cancer Res*, 77:25–79, 2000.

[127] R. Koenig, L. Y. Huang, and R. N. Germain. MHC class II interaction with CD4 mediated by a region analogous to the MHC class I binding site for CD8. *Nature*, 356(6372):796–798, Apr 1992.

[128] Natsuko Kondo, Akihisa Takahashi, Koji Ono, and Takeo Ohnishi. DNA damage induced by alkylating agents and repair pathways. *J Nucleic Acids*, 2010:543531, 2010.

[129] Gottfried E. Konecny, Y Gloria Meng, Michael Untch, He-Jing Wang, Ingo Bauerfeind, Melinda Epstein, Petra Stieber, Jean-Michel Vernes, Johnny Gutierrez, Kyu Hong, Malgorzata Beryt, Hermann Hepp, Dennis J. Slamon, and Mark D. Pegram. Association between HER-2/neu and vascular endothelial growth factor expression predicts clinical outcome in primary breast cancer patients. *Clin Cancer Res*, 10(5):1706–1716, Mar 2004.

[130] Y. C. Kong, L. C. Lomo, R. W. Motte, A. A. Giraldo, J. Baisch, G. Strauss, G. J. Haemmerling, and C. S. David. HLA-DRB1 polymorphism determines susceptibility to autoimmune thyroiditis in transgenic mice: definitive association with HLA-DRB1*0301 (DR3) gene. *J Exp Med*, 184(3):1167–1172, Sep 1996.

[131] Keiichi Kontani, Osamu Taguchi, Yoshitomo Ozaki, Jun Hanaoka, Satoru Sawai, Shuhei Inoue, Hajime Abe, Kazuyoshi Hanasawa, and Shozo Fujino. Dendritic cell vaccine immunotherapy of cancer targeting MUC1 mucin. *Int J Mol Med*, 12(4):493–502, Oct 2003.

[132] Thomas Korn, Estelle Bettelli, Mohamed Oukka, and Vijay K. Kuchroo. IL-17 and Th17 Cells. *Annu Rev Immunol*, 27:485–517, 2009.

[133] Gary K. Koski, Ursula Koldovsky, Shuwen Xu, Rosemarie Mick, Anupama Sharma, Elizabeth Fitzpatrick, Susan Weinstein, Harvey Nisenbaum, Bruce L. Levine, Kevin Fox, Paul

Zhang, and Brian J. Czerniecki. A novel dendritic cell-based immunization approach for the induction of durable Th1-polarized anti-HER-2/neu responses in women with early breast cancer. *J Immunother*, 35(1):54–65, Jan 2012.

[134] R. Kumar and R. Yarmand-Bagheri. The role of HER2 in angiogenesis. *Semin Oncol*, 28(5 Suppl 16):27–32, Oct 2001.

[135] Yo-Ping Lai, Chia-Ching Lin, Wan-Jung Liao, Chih-Yung Tang, and Shu-Ching Chen. CD4+ T cell-derived IL-2 signals during early priming advances primary CD8+ T cell responses. *PLoS One*, 4(11):e7766, 2009.

[136] Istvan Lang, Gabor Rubovszky, Zsolt Horvath, Erna Ganofszky, Eszter Szabo, Magdolna Dank, Katalin Boer, and Erika Hitre. A comparative analysis on the efficacy and safety of intaxel and taxol in advanced metastatic breast cancer. *J Clin Diagn Res*, 7(6):1120–1124, Jun 2013.

[137] Courtney M. Lappas, Jayson M. Rieger, and Joel Linden. A2A adenosine receptor induction inhibits IFN-gamma production in murine CD4+ T cells. *J Immunol*, 174(2):1073–1080, Jan 2005.

[138] E. Laurent, M. Talpaz, H. Kantarjian, and R. Kurzrock. The BCR gene and philadelphia chromosome-positive leukemogenesis. *Cancer Res*, 61(6):2343–2355, Mar 2001.

[139] N. T. Le and N. Chao. Regulating regulatory T cells. *Bone Marrow Transplant*, 39(1):1–9, Jan 2007.

[140] K. M. Lee, E. Chuang, M. Griffin, R. Khattri, D. K. Hong, W. Zhang, D. Straus, L. E. Samelson, C. B. Thompson, and J. A. Bluestone. Molecular basis of T cell inactivation by CTLA-4. *Science*, 282(5397):2263–2266, Dec 1998.

[141] Junan Li, Anjali Mahajan, and Ming-Daw Tsai. Ankyrin repeat: a unique motif mediating protein-protein interactions. *Biochemistry*, 45(51):15168–15178, Dec 2006.

[142] Elaine Y. Lin, Jiu-Feng Li, Leoid Gnatovskiy, Yan Deng, Liyin Zhu, Dustin A. Grzesik, Hong Qian, Xiao-nan Xue, and Jeffrey W. Pollard. Macrophages regulate the angiogenic switch in a mouse model of breast cancer. *Cancer Res*, 66(23):11238–11246, Dec 2006.

[143] S. Y. Lin, K. Makino, W. Xia, A. Matin, Y. Wen, K. Y. Kwong, L. Bourguignon, and M. C. Hung. Nuclear localization of EGF receptor and its potential new role as a transcription factor. *Nat Cell Biol*, 3(9):802–808, Sep 2001.

[144] Bryan Linggi and Graham Carpenter. ErbB receptors: new insights on mechanisms and biology. *Trends Cell Biol*, 16(12):649–656, Dec 2006.

[145] P. S. Linsley, J. Bradshaw, J. Greene, R. Peach, K. L. Bennett, and R. S. Mittler. Intracellular trafficking of CTLA-4 and focal localization towards sites of TCR engagement. *Immunity*, 4(6):535–543, Jun 1996.

[146] Udaya K. Liyanage, Todd T. Moore, Hong-Gu Joo, Yoshiyuki Tanaka, Virginia Herrmann, Gerard Doherty, Jeffrey A. Drebin, Steven M. Strasberg, Timothy J. Eberlein, Peter S. Goedegebuure, and David C. Linehan. Prevalence of regulatory T cells is increased in peripheral blood and tumor microenvironment of patients with pancreas or breast adenocarcinoma. *J Immunol*, 169(5):2756–2761, Sep 2002.

[147] Hui-Wen Lo, Sheng-Chieh Hsu, and Mien-Chie Hung. EGFR signaling pathway in breast cancers: from traditional signal transduction to direct nuclear translocalization. *Breast Cancer Res Treat*, 95(3):211–218, Feb 2006.

[148] Sherene Loi, Nicolas Sirtaine, Fanny Piette, Roberto Salgado, Giuseppe Viale, FranÃ§oise Van Eenoo, Ghizlane Rouas, Prudence Francis, John P A. Crown, Erika Hitre, Evandro de Azambuja, Emmanuel Quinaux, Angelo Di Leo, Stefan Michiels, Martine J. Piccart, and Christos Sotiriou. Prognostic and predictive value of tumor-infiltrating lymphocytes in a phase III randomized adjuvant breast cancer trial in node-positive breast cancer comparing the addition of docetaxel to doxorubicin with doxorubicin-based chemotherapy: BIG 02-98. *J Clin Oncol*, 31(7):860–867, Mar 2013.

[149] Xinghua Long and Kenneth P. Nephew. Fulvestrant (ICI 182,780)-dependent interacting proteins mediate immobilization and degradation of estrogen receptor-alpha. *J Biol Chem*, 281(14):9607–9615, Apr 2006.

[150] Daniel B. Longley, D Paul Harkin, and Patrick G. Johnston. 5-fluorouracil: mechanisms of action and clinical strategies. *Nat Rev Cancer*, 3(5):330–338, May 2003.

[151] Jamie A. Lopez, Olivia Susanto, Misty R. Jenkins, Natalya Lukoyanova, Vivien R. Sutton, Ruby H P. Law, Angus Johnston, Catherina H. Bird, Phillip I. Bird, James C. Whisstock, Joseph A. Trapani, Helen R. Saibil, and Ilia Voskoboinik. Perforin forms transient pores on the target cell plasma membrane to facilitate rapid access of granzymes during killer cell attack. *Blood*, 121(14):2659–2668, Apr 2013.

[152] Patricia M. LoRusso, Denise Weiss, Ellie Guardino, Sandhya Girish, and Mark X. Sliwkowski. Trastuzumab emtansine: a unique antibody-drug conjugate in development for human epi-

dermal growth factor receptor 2-positive cancer. *Clin Cancer Res*, 17(20):6437–6447, Oct 2011.

[153] Alberto Mantovani, Paola Allavena, and Antonio Sica. Tumour-associated macrophages as a prototypic type II polarised phagocyte population: role in tumour progression. *Eur J Cancer*, 40(11):1660–1667, Jul 2004.

[154] Alberto Mantovani, Silvano Sozzani, Massimo Locati, Paola Allavena, and Antonio Sica. Macrophage polarization: tumor-associated macrophages as a paradigm for polarized M2 mononuclear phagocytes. *Trends Immunol*, 23(11):549–555, Nov 2002.

[155] Chen Mao, Zu-Yao Yang, Ben-Fu He, Shan Liu, Jun-Hua Zhou, Rong-Cheng Luo, Qing Chen, and Jin Ling Tang. Toremifene versus tamoxifen for advanced breast cancer. *Cochrane Database Syst Rev*, 7:CD008926, 2012.

[156] F. M. Marincola, Y. M. Hijazi, P. Fetsch, M. L. Salgaller, L. Rivoltini, J. Cormier, T. B. Simonis, P. H. Duray, M. Herlyn, Y. Kawakami, and S. A. Rosenberg. Analysis of expression of the melanoma-associated antigens MART-1 and gp100 in metastatic melanoma cell lines and in in situ lesions. *J Immunother Emphasis Tumor Immunol*, 19(3):192–205, May 1996.

[157] Denis Martinvalet, Derek M. Dykxhoorn, Roger Ferrini, and Judy Lieberman. Granzyme A cleaves a mitochondrial complex I protein to initiate caspase-independent cell death. *Cell*, 133(4):681–692, May 2008.

[158] Kunio Matsumoto and Toshikazu Nakamura. Hepatocyte growth factor and the Met system as a mediator of tumor-stromal interactions. *Int J Cancer*, 119(3):477–483, Aug 2006.

[159] A. D. McLellan, R. V. Sorg, L. A. Williams, and D. N. Hart. Human dendritic cells activate T lymphocytes via a CD40: CD40 ligand-dependent pathway. *Eur J Immunol*, 26(6):1204–1210, Jun 1996.

[160] Cornelis J M. Melief and Sjoerd H. van der Burg. Immunotherapy of established (pre)malignant disease by synthetic long peptide vaccines. *Nat Rev Cancer*, 8(5):351–360, May 2008.

[161] Kathy Miller, Molin Wang, Julie Gralow, Maura Dickler, Melody Cobleigh, Edith A. Perez, Tamara Shenkier, David Cella, and Nancy E. Davidson. Paclitaxel plus bevacizumab versus paclitaxel alone for metastatic breast cancer. *N Engl J Med*, 357(26):2666–2676, Dec 2007.

[162] Giorgio Minotti, Pierantonio Menna, Emanuela Salvatorelli, Gaetano Cairo, and Luca Gianni. Anthracyclines: molecular advances and pharmacologic developments in antitumor activity and cardiotoxicity. *Pharmacol Rev*, 56(2):185–229, Jun 2004.

[163] Elizabeth A. Mittendorf, Guy T. Clifton, Jarrod P. Holmes, Kevin S. Clive, Ritesh Patil, Linda C. Benavides, Jeremy D. Gates, Alan K. Sears, Alexander Stojadinovic, Sathibalan Ponniah, and George E. Peoples. Clinical trial results of the HER-2/neu (E75) vaccine to prevent breast cancer recurrence in high-risk patients: from US Military Cancer Institute Clinical Trials Group Study I-01 and I-02. *Cancer*, 118(10):2594–2602, May 2012.

[164] Elizabeth A. Mittendorf, Catherine E. Storrer, Rebecca J. Foley, Katie Harris, Yusuf Jama, Craig D. Shriver, Sathibalan Ponniah, and George E. Peoples. Evaluation of the HER2/neu-derived peptide GP2 for use in a peptide-based breast cancer vaccine trial. *Cancer*, 106(11):2309–2317, Jun 2006.

[165] F. Momburg, J. Roelse, J. Neefjes, and G. J. Haemmerling. Peptide transporters and antigen processing. *Behring Inst Mitt*, (94):26–36, Jul 1994.

[166] T. Morisaki, D. L. Morton, A. Uchiyama, D. Yuzuki, A. Barth, and D. S. Hoon. Characterization and augmentation of CD4+ cytotoxic T cell lines against melanoma. *Cancer Immunol Immunother*, 39(3):172–178, Sep 1994.

[167] R. Moro, J. Gulyaeva-Tcherkassova, and P. Stieber. Increased alpha-fetoprotein receptor in the serum of patients with early-stage breast cancer. *Curr Oncol*, 19(1):e1–e8, Feb 2012.

[168] Yukie Murata, Toshiaki Ohteki, Shigeo Koyasu, and Junji Hamuro. IFN-gamma and pro-inflammatory cytokine production by antigen-presenting cells is dictated by intracellular thiol redox status regulated by oxygen tension. *Eur J Immunol*, 32(10):2866–2873, Oct 2002.

[169] Yuichi Nagakawa, Tatsuya Aoki, Kazuhiko Kasuya, Akihiko Tsuchida, and Yasuhisa Koyanagi. Histologic features of venous invasion, expression of vascular endothelial growth factor and matrix metalloproteinase-2 and matrix metalloproteinase-9, and the relation with liver metastasis in pancreatic cancer. *Pancreas*, 24(2):169–178, Mar 2002.

[170] Rodrigo Naves, Ana Maria Lennon, Giovanna Barbieri, Lilian Reyes, Gisella Puga, Laura Salas, Virginie Deffrennes, Mario Rosemblatt, Marc Fellous, Dominique Charron, Catherine Alcaide-Loridan, and Maria Rosa Bono. MHC class II-deficient tumor cell lines with a defective expression of the class II transactivator. *Int Immunol*, 14(5):481–491, May 2002.

[171] Jacques Neefjes, Marlieke L M. Jongsma, Petra Paul, and Oddmund Bakke. Towards a systems understanding of MHC class I and MHC class II antigen presentation. *Nat Rev Immunol*, 11(12):823–836, Dec 2011.

[172] L. R. Nelson and S. E. Bulun. Estrogen production and action. *J Am Acad Dermatol*, 45(3 Suppl):S116–S124, Sep 2001.

[173] Gerald T. Nepom. MHC class II tetramers. *J Immunol*, 188(6):2477–2482, Mar 2012.

[174] Charlotte K Y. Ng, Helen N. Pemberton, and Jorge S. Reis-Filho. Breast cancer intratumor genetic heterogeneity: causes and implications. *Expert Rev Anticancer Ther*, 12(8):1021–1032, Aug 2012.

[175] S. Nilsson, S. Maekelae, E. Treuter, M. Tujague, J. Thomsen, G. Andersson, E. Enmark, K. Pettersson, M. Warner, and J. A. Gustafsson. Mechanisms of estrogen action. *Physiol Rev*, 81(4):1535–1565, Oct 2001.

[176] Shinzaburo Noguchi, Norikazu Masuda, Hiroji Iwata, Hirofumi Mukai, Jun Horiguchi, Puttisak Puttawibul, Vichien Srimuninnimit, Yutaka Tokuda, Katsumasa Kuroi, Hirotaka Iwase, Hideo Inaji, Shozo Ohsumi, Woo-Chul Noh, Takahiro Nakayama, Shinji Ohno, Yoshiaki Rai, Byeong-Woo Park, Ashok Panneerselvam, Mona El-Hashimy, Tetiana Taran, Tarek Sahmoud, and Yoshinori Ito. Efficacy of everolimus with exemestane versus exemestane alone in Asian patients with HER2-negative, hormone-receptor-positive breast cancer in BOLERO-2. *Breast Cancer*, Feb 2013.

[177] P. Noordhuis, U. Holwerda, C. L. Van der Wilt, C. J. Van Groeningen, K. Smid, S. Meijer, H. M. Pinedo, and G. J. Peters. 5-Fluorouracil incorporation into RNA and DNA in relation to thymidylate synthase inhibition of human colorectal cancers. *Ann Oncol*, 15(7):1025–1032, Jul 2004.

[178] Hakan Norell, Isabel Poschke, Jehad Charo, Wei Z. Wei, Courtney Erskine, Marie P. Piechocki, Keith L. Knutson, Jonas Bergh, Elisabet Lidbrink, and Rolf Kiessling. Vaccination with a plasmid DNA encoding HER-2/neu together with low doses of GM-CSF and IL-2 in patients with metastatic breast carcinoma: a pilot clinical trial. *J Transl Med*, 8:53, 2010.

[179] Elias Obeid, Rita Nanda, Yang-Xin Fu, and Olufunmilayo I. Olopade. The role of tumor-associated macrophages in breast cancer progression (review). *Int J Oncol*, 43(1):5–12, Jul 2013.

[180] Mari Ohmura-Hoshino, Eiji Goto, Yohei Matsuki, Masami Aoki, Mari Mito, Mika Uematsu, Hak Hotta, and Satoshi Ishido. A novel family of membrane-bound E3 ubiquitin ligases. *J Biochem*, 140(2):147–154, Aug 2006.

[181] M. A. Olayioye, R. M. Neve, H. A. Lane, and N. E. Hynes. The ErbB signaling network: receptor heterodimerization in development and cancer. *EMBO J*, 19(13):3159–3167, Jul 2000.

[182] Guillaume Oldenhove, Nicolas Bouladoux, Elizabeth A. Wohlfert, Jason A. Hall, David Chou, Liliane Dos Santos, Shaun O'Brien, Rebecca Blank, Erika Lamb, Sundar Natarajan, Robin Kastenmayer, Christopher Hunter, Michael E. Grigg, and Yasmine Belkaid. Decrease of Foxp3+ Treg cell number and acquisition of effector cell phenotype during lethal infection. *Immunity*, 31(5):772–786, Nov 2009.

[183] Wolfram Osen, Sabine Soltek, Mingxia Song, Barbara Leuchs, Julia Steitz, Thomas Tueting, Stefan B. Eichmueller, Xuan-Duc Nguyen, Dirk Schadendorf, and Annette Paschen. Screening of human tumor antigens for CD4 T cell epitopes by combination of HLA-transgenic mice, recombinant adenovirus and antigen peptide libraries. *PLoS One*, 5(11):e14137, 2010.

[184] Warwick G. P. The mechanism of action of alkylating agents. *Cancer Res*, 23:1315–1333, Sep 1963.

[185] C. Palmieri, G. J. Cheng, S. Saji, M. Zelada-Hedman, A. Waerri, Z. Weihua, S. Van Noorden, T. Wahlstrom, R. C. Coombes, M. Warner, and J-A. Gustafsson. Estrogen receptor beta in breast cancer. *Endocr Relat Cancer*, 9(1):1–13, Mar 2002.

[186] S. Pan, T. Trejo, J. Hansen, M. Smart, and C. S. David. HLA-DR4 (DRB1*0401) transgenic mice expressing an altered CD4-binding site: specificity and magnitude of DR4-restricted T cell response. *J Immunol*, 161(6):2925–2929, Sep 1998.

[187] Pushpa Pandiyan, Lixin Zheng, Satoru Ishihara, Jennifer Reed, and Michael J. Lenardo. CD4+CD25+Foxp3+ regulatory T cells induce cytokine deprivation-mediated apoptosis of effector CD4+ T cells. *Nat Immunol*, 8(12):1353–1362, Dec 2007.

[188] Seho Park, Ja Seung Koo, Min Suk Kim, Hyung Seok Park, Jun Sang Lee, Jong Seok Lee, Seung Il Kim, and Byeong-Woo Park. Characteristics and outcomes according to molecular subtypes of breast cancer as classified by a panel of four biomarkers using immunohistochemistry. *Breast*, 21(1):50–57, Feb 2012.

[189] K. C. Parker, M. A. Bednarek, L. K. Hull, U. Utz, B. Cunningham, H. J. Zweerink, W. E. Biddison, and J. E. Coligan. Sequence motifs important for peptide binding to the human MHC class I molecule, HLA-A2. *J Immunol*, 149(11):3580–3587, Dec 1992.

[190] S. Pascolo, N. Bervas, J. M. Ure, A. G. Smith, F. A. Lemonnier, and B. Perarnau. HLA-A2.1-restricted education and cytolytic activity of CD8(+) T lymphocytes from beta2 microglobulin (beta2m) HLA-A2.1 monochain transgenic H-2Db beta2m double knockout mice. *J Exp Med*, 185(12):2043–2051, Jun 1997.

[191] W. S. Pear, G. P. Nolan, M. L. Scott, and D. Baltimore. Production of high-titer helper-free retroviruses by transient transfection. *Proc Natl Acad Sci U S A*, 90(18):8392–8396, Sep 1993.

[192] George E. Peoples, Jennifer M. Gurney, Matthew T. Hueman, Mike M. Woll, Gayle B. Ryan, Catherine E. Storrer, Christine Fisher, Craig D. Shriver, Constantin G. Ioannides, and Sathibalan Ponniah. Clinical trial results of a HER2/neu (E75) vaccine to prevent recurrence in high-risk breast cancer patients. *J Clin Oncol*, 23(30):7536–7545, Oct 2005.

[193] C. M. Perou, S. S. Jeffrey, M. van de Rijn, C. A. Rees, M. B. Eisen, D. T. Ross, A. Pergamenschikov, C. F. Williams, S. X. Zhu, J. C. Lee, D. Lashkari, D. Shalon, P. O. Brown, and D. Botstein. Distinctive gene expression patterns in human mammary epithelial cells and breast cancers. *Proc Natl Acad Sci U S A*, 96(16):9212–9217, Aug 1999.

[194] W. F. Pickl, O. Majdic, P. Kohl, J. StÃ¶ckl, E. Riedl, C. Scheinecker, C. Bello-Fernandez, and W. Knapp. Molecular and functional characteristics of dendritic cells generated from highly purified CD14+ peripheral blood monocytes. *J Immunol*, 157(9):3850–3859, Nov 1996.

[195] Anouk Pijpe, Nadine Andrieu, Douglas F. Easton, Ausrele Kesminiene, Elisabeth Cardis, Catherine Nogues, Marion Gauthier-Villars, Christine Lasset, Jean-Pierre Fricker, Susan Peock, Debra Frost, D Gareth Evans, Rosalind A. Eeles, Joan Paterson, Peggy Manders, Christi J. van Asperen, Margreet G E M. Ausems, Hanne Meijers-Heijboer, Isabelle Thierry-Chef, Michael Hauptmann, David Goldgar, Matti A. Rookus, Flora E. van Leeuwen, G. E. N. E. P. S. O. , E. M. B. R. A. C. E. , and H. E. B. O. N. . Exposure to diagnostic radiation and risk of breast cancer among carriers of BRCA1/2 mutations: retrospective cohort study (GENE-RAD-RISK). *BMJ*, 345:e5660, 2012.

[196] Jeffrey W. Pollard. Tumour-educated macrophages promote tumour progression and metastasis. *Nat Rev Cancer*, 4(1):71–78, Jan 2004.

[197] Kornelia Polyak. Breast cancer: origins and evolution. *J Clin Invest*, 117(11):3155–3163, Nov 2007.

[198] Adi Prayitno. Cervical cancer with human papilloma virus and Epstein Barr virus positive. *J Carcinog*, 5:13, 2006.

[199] H. M. Prince, S. Dessureault, S. Gallinger, M. Krajden, D. R. Sutherland, C. Addison, Y. Zhang, F. L. Graham, and A. K. Stewart. Efficient adenovirus-mediated gene expression

in malignant human plasma cells: relative lymphoid cell resistance. *Exp Hematol*, 26(1):27–36, Jan 1998.

[200] Binzhi Qian, Yan Deng, Jae Hong Im, Ruth J. Muschel, Yiyu Zou, Jiufeng Li, Richard A. Lang, and Jeffrey W. Pollard. A distinct macrophage population mediates metastatic breast cancer cell extravasation, establishment and growth. *PLoS One*, 4(8):e6562, 2009.

[201] Jon G. Quatromoni and Evgeniy Eruslanov. Tumor-associated macrophages: function, phenotype, and link to prognosis in human lung cancer. *Am J Transl Res*, 4(4):376–389, 2012.

[202] Ganiyu A. Rahman. Breast Conserving Therapy: A surgical Technique where Little can Mean More. *J Surg Tech Case Rep*, 3(1):1–4, Jan 2011.

[203] P. Ramesh, L. Barber, J. R. Batchelor, and R. I. Lechler. Structural analysis of human anti-mouse H-2E xenorecognition: T cell receptor bias and impaired CD4 interaction contribute to weak xenoresponses. *Int Immunol*, 4(8):935–943, Aug 1992.

[204] H. Rammensee, J. Bachmann, N. P. Emmerich, O. A. Bachor, and S. Stevanovic. SYFPEITHI: database for MHC ligands and peptide motifs. *Immunogenetics*, 50(3-4):213–219, Nov 1999.

[205] Pedro A. Reche, John-Paul Glutting, and Ellis L. Reinherz. Prediction of MHC class I binding peptides using profile motifs. *Hum Immunol*, 63(9):701–709, Sep 2002.

[206] M. Reddish, G. D. MacLean, R. R. Koganty, J. Kan-Mitchell, V. Jones, M. S. Mitchell, and B. M. Longenecker. Anti-MUC1 class I restricted CTLs in metastatic breast cancer patients immunized with a synthetic MUC1 peptide. *Int J Cancer*, 76(6):817–823, Jun 1998.

[207] Kelly Marie Redmond, Timothy Richard Wilson, Patrick Gerard Johnston, and Daniel Broderick Longley. Resistance mechanisms to cancer chemotherapy. *Front Biosci*, 13:5138–5154, 2008.

[208] Nicholas P. Restifo, Mark E. Dudley, and Steven A. Rosenberg. Adoptive immunotherapy for cancer: harnessing the T cell response. *Nat Rev Immunol*, 12(4):269–281, Apr 2012.

[209] Katayoun Rezvani, Matthias Grube, Jason M. Brenchley, Giuseppe Sconocchia, Hiroshi Fujiwara, David A. Price, Emma Gostick, Ko Yamada, Jan Melenhorst, Richard Childs, Nancy Hensel, Daniel C. Douek, and A John Barrett. Functional leukemia-associated antigen-specific memory CD8+ T cells exist in healthy individuals and in patients with chronic

myelogenous leukemia before and after stem cell transplantation. *Blood*, 102(8):2892–2900, Oct 2003.

[210] M. P. Roberti, M. M. Barrio, A. I. Bravo, Y. S. Rocca, J. M. Arriaga, M. Bianchini, J. Mordoh, and E. M. Levy. IL-15 and IL-2 increase Cetuximab-mediated cellular cytotoxicity against triple negative breast cancer cell lines expressing EGFR. *Breast Cancer Res Treat*, 130(2):465–475, Nov 2011.

[211] James Robinson, Matthew J. Waller, Sylvie C. Fail, Hamish McWilliam, Rodrigo Lopez, Peter Parham, and Steven G E. Marsh. The IMGT/HLA database. *Nucleic Acids Res*, 37(Database issue):D1013–D1017, Jan 2009.

[212] Christoph Rochlitz, Robert Figlin, Patrick Squiban, Marc Salzberg, Miklos Pless, Richard Herrmann, Eric Tartour, Yongxiang Zhao, Nadine Bizouarne, Martine Baudin, and Bruce Acres. Phase I immunotherapy with a modified vaccinia virus (MVA) expressing human MUC1 as antigen-specific immunotherapy in patients with MUC1-positive advanced cancer. *J Gene Med*, 5(8):690–699, Aug 2003.

[213] Kenneth L. Rock and Lianjun Shen. Cross-presentation: underlying mechanisms and role in immune surveillance. *Immunol Rev*, 207:166–183, Oct 2005.

[214] Jose Manuel Rojas, Stephanie E B. McArdle, Roger B V. Horton, Matthew Bell, Shahid Mian, Geng Li, Selman A. Ali, and Robert C. Rees. Peptide immunisation of HLA-DR-transgenic mice permits the identification of a novel HLA-DRbeta1*0101- and HLA-DRbeta1*0401-restricted epitope from p53. *Cancer Immunol Immunother*, 54(3):243–253, Mar 2005.

[215] S. Romagnani. T-cell subsets (Th1 versus Th2). *Ann Allergy Asthma Immunol*, 85(1):9–18; quiz 18, 21, Jul 2000.

[216] R. K. Ross, A. Paganini-Hill, P. C. Wan, and M. C. Pike. Effect of hormone replacement therapy on breast cancer risk: estrogen versus estrogen plus progestin. *J Natl Cancer Inst*, 92(4):328–332, Feb 2000.

[217] Carmen Ruiz-Ruiz, Gema Robledo, Eva Cano, Juan Miguel Redondo, and Abelardo Lopez-Rivas. Characterization of p53-mediated up-regulation of CD95 gene expression upon genotoxic treatment in human breast tumor cells. *J Biol Chem*, 278(34):31667–31675, Aug 2003.

[218] Qin Ryan, Amna Ibrahim, Martin H. Cohen, John Johnson, Chia-wen Ko, Rajeshwari Sridhara, Robert Justice, and Richard Pazdur. FDA drug approval summary: lapatinib in combi-

nation with capecitabine for previously treated metastatic breast cancer that overexpresses HER-2. *Oncologist*, 13(10):1114–1119, Oct 2008.

[219] Shimon Sakaguchi, Kajsa Wing, Yasushi Onishi, Paz Prieto-Martin, and Tomoyuki Yamaguchi. Regulatory T cells: how do they suppress immune responses? *Int Immunol*, 21(10):1105–1111, Oct 2009.

[220] R. D. Salter, D. N. Howell, and P. Cresswell. Genes regulating HLA class I antigen expression in T-B lymphoblast hybrids. *Immunogenetics*, 21(3):235–246, 1985.

[221] Dos D. Sarbassov, Siraj M. Ali, and David M. Sabatini. Growing roles for the mTOR pathway. *Curr Opin Cell Biol*, 17(6):596–603, Dec 2005.

[222] Hans-Henning Schmidt, Yingzi Ge, Felix J. Hartmann, Heinke Conrad, Felix Klug, Sina Nittel, Helga Bernhard, Christoph Domschke, Florian Schuetz, Christof Sohn, and Philipp Beckhove. HLA Class II tetramers reveal tissue-specific regulatory T cells that suppress T-cell responses in breast carcinoma patients. *Oncoimmunology*, 2(6):e24962, Jun 2013.

[223] U. Schubert, L. C. Anton, J. Gibbs, C. C. Norbury, J. W. Yewdell, and J. R. Bennink. Rapid degradation of a large fraction of newly synthesized proteins by proteasomes. *Nature*, 404(6779):770–774, Apr 2000.

[224] T. N. Schumacher, D. V. Kantesaria, M. T. Heemels, P. G. Ashton-Rickardt, J. C. Shepherd, K. Fruh, Y. Yang, P. A. Peterson, S. Tonegawa, and H. L. Ploegh. Peptide length and sequence specificity of the mouse TAP1/TAP2 translocator. *J Exp Med*, 179(2):533–540, Feb 1994.

[225] Inka Seil, Claudia Frei, Holger Sueltmann, Shirley K. Knauer, Knut Engels, Elke Jaeger, Kurt Zatloukal, Michael Pfreundschuh, Alexander Knuth, Yao Tseng-Chen, Achim A. Jungbluth, Roland H. Stauber, and Dirk Jaeger, D.ger. The differentiation antigen NY-BR-1 is a potential target for antibody-based therapies in breast cancer. *Int J Cancer*, 120(12):2635–2642, Jun 2007.

[226] Raffaele Serra, Anna Maria Miglietta, Sergio Abonante, Vincent Giordano, Gianluca Buffone, and Stefano de Franciscis. Skin-sparing mastectomy with immediate breast and nipple reconstruction: a new technique of nipple reconstruction. *Plast Surg Int*, 2013:406375, 2013.

[227] S. K. Shapira, H. H. Jabara, C. P. Thienes, D. J. Ahern, D. Vercelli, H. J. Gould, and R. S. Geha. Deletional switch recombination occurs in interleukin-4-induced isotype switching to IgE expression by human B cells. *Proc Natl Acad Sci U S A*, 88(17):7528–7532, Sep 1991.

[228] D. J. Sharp, G. C. Rogers, and J. M. Scholey. Microtubule motors in mitosis. *Nature*, 407(6800):41–47, Sep 2000.

[229] Lei Shen, Roland Schroers, Juergen Hammer, Xue F. Huang, and Si-Yi Chen. Identification of a MHC class-II restricted epitope in carcinoembryonic antigen. *Cancer Immunol Immunother*, 53(5):391–403, May 2004.

[230] E. M. Shevach, J. D. Stobo, and I. Green. Immunoglobulin and theta-bearing murine leukemias and lymphomas. *J Immunol*, 108(5):1146–1151, May 1972.

[231] G. P. Shi, R. A. Bryant, R. Riese, S. Verhelst, C. Driessen, Z. Li, D. Bromme, H. L. Ploegh, and H. A. Chapman. Role for cathepsin F in invariant chain processing and major histocompatibility complex class II peptide loading by macrophages. *J Exp Med*, 191(7):1177–1186, Apr 2000.

[232] Masayuki Shimoda, Kieran T. Mellody, and Akira Orimo. Carcinoma-associated fibroblasts are a rate-limiting determinant for tumour progression. *Semin Cell Dev Biol*, 21(1):19–25, Feb 2010.

[233] S. Shresta, C. T. Pham, D. A. Thomas, T. A. Graubert, and T. J. Ley. How do cytotoxic lymphocytes kill their targets? *Curr Opin Immunol*, 10(5):581–587, Oct 1998.

[234] E. R. Simpson. Sources of estrogen and their importance. *J Steroid Biochem Mol Biol*, 86(3-5):225–230, Sep 2003.

[235] S Eva Singletary. Radiofrequency ablation of breast cancer. *Am Surg*, 69(1):37–40, Jan 2003.

[236] D. J. Slamon, G. M. Clark, S. G. Wong, W. J. Levin, A. Ullrich, and W. L. McGuire. Human breast cancer: correlation of relapse and survival with amplification of the HER-2/neu oncogene. *Science*, 235(4785):177–182, Jan 1987.

[237] F. G. Snijdewint, S. von Mensdorff-Pouilly, A. H. Karuntu-Wanamarta, A. A. Verstraeten, P. O. Livingston, J. Hilgers, and P. Kenemans. Antibody-dependent cell-mediated cytotoxicity can be induced by MUC1 peptide vaccination of breast cancer patients. *Int J Cancer*, 93(1):97–106, Jul 2001.

[238] Patsy S H. Soon, Edward Kim, Cindy K. Pon, Anthony J. Gill, Katrina Moore, Andrew J. Spillane, Diana E. Benn, and Robert C. Baxter. Breast cancer-associated fibroblasts induce epithelial-to-mesenchymal transition in breast cancer cells. *Endocr Relat Cancer*, 20(1):1–12, Feb 2013.

[239] Therese Sorlie, Yulei Wang, Chunlin Xiao, Hilde Johnsen, BjÃžrn Naume, Raymond R. Samaha, and Anne-Lise Borresen-Dale. Distinct molecular mechanisms underlying clinically relevant subtypes of breast cancer: gene expression analyses across three different platforms. *BMC Genomics*, 7:127, 2006.

[240] H. D. Soule, J. Vazguez, A. Long, S. Albert, and M. Brennan. A human cell line from a pleural effusion derived from a breast carcinoma. *J Natl Cancer Inst*, 51(5):1409–1416, Nov 1973.

[241] E. D. Staren, M. S. Sabel, L. M. Gianakakis, G. A. Wiener, V. M. Hart, M. Gorski, K. Dowlatshahi, B. F. Corning, M. F. Haklin, and G. Koukoulis. Cryosurgery of breast cancer. *Arch Surg*, 132(1):28–33; discussion 34, Jan 1997.

[242] V. Steimle, C. A. Siegrist, A. Mottet, B. Lisowska-Grospierre, and B. Mach. Regulation of MHC class II expression by interferon-gamma mediated by the transactivator gene CIITA. *Science*, 265(5168):106–109, Jul 1994.

[243] Michael D. Street, Tracy Doan, Karen A. Herd, and Robert W. Tindle. Limitations of HLA-transgenic mice in presentation of HLA-restricted cytotoxic T-cell epitopes from endogenously processed human papillomavirus type 16 E7 protein. *Immunology*, 106(4):526–536, Aug 2002.

[244] Gerd Sutter and Caroline Staib. Vaccinia vectors as candidate vaccines: the development of modified vaccinia virus Ankara for antigen delivery. *Curr Drug Targets Infect Disord*, 3(3):263–271, Sep 2003.

[245] Tuende Szatmari, Katalin Lumniczky, Szilvia Desaknai, Stephane Trajcevski, Egon J. HÃdvÃ©gi, Hirofumi Hamada, and Geza Safrany. Detailed characterization of the mouse glioma 261 tumor model for experimental glioblastoma therapy. *Cancer Sci*, 97(6):546–553, Jun 2006.

[246] Yan Tang, Li Jiang, Yanhua Zheng, Bing Ni, and Yuzhang Wu. Expression of CD39 on FoxP3+ T regulatory cells correlates with progression of HBV infection. *BMC Immunol*, 13:17, 2012.

[247] Jean-Philippe Theurillat, Ursina Zuerrer-Haerdi, Zsuzsanna Varga, Andre Barghorn, Elisabeth Saller, Claudia Frei, Martina Storz, Silvia Behnke, Burkhardt Seifert, Mathias Fehr, Daniel Fink, Christoph Rageth, Claudia Linsenmeier, Bernhard Pestalozzi, Yao-Tseng Chen, Alexander Knuth, Dirk Jaeger, and Holger Moch. Distinct expression patterns of the immunogenic differentiation antigen NY-BR-1 in normal breast, testis and their malignant counterparts. *Int J Cancer*, 122(7):1585–1591, Apr 2008.

[248] Jean-Philippe Theurillat, Ursina Zuerrer-Haerdi, Zsuzsanna Varga, Martina Storz, Nicole M. Probst-Hensch, Burkhardt Seifert, Mathias K. Fehr, Daniel Fink, Soldano Ferrone, Bernhard Pestalozzi, Achim A. Jungbluth, Yao-Tseng Chen, Dirk Jaeger, Alexander Knuth, and Holger Moch. NY-BR-1 protein expression in breast carcinoma: a mammary gland differentiation antigen as target for cancer immunotherapy. *Cancer Immunol Immunother*, 56(11):1723–1731, Nov 2007.

[249] Venkataswarup Tiriveedhi, Timothy P. Fleming, Peter S. Goedegebuure, Michael Naughton, Cynthia Ma, Craig Lockhart, Feng Gao, William E. Gillanders, and T. Mohanakumar. Mammaglobin-A cDNA vaccination of breast cancer patients induces antigen-specific cytotoxic CD4+ICOShi T cells. *Breast Cancer Res Treat*, 138(1):109–118, Feb 2013.

[250] Khoi Q. Tran, Juhua Zhou, Katherine H. Durflinger, Michelle M. Langhan, Thomas E. Shelton, John R. Wunderlich, Paul F. Robbins, Steven A. Rosenberg, and Mark E. Dudley. Minimally cultured tumor-infiltrating lymphocytes display optimal characteristics for adoptive cell therapy. *J Immunother*, 31(8):742–751, Oct 2008.

[251] G. L. Trempe. Human breast cancer in culture. *Recent Results Cancer Res*, (57):33–41, 1976.

[252] E Sergio Trombetta and Ira Mellman. Cell biology of antigen processing in vitro and in vivo. *Annu Rev Immunol*, 23:975–1028, 2005.

[253] Shaw-Wei D. Tsen, Augustine H. Paik, Chien-Fu Hung, and T-C. Wu. Enhancing DNA vaccine potency by modifying the properties of antigen-presenting cells. *Expert Rev Vaccines*, 6(2):227–239, Apr 2007.

[254] M. Van de Craen, I. Van den Brande, W. Declercq, M. Irmler, R. Beyaert, J. Tschopp, W. Fiers, and P. Vandenabeele. Cleavage of caspase family members by granzyme B: a comparative study in vitro. *Eur J Immunol*, 27(5):1296–1299, May 1997.

[255] J. Van de Steene, G. Soete, and G. Storme. Adjuvant radiotherapy for breast cancer significantly improves overall survival: the missing link. *Radiother Oncol*, 55(3):263–272, Jun 2000.

[256] P. A. van der Merwe, D. L. Bodian, S. Daenke, P. Linsley, and S. J. Davis. CD80 (B7-1) binds both CD28 and CTLA-4 with a low affinity and very fast kinetics. *J Exp Med*, 185(3):393–403, Feb 1997.

[257] Zsuzsanna Varga, Jean-Philippe Theurillat, Valeriy Filonenko, Bernd Sasse, Bernhard Odermatt, Achim A. Jungbluth, Yao-Tseng Chen, Lloyd J. Old, Alexander Knuth, Dirk Jaeger,

and Holger Moch. Preferential nuclear and cytoplasmic NY-BR-1 protein expression in primary breast cancer and lymph node metastases. *Clin Cancer Res*, 12(9):2745–2751, May 2006.

[258] Ashok R. Venkitaraman. Cancer susceptibility and the functions of BRCA1 and BRCA2. *Cell*, 108(2):171–182, Jan 2002.

[259] Sunil Verma, David Miles, Luca Gianni, Ian E. Krop, Manfred Welslau, Jose Baselga, Mark Pegram, Do-Youn Oh, Veronique Dieras, Ellie Guardino, Liang Fang, Michael W. Lu, Steven Olsen, Kim Blackwell, and E. M. I. L. I. A Study Group . Trastuzumab emtansine for HER2-positive advanced breast cancer. *N Engl J Med*, 367(19):1783–1791, Nov 2012.

[260] Robert H. Vonderheide, Patricia M. LoRusso, Magi Khalil, Elaina M. Gartner, Divis Khaira, Denis Soulieres, Prudence Dorazio, Jennifer A. Trosko, Jens RÃŒter, Gabriella L. Mariani, Tiziana Usari, and Susan M. Domchek. Tremelimumab in combination with exemestane in patients with advanced breast cancer and treatment-associated modulation of inducible costimulator expression on patient T cells. *Clin Cancer Res*, 16(13):3485–3494, Jul 2010.

[261] Ralf-Holger Voss, Simone Thomas, Christina Pfirschke, Beate Hauptrock, Sebastian Klobuch, Juergen Kuball, Margarete Grabowski, Renate Engel, Philippe Guillaume, Pedro Romero, Christoph Huber, Philipp Beckhove, and Matthias Theobald. Coexpression of the T-cell receptor constant alpha domain triggers tumor reactivity of single-chain TCR-transduced human T cells. *Blood*, 115(25):5154–5163, Jun 2010.

[262] Zev A. Wainberg, Adrian Anghel, Amrita J. Desai, Raul Ayala, Tong Luo, Brent Safran, Marlena S. Fejzo, J Randolph Hecht, Dennis J. Slamon, and Richard S. Finn. Lapatinib, a dual EGFR and HER2 kinase inhibitor, selectively inhibits HER2-amplified human gastric cancer cells and is synergistic with trastuzumab in vitro and in vivo. *Clin Cancer Res*, 16(5):1509–1519, Mar 2010.

[263] Even Walseng, Kazuyuki Furuta, Berta Bosch, Karis A. Weih, Yohei Matsuki, Oddmund Bakke, Satoshi Ishido, and Paul A. Roche. Ubiquitination regulates MHC class II-peptide complex retention and degradation in dendritic cells. *Proc Natl Acad Sci U S A*, 107(47):20465–20470, Nov 2010.

[264] Zhi-kuan Wang, Bo Yang, Hui Liu, Yi Hu, Jun-lan Yang, Liang-liang Wu, Zhen-hong Zhou, and Shun-chang Jiao. Regulatory T cells increase in breast cancer and in stage IV breast cancer. *Cancer Immunol Immunother*, 61(6):911–916, Jun 2012.

[265] Ulrich Warnke, Christina Rappel, Heiko Meier, Charlotte Kloft, Markus Galanski, Christian G. Hartinger, Bernhard K. Keppler, and Ulrich Jaehde. Analysis of platinum adducts with DNA nucleotides and nucleosides by capillary electrophoresis coupled to ESI-MS: indications of guanosine 5'-monophosphate O6-N7 chelation. *Chembiochem*, 5(11):1543–1549, Nov 2004.

[266] Norihiko Watanabe, Yi-Hong Wang, Heung Kyu Lee, Tomoki Ito, Yui-Hsi Wang, Wei Cao, and Yong-Jun Liu. Hassall's corpuscles instruct dendritic cells to induce CD4+CD25+ regulatory T cells in human thymus. *Nature*, 436(7054):1181–1185, Aug 2005.

[267] M. A. Watson and T. P. Fleming. Mammaglobin, a mammary-specific member of the uteroglobin gene family, is overexpressed in human breast cancer. *Cancer Res*, 56(4):860–865, Feb 1996.

[268] Britta Weigelt, Johannes L. Peterse, and Laura J. van 't Veer. Breast cancer metastasis: markers and models. *Nat Rev Cancer*, 5(8):591–602, Aug 2005.

[269] Marij J P. Welters, Gemma G. Kenter, Sytse J. Piersma, Annelies P G. Vloon, Margriet J G. Loewik, Dorien M A. Berends-van der Meer, Jan W. Drijfhout, A Rob P M. Valentijn, Amon R. Wafelman, Jaap Oostendorp, Gert Jan Fleuren, Rienk Offringa, Cornelis J M. Melief, and Sjoerd H. van der Burg. Induction of tumor-specific CD4+ and CD8+ T-cell immunity in cervical cancer patients by a human papillomavirus type 16 E6 and E7 long peptides vaccine. *Clin Cancer Res*, 14(1):178–187, Jan 2008.

[270] E John Wherry. T cell exhaustion. *Nat Immunol*, 12(6):492–499, Jun 2011.

[271] Melanie Widenmeyer, Yuriy Shebzukhov, Sebastian P. Haen, Diethard Schmidt, Stephan Clasen, Andreas Boss, Dmitri V. Kuprash, Sergei A. Nedospasov, Arnulf Stenzl, Hermann Aebert, Dorothee Wernet, Stefan Stevanovic, Philippe L. Pereira, Hans-Georg Rammensee, and Cecile Gouttefangeas. Analysis of tumor antigen-specific T cells and antibodies in cancer patients treated with radiofrequency ablation. *Int J Cancer*, 128(11):2653–2662, Jun 2011.

[272] Scott Wilkie, May C I. van Schalkwyk, Steve Hobbs, David M. Davies, Sjoukje J C. van der Stegen, Ana C Parente Pereira, Sophie E. Burbridge, Carol Box, Suzanne A. Eccles, and John Maher. Dual targeting of ErbB2 and MUC1 in breast cancer using chimeric antigen receptors engineered to provide complementary signaling. *J Clin Immunol*, 32(5):1059–1070, Oct 2012.

[273] Vaughan P. Wittman, David Woodburn, Tiffany Nguyen, Francisca A. Neethling, Stephen Wright, and Jon A. Weidanz. Antibody targeting to a class I MHC-peptide epitope promotes tumor cell death. *J Immunol*, 177(6):4187–4195, Sep 2006.

[274] James D. Yager and Nancy E. Davidson. Estrogen carcinogenesis in breast cancer. *N Engl J Med*, 354(3):270–282, Jan 2006.

[275] F Michael Yakes, Wichai Chinratanalab, Christoph A. Ritter, Walter King, Steven Seelig, and Carlos L. Arteaga. Herceptin-induced inhibition of phosphatidylinositol-3 kinase and Akt Is required for antibody-mediated effects on p27, cyclin D1, and antitumor action. *Cancer Res*, 62(14):4132–4141, Jul 2002.

[276] H. Yang, N-H. Cho, and S-Y. Seong. The Tat-conjugated N-terminal region of mucin antigen 1 (MUC1) induces protective immunity against MUC1-expressing tumours. *Clin Exp Immunol*, 158(2):174–185, Nov 2009.

[277] X. Yang, L. Yan, and N. E. Davidson. DNA methylation in breast cancer. *Endocr Relat Cancer*, 8(2):115–127, Jun 2001.

[278] Y. Yarden. Biology of HER2 and its importance in breast cancer. *Oncology*, 61 Suppl 2:1–13, 2001.

[279] P. Ye, F. H. Rodriguez, S. Kanaly, K. L. Stocking, J. Schurr, P. Schwarzenberger, P. Oliver, W. Huang, P. Zhang, J. Zhang, J. E. Shellito, G. J. Bagby, S. Nelson, K. Charrier, J. J. Peschon, and J. K. Kolls. Requirement of interleukin 17 receptor signaling for lung CXC chemokine and granulocyte colony-stimulating factor expression, neutrophil recruitment, and host defense. *J Exp Med*, 194(4):519–527, Aug 2001.

[280] John S. Yi, Maureen A. Cox, and Allan J. Zajac. T-cell exhaustion: characteristics, causes and conversion. *Immunology*, 129(4):474–481, Apr 2010.

[281] Tadashi Yokosuka, Masako Takamatsu, Wakana Kobayashi-Imanishi, Akiko Hashimoto-Tane, Miyuki Azuma, and Takashi Saito. Programmed cell death 1 forms negative costimulatory microclusters that directly inhibit T cell receptor signaling by recruiting phosphatase SHP2. *J Exp Med*, 209(6):1201–1217, Jun 2012.

[282] A. M. Yvon, P. Wadsworth, and M. A. Jordan. Taxol suppresses dynamics of individual microtubules in living human tumor cells. *Mol Biol Cell*, 10(4):947–959, Apr 1999.

[283] Thorsten Zenz. Exhausting T cells in CLL. *Blood*, 121(9):1485–1486, Feb 2013.

[284] Yuanming Zhang and Jeffrey M. Bergelson. Adenovirus receptors. *J Virol*, 79(19):12125–12131, Oct 2005.

[285] Fang Zhou. Molecular mechanisms of IFN-gamma to up-regulate MHC class I antigen processing and presentation. *Int Rev Immunol*, 28(3-4):239–260, 2009.

[286] Jinfang Zhu, Hidehiro Yamane, and William E. Paul. Differentiation of effector CD4 T cell populations (*). *Annu Rev Immunol*, 28:445–489, 2010.

8 Publications and Presentations

8.1 Publications

Hübener J, Vauti F, Funke C, Wolburg H, Ye Y, Schmidt T, Wolburg-Buchholz K, Schmitt I, Gardyan A, Driessen S, Arnold HH, Nguyen HP, Riess O. N-terminal ataxin-3 causes neurological symptoms with inclusions, endoplasmic reticulum stress and ribosomal dislocation. Brain 2011; Jul;134 Pt 7):1925-42

8.2 Presentations

Adriane Gardyan, Wolfram Osen, Inka Zörnig, Dirk Jäger, Stefan B. Eichmüller. **Identification of novel HLA-restricted T cell epitopes specific fort he breast cancer associated tumor antigen NY-BR-1.** Cancer Immunotherapy Meeting 2011, Mainz, Germany

Adriane Gardyan, Wolfram Osen, Maria Jesiak, Sabine Soltek, Inka Zörnig, Dirk Jäger, Stefan B. Eichmüller. **Identification of novel HLA-restricted T cell epitopes specific for the breast cancer associated tumor antigen NY-BR-1.** Annual KI Cancer Retreat 2011, Stockholm, Sweden.

Adriane Gardyan, Wolfram Osen, Maria Jesiak, Inka Zörnig, Dirk Jäger, Stefan B. Eichmüller. **Identification of novel HLA-restricted T cell epitopes specific for the breast cancer associated tumor antigen NY-BR-1**. AACR Annual Meeting 2012 Chicago, USA.

Adriane Gardyan, Wolfram Osen, Maria Jesiak, Inka Zörnig, Dirk Jäger, Stefan B. Eichmüller. **Characterization of CD4$^+$ T cell responses specific for novel HLA-DR-restricted epitopes derived from the breast tumor antigen NY-BR-1.** Cancer Immunotherapy Meeting 2012, Mainz, Germany

Adriane Gardyan, Wolfram Osen, Maria Jesiak, Inka Zörnig, Dirk Jäger, Stefan B. Eichmüller. Murine **HLA-restricted CD4$^+$ T cell lines as source of high affinity TCRs specific for the human breast cancer associated tumor antigen NY-BR-1**. AACR Annual Meeting 2013 Washington DC, USA.

Adriane Gardyan, Wolfram Osen, Maria Jesiak, Inka Zörnig, Dirk Jäger, Stefan B. Eichmüller. **Murine HLA-restricted CD4$^+$ T cell lines as source of high affinity TCRs specific for the human breast cancer associated tumor antigen NY-BR-1.** Cancer Immunotherapy

Meeting 2013, Mainz, Germany

9 Acknowledgments

At this point I would like to thank all the people who supported me to make this Dissertation possible.

Ganz besonderer Dank geht an Herrn Prof. Stefan Eichmüller für die Möglichkeit in einem wunderbaren Team an diesem Projekt zu arbeiten. Danke für die unermüdliche Unterstützung, wissenschaftlichen Diskussionen und die fantastische Arbeitsatmosphäre in unserem Labor.

Ich möchte mich ganz herzlich bei meinem Betreuer Dr. Wolfram Osen bedanken. Sein beständiger Einsatz bezüglich der experimentellen Unterstützung des Projektes, sowie sein stets offenes Ohr und enormes Fachwissen zu jeglicher wissenschaftlichen Fragestellung, gingen weit über das Maß einer erwarteten Betreuung hinaus.

Des Weitern möchte ich meinen TAC-Komitee Mitgliedern: Prof. Philipp Beckhove und Prof. Dirk Jäger für Ihr stetiges Interesse an diesem Projekt und vor allem für ihre konstruktiven wissenschaftlichen Beiträge, die zum Gelingen diese Arbeit beigetragen haben, danken.

Ich danke den Mitgliedern meiner Prüfungskommission, Prof. Ralf Bartenschlager und Prof. Viktor Umansky, für ihre Bereitschaft mich auf dem so wichtigen letzten Schritt zum Erlangen der Doktorwürde zu unterstützen.

Mein größter Dank geht an alle Brustkrebspatienten, die bereit waren mir ihr Blut zu wissenschaftlichen Zwecken zur Verfügung zu stellen. In diesem Zusammenhang möchte ich mich gerne bei Prof. Schneeweis für die Entnahme der Gewebeproben, bei Sebastian Aulman für die pathologische Einschätzung der Proben und bei Jutta Funk für die riesige Hilfe bei der allgemeine Organisation und dem Aufbereiten der Blutproben, bedanken. Inka Zörnig danke ich für die wissenschaftlichen Diskussionen und die Unterstützung in der Organisation der Verfügbarkeit von Patientenproben.
Mein Dank gilt auch den gesunden Spendern, welche bereitwillig immer wieder zur Probenentnahme zur Verfügung standen und somit maßgeblich zum Gelingen diese Arbeit beigetragen haben.

Ohne meine lieben Kollegen wäre diese Arbeit nicht möglich gewesen. First of all I would like to thank Maria Argawal who did not only make work so much easier but also always was there to help to solve scientific as well as privat life related questions. Thank you so much for the great time we had in the lab in Heidelberg, in the USA and in India. Auch meinen weitern Kollegen Claudia

Weber, Chonglin Luo, Krishna Das und Elke Dickes möchte ich von Herzen für die wunderbare Arbeitsatmosphäre in unserem Labor danke, ohne Eure Unterstützung und Verständnis wäre diese Arbeit nicht möglich gewesen, Danke nochmals dafür.

Freunde begleiten einen auf wichtigen Wegen, ich hatte das Glück Freunde an meiner Seite zu haben, die mit mir gelacht haben, mich aufgemuntert und ermutigt haben wenn es mal nicht so gut mit der wissenschaftlichen Arbeit lief, und mir viele schöne gemeinsame Erlebnisse geschenkt haben, Danke an Euch alle. Besondern Danke an Kerstin, die seit Jahren als wahrhaftige Freundin an meiner Seite ist, ich möchte dich nicht missen. Ganz lieben Dank auch an Theresa, in dir habe ich eine sehr wertvolle Freundin gefunden, für deren Rat, arbeitstechnisch und privat, ich immer offen bin. Allerliebsten Dank auch an meine längste Freundin Sina, die sogar mit der ganzen Familie angereist ist um mich in meinem "Projekt-Doktorarbeit" zu unterstützen.

Letztendlich wäre ohne die stetige Unterstützung meiner Familie auf meinem bisherigen Lebensweg diese Arbeit nicht entstanden. Voran möchte ich meinen Eltern und meinem Bruder danken, die es mir ermöglicht haben eine wissenschaftliche Laufbahn einzuschlagen und es immer wieder geschafft haben mich in meinen Zielen zu bestärken und zu unterstützen. Ein großer Dank geht auch an meine beiden Großelternpaare, die mir auf vielfältige Weise sehr geholfen haben das große Ziel des Erlangens einer Doktorwürde, zu erreichen. Besonders hervorheben möchte ich auch den unermüdlichen Einsatz seitens meiner Tante und Onkel, Danke für die zur jeder Zeit verfügbare Unterstützung, die ich von Euch erfahren habe. Besonderer Dank gilt Benny, ich danke Dir von Herzen dafür, dass Du mich nicht nur in der Zeit meiner Doktorarbeit immer unterstützt hast, sondern auch sonst immer zu mir stehst und mir das wunderbare Gefühl gibst geliebt zu werden.